1

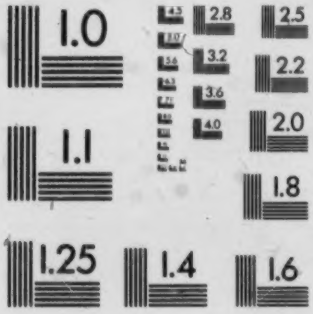
1.0
1.1
1.25
1.4
1.6
1.8
2.0
2.2
2.5
2.8
3.2
3.6
4.0

MICRO-D

# CANADIAN THESES ON MICROFICHE

# THÈSES CANADIENNES SUR MICROFICHE

National Library of Canada
Collections Development Branch

Canadian Theses on
Microfiche Service

Ottawa, Canada
K1A 0N4

Bibliothèque nationale du Canada
Direction du développement des collections

Service des thèses canadiennes
sur microfiche

## NOTICE

The quality of this microfiche is heavily dependent upon the quality of the original thesis submitted for microfilming. Every effort has been made to ensure the highest quality of reproduction possible.

If pages are missing, contact the university which granted the degree.

Some pages may have indistinct print especially if the original pages were typed with a poor typewriter ribbon or if the university sent us an inferior photocopy.

Previously copyrighted materials (journal articles, published tests, etc.) are not filmed.

Reproduction in full or in part of this film is governed by the Canadian Copyright Act, R.S.C. 1970, c. C-30. Please read the authorization forms which accompany this thesis.

## AVIS

La qualité de cette microfiche dépend grandement de la qualité de la thèse soumise au microfilmage. Nous avons tout fait pour assurer une qualité supérieure de reproduction.

S'il manque des pages, veuillez communiquer avec l'université qui a conféré le grade.

La qualité d'impression de certaines pages peut laisser à désirer, surtout si les pages originales ont été dactylographiées à l'aide d'un ruban usé ou si l'université nous a fait parvenir une photocopie de qualité inférieure.

Les documents qui font déjà l'objet d'un droit d'auteur (articles de revue, examens publiés, etc.) ne sont pas microfilmés.

La reproduction, même partielle, de ce microfilm est soumise à la Loi canadienne sur le droit d'auteur, SRC 1970, c. C-30. Veuillez prendre connaissance des formules d'autorisation qui accompagnent cette thèse.

**THIS DISSERTATION HAS BEEN MICROFILMED EXACTLY AS RECEIVED**

**LA THÈSE A ÉTÉ MICROFILMÉE TELLE QUE NOUS L'AVONS REÇUE**

Canada

NL-339 (r. 85/09)

THE UNIVERSITY OF ALBERTA

# A PLEISTOCENE HIGH-LATITUDE GEOMAGNETIC STUDY

by

© MICHAEL A. H. HEDLIN

A THESIS

SUBMITTED TO THE FACULTY OF GRADUATE STUDIES AND RESEARCH

IN PARTIAL FULFILMENT OF THE REQUIREMENTS FOR THE DEGREE

OF MASTER OF SCIENCE

IN

GEOPHYSICS

DEPARTMENT OF PHYSICS

EDMONTON, ALBERTA

FALL 1986

Permission has been granted to the National Library of Canada to microfilm this thesis and to lend or sell copies of the film.

The author (copyright owner) has reserved other publication rights, and neither the thesis nor extensive extracts from it may be printed or otherwise reproduced without his/her written permission.

L'autorisation a été accordée à la Bibliothèque nationale du Canada de microfilmer cette thèse et de prêter ou de vendre des exemplaires du film.

L'auteur (titulaire du droit d'auteur) se réserve les autres droits de publication; ni la thèse ni de longs extraits de celle-ci ne doivent être imprimés ou autrement reproduits sans son autorisation écrite.

ISBN 0-315-32558-5

THE UNIVERSITY OF ALBERTA

**RELEASE FORM**

NAME OF AUTHOR MICHAEL A. H. HEDLIN

TITLE OF THESIS A PLEISTOCENE HIGH-LATITUDE GEOMAGNETIC STUDY

DEGREE FOR WHICH THESIS WAS PRESENTED MASTER OF SCIENCE

YEAR THIS DEGREE GRANTED FALL 1986

Permission is hereby granted to THE UNIVERSITY OF ALBERTA LIBRARY to reproduce single copies of this thesis and to lend or sell such copies for private, scholarly or scientific research purposes only.

The author reserves other publication rights, and neither the thesis nor extensive extracts from it may be printed or otherwise reproduced without the author's written permission.

(SIGNED) Michael Hedlin

PERMANENT ADDRESS:

26 Weir Crescent
Saskatoon, Saskatchewan, Canada
S7H 3A9

DATED September 2 1986

THE UNIVERSITY OF ALBERTA

FACULTY OF GRADUATE STUDIES AND RESEARCH

The undersigned certify that they have read, and recommend to the Faculty of Graduate Studies and Research, for acceptance, a thesis entitled A PLEISTOCENE HIGH-LATITUDE GEOMAGNETIC STUDY submitted by MICHAEL A. H. HEDLIN in partial fulfilment of the requirements for the degree of MASTER OF SCIENCE in GEOPHYSICS.

Michael Evans
......................
Supervisor

......................

......................

Charles Schweger
......................

Date September 2, 1986

## Dedication

to my parents, Charles and Phyllis Hedlin

# Abstract

This thesis reports paleomagnetic results from four vertical sequences of samples of Pleistocene sediments at 68° N latitude in the Yukon territory. Each sequence is believed to cover some, or all, of the time between 80,000 and 140,000 years B.P.. The initial goal was to study the long-term changes in the geomagnetic field, but a feature of particular interest was the so-called Blake Event which is believed by many to have been a time of global reversed polarity that occurred about 100,000 years ago.

No reversed interval is recorded in these sediments, most likely because of a hiatus, but twice in each sedimentary sequence linear perturbations of the geomagnetic field are recorded. These perturbations involve outward trajectories with 22° movement to a westerly declination and shallow inclination and superimposed return trajectories. The reality of these perturbations is supported by the fact that they are recorded with similar character in each sequence and by a time series analysis which reveals a strong power peak, with a high degree of polarization, at the wavelength corresponding to the perturbations.

Analyses of two aspects of the data sets; the far-sidedness of the mean virtual geomagnetic pole (VGP) and the angular dispersion of the VGPs about this mean, as well as consideration of likely sedimentation rates leads to the conclusion that the span of time covered by the samples is not sufficient to average out the effect of dipole wobble.

It is concluded that the perturbations were due to fluctuations in the non-dipole field caused by an intermittent eddy located beneath a stationary bump, or inhomogeneity, at the core-mantle boundary. It is believed that this eddy led to a radially orientated magnetic dipole that posessed a time varying amplitude. Elementary magnetostatic theory shows that such a radial dipole with a magnetic moment as low as 8% that of the Earth's main dipole could cause the perturbations observed in this study. Furthermore, stationary radial dipoles with outwardly directed magnetic flux could cause the far-sidedness of average VGPs that has been observed in sequences of paleomagnetic observations made over the last 20 years.

The effect of cryoturbation on the natural remanent magnetization preserved in poorly consolidated sediments was investigated. It is concluded that in some cases cryoturbation may allow the resetting of magnetization at a time significantly later than the time of deposition by providing the interstitial water necessary to allow the magnetic particles to re-orientate themselves.

## Acknowledgements

I wish to express my sincerest appreciation to Dr. M. E. Evans for his supervision and many useful discussions throughout the course of this research. This project could not have been completed without his assistance.

I would like to thank the Natural Sciences and Engineering Research Council for awarding me a post-graduate scholarship. I would also like to thank the Boreal Institute for Northern Research for providing partial funding for the field work. I am greatly indebted to Dr. C. E. Schweger for his invaluable assistance in the field, and for further discussions afterwards regarding the geology of Beringia. I am also indebted to Dr. J. V. Matthews for his assistance in the field, and to Dr. J. C. Samson for his advice on the the time series analysis of the data. I wish to extend my thanks to Bobby Benjamin who accompanied my wife and I in the field and greatly assisted with the hard labour. I would also like to thank Vaclav Frnoch and Wendy Gough for the many hours they spent in the laboratory working on my samples.

Finally, this project could not have been completed without the encouragement and moral support of my wife, Catherine.

## Table of Contents

Chapter Page

1. GEOMAGNETISM AND PALEOMAGNETISM ....................1

A. Spatial and Temporal Characteristics of the Geomagnetic Field ....................1

B. Natural Recording Processes ....................12

C. Scope of this thesis ....................13

2. GEOLOGICAL AND SAMPLING DETAILS ....................14

A. Geographic Location of Study ....................14

B. Surficial Geology ....................14

C. Paleomagnetic studies in Beringia ....................20

D. Field Procedure ....................22

3. LABORATORY MEASUREMENTS ....................27

A. The Equipment ....................27

B. Partial Demagnetization of Pilot samples ....................28

C. Partial Demagnetization of the remaining samples .30

The Elimination of Inferior Data ....................36

Selection of Optimum Demagnetization Level ....47

D. Temporal Decay of Natural Remanence ....................48

E. Effect of Cryoturbation ....................51

F. Combination of Sections A,B,C and D ....................56

G. Smoothing the Combined Sections ....................61

H. Quality of the Data ....................62

4. ANALYSIS OF THE SECULAR VARIATION ....................72

A. Introduction ....................72

B. Sedimentological Considerations ....................72

C. Analysis of the Temporal Variation ....................76

Geomagnetic Perturbations caused by Dipole Wobble ....................77

Perturbations caused by Dipole(s) at the Core-Mantle Boundary ....78

Space Series Analysis ....94

D. Dispersion Analysis ....97

E. The time averaged paleomagnetic field vector ....101

Landslip ....101

Depositional Inclination Error ....103

Quadrupole far-sidedness ....104

Dipole Wobble ....105

F. The Absence of the Blake Event ....106

5. SUMMARY AND CONCLUSIONS ....111

BIBLIOGRAPHY ....118

APPENDIX A (UNIT DESCRIPTIONS) ....125

A. Section 1 ....125

B. Section C ....128

C. Section D ....130

APPENDIX B (THE INCLINOMETER) ....132

APPENDIX C (MODELLING OF GEOMAGNETIC PERTURBATIONS) ....134

APPENDIX D (DATA ARCHIVE) ....141

## List of Tables

Table Page

3.1 Table illustrating the effect of cryoturbation on orientation, intensity and scatter of remanence preserved in sediments ....................................52

## List of Figures

Figure Page

1.1 The vertical component of the non-dipole field in 1980 ........................................2

1.2 The direction of the Earth's magnetic field at Greenwich over the last 400 years ........................................4

1.3 The twisting of a toroidal magnetic field into a poloidal field ................................6

1.4 Diagram illustrating the effect of a radial dipole just below the core-mantle boundary ........................................10

2.1 Map of Northeastern Beringia ........................15

2.2 Detail of figure 2-1 in the vicinity of sampling sites and the village of Old Crow ........................................16

2.3 A drawing of the cutbank at site 15 as seen from the Old Crow River ........................18

2.4 Old Crow Basin Composite Section ..................19

2.5 Photograph illustrating typical prepared exposure ........................................23

2.6 Photograph illustrating strata and typical sample pairs prior to retrieval ............25

2.7 Drawing of sampling procedure .......................26

3.1 A.F. Demagnetization of Pilot samples ..............29

3.2 Plots showing the dependance of direction of remanence on A.F. demagnetizing field for 3 pilot samples ........................................31

3.3 Section A, 0mT, θ=99° magnetogram ....................32

3.4 Section B, 0mT, θ=99° magnetogram ....................33

3.5 Section C, 0mT, θ=99° magnetogram ....................34

3.6 Section D, 0mT, θ=99° magnetogram ....................35

3.7 Plot illustrating the average directions of magnetization in all samples at 0,10 and 20 mT, and the average remanence vectors removed between these levels ...............37

Figure Page

3.8 Angular difference histograms for sections 1 (A+B) and 2 (C+D) ....................39

3.9 Plot of Angular difference between sample pairs versus Intensity of magnetization ............40

3.10 Section A, 0mt, $\theta=99°$, Intensity Cutoff=$0.3x10^{-2}Am^{-1}$ magnetogram ..................42

3.11 Section A, 0mT, $\theta=10°$ magnetogram ..................43

3.12 Section B, 0mT, $\theta=10°$ magnetogram ..................44

3.13 Section C, 0mT, $\theta=10°$ magnetogram ..................45

3.14 Section D, 0mT, $\theta=10°$ magnetogram ..................46

3.15 Decay of Natural Remanence with time ...............49

3.16 Plot illustrating lack of movement of magnetization vector over a period of 21 weeks in 2 samples ..................................50

3.17 Photograph illustrating intensely cryoturbated sediments in section A ...............53

3.18 Photograph illustrating an apparant thickening of strata at location of ice wedge cast in section C ..........................54

3.19 The intensities of the natural remanent magnetization preserved in sections C and D as a function of depth ..........................58

3.20 Section 1, 10mT, $\theta=10°$ ..............................59

3.21 Section 2, 0mT, $\theta=10°$ ...............................60

3.22 Section 1, 10mT, $\theta=10°$, 5 horizons per group ...........................................63

3.23 Section 2, 0mT, $\theta=10°$, 5 horizons per group ...........................................64

3.24 Bauer plots illustrating the secular variation of the geomagnetic field in section 1 .........................................65

3.25 Bauer plots illustrating the secular variation of the geomagnetic field in section 2 .........................................66

Figure Page

3.26 Histograms illustrating the dependence of $\alpha95$ on size of sampling window ....................68

3.27 The distribution of Fisher's precision parameter $\kappa$ in sections 1 and 2 ..................69

3.28 $\alpha95$ and precision parameter ($\kappa$) distributions in four studies of volcanic rocks ....................................71

4.1 Sedimentation rates observed in a variety of depositional environments .....................74

4.2 Geomagnetic field variation at site HH68-10 due to the dipole precessing at 80° N. latitude ...............................79

4.3 Bauer plot corresponding to figure 4-2 .............80

4.4 Geomagnetic field variation at site HH68-10 that would result from sinusoidal dipole nodding in a plane 45° E, or 135° W, from the site ...............................81

4.5 Bauer plot corresponding to figure 4-4 .............82

4.6 The locus on which radial dipoles located at the core-mantle boundary would cause perturbations of the geomagnetic field observed in this study and by Turner et al (1982) ....................................84

4.7 The magnetic moments of radial dipoles situated at the core-mantle boundary required to cause the perturbations observed in section 1 ...........................86

4.8 Bauer plot illustrating the effect a perturbing RD at the core-mantle boundary has on the total geomagnetic field ................88

4.9 Synthetic magnetogram resulting from a periodically recurring perturbation of the geomagnetic field resulting from the radial dipole described in figure 4-8 ..............89

4.10 Bauer plot of a perturbation of the paleomagnetic field observed by Turner et al (1982) ....................................90

Figure Page

4.11 The magnetic moments of radial dipoles situated at the core-mantle boundary required to cause the paleomagnetic field perturbation observed by Turner et al (1982) ........................................91

4.12 Plot of total power versus frequency in section 1 ........................................96

4.13 The VGP angular dispersion observed in lava flows less than 5 million years old ...........99

4.14 The average VGP's from section 1 before and after removing the perturbations of the paleomagnetic field ...........................102

4.15 The paleolongitude and paleolatitude of the VGP as a function of stratigraphic level relative to the Old Crow Tephra near the town of Old Crow ........................107

5.1 Drawing of the inclinometer ......................133

# 1. GEOMAGNETISM AND PALEOMAGNETISM

## A. Spatial and Temporal Characteristics of the Geomagnetic Field

Although magnetism was discovered by the Chinese over 2,000 years ago, it was not until the fifteenth century that a direct relationship between this phenomenon and the Earth itself was firmly established. In 1600 William Gilbert correctly deduced that the geomagnetic field closely corresponds to the dipolar field that would be expected from a uniformly magnetized sphere. It varies in strength from about 30,000 nT near the equator to about 60,000 nT at the poles. Currently the best fitting dipole is inclined at 11.5 degrees to the rotation axis, so that its axis intersects the surface at 78.5° North, 70° West and 78.5° South, 110° East. In the 1830's C.F. Gauss used spherical harmonic analysis to demonstrate conclusively that the field is of internal origin although there are components, now known collectively as the non-dipole field, that are superimposed on the central dipole and comprise roughly $\frac{1}{20}$ of the total field strength (Irving, 1964) (fig. 1-1). These components involve all terms above order 1 in the spherical harmonic expansion.

Direct observation of the direction of the field over the last 400 years at observatories in London and Paris (and many other locations over shorter time spans) has revealed that the field is not stationary, but undergoes gradual

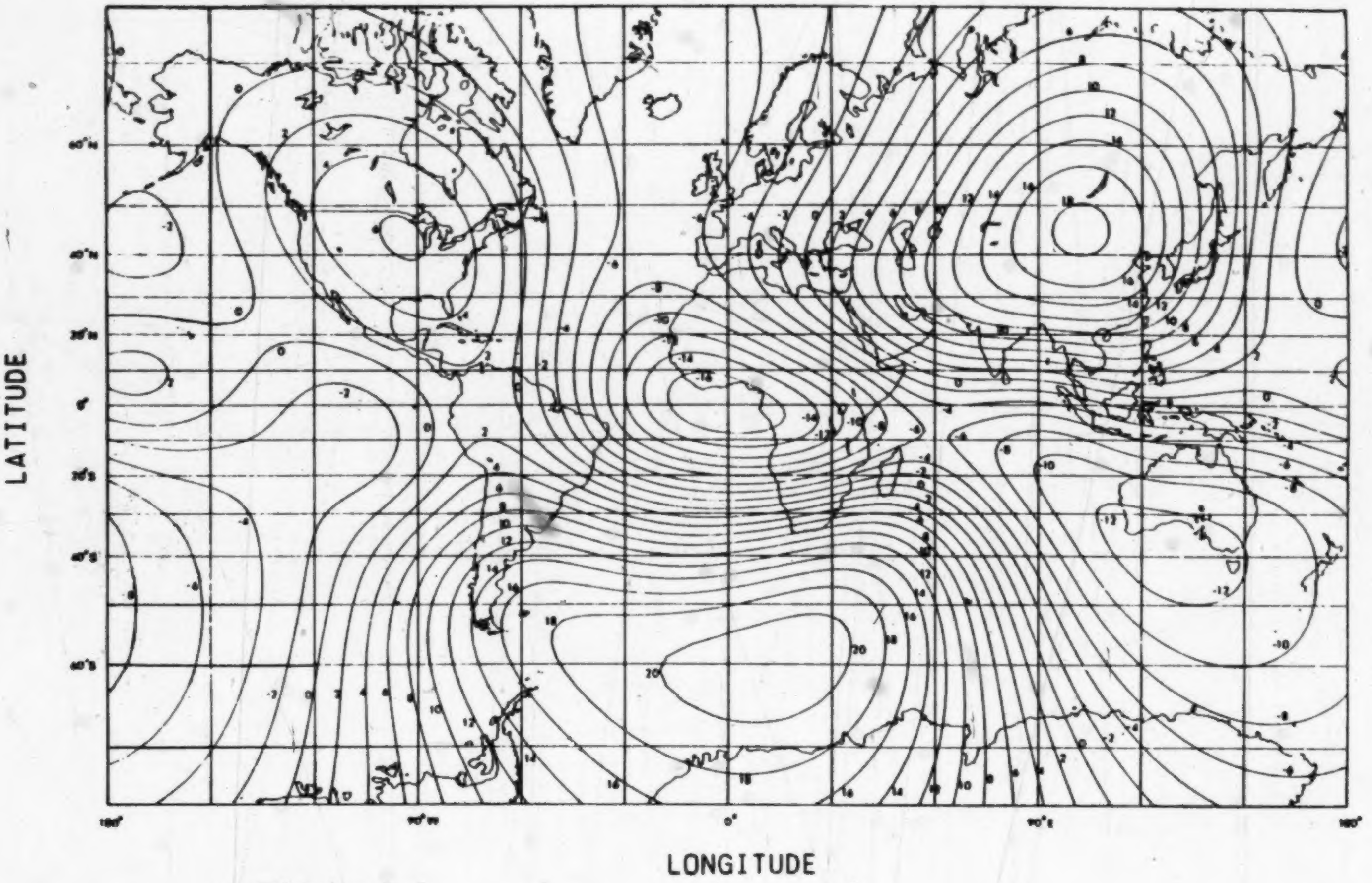
LATITUDE
60°N
40°N
20°N
0°
20°S
40°S
60°S
180°
90°W
0°
90°E
180°
LONGITUDE

**Figure 1-1**

The vertical component of the non-dipole field in 1980. Contour interval is 2000 nT.

changes known as the secular variation (fig. 1-2). In the twentieth century, paleomagnetic investigations have shown that these gradual changes have been occurring for millions of years and involve a rich spectrum of phenomena (Merrill and McElhinny,1983). The discovery by H. Gellibrand in 1635 that the geomagnetic field varies with time, and the fact that no material can possess a permanent magnetization at high temperatures, quickly led researchers to discard Gilbert's notion of a permanently magnetized source in the Earth's interior. Instead, it is now generally accepted that the field is due to magnetohydrodynamic motions in the Earth's fluid outer core. Critical to the development of this theory was the discovery by Oldham in 1906 that the transmission of seismic shear waves ceases abruptly at a depth of 2900 kilometers. It is now known that this is due to the presence of a liquid zone, the outer core, which consists of a Ni-Fe mixture extending down to a depth of about 5,000 kilometers. Beneath this is the solid inner core.

Because of heat produced in the core - either by the decay of radioactive elements or latent heat produced by its gradual solidification, or because of gravitational stirring - convection cells are believed to exist in the outer core. It is believed by many (including Jacobs, 1984 and Bullard, 1968) that the combined effects of this mechanical movement, the metallic nature of the material involved, and the initial presence of an ambient magnetic field, may be

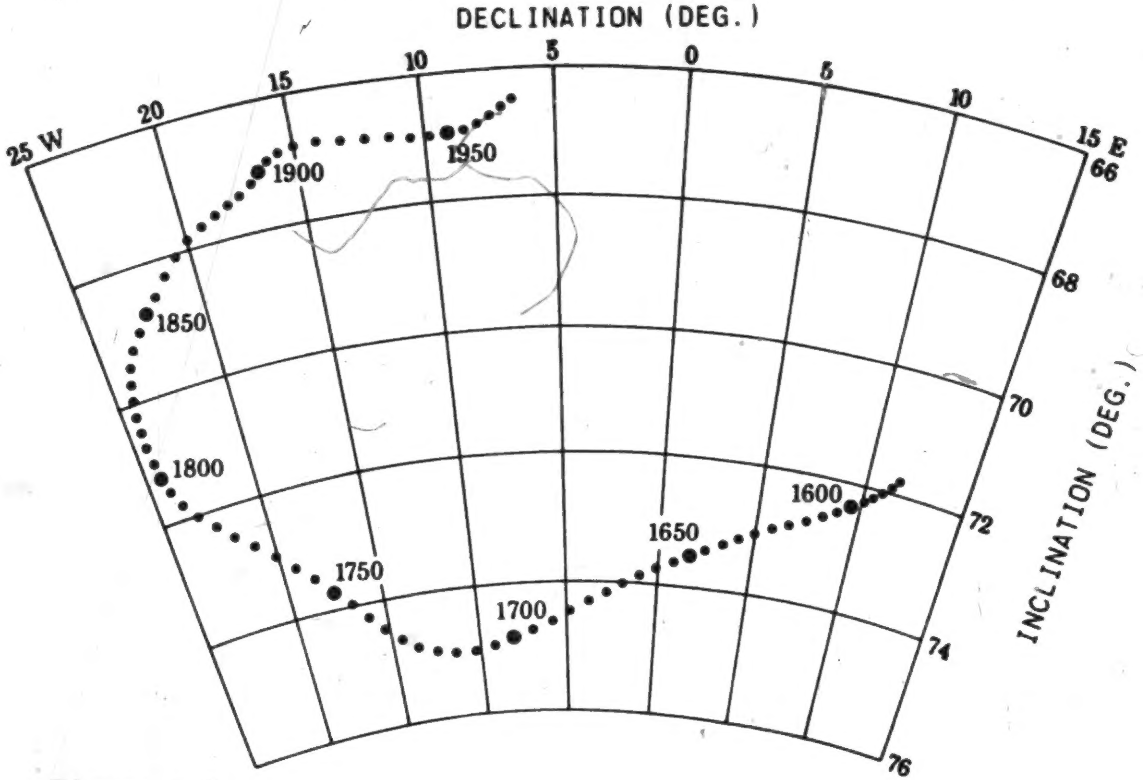

Figure 1-2

The direction of the Earth's magnetic field at Greenwich.
Zenithal equidistant projection.
Inclination is the angle between the horizontal plane and the total field vector (positive down).
Declination is the angle between geographic north and the horizontal component of the total field vector.
From S. Malin and E. Bullard (1981)

sufficient to give rise to an external magnetic field. As described by Bullard (1968), the generation of a magnetic field observable at the Earth's surface by the movement of electrically conducting fluids in the outer core may resemble that which occurs in a self-exciting dynamo. If a conducting disk is rotated perpendicular to a magnetic field any charges present will be acted on by the Lorentz force and will move in the radial direction. If the resulting current is fed into a suitable closed loop, a magnetic field which is parallel to the original field can be set up. The Lorentz force will then be increased and the entire system will be self-sustaining, provided a torque is applied to rotate the disk. The convection cells in the outer core form closed loops of moving charge, but because the Earth is rotating these cells are acted upon by the Coriolis force and must conserve angular momentum as they rise and fall so they are twisted so that the magnetic field they produce is directed along their axes. The bulk of the magnetic field in the core is toroidal and is never seen at the Earth's surface, but because of cyclonic convective motions this toroidal field is twisted into loops which are orientated by the Coriolis force to produce a poloidal field (Parker,1955)(fig. 1-3). The toroidal field serves to regenerate the dynamo; the poloidal field is a small by-product which is observed at the Earth's surface. Because of the remoteness of the Earth's core, this theory and all others regarding the generation of the geomagnetic field is

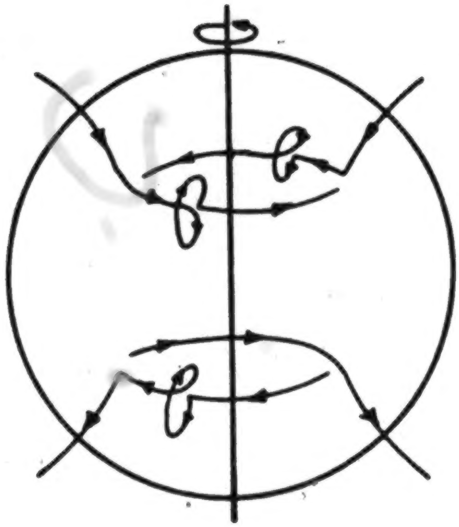

Figure 1-3

The twisting of a toroidal magnetic field into a poloidal field.
**From Jacobs (1984)**

still far from established.

Since the magnetic field is controlled to some extent by the Earth's rotation, one might expect a relationship between the location of the geomagnetic poles and the Earth's rotation axis. In fact it has been shown by Merrill and McElhinny(1977) that when averaged over sufficiently long time intervals the geomagnetic poles do indeed coincide with the rotation axis. The present divergence of 11.5° is the result of dipole wobble. Currently, there is no consensus on the exact nature and cause of the wobbling of the dipole, but it apparently involves time scales on the order of $10^5$ years with an average deflection on the order of 10° (McElhinny and Merrill, 1975).

Far more dramatic than dipole wobble is the phenomenon of polarity reversal, which the geological record indicates take place several times every million years. Because reversals occur so rapidly (perhaps requiring as little as $10^3$ years) they are hard to find and are consequently poorly documented. Reversals are so significant that the Earth's history has been divided into *epochs* defined by periods of one dominant polarity. The most recent reversal that is established beyond all doubt is that which divides the current Brunhes Epoch from the preceeding Matuyama Epoch, some 690,000 years ago.

Polarity intervals that lie within epochs and last for only $10^3$ to $10^4$ years are known as *events*. One event that is very relevant to the present study is the Blake Event which occurred roughly 100,000 years ago, and is estimated to have lasted anywhere from 5,000 to 40,000 years. It was originally discovered in the north Atlantic by Smith and Foster(1969), but has been subsequently located in Japan (Sasajima et al,1980; Yaskawa et al,1973), Italy (Creer et al,1980), and northern Canada (Westgate et al, 1985). This wide geographic spread strongly supports the reality of a genuine occurrence involving the main dipole. The event has been observed to be split into two stages by a short time of normal polarity (Smith and Foster,1969; Creer et al,1980; Denham et al,1977), but whether or not a full 180° movement of the poles is involved has not yet been fully established.

In addition to complete reversals, short *excursions* on the order of $10^4$ years in duration and involving more than 40° movement from the rotation axis, have been observed. There is debate on whether excursions involve the main dipole, and are abortive attempts of the field to reverse, or are simply due to large, rapid enhancements of the non-dipole field. It has even been suggested (e.g. Verosub et al,1977) that some proposed excursions may be simply due to disturbances in the sediment occurring during, or after, deposition. As is the case with establishing the validity and cause of events, determining the geographic extent of excursions is critical. If an excursion is only observed over a limited area it was most likely a non-dipole field phenomenon, whereas if it was observed on a global scale the main dipole must have been involved. As explained by

Yukutake(1961) the fact that changes in the non-dipole field occur so rapidly demands that their source be in the outer regions of the core. Deeper, small-scale, electromagnetic fluctuations will inevitably be shielded by the outer conductive layers and therefore never be observed at the surface. It has been shown by Alldredge and Hurwitz (1964) that 8 eddies occurring under irregularities at the core-mantle interface can accurately simulate the observed non-dipole field. Short term enhancement of one of these eddies could have a pronounced effect on the observed field just above the eddy and could lead to a localized polar excursion (Harrison and Ramirez,1975) (fig. 1-4).

Since changes in the non-dipole field occur so rapidly it is possible to observe them by comparing maps of directly observed field intensity and direction constructed several years apart. The most notable feature of recent secular variation, originally discovered by Halley in 1692, is a gradual westward drift at approximately 0.2° per year (Bullard et al,1950). By studying archaeomagnetic data from the years 1200 to 1800 Burlatskaya(1965) claimed to have established that westward drift has persisted over at least the last 750 years. Recent study has complicated the matter somewhat. Yukutake and Tachinaka (1968) discuss the division of the non-dipole field into stationary and drifting components (see also Evans,1984). This followed the discovery of some very large anomalies that display growth or decay, but which do not appear to drift. Furthermore,

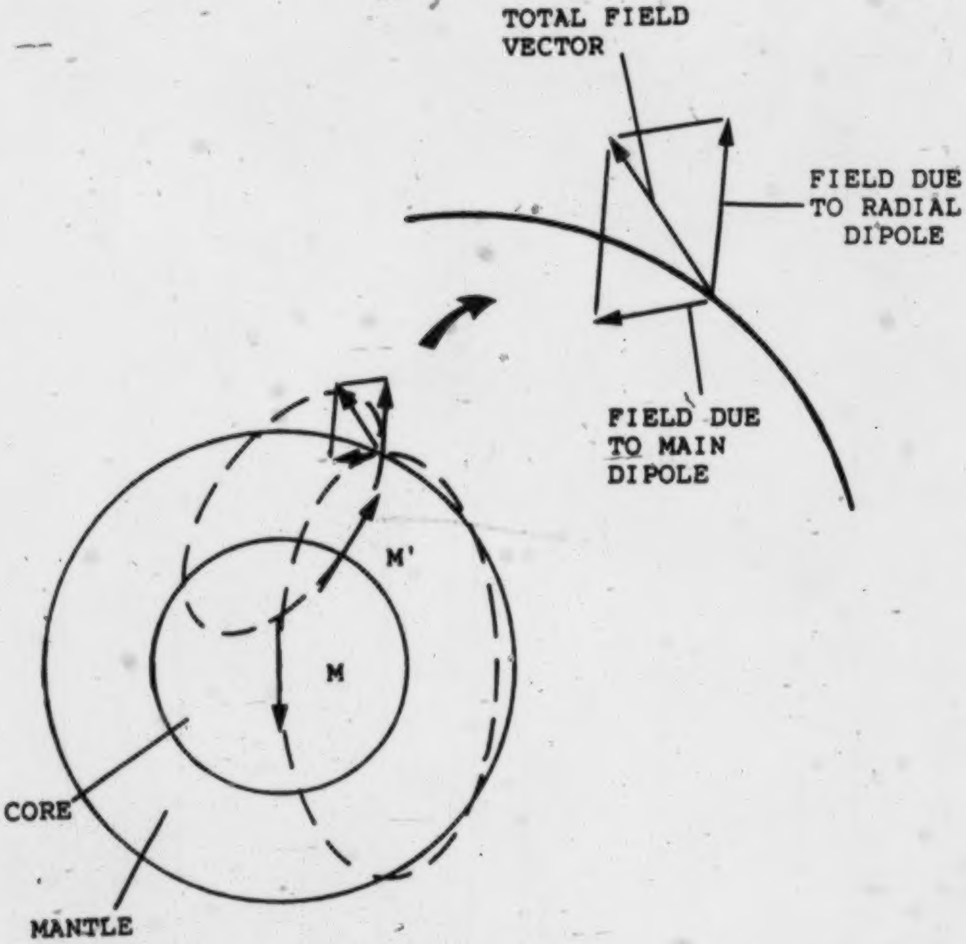
TOTAL FIELD VECTOR
FIELD DUE TO RADIAL DIPOLE
FIELD DUE TO MAIN DIPOLE
M'
M
CORE
MANTLE

**Figure 1-4**

Diagram illustrating the effect of a radial dipole due to a fluid eddy just below the core-mantle boundary.

In the case depicted here the relative positions and magnetic moments of the central dipole (M) and the eddy dipole (M') lead to a total field vector which is deflected some 50° from the field expected from the main central dipole alone. (Since the resulting inclination has switched from positive (below the horizontal) to negative, some authors would label the outcome a reversal.)

several authors including Bullard et al(1950) and Adam et al(1964) discuss a dependence of drift rate on latitude. The northern hemisphere seems to have a slower drift rate than the southern hemisphere, and negative (i.e. eastward) drift rates have been reported in some areas of Canada and Alaska (Bullard et al,1950). In addition, several authors (including Harwood and Malin,1976; Hoye,1981; and Yukutake,1967) have demonstrated that the drift rate has been changing with time. From studying direct observations of the field made over a 30 year span Harwood and Malin (1976) concluded that the westward drift had a mean deceleration of .01°/year$^2$. Paleomagnetic data from Vesuvian lavas led Hoye to deduce a mean deceleration rate of .004°/yr$^2$ over the last 200 years. Yukutake (1967) claims that archaeomagnetic data indicate that present rates are 50% slower than those of 1,000 years ago.

Although the westward drift of the non-dipole field appears to be a very complex process it has been postulated by Bullard et al (1950) that it may be due to the conservation of angular momentum in convection cells in the outer core and the imperfect coupling between the core and mantle. As plumes of fluid rise in the convection process they would have to slow down and drift westward relative to the mantle and surface of the Earth in order to conserve angular momentum. The effects of downward moving, eastward drifting, plumes would never be seen at the surface of the Earth because of electromagnetic screening in the outermost layers of the core. As a result the trend would be for secular variation to have an overall westward movement as observed.

## B. Natural Recording Processes

Several excellent books have been written which cover in detail the acquisition of a *natural remanent magnetization* (NRM) and the recording of secular variation in the rock record (including Irving,1964; McElhinny,1973; Jacobs,1984). In this chapter therefore, only a brief description of the five main mechanisms is given, in order to introduce the proper terminology.

In an igneous or metamorphic environment cooling of the rock allows any ferromagnetic particles to reach the Curie temperature and acquire a magnetization. This is known as *thermoremanent magnetization* (TRM). Remanence can also arise when ferromagnetic particles form by chemical precipitation, leading to a *chemical remanent magnetization* (CRM).

More relevant to this study however is the recording process that occurs in sedimentary environments. As a sediment is being deposited, any magnetic particles present will be forced into a rough alignment with the ambient geomagnetic field, provided the medium (usually water) in which the particles are being deposited is not too agitated. As a result the sediment will posess a *detrital remanent magnetization* (DRM). After deposition, if magnetic particles are free to rotate in water-filled voids, *a post* *depositional remanent magnetization* (PDRM) may replace the original DRM.

Once the remanent magnetization has been acquired it is subject to a process known as viscous decay. The intensity of magnetization drops as the magnetic moments of some grains are thermally agitated such that they acquire a new direction of magnetization. If an ambient field is present it will bias the new directions of magnetization such that a *viscous remanent magnetization* (VRM) is overprinted onto the original. Fortunately those grains that tend to get remagnetized in this manner have a low coercive force and their effects can be reduced , or eliminated, by partial demagnetization of the sediment in a manner discussed in chapter 3.

## C. Scope of this thesis

Critical to the understanding of the secular variation of the geomagnetic field is the collection of samples containing its history from as many parts of the Earth as possible. One region that is in need of further attention is the far North (especially above the Arctic Circle). In this study long sequences of sediments from a latitude of 67°51' have been sampled in the hope that they will reveal not only the secular variation, but rarer phenomena such as polar reversals. To increase the likelihood of this an interval roughly $10^5$ years old that is believed to span the time of the Blake Event has been sampled.

## 2. GEOLOGICAL AND SAMPLING DETAILS

### A. Geographic Location of Study

The samples for this study were collected from two cutbanks along the Old Crow River in the Yukon Territory. These sections are located at 67°51' North, 139°48' West, and are separated from one another by 1 kilometer (figs. 2-1 and 2-2). The river itself traverses the Old Crow Basin which is the largest (roughly 6500 km$^2$) of three in the northern Yukon, the others being the Bluefish and the Bell Basins. The general area is part of a much larger region extending from the Richardson Mountains in the East to the Bering Strait, and South from the Beaufort Sea to Whitehorse, Yukon; some authors (e.g. Morlan, 1980) refer to this broad area as *Beringia*.

### B. Surficial Geology

For some years now this area has attracted scientists from a wide range of disciplines because it has remained unglaciated to the present day. The maximum ice advance is shown in figure 2-1. During times of advanced glaciation in the Cenozoic this area served as a refuge for plant and animal life, including possibly the first humans in North America, who arrived across the Bering Strait. As the glaciers melted and receeded from the surrounding areas Beringia received sediments carried by the meltwaters. As a result considerable thicknesses of upper Pleistocene fluvial

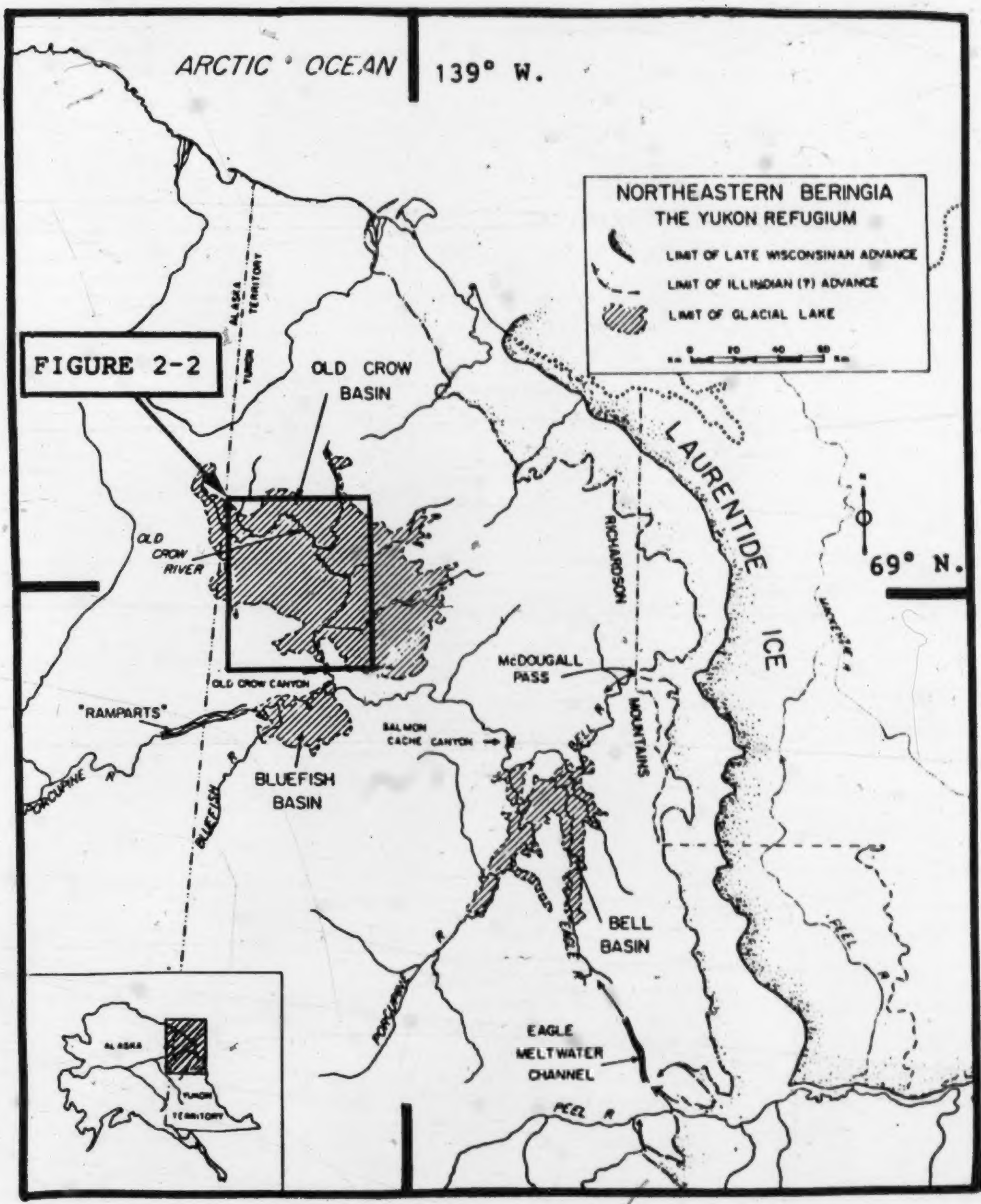
ARCTIC OCEAN
139° W.
NORTHEASTERN BERINGIA
THE YUKON REFUGIUM
LIMIT OF LATE WISCONSINAN ADVANCE
LIMIT OF ILLINOIAN (?) ADVANCE
LIMIT OF GLACIAL LAKE
0 20 40 60
km
FIGURE 2-2
ALASKA
YUKON TERRITORY
OLD CROW BASIN
OLD CROW RIVER
LAURENTIDE ICE
69° N.
RICHARDSON MOUNTAINS
McDOUGALL PASS
OLD CROW CANYON
"RAMPARTS"
PORCUPINE R
BLUEFISH R
BLUEFISH BASIN
SALMON CACHE CANYON
BELL R
BELL BASIN
EAGLE R
PEEL R
EAGLE MELTWATER CHANNEL
ALASKA
YUKON TERRITORY

Figure 2-1

Map of Northeastern Beringia

From Morlan(1980)

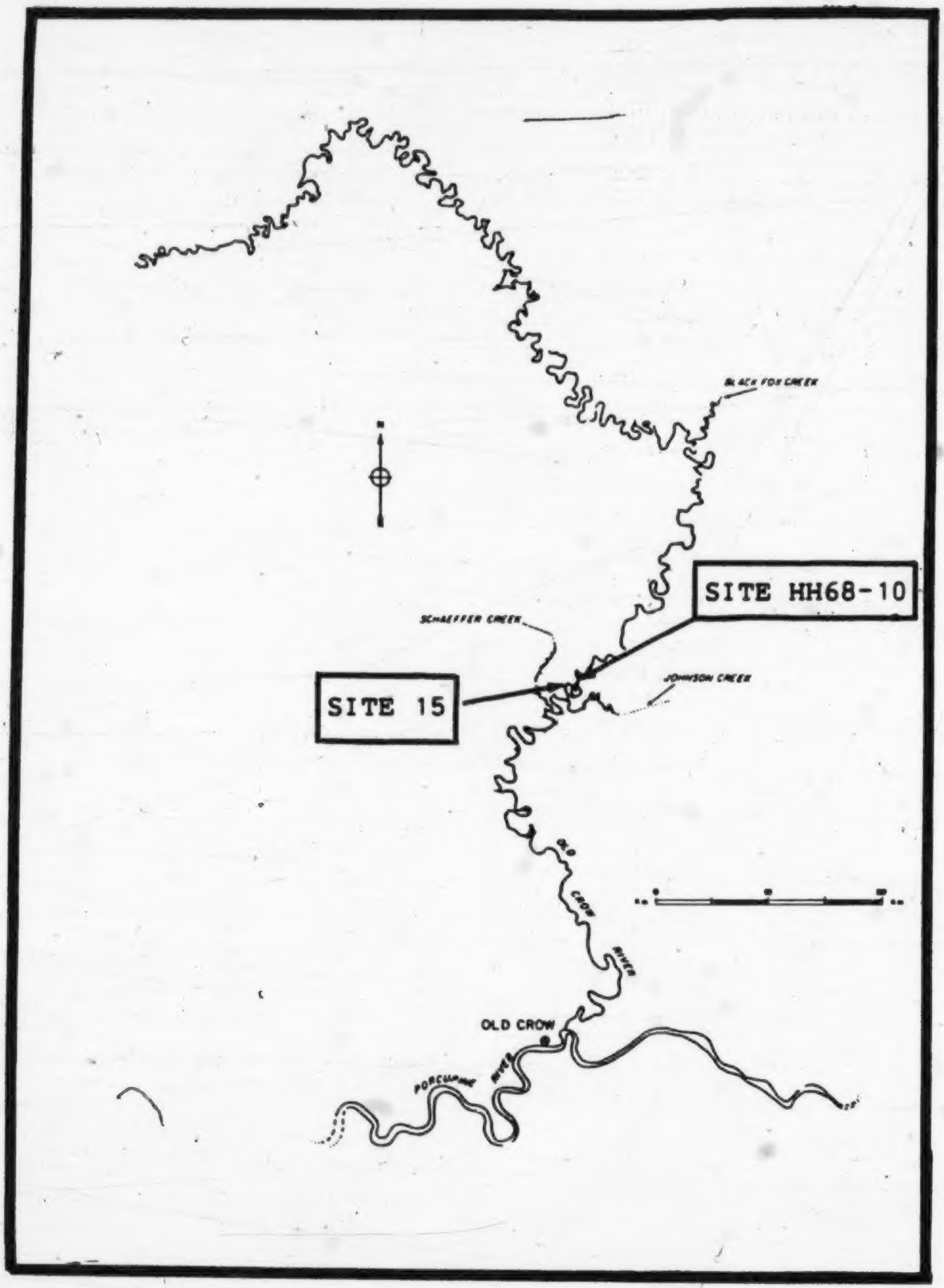
BLACK FOX CREEK
SITE HH68-10
SCHAEFFER CREEK
JOHNSON CREEK
SITE 15
OLD CROW RIVER
OLD CROW
PORCUPINE RIVER

**Figure 2-2**

Detail of figure 2-1 in the vicinity of sampling sites and the village of Old Crow.

From Morlan(1980)

and lacustrine sediments have been deposited along with well preserved plant and animal remains. Subsequent downcutting by the Old Crow and other rivers has resulted in the present exposure. Sketches of a typical exposure are shown in figures 2-3 and 2-4. The stratigraphic subdivisions were originally defined by Hughes(1969,1972) and have been extended by Morlan(1978,1980) and others. As is shown in figure 2-4, nine major units have been defined. All samples in this study were collected from unit 3, which has been described by Morlan(1980) as follows:

> Largely composed of bedded sands, silts and clays. Vertical, and lateral, facies changes occur abruptly and are common. Sediments believed to be of Sangamon Interglacial and/or early Wisconsin age. No widely recognised disconformities have been located within this unit. The upper limit is defined by an erosional surface which contains ice wedge pseudomorphs (Disconformity A). Just beneath Disconformity A is a volcanic ash known as the 'Old Crow Tephra'.

The Old Crow Tephra has been dated by Westgate and Wintle (1986) using thermoluminesence techniques to be 86,000 ± 8,000 years old. Disconformity A has been dated by Morlan (1986) at 39,000 years of age using bone matter (this date is believed to represent the time when sedimentation began after the hiatus). At present no other dates have been obtained from unit 3. The only other date available is derived from the Little Timber Tephra which has been

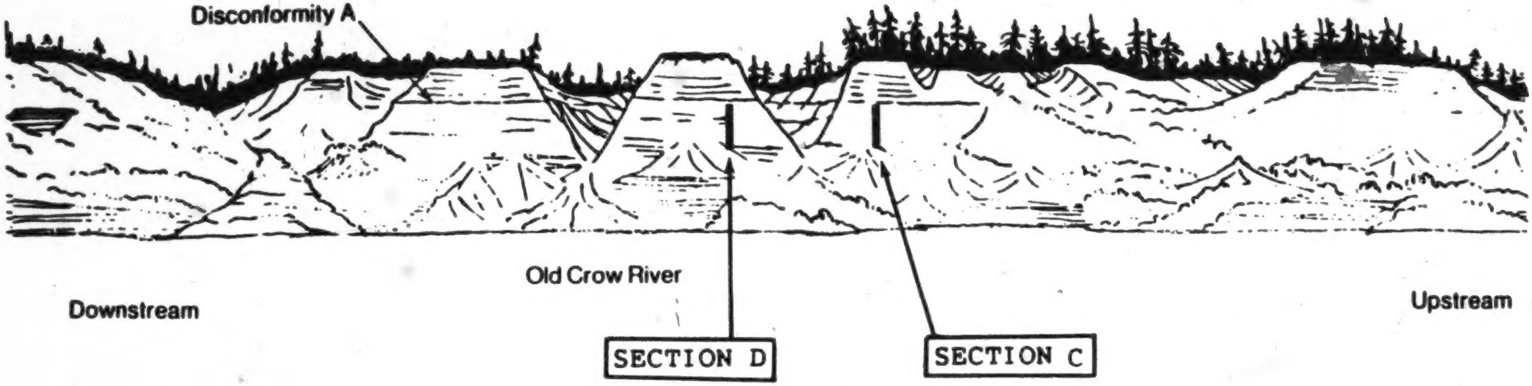
Disconformity A
Old Crow River
Downstream
Upstream
SECTION D
SECTION C

**Figure 2-3**

A drawing of the cutbank at site 15 as seen from the Old Crow River.

Modified from Walde (1986)

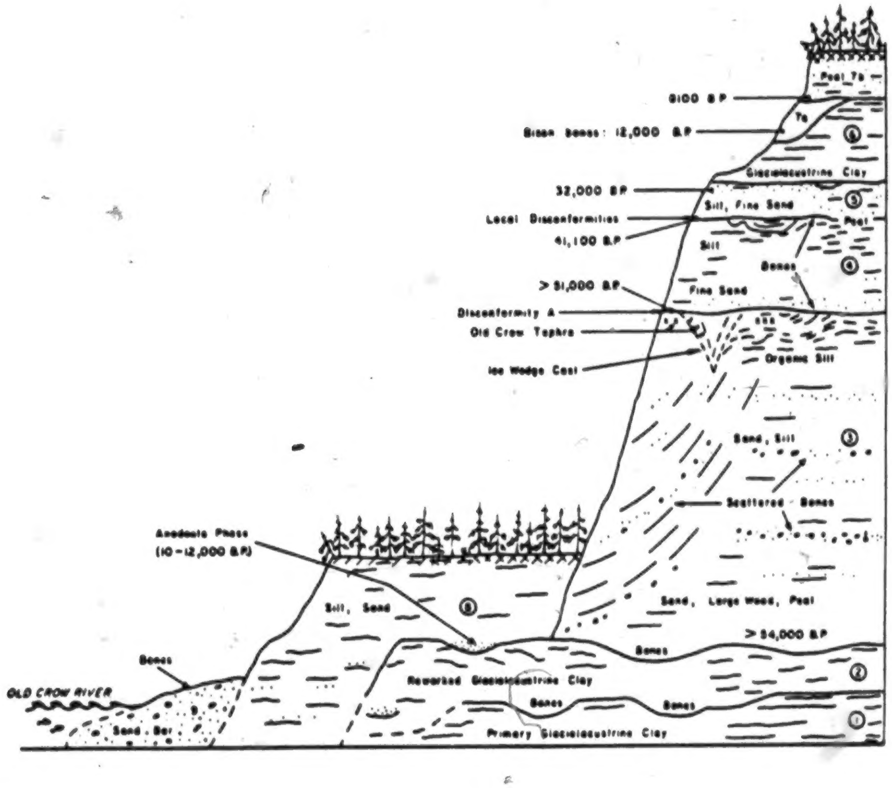
Peat Ts
8100 B.P
Ts
Bison Bones: 12,000 B.P
⑥
Glaciolacustrine Clay
32,000 B.P
Silt, Fine Sand
⑤
Local Disconformities
Peat
41,100 B.P
Silt
Bones
④
> 51,000 B.P
Fine Sand
Disconformity A
Old Crow Tephra
Ice Wedge Cast
Organic Silt
Sand, Silt
③
Scattered Bones
Anodonta Phase
(10-12,000 B.P)
Silt, Sand
Sand, Large Wood, Peat
> 54,000 B.P
Bones
Bones
OLD CROW RIVER
Reworked Glaciolacustrine Clay
②
Bones
Bones
Sand Bar
Primary Glaciolacustrine Clay
①

Figure 2-4

Old Crow Basin composite section

From Morlan (1980)

observed at location 94 (≃ 40 km up the Old Crow River from site HH68-10) and is believed to be correlated with part of the underlying unit 2. Using fission track methods Westgate (personal communication) has dated it at an age of between 1.2 and 1.4 million years.

## C. Paleomagnetic studies in Beringia

There are two main reasons for conducting paleomagnetic investigations in Beringia:

1) To elucidate the history of the geomagnetic field. To the present day very little paleomagnetic data has been collected this far North and thus any additional data can be expected to constrain geomagnetic field models, particularly those concerned with the secular variation.

2) To help date the strata. Because Beringia is such an important area, geologically and archaeologically, it is critical that the ages of the strata are known as accurately as possible. The most reliable technique for obtaining absolute dates of recent strata involves the decay of $C^{14}$ in organic matter. Since the half life of $C^{14}$ is 5730 years this method can rarely be used in sediments older than 40,000 years. In its place scientists have resorted to other methods, such as fission-track dating and thermoluminescence. It is hoped that by retrieving the changes in the geomagnetic field from sediments in which they are recorded,

paleomagnetic studies may provide another dating tool.

Two earlier paleomagnetic studies have been conducted on Pleistocene sediments in the Old Crow area. Pearce et al(1982) collected samples from a 50 metre thick section at a site on the Porcupine river just southwest of the village of Old Crow (67°28' North, 137°54' West), known as HH-228. They found that the sediments possess a stable natural remanence although some samples had apparently been disturbed by cryoturbation. Within the section was a zone of reversed polarity. They concluded that it was a true reversed interval because of its long duration and was likely due to the Matuyama reversed epoch and thus greater than 690,000 years old.

Westgate et al(1985) collected paleomagnetic samples from Pleistocene sediments in the Fairbanks area as well as near Old Crow. They were also able to retrieve a stable paleomagnetic signal. At the Old Crow site (67°28' North, 139°54' West) they located a full reversal in the sediment 4 metres beneath the Old Crow Tephra. At Halfway House (64°55' North, 148°30' West) roughly 50 centimeters beneath the same tephra they located a geomagnetic excursion during which the field becomes distinctly more shallow but does not reverse. Westgate and Wintle (1986) concluded these two features were likely both from the same geomagnetic phenomenon. Because of the proximity to the Old Crow Tephra they concluded that the features were from within the Brunhes Epoch and likely due to the Blake Event.

A third study by Marino(1977) also located an excursion just beneath the Old Crow Tephra in a core taken from Imuruk Lake (65°36' North, 163°12' West) on the Seward Peninsula. He concluded this feature was likely due to the Blake Event.

With these encouraging results in mind the present study was carried out on sediments that include the Old Crow Tephra. A total of four sections, each roughly six metres thick, were sampled. Two (A and B) were taken at site HH68-10 and separated laterally by 20 metres. Two (C and D) from site 15 were separated by 30 metres. The Old Crow Tephra was present in sections A, B and C and sampling began 0.5 m above and ended 5.5 m below it. In section D the tephra was not present and sampling began at Disconformity A (which generally lies about 80 cm above the tephra). Section D was located in an area with no tephra to test if correlations could be made solely on the basis of paleomagnetic data. The Old Crow Tephra is not ubiquitous in Beringia and if this exercise is successful it may prove to be useful for future stratigraphic work.

## D. Field Procedure

Prior to sample collection, trenches were dug to provide a fresh vertical face from which samples could be removed, and also to get beyond any recent slump material to the original in situ strata (fig. 2-5). Samples were collected by tapping small plastic boxes (2 cm on a side), into the prepared exposure, two samples being taken at each

Figure 2-5

Photograph illustrating a typical prepared exposure.

From section B, yellow stake is 404 cm beneath the Old Crow Tephra.

horizon (fig. 2-6). The orientations of the cubical boxes were obtained using a Brunton compass to determine strike, and a specially designed inclinometer to measure dip and roll (fig. 2-7, Appendix B). The procedure is described in detail by Oberg(1978). Each angle was measured with an accuracy of 0.5 degrees. A total of 26 solar bearings accurately determined the local magnetic declination to be 33°30' east, with a standard error of 5'.

All samples, with the exception of those in section D, were located vertically with respect to the Old Crow Tephra. In section D all elevations were measured from Disconformity A. The vertical separation between sampled horizons averaged 6 cm. The number of samples collected in sections A,B,C and D were 196,158,194 and 174 respectively, giving a total of 722. After removal from the outcrop a snugly fitting cap was placed on each cube to prevent the loss of moisture. Upon returning to Edmonton all samples were stored in a magnetically shielded room in which the ambient field is less than 50 nT (Reid,1972).

**Figure 2-6**

Photograph illustrating strata and typical sample pairs prior to retrieval.

From section D, 231 to 266 cm beneath Old Crow Tephra, samples D053 to D066.

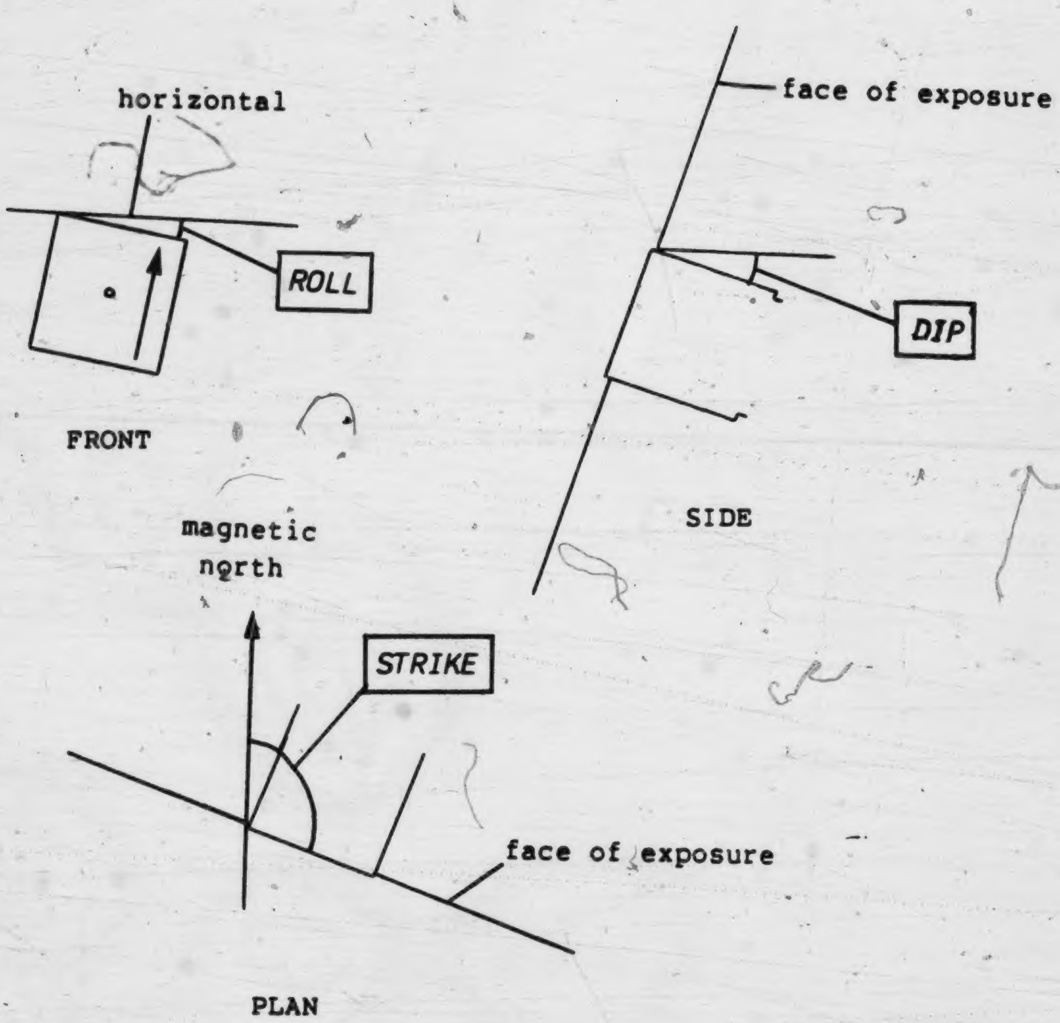
horizontal
ROLL
FRONT
face of exposure
DIP
SIDE
magnetic north
STRIKE
face of exposure
PLAN

**Figure 2-7**

Drawing of a typical sampling cube in 3 positions illustrating the angles (strike, dip and roll) used in its orientation.

## 3. LABORATORY MEASUREMENTS

In this chapter, sections A to C contain details regarding the laboratory work which principally involves the partial demagnetization of the samples. In addition, the effects of prolonged storage of the samples prior to measurement (section D) and cryoturbation of the sediments (section E) are discussed. Sections F to H are concerned with the steps taken to arrive at a final data set and the assessment of its quality.

### A. The Equipment

The remanences of all 722 samples were measured using a Digico balanced fluxgate spinner magnetometer. The intensities of the samples ranged from $1.0\mathrm{x}10^{-3}$ to $3.0\mathrm{x}10^{-2}$ $\mathrm{Am}^{-1}$ , well above the instrumental noise level quoted by the manufacturer (Molyneux,1971). The integration time required for each sample is determined by, and inversely proportional to, its intensity of magnetization. Since each of the 3 orthogonal components of the remanence vector is measured 4 times, the Digico is programmed to compute the internal variance. The RMS deviation of any orthogonal component, R, is

$$\mathrm{Dev}(R) = \frac{1}{4}\sqrt{\Sigma(\bar{R}-R)^2}$$

The internal variance can be conveniently expressed as an angle $\phi$, where

$$\phi=\sin^{-1}\left(\frac{\sqrt{(Dev(X)^2+Dev(Y)^2+Dev(Z)^2)}}{I}\right)$$

X,Y,and Z being the three orthogonal components and

$I = \sqrt{(X^2+Y^2+Z^2)}$

This angle gives the maximum radius of the cone within which the true vector lies; it is simply used to compare samples relative to one another. Any measurement for which $\phi$ exceeded 5° was repeated at a longer integration time. The most commonly used spin time was 18 seconds (128 revolutions), but this ranged from 9 to 73 seconds (64 to 512 revolutions respectively).

Because each sample may have acquired a viscous remanent magnetization subsequent to deposition and possibly during sampling and transportation, partial demagnetization was necessary. An alternating field (AF) demagnetization apparatus following the original design by McElhinny(1966) was used (Murthy,1969). Equipment and procedures of this kind are now standard in paleomagnetic research.

### B. Partial Demagnetization of Pilot samples

To determine appropriate demagnetization levels 20 pilot samples (10 each from sections A and C) were taken in steps to peak AF levels of up to 100 mT. The average median destructive field (MDF) of these samples was 19 ± 1 mT (fig. 3-1). This rapid intensity drop is not conclusive, but indicates that the magnetic carrier is magnetite or a titanomagnetite. The other common carrier of magnetization

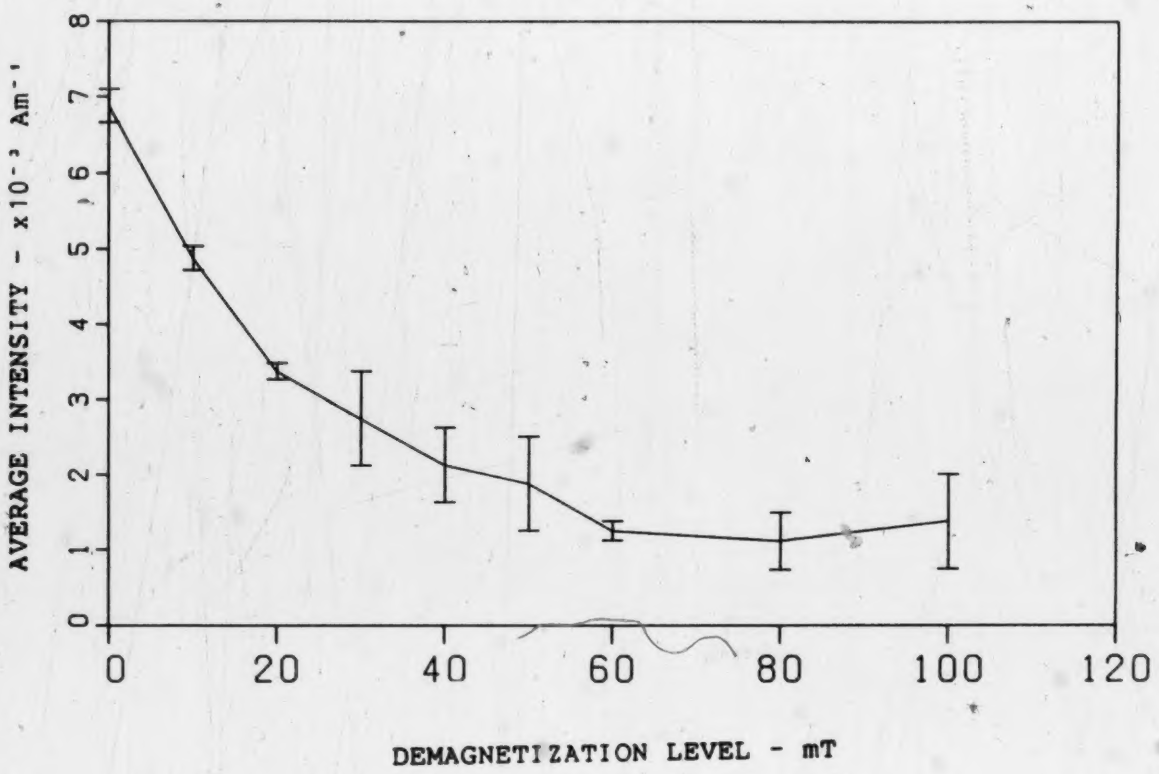

**Figure 3-1**

A.F. demagnetization of the pilot samples.

(0, 10 and 20 mT include the data from the blanket demagnetization)

Standard errors are included.

in sedimentary environments is hematite which has a much higher coercive force so that its intensity drops much more slowly.

Apart from one very weakly magnetized sample which moved to a negatively inclined magnetization above 40mT, the pilot samples in general displayed little movement. Of the 20 samples, 16 moved an average of only 4.3°±0.5° and 3.5°±0.6° in the 0 to 10 mT and 10 to 20 mT intervals respectively, before becoming unstable at higher fields. The remaining samples (C089, C090 and A071) located about 2m beneath the Old Crow Tephra all showed systematic movement toward a shallow inclination and a declination of 200 to 240° (fig. 3-2). Such movement towards shallow inclinations is suggestive of a negatively inclined original magnetization but this evidence, in itself, is far from compelling. This point is discussed further in Chapter 4.

### C. Partial Demagnetization of the remaining samples

Figures 3-3 to 3-6 are magnetograms of the results from the four stratigraphic sections before any AF treatment (0 mT). Partial demagnetization of these samples at 10 and 20 mT was carried out based on the MDF and the general lack of movement of the pilot samples. In the majority of paleomagnetic studies a single (blanket) AF cleaning treatment is chosen (following the guidance offered by the detailed pilot studies) but in this case it was decided to choose 2 levels in order to provide a check on individual

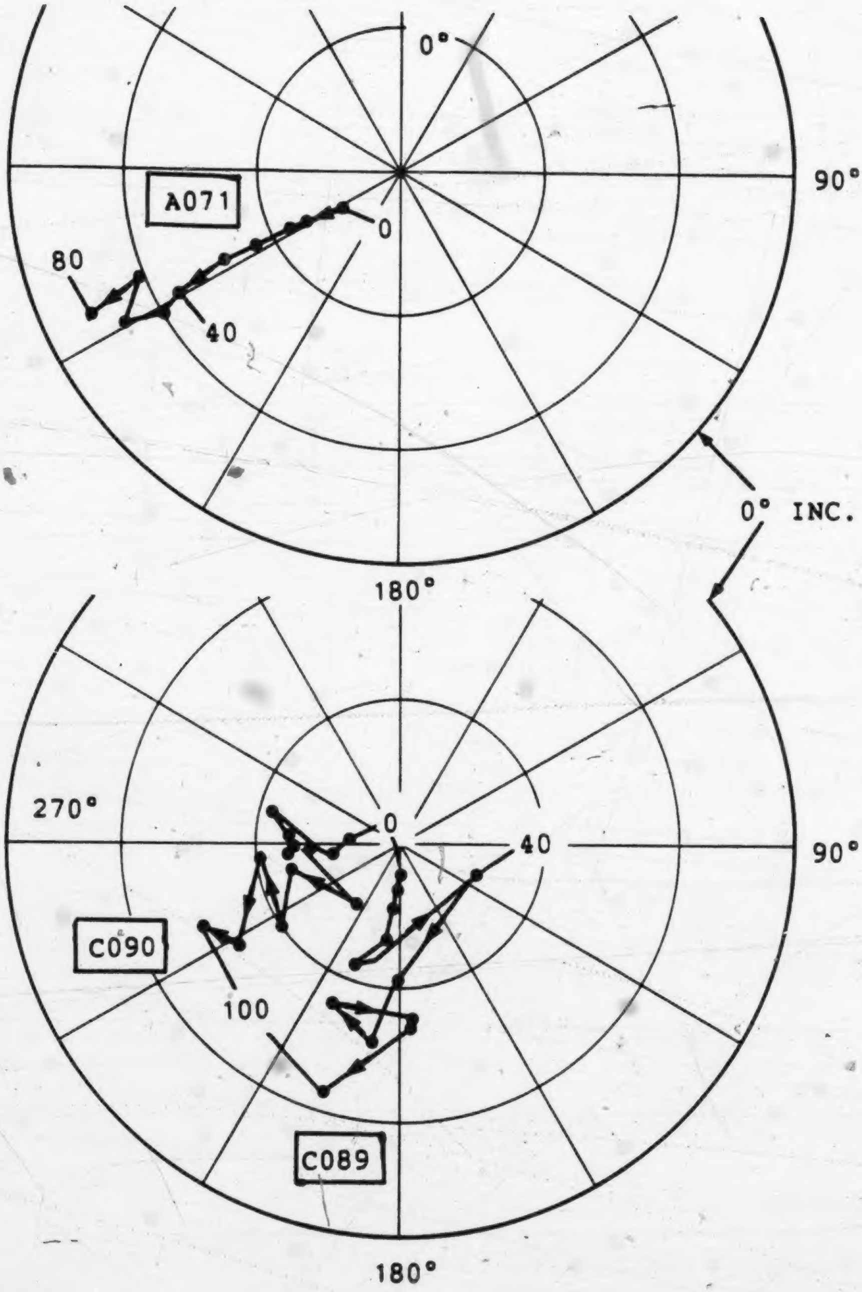

**Figure 3-2**

Plots showing the dependence of direction of remanence on A.F. demagnetizing field for 3 samples (A071, C089 and C090).

(A.F. levels are given in mT)
(equal area projection)

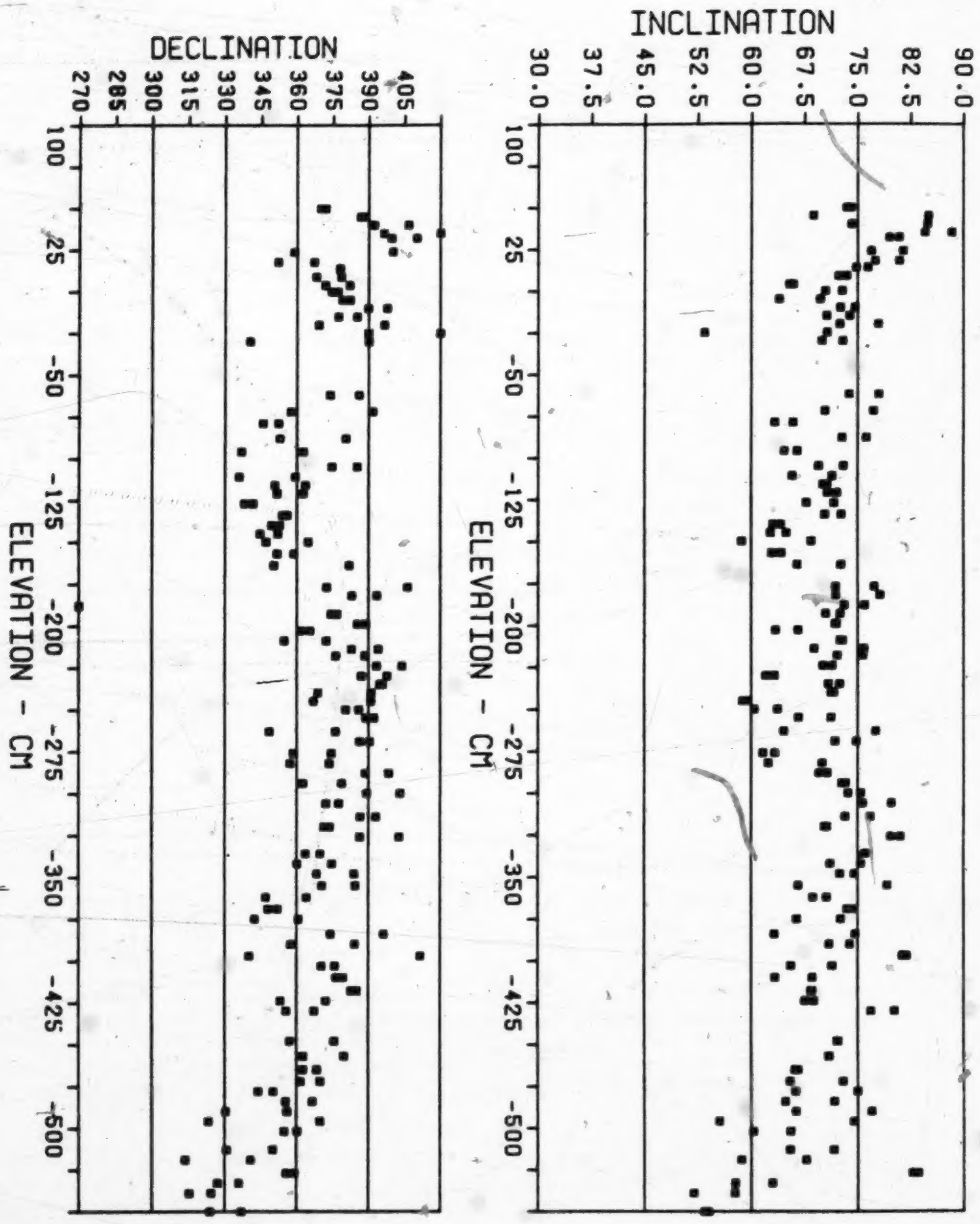

Figure 3-3

Section A, 0mT

In sections A,B,C,1 and 2, depths are relative to the Old Crow tephra. In section D depths are relative to disconformity A.
Declinations less than (greater than) 360° are west (east), of true north.
Positive inclinations are below the horizontal.

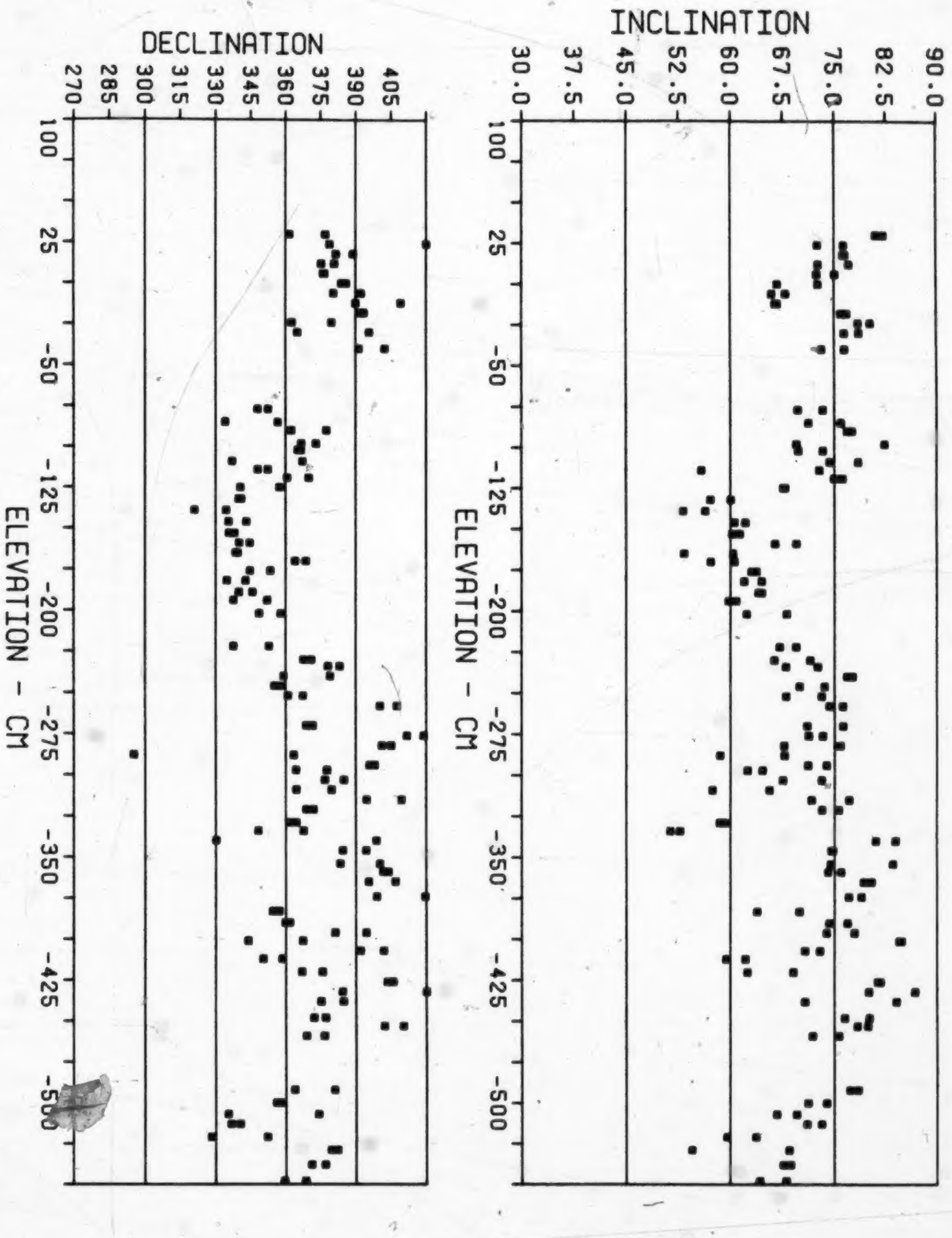

Figure 3-4

Section B, 0mT

(refer to figure 3-3 for further details)

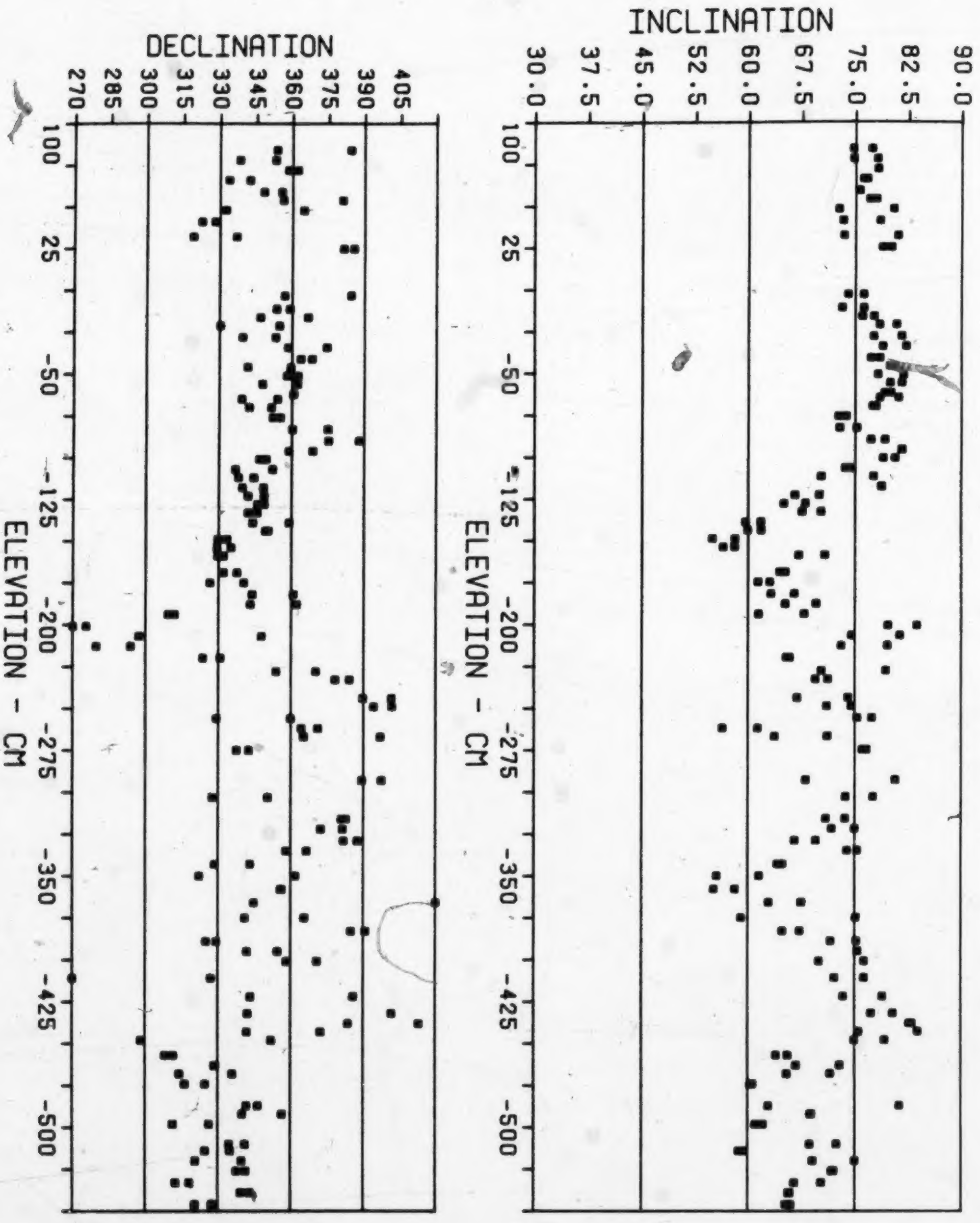

**Figure 3-5**

Section C, 0mT

(refer to figure 3-3 for further details)

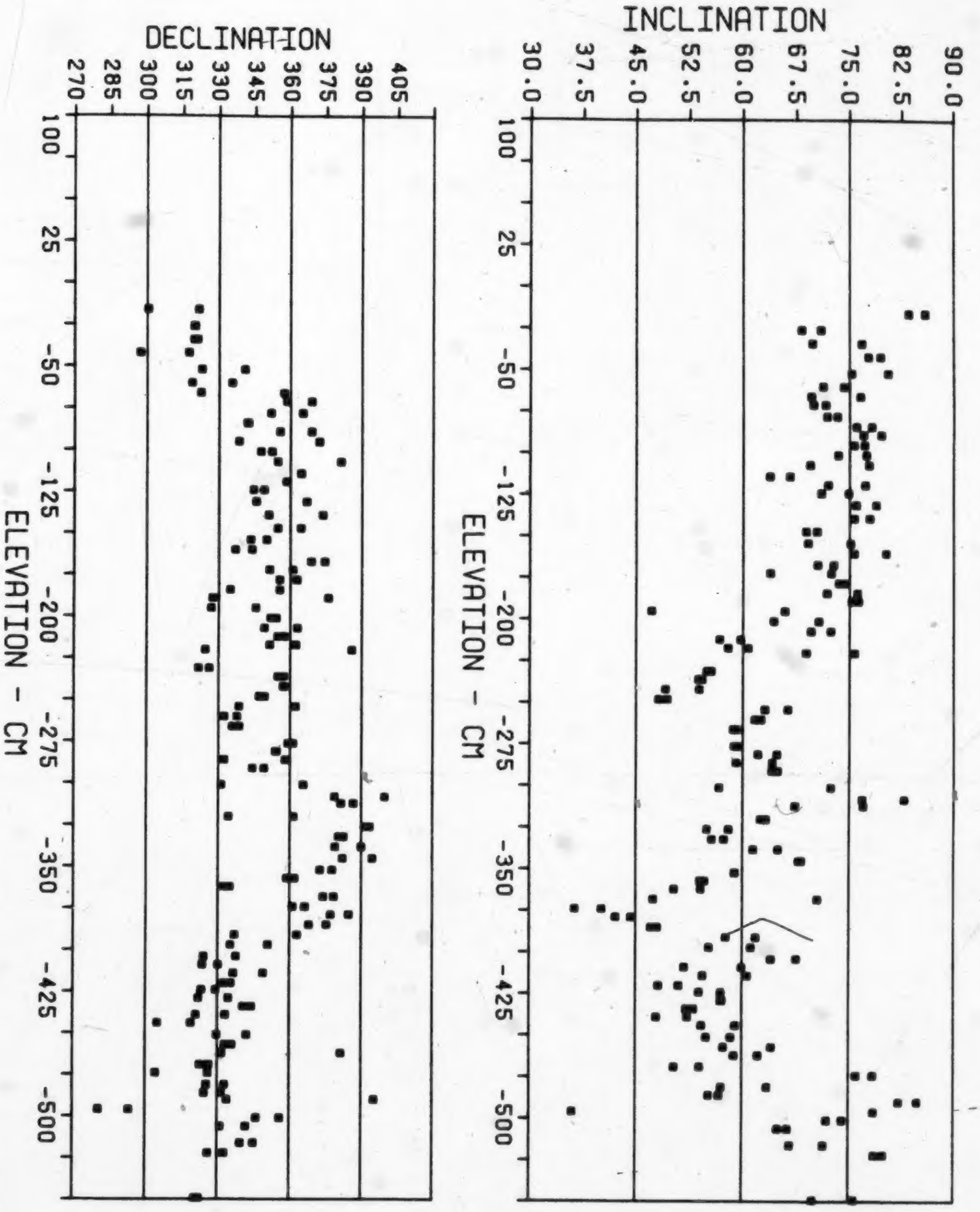

**Figure 3-6**

Section D, 0mT

(refer to figure 3-3 for further details)

sample stability. An archive of all the data can be found in appendix D.

Between 0 and 10 mT, the mean direction of remanence of all samples moved from $\overline{D}$ = 356.4°,$\overline{I}$ = +71.5° (α95 = 1.1°) to $\overline{D}$ = 349.4°, $\overline{I}$ = +68.9° (α95=1.3°) (fig. 3-7). See section 3-H for a discussion of the α95 statistic. The average difference vector ($\overline{D}$ = 20.4°, $\overline{I}$ = +75.1°, α95 1.1°) is not coplanar with the present field direction and the 0 and 10 mT mean remanence vectors suggesting that the viscous component removed had a shallower inclination (by at least 8°) than the present field. This in turn suggests that the bulk of the VRM is likely not recent but was acquired at some time in the past. Between the 10 and 20 mT demagnetization levels the average remanence shifted to $\overline{D}$ = 348.9°, $\overline{I}$ = +68.7° with an α95 of 1.4°. This negligible shift indicates that beyond 10 mT the demagnetization is removing the original magnetization, the overprinted VRM having been totally eliminated.

## The Elimination of Inferior Data

In general the angular difference between samples collected at the same horizon results from internal variance of the magnetometer measurements, inaccuracy caused by the sampling process, and actual angular deviation between the remanences preserved within the samples. One of the purposes of AF cleaning is to reduce the angular differences by removing viscous components of magnetization. In this study

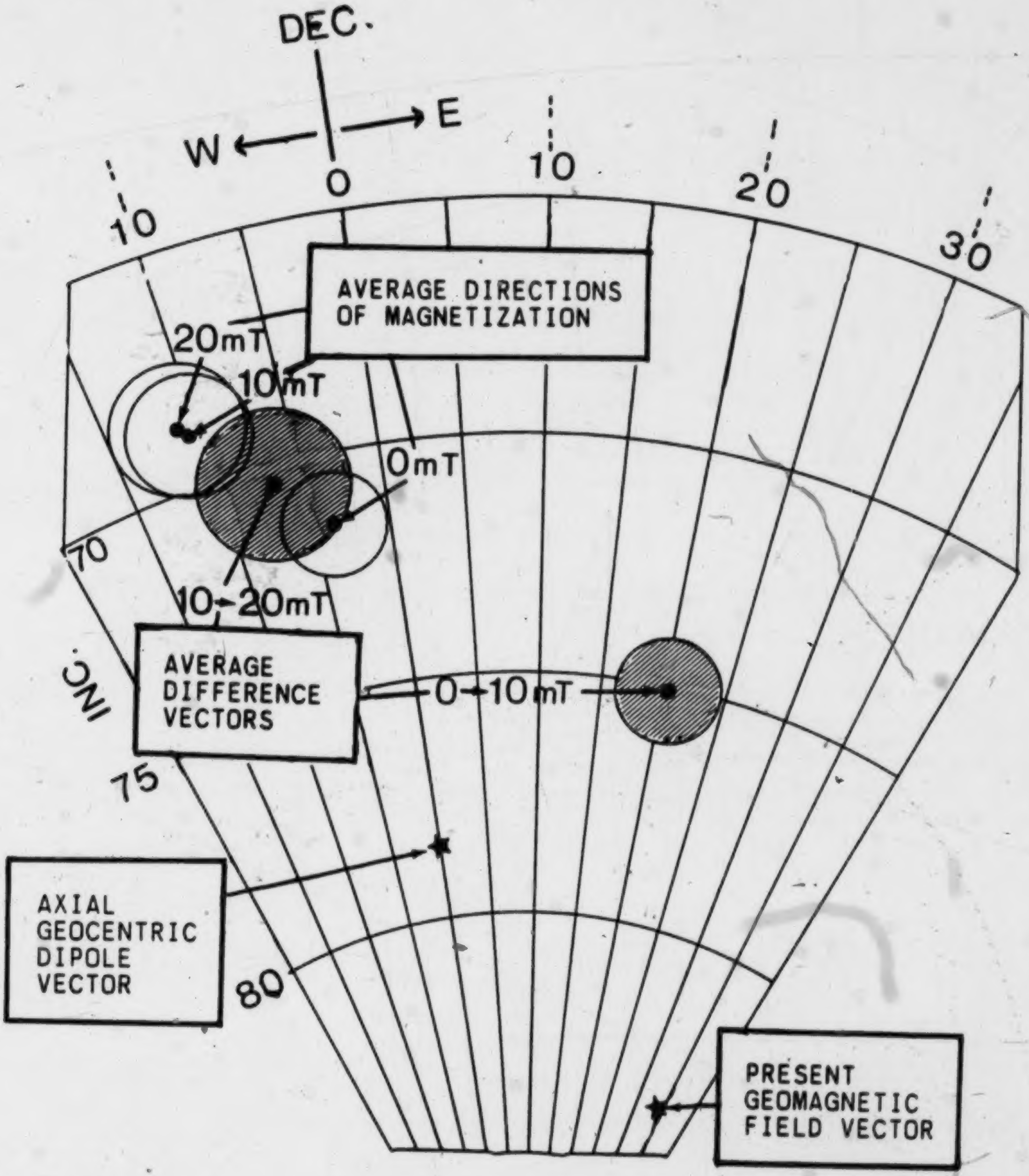

**Figure 3-7**

Plot illustrating the average directions of magnetization in all samples at 0, 10 and 20 mT, and the average remanence vectors removed between these levels.

(equal area projection)

even after AF cleaning the angular differences between samples were generally not insignificant. In fact they generally increased with increasing AF demagnetization (fig. 3-8). The median angular differences, and the 25% and 75% quartiles (in brackets), rose from 4.9°,(3.2°,7.9°) to 6.6°,(3.8°,9.9°) and then to 7.1°,(3.9°,10.7°) at 0,10, and 20 mT respectively. Ideally one would expect a decrease at low demagnetization levels as the viscous component is removed, followed by an increase as the original remanence is attacked. These results indicate that either the steps of 0-10-20 mT were too coarse or more likely that the resulting intensity drop produced a higher internal variance. Regardless of the cause of angular difference between sample pairs, those pairs that have high values inevitably contribute *noise* to the magnetograms. For the present purposes, noise can be loosely defined as erratic variation in declination and inclination between neighboring sample pairs. Two approaches have been tried in the attempt to reduce the noise.

One method employed was an attempt to remove the instrumental noise caused by the magnetometer itself. Figure 3-9 illustrates a general increase in the angular difference at low intensity levels which can be attributed to the magnetometer. This result suggests that removing all samples with intensities of magnetization below a certain level should reduce the adverse effect of the instrumental noise and as a result reduce scatter in the data. Section A

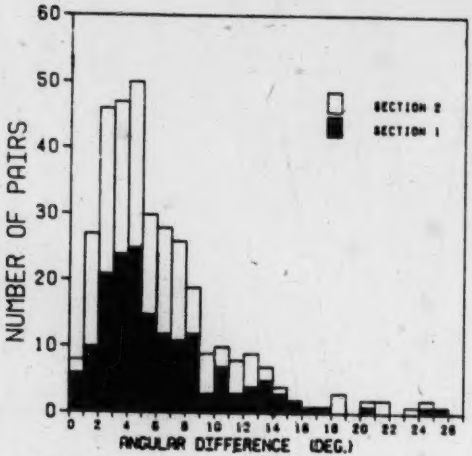

0mT

Median angular difference = 4.9°

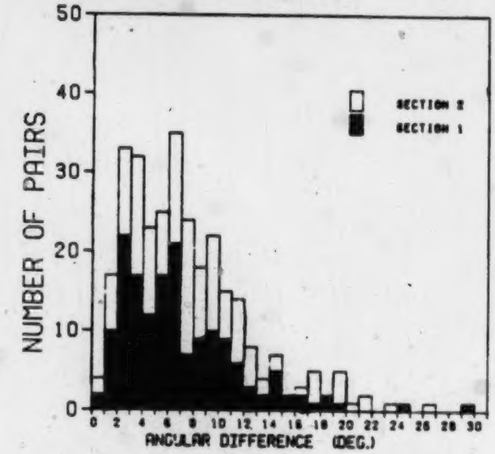

10mT

Median angular difference = 6.6°

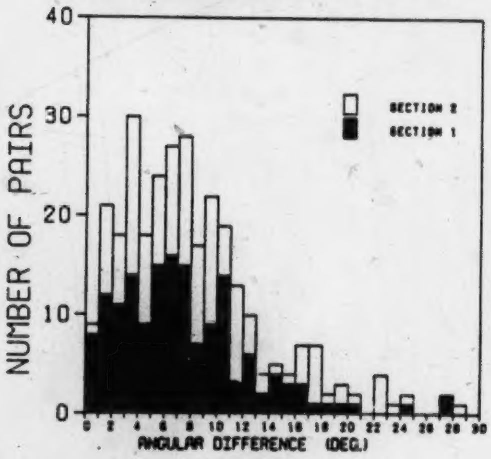

20mT

Median angular difference = 7.1°

Figure 3-8

Angular difference histograms for sections 1 (A+B) and 2 (C+D).

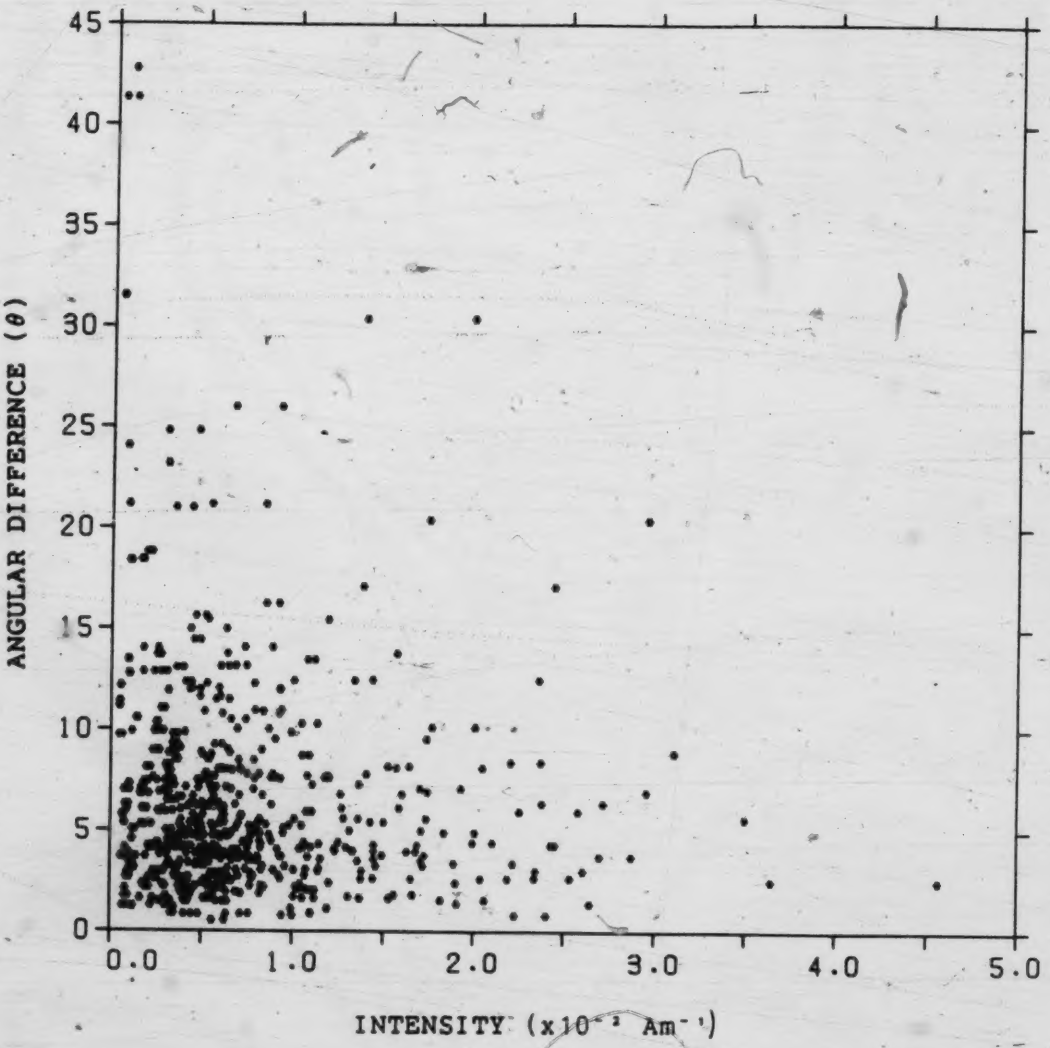

**Figure 3-9**

Plot of angular difference between sample pairs versus intensity of magnetization illustrating increase in scatter as intensity decreases.

(data from sections A,B,C and D at 0mT)

plotted after all samples with intensities less than $0.3\times10^{-2}$ $Am^{-1}$ have been removed is contained in figure 3-10. In comparing this result with the original (fig. 3-3) it is difficult to discern any improvement. In fact the median angular difference (and 25% and 75% quartiles) have actually increased slightly from 5.3°,(3.7°,8.9°) to 5.4°,(3.8°,8.9°). Although the scatter and average of angular difference are relatively high at low intensity levels, the bulk of these points still possess low angular differences (less than 10°). This is because of the policy described in section 3-A which demanded that weak samples with high internal variance be remeasured at a higher integration time. As a result this approach mainly just thinned out the magnetograms and was therefore discarded.

A second method, one that attacks the problem of noise more directly, is simply to remove all sample pairs with angular differences above a certain level. Although this penalizes both samples at a given horizon, when only one may have been at fault, it will certainly lead to a reduction of the noise level in the magnetograms. Figures 3-8 and 3-9 illustrate that removing all sample pairs with angular differences greater than 10° leaves the bulk of the data (2[illegible] out of 343 pairs at 0 mT for example) while removing most or all of the poor samples. In figures 3-11 to 3-14 are contained the 0 mT data for sections A to D after this exercise. Comparison of these figures with figures 3-3 to 3-6 reveals a distinct reduction in the noise level.

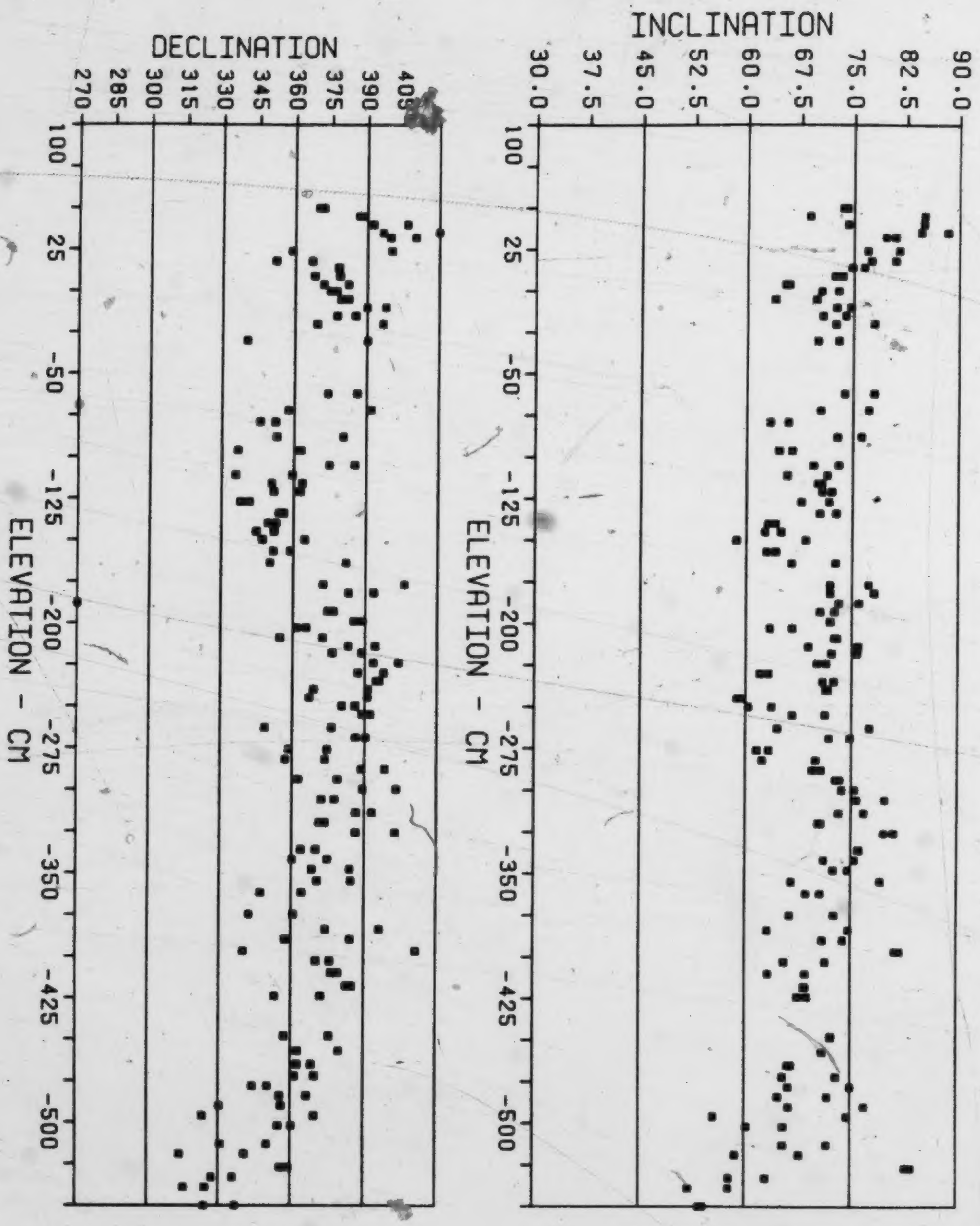

**Figure 3-10**

Section A, 0mT, Intensity cutoff = $0.3\times10^{-3}$ Am$^{-1}$

The intensity cutoff refers to the intensity below which no sample, or its pair, are plotted.
(refer to figure 3-3 for further details)

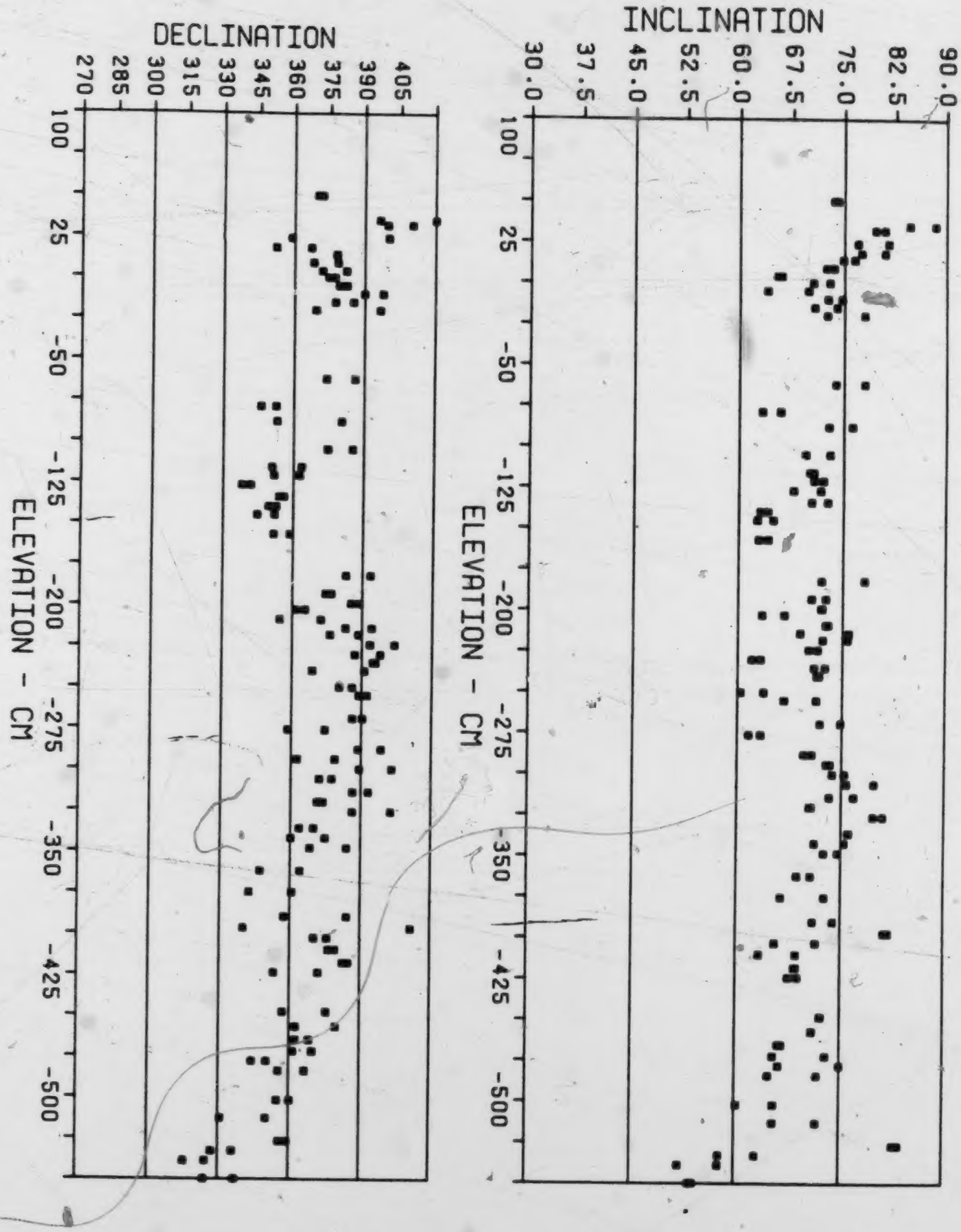

**Figure 3-11**

Section A, 0mT, $\theta=10°$

The angle $\theta$ in this and all following figures is the angular difference between two samples at the same horizon beyond which they are not plotted (refer to figure 3-3 for further details).

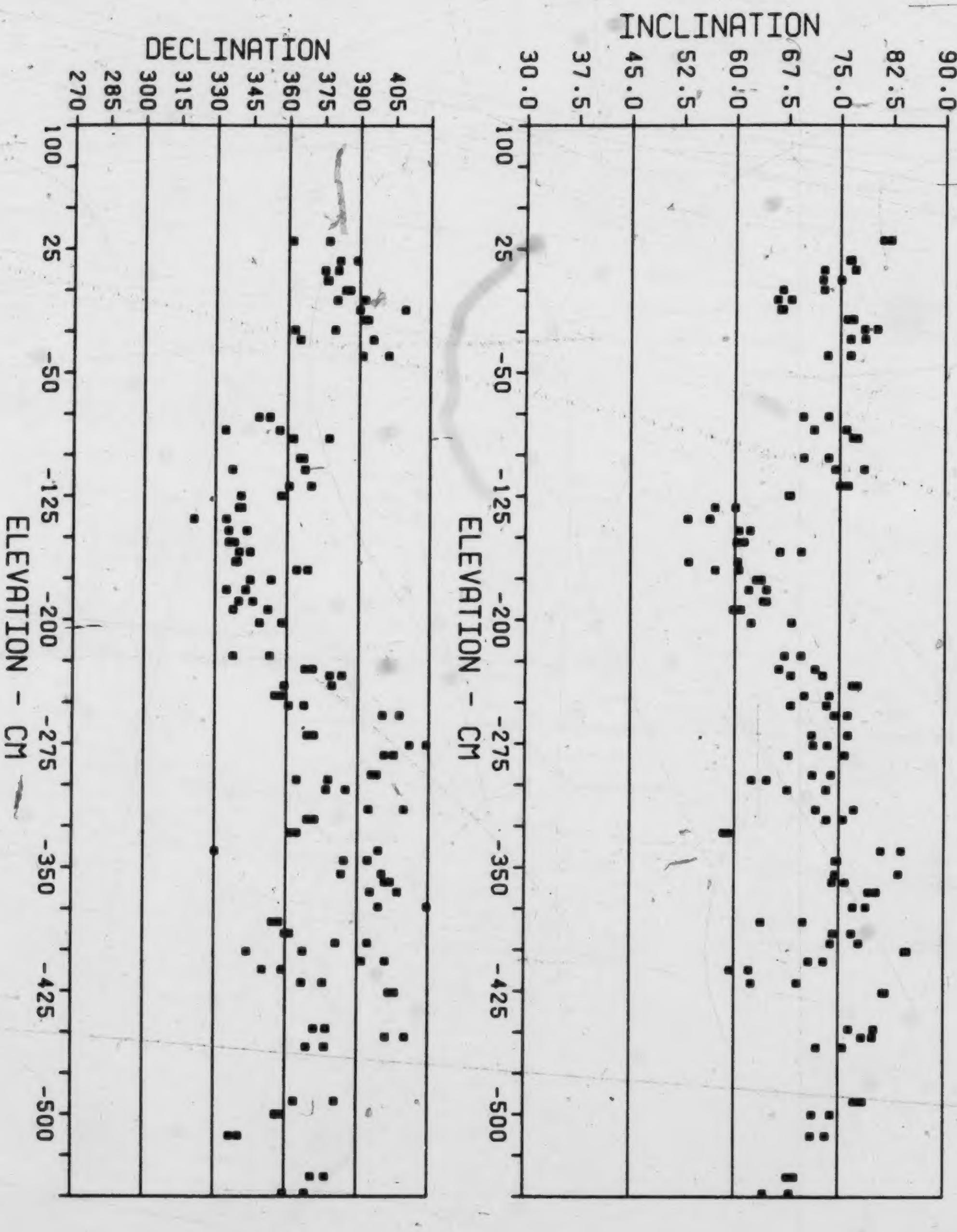

Figure 3-12

Section B, 0mT, $\theta=10°$

(refer to figures 3-3 and 3-11 for further details)

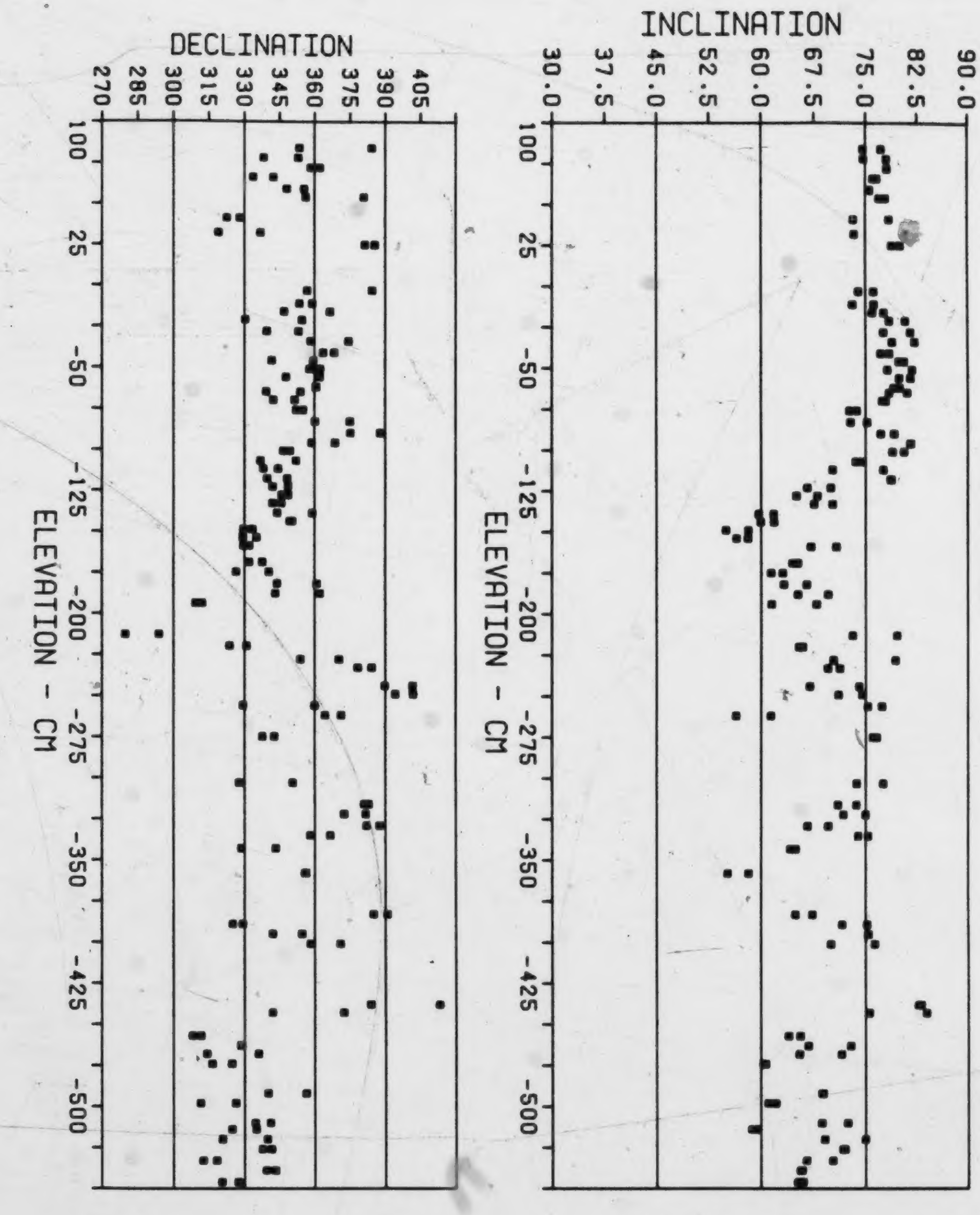

Figure 3-13

Section C, 0mT, θ=10°

(refer to figures 3-3 and 3-11 for further details)

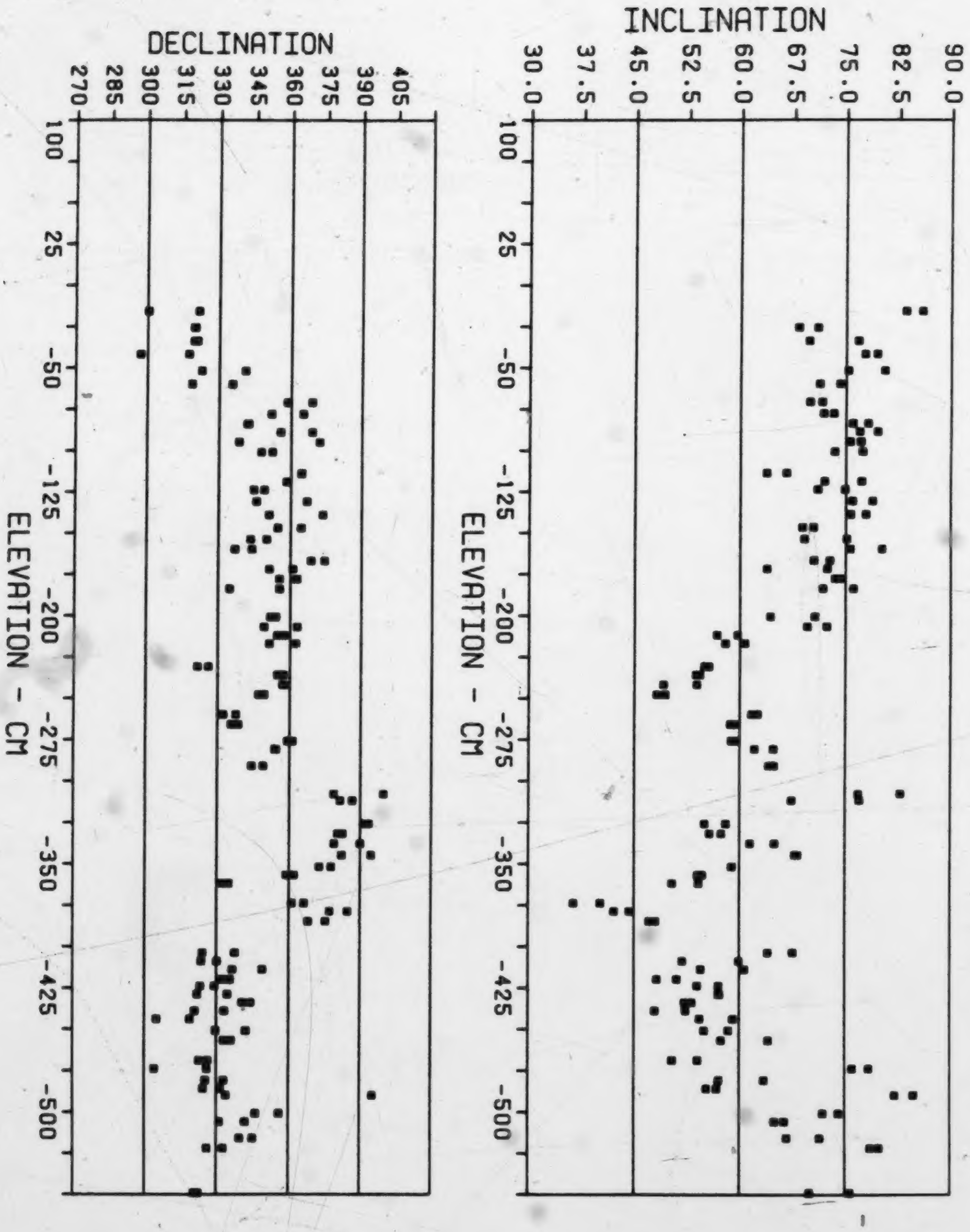

Figure 3-14

Section D, 0mT, $\theta=10°$

(refer to figures 3-3 and 3-11 for further details)

## Selection of Optimum Demagnetization Level

Considering only the angular movement results, it seems clear that since the 0 to 10 mT demagnetization has removed an overprinted viscous, and therefore undesired, component of magnetization, the 10 mT data is superior. Even though only a small component has been removed, this treatment should reveal more accurately the secular variation originally preserved in the sediments. Unfortunately the angular differences are generally increased by the same treatment and will therefore counteract this improvement. Sections C and D, which had the weakest NRM, showed the largest increase in average angular difference. Keeping both these factors in mind it was decided that the NRM data in sections C and D would be used in the final data set. The 10 mT results from sections A and B were chosen because the corresponding samples showed a much less pronounced increase in angular difference.

In the end, after the demagnetization program had been carried out, comparison of the magnetograms at 0, 10 and 20 mT showed very little difference between them. So although the partial demagnetization was a necessary step to test the magnetic stability of the samples it does not greatly influence the final geophysical interpretation.

### D. Temporal Decay of Natural Remanence

Further evidence of a recent viscous component of magnetization came from a study of the decay in NRM that occurred in 2 samples over a period of 21 weeks immediately following collection. To see if the temporal decay depended on lithology relatively silty and clayey samples (A116 and B006 respectively) were chosen. The intensity of A116 fell from $5.7\text{x}10^{-3}$ to $4.7\text{x}10^{-3}$ $Am^{-1}$ (an 18% drop) in 21 weeks but as is clear from figure 3-15 the bulk of this decay occurred in the first 5 weeks. The intensity in B006 dropped from $1.3\text{x}10^{-2}$ to $1.0\text{x}10^{-2}$ $Am^{-1}$ (a 23% drop) in the same period but again it is clear that this drop occurred mainly within 5 to 6 weeks of collection.

Such rapid intensity drops followed by little or no further loss strongly indicates that either:

1) a viscous remanence was picked up in the sampling and handling of the samples.

2) loss of moisture caused by removal from the outcrop and imperfect sealing has led to a loss of intensity.

Since, of course, the intensity before collection is not known it is not possible to distinguish between these possibilities. A high original intensity would support the latter option and vice versa. Since the directions of the remanence stayed virtually constant in both samples (fig. 3-16) this temporal decay of NRM will have no effect on our results.

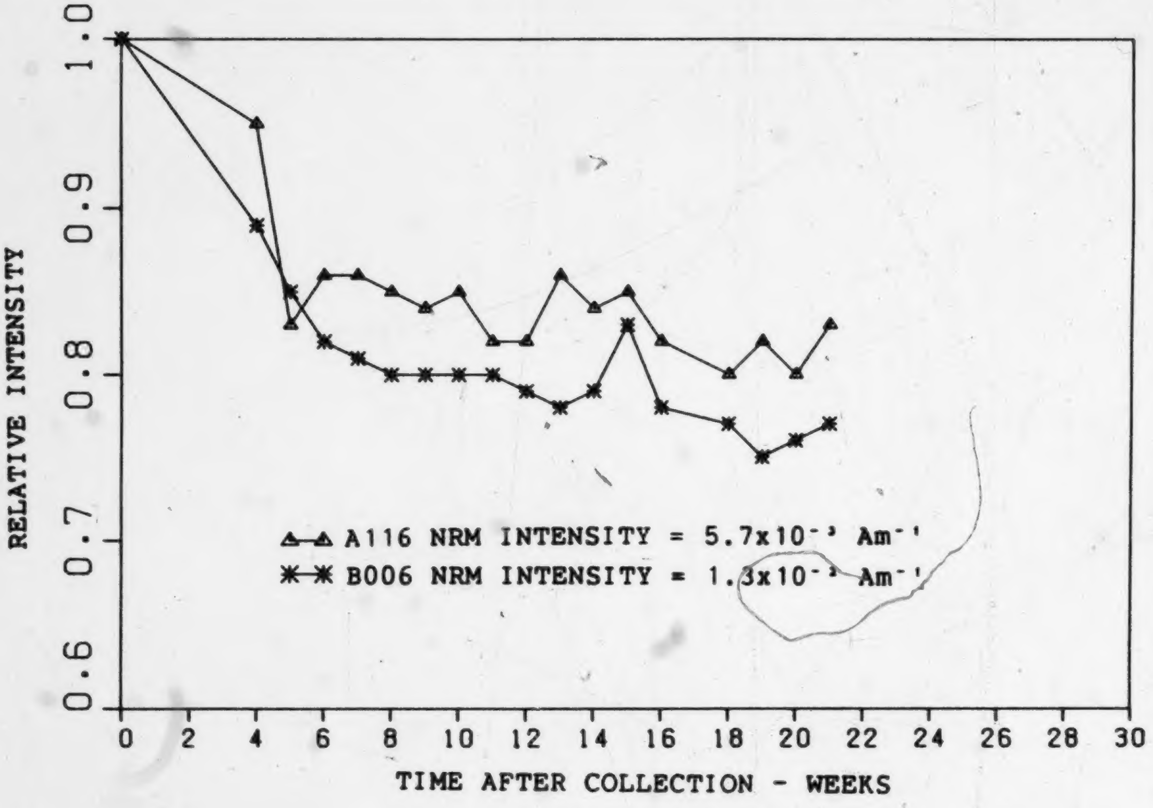

**Figure 3-15**

Decay of natural remanence with time (normalized to initial intensity).

Sample A116 was collected from a silt. Sample B006 was collected from a silty clay.

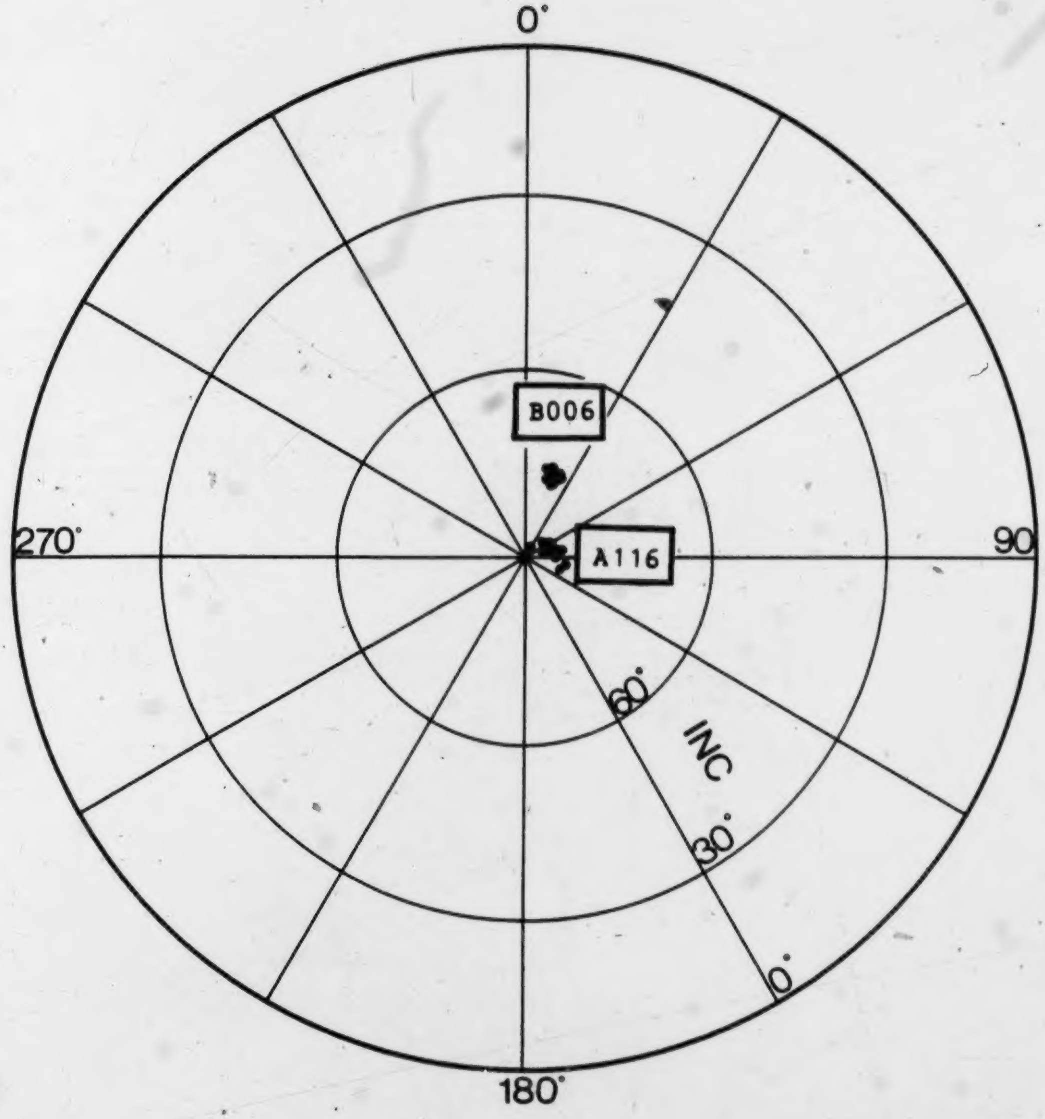

**Figure 3-16**

Plot illustrating lack of movement of magnetization vector over a period of 21 weeks in two samples.

(to avoid the overlapping of the two vector sets all A116 vectors have been shifted an arbitrary amount)
(equal area projection)

## E. Effect of Cryoturbation

Cryoturbation is a process in which subaerally or subaqueously exposed sediments are deformed by the repeated freezing and thawing of interstitially bound water. Cryoturbated strata are easily identified by the distortion of the originally horizontal bedding into convoluted patterns, for example compare the disturbed beds shown in figures 3-17 and 3-18 with those of figures 2-5 and 2-6. In all sections in this study there were intervals which had undergone cryoturbation at some time in their past. The most intense zone of distortion occurred between 1.5 and 3.5 metres beneath the Old Crow Tephra.

In an attempt to study the effect of cryoturbation on NRM this interval was sampled four times (one cryoturbated and one relatively uncryoturbated in each of sections A and C). The results from these corresponding intervals are summarized in table 3-1. Considering section A it is clear that the intensity, the inclination and the scatter ($\alpha95$) of the remanences preserved have not been affected by cryoturbation. However the declination has shifted a statistically significant amount to the West - the cryoturbated and uncryoturbated vector distributions have an F-ratio of 9.12 which fails the F-ratio test at the 95% confidence level (Watson 1956a). This is not the case in section C where the corresponding vector distributions pass the F-ratio test at the 95% confidence level, the F-ratio being 2.67.

**Figure 3-17**

Photograph illustrating intensely cryoturbated sediments. From Section A, 164 to 235 cm beneath the Old Crow Tephra.

**Figure 3-18**

Photograph illustrating an apparent thickening of strata at the location of an ice wedge cast.

From Section C, tip of knife is 100 cm beneath the Old Crow Tephra.

| Interval | N | Declination<br>$\pm\frac{\alpha 95}{\cos(\mathrm{Inc.})}$ | Inclination<br>$\pm\alpha 95$ | Intensity<br>$\mathrm{Am}^{-1}$<br>±standard error |
|---|---|---|---|---|
| **Section A**<br>**NRM**<br>-173 to -219 cm | | | | |
| **CRYOTURBATED** | 8 | 353±12° | 72±4° | 1.3±0.1 |
| **UNCRYOTURBATED** | 8 | 018±10° | 73±3° | 1.2±0.1 |
| **Section C**<br>**NRM**<br>-107 to -144 cm | | | | |
| **CRYOTURBATED** | 6 | 359±6° | 71±2° | 0.55±0.06 |
| **UNCRYOTURBATED** | 8 | 347±12° | 69±4° | 0.39±0.04 |

**Table 3-1**

Table illustrating the effect of cryoturbation on orientation, intensity and scatter of remanences preserved in sediments.

At first sight, it is quite surprising that the scatter in the data has not been increased by cryoturbation. Figures 3-17 and 3-18 illustrate the cryoturbated intervals that were sampled and show an intense degree of distortion (at the macroscopic level) caused by ice wedges. Although the sampling of only two cryoturbated zones does not allow any firm conclusions, these results suggest that while cryoturbation is occurring, and distorting the large particles, the magnetic particles are free to orientate themselves parallel to the ambient field. The melting of ice associated with cryoturbation seems to provide the interstitial water necessary to give the magnetic particles the freedom to move. The westward shift in declination that occurs because of cryoturbation in section A suggests that it has allowed a PDRM to replace pre-existing magnetization. An examination of the magnetogram for section A (fig. 3-10) shows that a declination of 353° and inclination of 72°, which the cryoturbated interval has preserved, occurs at -100 cm (roughly 75 cm above the top of the cryoturbated zone). As mentioned earlier the cryoturbation in section C has had no effect on the preserved remanence indicating that the cryoturbation either occurred very shortly after or during the time the original remanence was acquired. Very striking support for this conclusion comes from the ice wedge pseudomorph illustrated in figure 3-18. By careful inspection of this photograph one can discern a thickening of the beds at the location of the ice wedge. This indicates that formation of the ice wedge pseudomorph was actually penecontemporaneous with the deposition of the sediments (Putnam and Bassett, 1971).

Admittedly, there is some speculation involved in these conclusions, due to the lack of data, but it seems reasonable to infer that cryoturbation in sediments such as these could allow a re-orientation of the magnetic particles and the acquisition of a PDRM at some time after deposition. Irving (1957) and Tucker (1983) observed sediments that underwent slumping shortly after deposition but subsequently acquired a PDRM that eliminated the effect of the slumping on the preserved magnetization. Both cryoturbation and slumping are processes that distort sediment while it is fairly saturated with water, so it seems reasonable to suggest that their effect on the magnetic remanence carried by the sediments may be similar.

Clearly there is a need for further research in this area. With more sampling of cryoturbated strata, and work in the laboratory done to model the cryoturbation process, it should be possible to test the conclusions reached above.

### F. Combination of Sections A,B,C and D

Since all sections sampled the same interval one would expect that they could be combined to give a clearer picture of the overall temporal variation of the geomagnetic field. This should certainly be true for sections A and B (separated by 20 metres) and for C and D (separated by 30 metres). Sites 15 and HH68-10 were roughly 1 kilometer apart and thus the combination of all data into one section may or may not be feasible.

Because all samples were located with respect to the Old Crow Tephra by distance, not time, it was necessary to use the measured thicknesses of the sub-units to adjust for differing sedimentation rates. Appendix A summarizes the unit descriptions involved. The units were very similar in sections A and B, however between sections C and D a clear correlation was only possible for the first 80 cm beneath the Old Crow Tephra. Correlations between these sections are made more obvious by comparing the NRM intensities (fig. 3-19), which strongly suggest that elevations in section D should be shifted upwards by 80 cm to give a proper correlation with section C. Using these results the elevations in sections A and D were adjusted to fit sections B and C respectively. The magnetograms of the combined sections are given in figures 3-20 and 3-21. (section 1 is A + B;section2 is C + D).

By determining the vector correlation between the sections A-B and C-D before and after this adjustment it was possible to assess its effect. The vector correlation (C) is defined as

$$C = \left(\frac{1}{N}\right)\frac{\Sigma f \bullet g}{|f||g|}$$

where N= the number of samples and

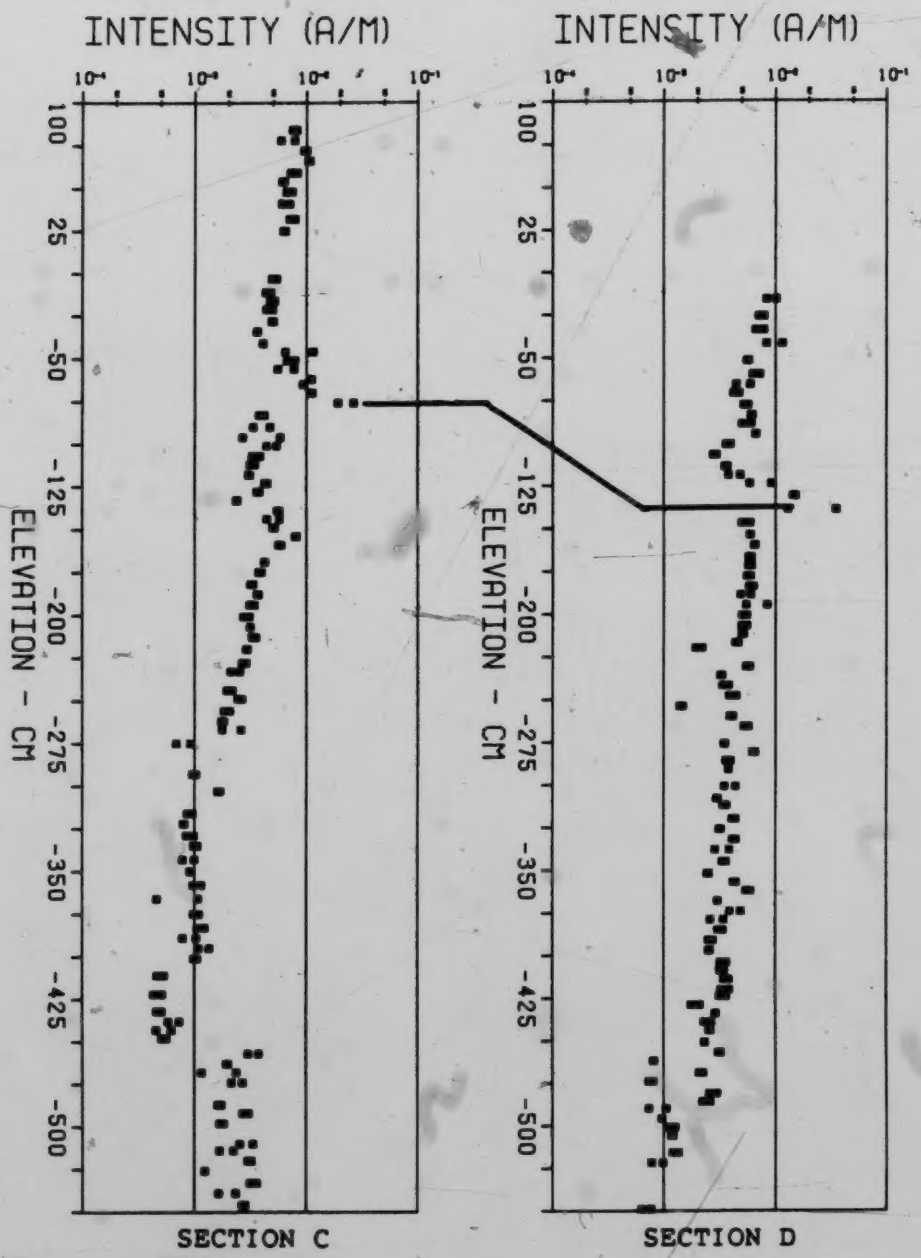

**Figure 3-19**

The intensities of the natural remanent magnetization preserved in sections C and D as a function of depth. (most likely correlation is indicated by solid line)

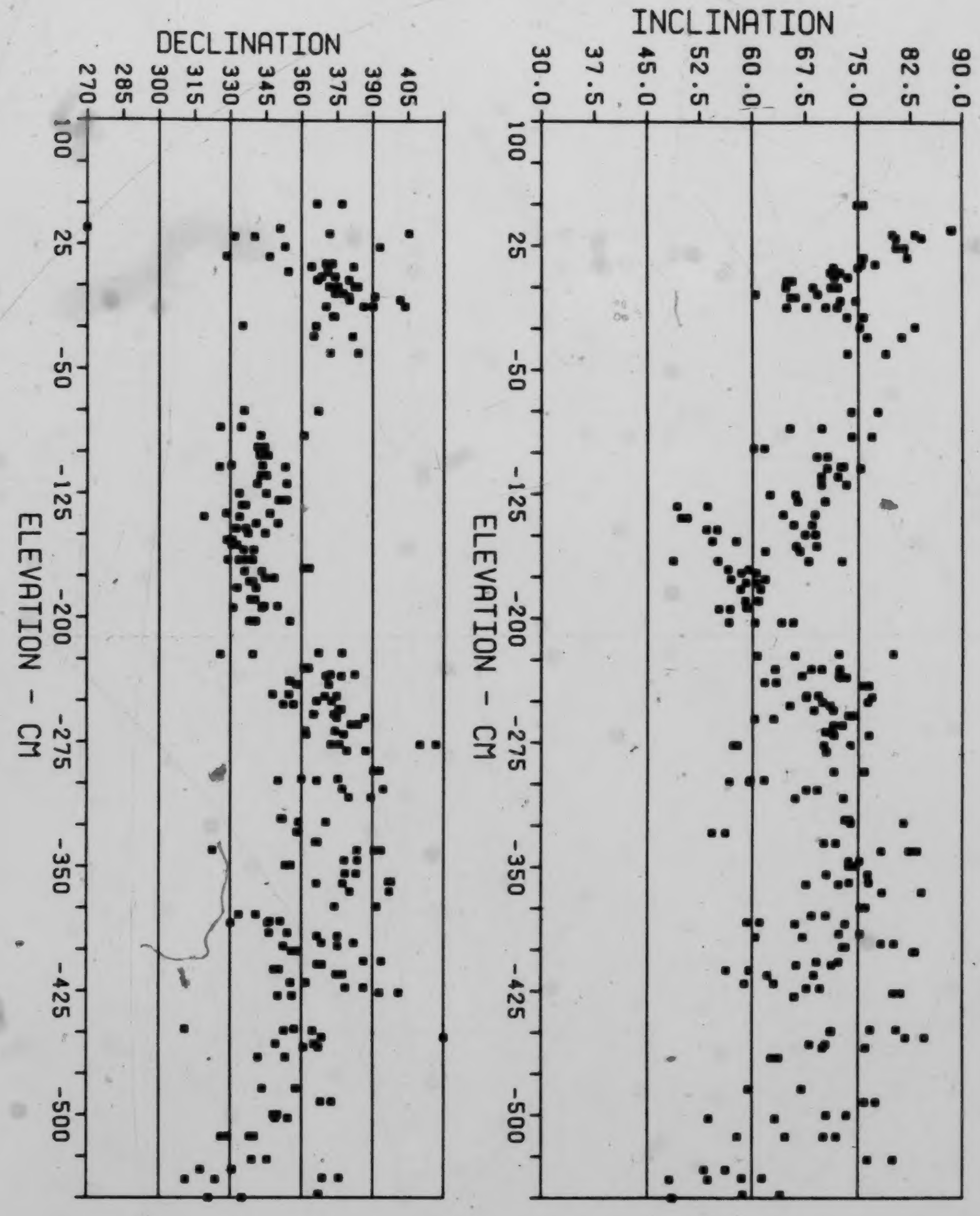

**Figure 3-20**

Section 1, 10mT, $\theta$=10°

(refer to figures 3-3 and 3-11 for further details)

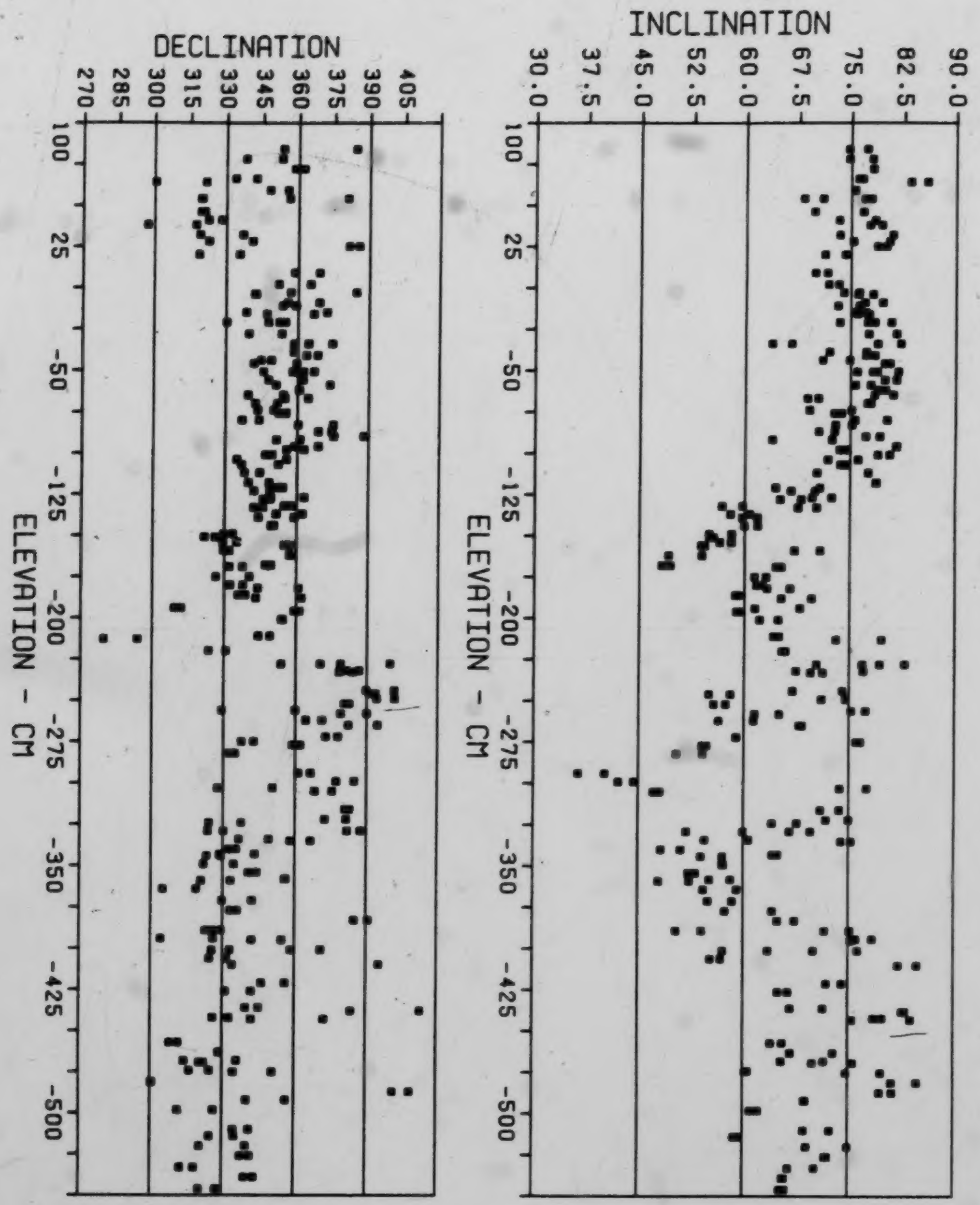

**Figure 3-21**

Section 2, 10mT, $\theta=10°$

(refer to figures 3-3 and 3-11 for further details)

f and g are the magnetization vectors at corresponding levels in the two sections being compared.

Because samples were not collected at exactly the same elevations it was necessary to linearly interpolate the data in one section to the levels sampled in the other. In both cases the correlation coefficient was increased a small amount by the elevation adjustments. In section 1 it rose from 0.969 to 0.976; in section 2 it rose from 0.956 to 0.964.

### G. Smoothing the Combined Sections

By applying a sliding window that averages the components of magnetization over more than one level it was possible to reduce the scatter in the data and replace it with error bars which define the angular range within which it is 95% probable the actual values of inclination or declination lie. This statistic was developed by Fisher (1953), and is now the standard yardstick used in all paleomagnetic research.

The size of the window was chosen such that the high frequency noise was smoothed out and the lower frequency signal was accentuated. The $\alpha95$ bars determine the lower thickness (i.e. time) limit of geomagnetic features that can be studied with any degree of confidence. The ideal section containing no sources of angular difference between sample pairs would have correspondingly small 95% confidence bars and would allow the study of extremely rapid geomagnetic phenomena. By visual inspection of figures 3-20 and 3-21 it is clear that no features less than about 20 cm thick can be resolved. For example, between +10 and -10 cm in section 1 is a feature involving low inclination and easterly declination. In order that this feature and others of similar thickness may be studied, a sliding window averaging over 5 horizons (≃16 cm on average) was chosen, but experiment showed that this choice is not critical. The smoothed sequences obtained after passing this sliding window over the data are given in figures 3-22 and 3-23.

Bauer plots (which show the combined variation of declination and inclination) are given in figures 3-24 and 3-25. The Bauer plots of sections 1 and 2 are very similar but because of the uncertainty of the correlations between sections C and D section 1 will be used as the final data set. Section 2 will serve as a back up. As a result figures 3-22 and 3-24 contain the final results from which most conclusions of this thesis will be drawn.

## H. Quality of the Data

There are a number of sources of error in a study of this type that cause a reduction in the precision of the final results. These include orientation errors, scatter introduced by the demagnetization process, measurement errors, and local magnetic anomalies.

An estimate of the precision of the remanence vectors can be obtained by grouping them and determining the spread

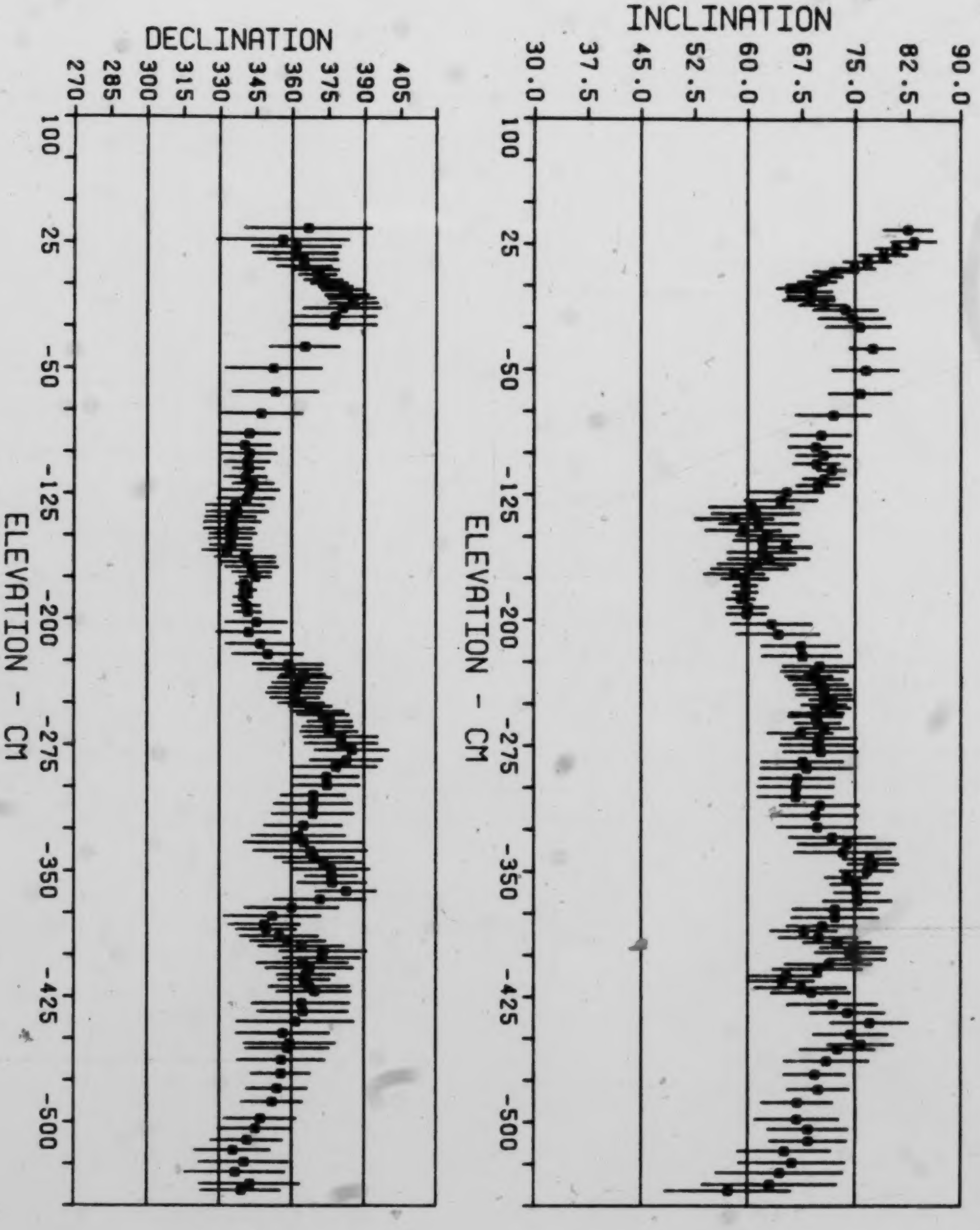

**Figure 3-22**

Section 1, 10mT, $\theta=10°$, 10 samples per group

(refer to figures 3-3 and 3-11 for further details)

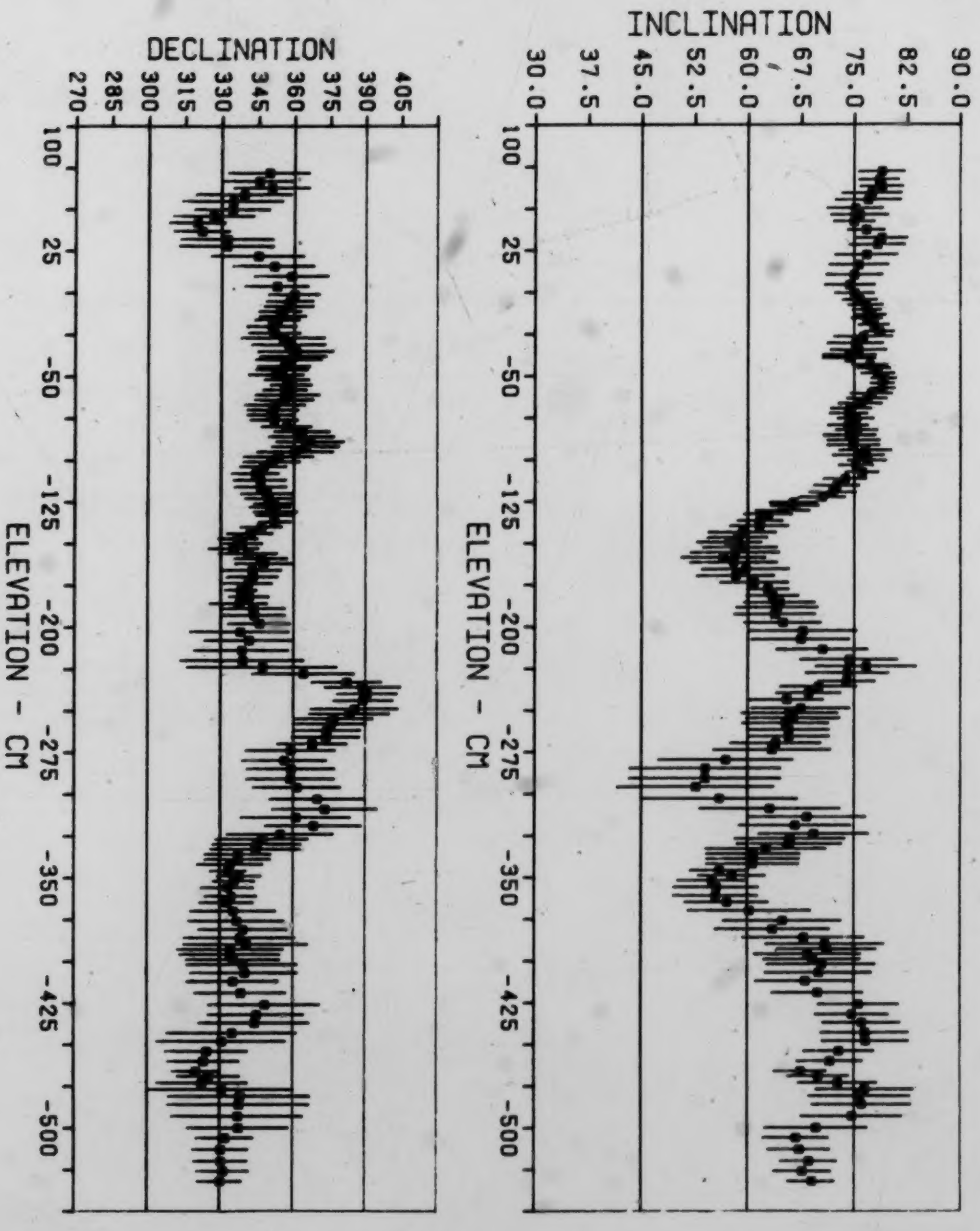

**Figure 3-23**

Section 2, 0mT, $\theta$=10°, 10 samples per group (refer to figures 3-3 and 3-11 for further details)

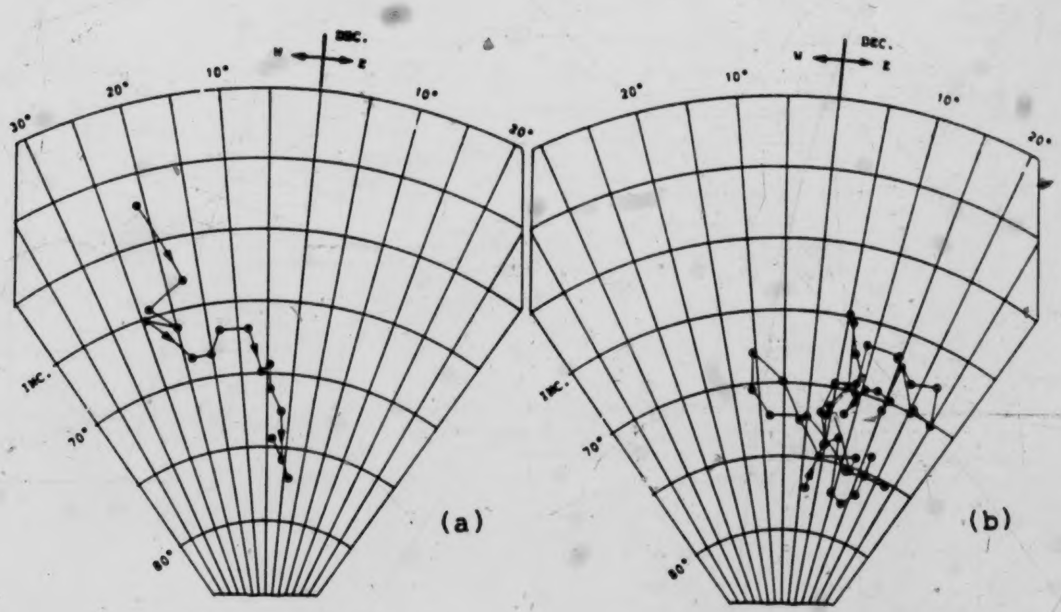

-550→ -419 cm

-419→ -241 cm

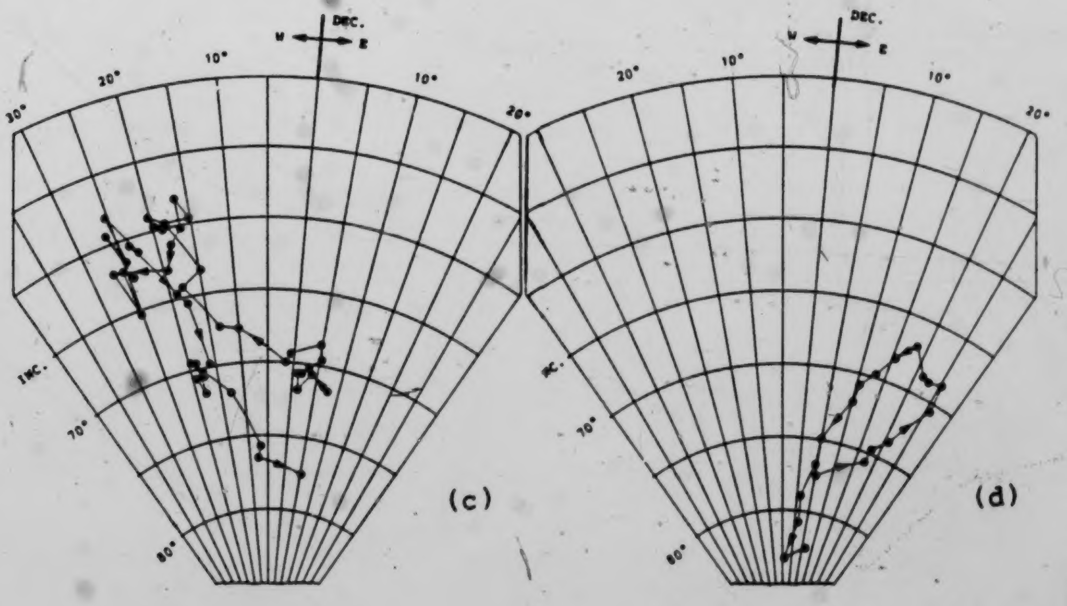

-241→ -11 cm

-11→ +50 cm

**Figure 3-24**

Bauer plots illustrating the secular variation of the geomagnetic field in section 1.

(equal area projections)
(refer to figure 3-22 for corresponding magnetogram)

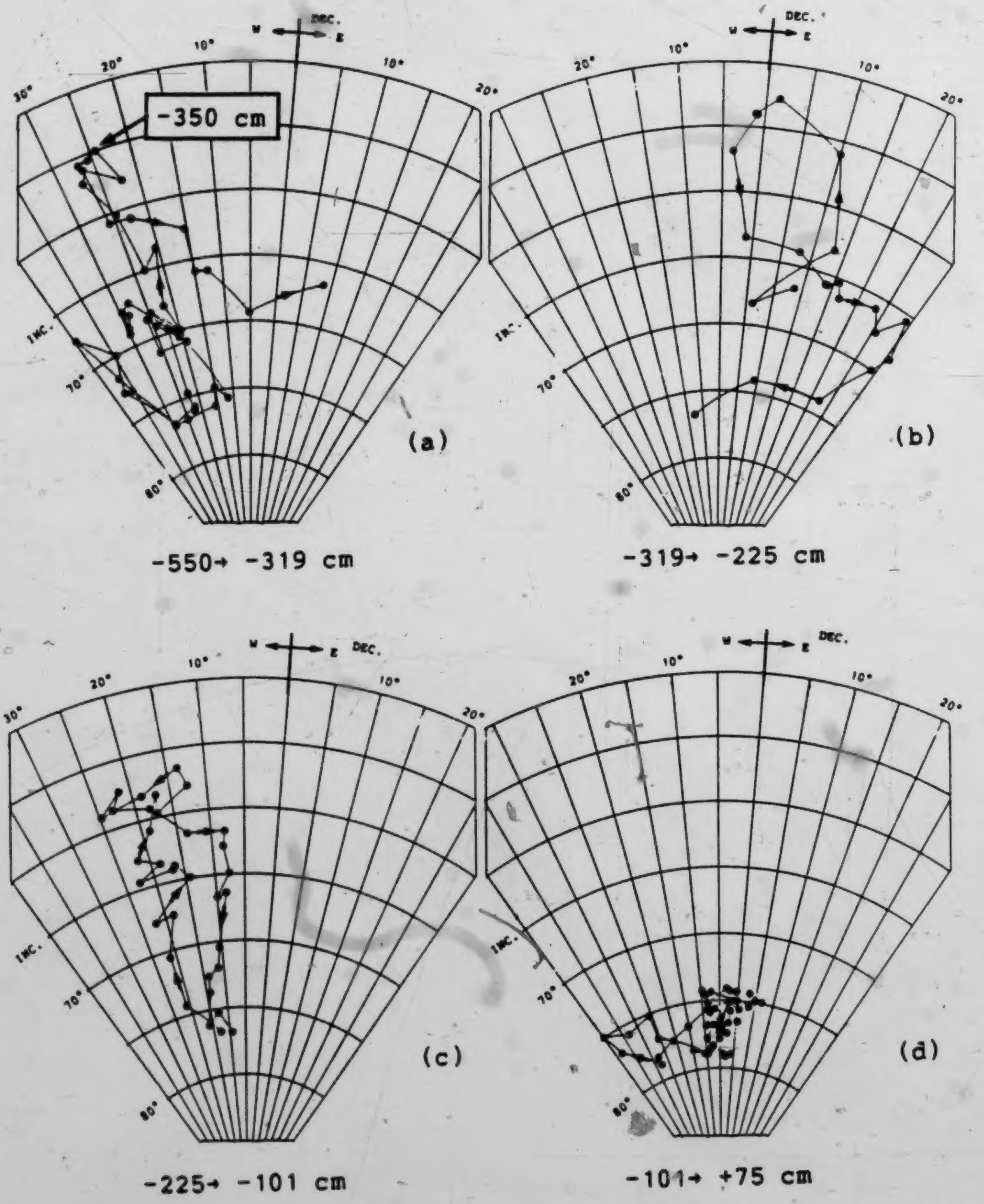

-550→ -319 cm

-319→ -225 cm

-225→ -101 cm

-101→ +75 cm

Figure 3-25

Bauer plots illustrating the secular variation of the geomagnetic field in section 2

(equal area projections) (refer to figure 3-23 for corresponding magnetogram) about the mean direction. For Fisherian distributions the two statistics that are commonly used are $\alpha95$ and the so-called precision parameter, $\kappa$. These are given by

$$\alpha95 = \cos^{-1}\{ 1 - \frac{N-R}{R}((20)^{1/(N-1)} - 1)\}$$

and by

$$\kappa = \frac{N-1}{N-R}$$

respectively, where N is the number of unit vectors involved and R is their vector sum (Fisher,1953). If $\kappa \geq 7$, these statistics can be related as follows

$$\alpha95 = \frac{140}{\sqrt{(\kappa N)}}$$

As the number of samples in the group (N) increases the mean direction is estimated more and more precisely and the $\alpha95$ decreases. The precision parameter ($\kappa$) describes the degree of scatter present in the underlying population and ranges from zero when the vectors are uniformly dispersed to infinity when they are all parallel (zero scatter).

Figure 3-26 presents histograms of $\alpha95$ for sections 1 and 2 combined. The median $\alpha95$ (and the 25% and 75% quartiles) drop from 4.6°,(3.5°,6.7°) to 3.8°,(2.9°,4.8°) as N increases from 8 to 14. The $\kappa$ histogram for N = 8 is given in figure 3-27 and has a median (and 25% and 75% quartiles) of 129,(64,235).

The quality of this data can assessed by comparing these statistics with those obtained from studies of

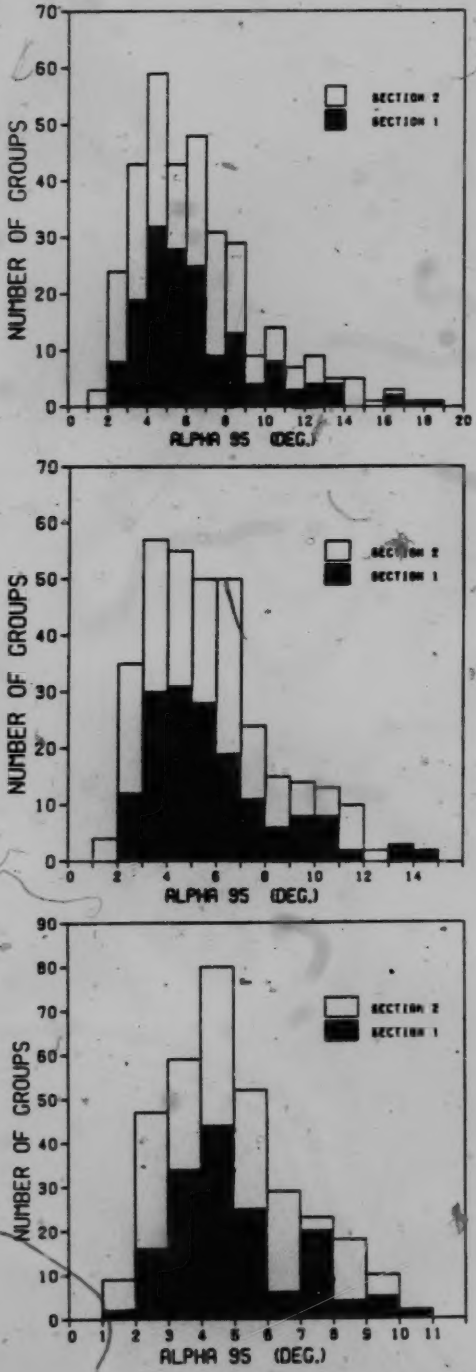

8 PER GROUP
Median $\alpha 95$ = 4.6°

10 PER GROUP
Median $\alpha 95$ = 4.2°

14 PER GROUP
Median $\alpha 95$ = 3.8°

**Figure 3-26**

Histograms illustrating the dependance of $\alpha 95$ on size of sampling window.

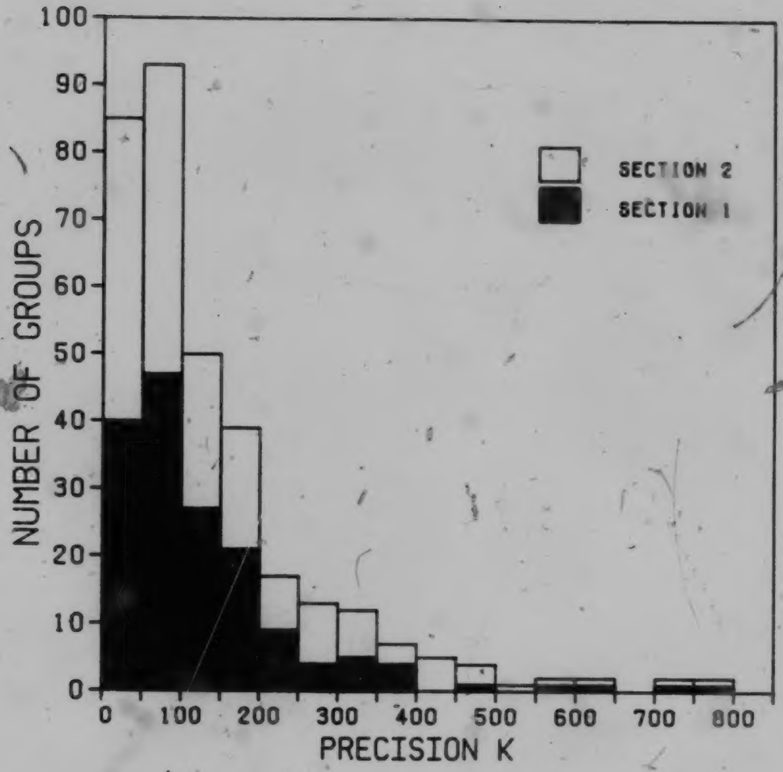

Figure 3-27

The distribution of Fisher's precision parameter k in sections 1 and 2

(8 samples per group)

Median k = 129

volcanic rocks. Since volcanics acquire their remanence very rapidly and are highly consolidated relative to the poorly consolidated sediments in the present work they can usually be studied with a high level of precision.

Four reports (Doell,1970,1972; Cox,1969; and Watkins and Nougier,1973), have been reviewed (fig. 3-28). The median $\alpha95$ (and 25% and 75% quartiles) for all four studies combined is 4.0°,(2.7°,5.9°). The corresponding $\kappa$ values are 192,(107,427). Although the precisions indicated by both statistics suggest the lava data is superior to the data from this study it must be remembered that the groups of measurements in the lava studies are separated by a few years at most. As will be discussed in more detail in the next chapter it is expected that adjacent sampled horizons in this study are separated by some 400 years. Thus when 8 samples are grouped, they come from 4 horizons and thus could span some 1200 years. Secular variation of the geomagnetic field over this time would lead to a certain degree of dispersion and thus apparently poorer precision statistics. Bearing this in mind, and the fact that the statistics from this study and the typical volcanic studies are comparable, it seems clear that the results in this study are of high precision.

Since the final data set has been established, and its precision has been shown to be of high order, it is now possible to turn to the analysis stage.

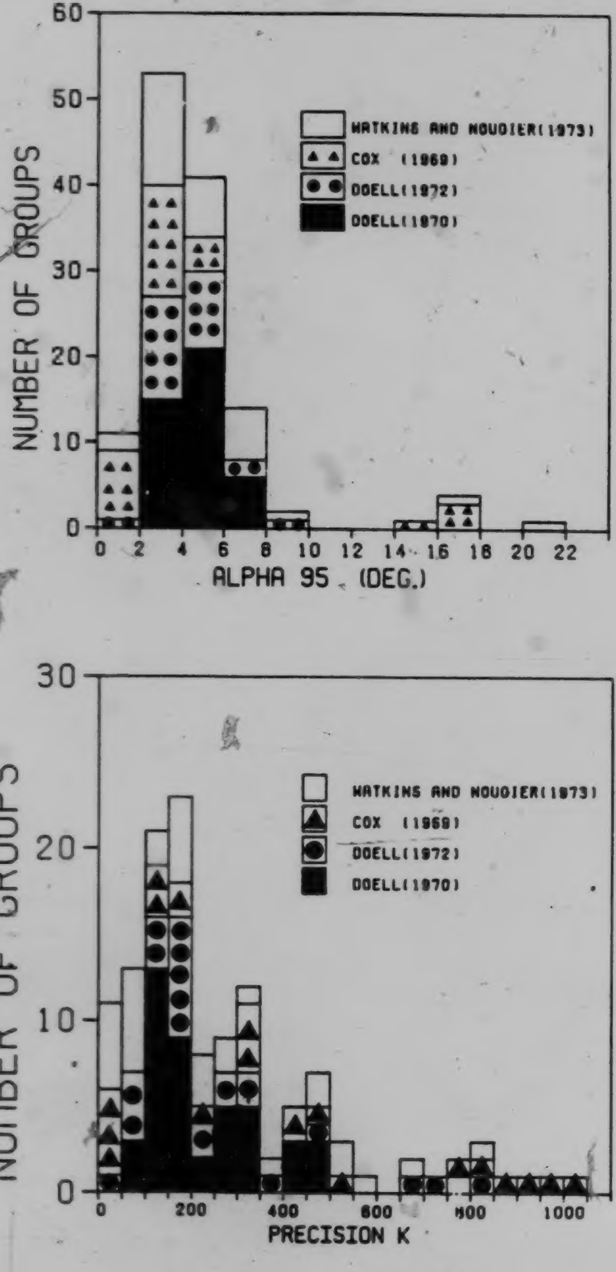

**Figure 3-28**

α95 and k distributions in four studies of volcanic rocks

(8 per group)
(median α95 = 4.0°)
(median k = 192)

# 4. ANALYSIS OF THE SECULAR VARIATION

## A. Introduction

Prior to detailed analysis of the data the question regarding whether or not the samples collected in section 1 represent a legitimate time series must be addressed. Legitimate time series are those in which the samples are not only ordered sequentially in time but are also separated by roughly equivalent time intervals. This is a very important point because it determines which mode of analysis is appropriate; if these conditions are not met then a time series analysis may not be warranted.

Before dealing with the two alternative procedures, we turn first to a discussion of the possible sedimentological problems (section B). In sections C and D the two analytical aproaches are described. The first assumes that the samples do constitute a legitimate time series, whereas the second does not. It ignores all information regarding the ordering of the samples. In section E the time-averaged paleomagnetic field is studied. Section F deals with the absence of the Blake Event.

## B. Sedimentological Considerations

It is virtually certain that the sedimentation rate was not constant throughout the sampled interval. Although sedimentation rates vary widely, it is generally true that coarser sediments are deposited more rapidly than fine grained sediments. Although the strata comprising section 1 are predominantly clayey silts (possibly deposited at a uniform rate) there are some units, for example AB-4 and AB-5, which comprise a total of 38 cm of fine-grained pebbly sands (appendix A). These were probably deposited very rapidly and represent a very short time.

The age information that is available (chapter 2), indicates that 1.1 million years may have elapsed from the base of unit 3 until the time of the Old Crow Tephra. At the location of section 1 this comprises 15 meters of sediment. If the sedimentation was unbroken this suggests an extremely low sedimentation rate of 1.5 cm/1,000 years. A review of sedimentation rates by Kukal(1971)(fig. 4-1) suggests that, for a fluvial or lacustrine environment, this rate is abnormally low, therefore it is far more likely that gaps in the sedimentary record exist. These may consist of times of non-deposition, or more seriously, times of erosion. The presence of a cryoturbated interval, roughly 2 metres beneath the Old Crow Tephra, strongly suggests that at least one hiatus is present. Cryoturbated sediments indicate subaereal exposure which in turn indicates a time of non-deposition. Any ice wedges present at such horizons can give some indication of the duration of subareal exposure. As discussed by Shumskii (1964b), ice wedges grow extremely slowly (from 1 to 20 mm per year). Ice wedge casts present in the cryoturbated strata sampled in this study range up to 0.5 m across, therefore the time of hiatus could be as much

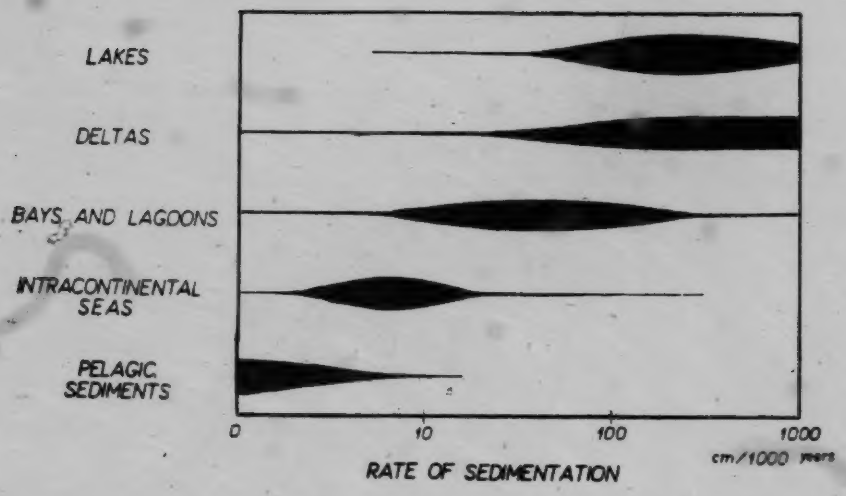

**Figure 4-1**

Sedimentation rates observed in a variety of depositional environments

Modified from Kukal (1971)

as 500 years. Fortunately only one cryoturbated interval was detected in the section sampled so it is possible that much of the loss occurred in the 10 m of unit 3 below the lowermost sampled horizons. The time loss at the cryoturbated horizon may not be significant in view of the fact that the sampled horizons are already separated by finite distances (an average of 4 cm in section 1) which, depending on the sedimentation rates, could be equivalent to several hundred years. Kukal's summary suggests that deltaic and lacustrine sediments are deposited most commonly at a rate in excess of 10 cm /1000 years (fig. 4-1). Therefore it is possible that adjacent horizons could be separated by some 400 years. Keeping this in mind the possible loss of sediments that may have occurred at the cryoturbated interval may represent the loss of only a few points in the discrete time series. As will be discussed in section C, the non-erratic nature of the paleomagnetic record in section 1, as illustrated in figure 3-24, indicates the time loss is not significant and that few, if any, points in the time series are missing.

If Kukal's conclusions are reasonable, and the sedimentation rate is not likely to be less than 10 cm/1,000 years, then the 6m of sediments covered by section 1 likely represent less than 60,000 years. Figure 4-1 suggests the sedimentation rate could be on the order of 100 cm/1,000 years resulting in the 6m of sediments being deposited in as little as 6,000 years. However, this latter figure is most likely too low, because of compaction and the effect of times of non-deposition or erosion. The paucity of dating information means it is possible to infer only that section 1 covers some length of time between 6,000 and 60,000 years.

## C. Analysis of the Temporal Variation

This approach assumes that the samples represent a discrete time series, and allows the elucidation and modelling of the temporal variation of the geomagnetic field preserved in the sediments. An extension of this approach is the formal *time series analysis* which is used to elucidate the frequency spectrum (ie. indicate if any periodic components are present). Such an analysis would at least in the early stages have to be a *space series analysis* due to the lack of detailed information on sedimentation rates.

Close inspection of the paleomagnetic record in section 1 (as illustrated in figure 3-24) reveals that the secular variation has proceeded with two distinctly different types of behavior. In segments (b) and (d) the paleomagnetic field vector undergoes relatively little movement away from a mean orientation of $\overline{D}$ = 010°, $\overline{I}$= 73°. In segment (c) however it is clear that the field vector was perturbed a significant angle (22° at the maximum) away from this unperturbed orientation to a shallow inclination of 57° and a westerly declination of 336°. The outward and return trajectories of this perturbation are superposed. Segment (a), which encompasses the lowermost portion of section 1, appears to have recorded the final stages of a perturbation very similar to that which is recorded fully in segment (c). Section 2 (figure 3-25) has recorded a paleomagnetic field history that bears a striking resemblance to that recorded in section 1. Two perturbations to a relatively westerly declination and a shallow inclination have again been recorded, however section 2 apparently extends further back in time and has recorded a complete perturbation in segment (a).

As discussed in section 4-B, the fact that a coherent pattern of geomagnetic field vectors is observed in both sections lends support to the assumption that the samples do represent an essentially unbroken time series.

Such perturbations could be due to fluctuations in either the dipole or the non-dipole fields, and we now turn to an investigation of its possible origin and the implications thereof for geomagnetic secular variation.

## Geomagnetic Perturbations caused by Dipole Wobble

As discussed in chapter 1 many workers have noted that the main dipole seems to be wobbling so that at any instant in time it is not likely to be aligned with the geographic axis but is inclined by a small amount. At the present time, for example, this deviation amounts to $11\frac{1}{2}°$. It has not yet been established how this wobbling occurs.

Dipole precession (in which the geomagnetic pole moves along a line of latitude) leads to an elliptical movement of the geomagnetic field vector. As an example, figures 4-2 and 4-3 illustrate the effect that a dipole precessing at 80° latitude would have at the location of this study. Comparison of this result with the actual data (fig. 3-24) immediately reveals the inadequacy of this model. On a Bauer plot the actual perturbations described above cover the same *path* as they develop and fade. A precessing dipole cannot produce such movement.

Constant longitude movement (dipole nodding) leads to the observed path *coincidence* and therefore provides a much superior model than precession. Figures 4-4 and 4-5 illustrate the effect of sinusoidal dipole nodding of 15° amplitude in a plane 45°E/135°W from the site. It is clear that manipulation of the longitude and amplitude could essentially re-create the perturbations observed. Intui[illegible]y it is hard to imagine why the dipole would underg[illegible] movement. Furthermore there is no support in the literature for such dipole behavior: a more viable alternative is much to be desired.

### Perturbations caused by Dipole(s) at the Core-Mantle Boundary

It is highly plausible that the observed perturbations may result from fluctuations in the non-dipole field. As pointed out in chapter 1 it is believed that the sources of the non-dipole field are located just below the Earth's core-mantle boundary. Recent geomagnetic study has revealed

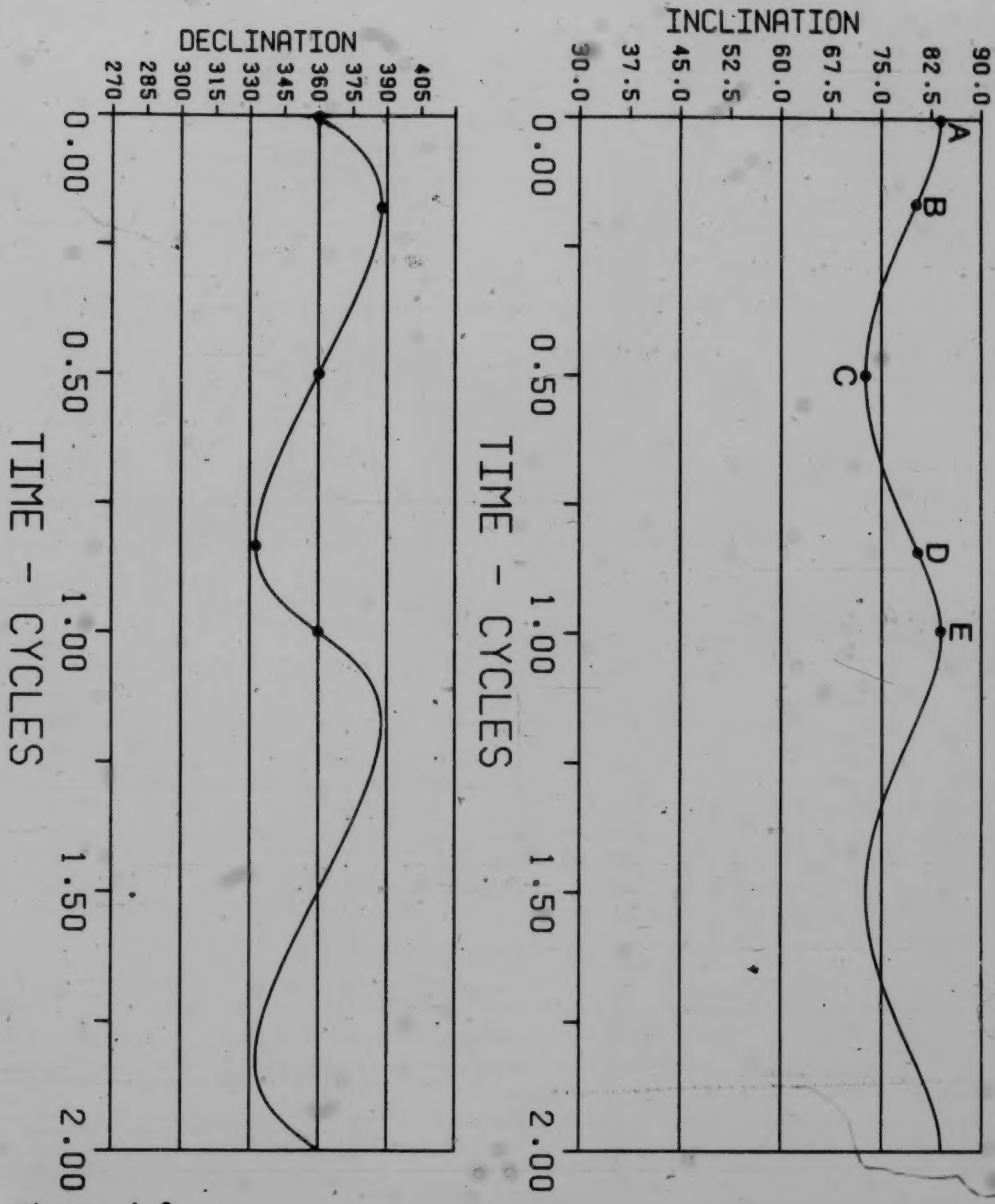

**Figure 4-2**

Geomagnetic field variation at site HH68-10 due to the dipole precessing at 80° N. latitude.

Two complete cycles representing an arbitrary time span are presented.

(refer to figure 4-3 for the corresponding Bauer plot)

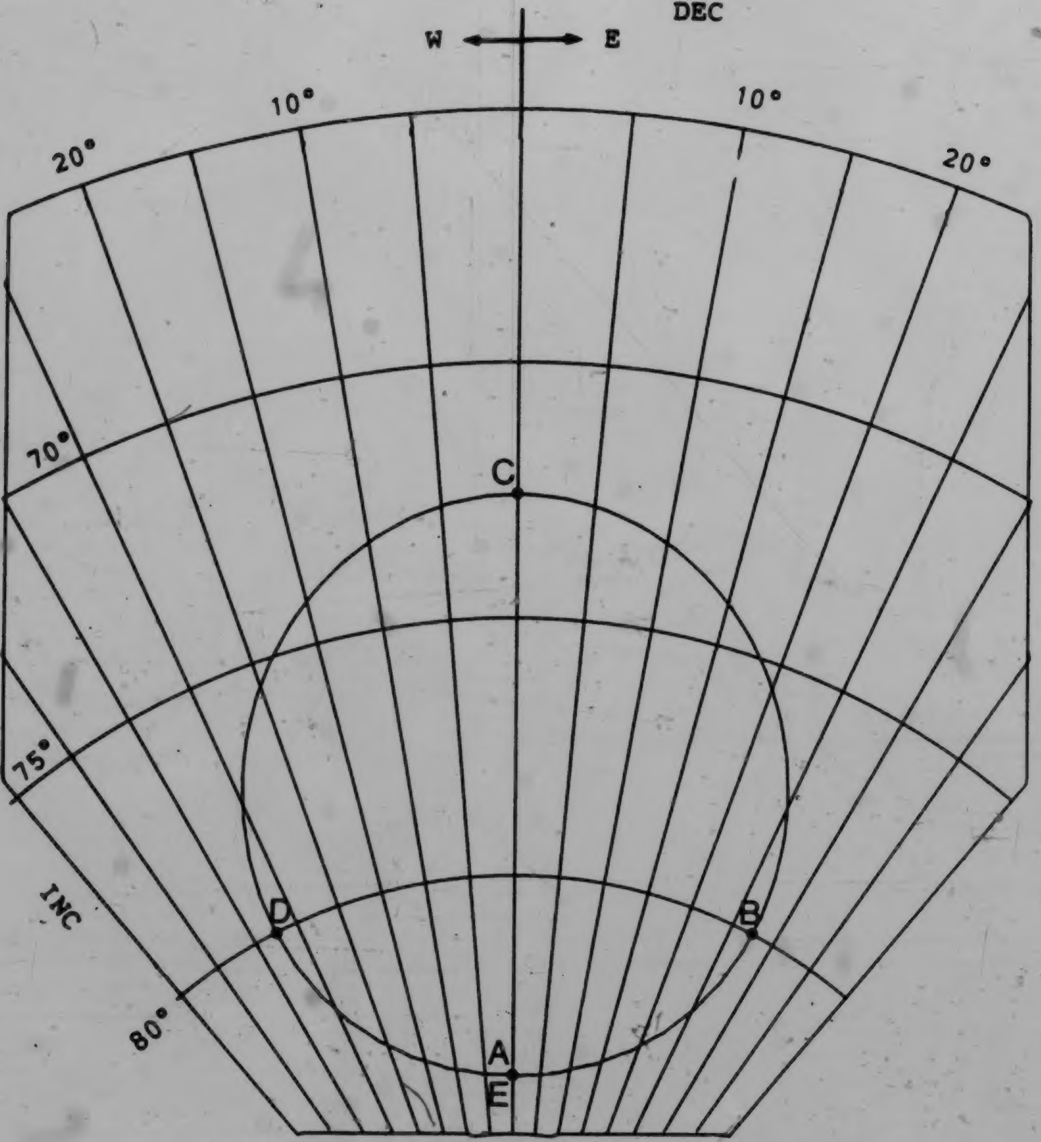

Figure 4-3

Bauer plot illustrating geomagnetic field variation at site HH68-10 that would result from the dipole precessing at 80° N. latitude.

(equal area projection)
(refer to figure 4-2 for corresponding magnetogram)

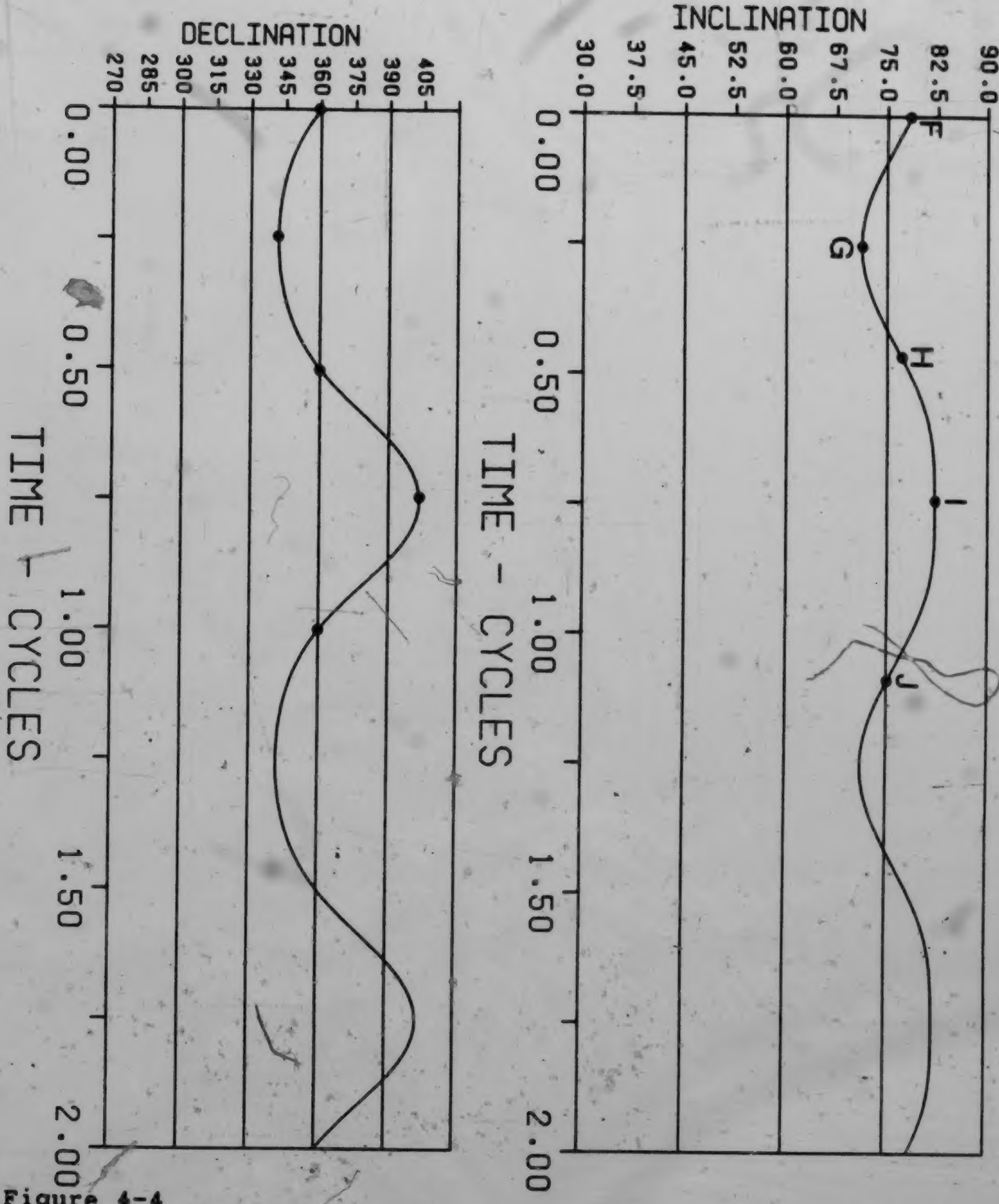

**Figure 4-4**

Geomagnetic field variation at site HH68-10 that would result from sinusoidal dipole nodding of 15° amplitude in a plane 45° E, or 135° W, from the site.

Two complete cycles representing an arbitrary time span are presented.

(refer to figure 4-5 for corresponding Bauer plot)

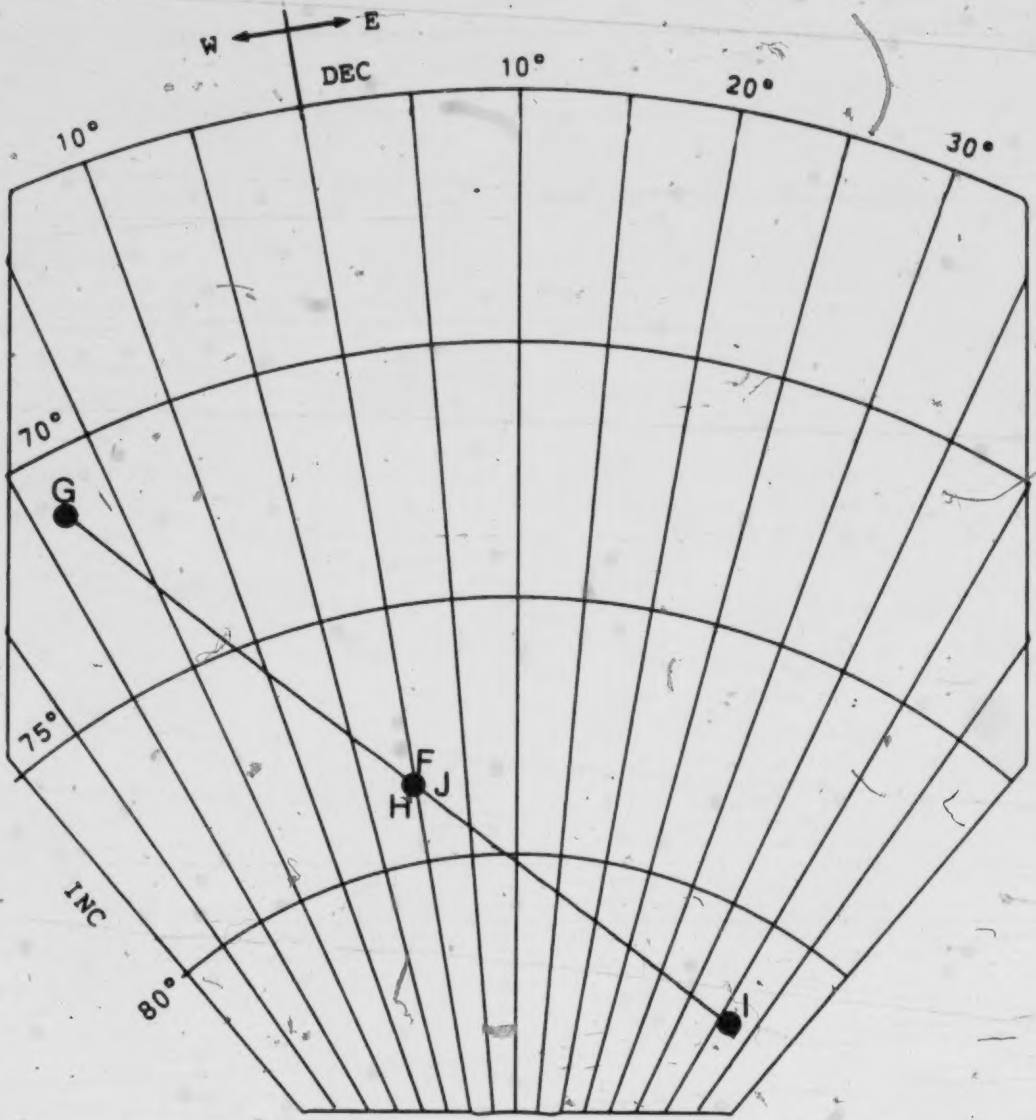

**Figure 4-5**

Bauer plot illustrating the geomagnetic field variation at site HH6B-10 that would result from sinusoidal dipole nodding of amplitude 15° in a plane 45° E, or 135° W, from the site.

(equal area projection)
(refer to figure 4-4 for corresponding magnetogram)

sources that drift westward relative to the Earth's surface and others that remain stationary (Yukutake and Tachinaka,1968).

As is the case with a precessing dipole, westward drifting non-dipole field sources lead to elliptical field vector movements and therefore cannot cause the observed perturbations. Naturally, the same objection holds for eastward drifting sources.

Stationary sources of the non-dipole field are believed by some (Creer et al,1973,1977) to arise from small horizontal eddies of liquid trapped beneath irregularities or lateral temperature variations at the core-mantle boundary. Such eddies are generally assumed (e.g. Cox,1968) to lead to radially orientated sources of magnetic flux. Assuming, at least for the present analysis, that this is true it is not possible to uniquely locate such a dipole but it is possible to locate the locus on which it must lie. The unperturbed and the perturbed field vectors define a plane in which the *perturbing vector* itself must also lie. This constrains any radial source of magnetic flux at the core-mantle boundary to lie on a curve. For the perturbation observed between -241 and -11 cm in section 1 (fig. 3-24) we obtain curve 1 in figure 4-6.

At the point of maximum perturbation (Dec.= 336°, Inc. = +57°) the geomagnetic field vector lies 22° away from its unperturbed orientation (Dec. = 010°, Inc.= +73°)(see fig. 3-24). In figure 4-7 the dependence of the required magnetic

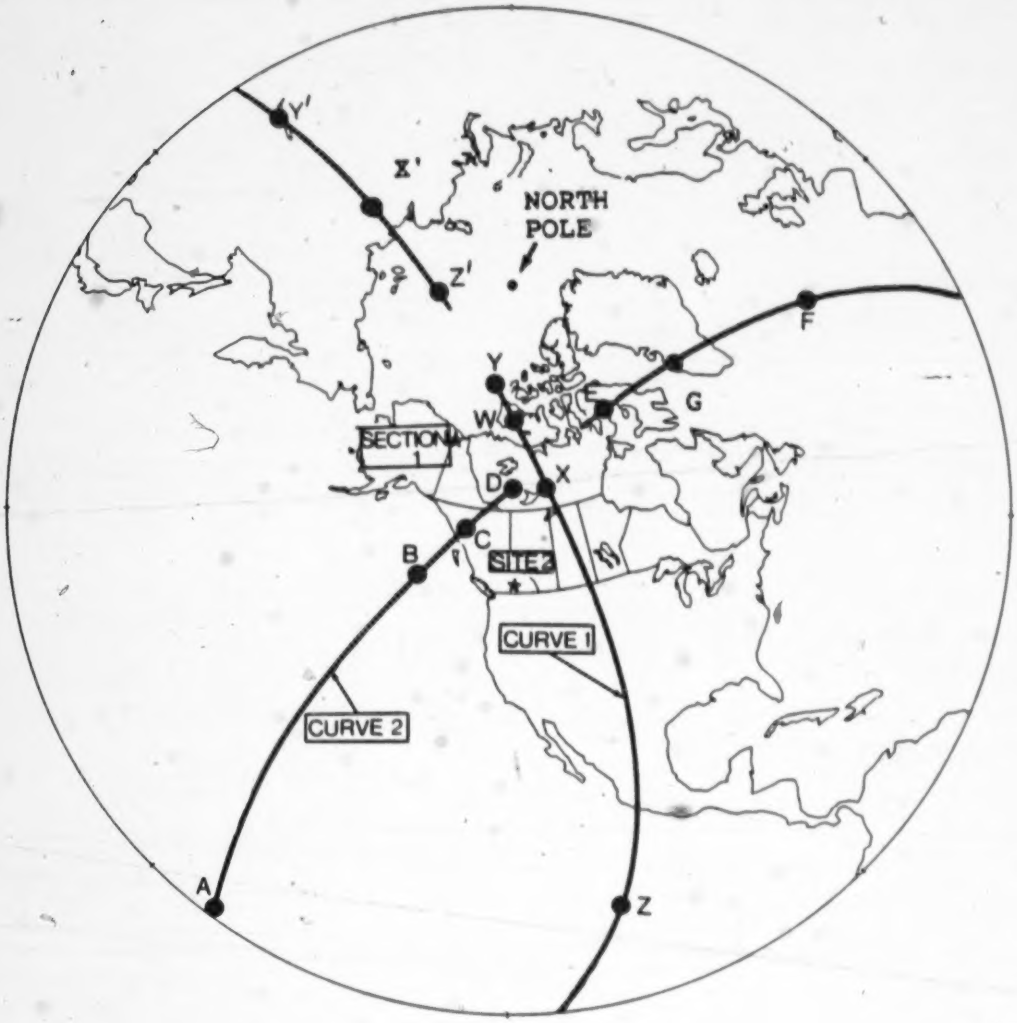
Y'
X'
NORTH
POLE
Z'
F
Y
G
E
W
SECTION 1
D
X
C
B
SITE 2
CURVE 1
CURVE 2
A
Z

**Figure 4-6**

The locus on which radial dipoles located at the core-mantle boundary would cause perturbations of the geomagnetic field observed in this study (section 1 - curve 1) and by Turner et al (1982) (site 2 - curve 2).

All points highlighted in this and following figures are explained in the text. See figures 4-7 and 4-11 for further details.

moment (M') of the radial dipole (RD) on location along curve 1 is illustrated. This curve was generated using elementary magnetostatic theory (appendix C). The gap in the curve between Δ=-8 and Δ=-20° exists because it is geometrically impossible for any RD in this range to cause the observed perturbation. The magnetic moment of the RD reaches a minimum of M' = +0.076M at point X, which is 11° away from point W (the point of closest approach of curve 1 to the site). This result is consistent with the magnetic moments obtained in previous studies of a similar nature. For example Harrison and Ramirez (1975) used RDs at the core-mantle boundary with magnetic moments ranging from 0.0794M to 0.274M to produce localized field reversals at the surface. It is not known how large RDs at the core-mantle boundary may be but it is very unlikely that their magnetic moments would exceed that of the Earth's main dipole. Given that this is true it is only possible to restrict any candidate RDs to the 75° between points Y and Z, or the 40° between Y' and Z' (figs. 4-6 and 4-7). With only one observation point more definite conclusions are not possible.

Since the perturbations in section 1 (segments (a) and (c) in figure 3-24) are isolated from each other in time it is necessary to give the candidate RD a magnetic moment that varies with time (physically this means that the postulated eddy at the core-mantle boundary must not be stable but must flare up from time to time). Assuming that this flaring up

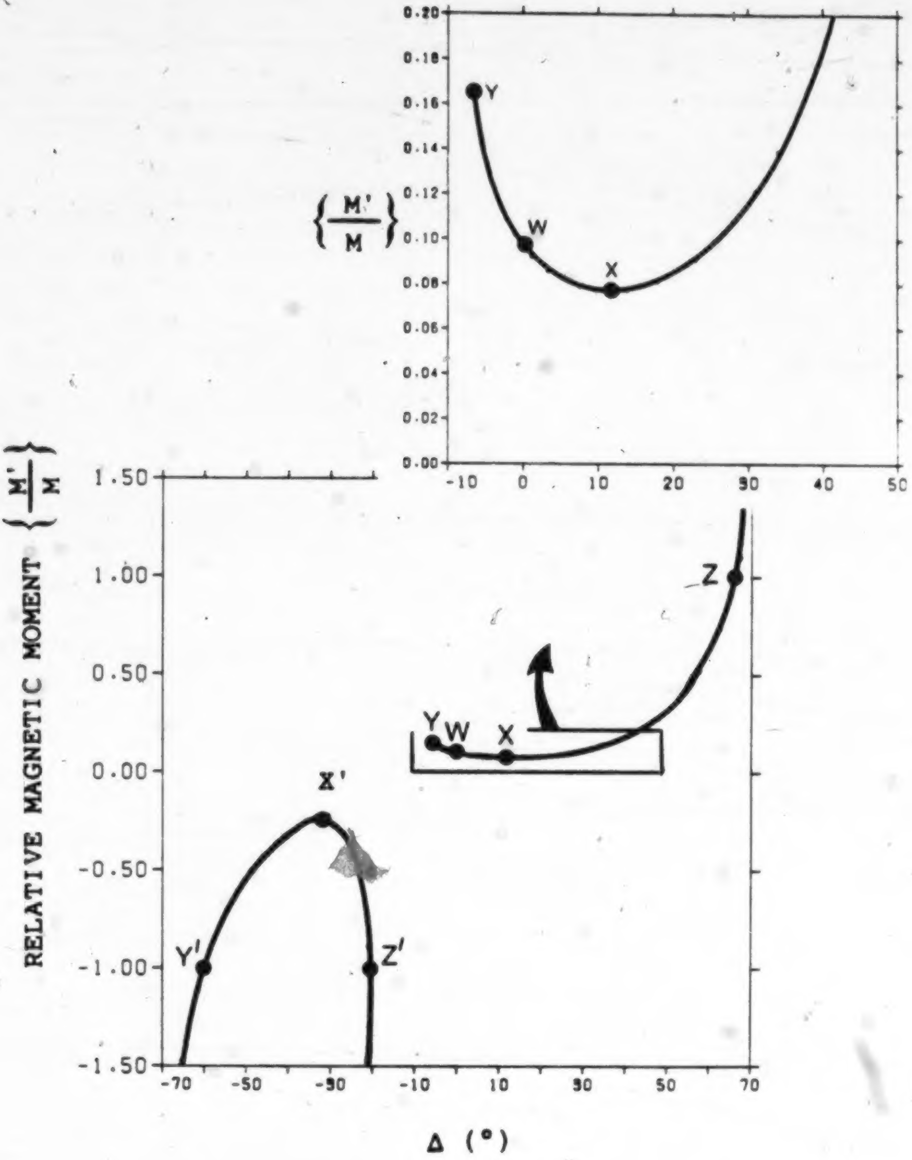

**Figure 4-7**

The magnetic moment (M') of a radial dipole situated at the core-mantle boundary along curve 1 (figure 4-6) required to cause the maximum paleomagnetic field perturbations observed in section 1.

The magnetic moments are relative to the Earth's main dipole moment (M). The angular distances (Δ) are from point W, the location at which curve 1 is closest to the site HH68-10. Negative values are assigned to radial dipoles that are directed toward the geocenter.

and down of magnetic moment occurs sinusoidally and ranges from zero to the maximum described in figure 4-7 it is possible to model the observed perturbation very precisely. Illustrated in figures 4-8 and 4-9 are the effects of such a RD located at point X (63° N, 250° E) in figures 4-6 and 4-7. Comparison of these results with the actual results in figures 3-22 and 3-24 shows a distinct similarity. Precisely the same results would arise from RDs located at any other point along the curve, provided that they have appropriatly stronger magnetic moments.

A very similar perturbation was located in sediments 20,000 to 30,000 years old in southeast British Columbia by Turner et al(1982)(fig.4-10). Evans(1984) discusses the possibility of such a perturbation being caused by a stationary RD at the core-mantle boundary. Although these sediments are much younger than the ones in this study the possibility that both perturbations could have had the same stationary source is worth investigating. The locus along which the radial source of Turner et al would lie is illustrated in figure 4-6 (curve 2). The corresponding dependence of magnetic moment on angular distance (Δ) is illustrated in figure 4-11. The geometry of this perturbation requires that any possible RD source at the core-mantle boundary cannot lie between longitudes of 240° and 269° east. Thus curves 1 and 2 do not coincide and it appears at first sight the perturbations could not have had the same source. However, there are a number of arguments in

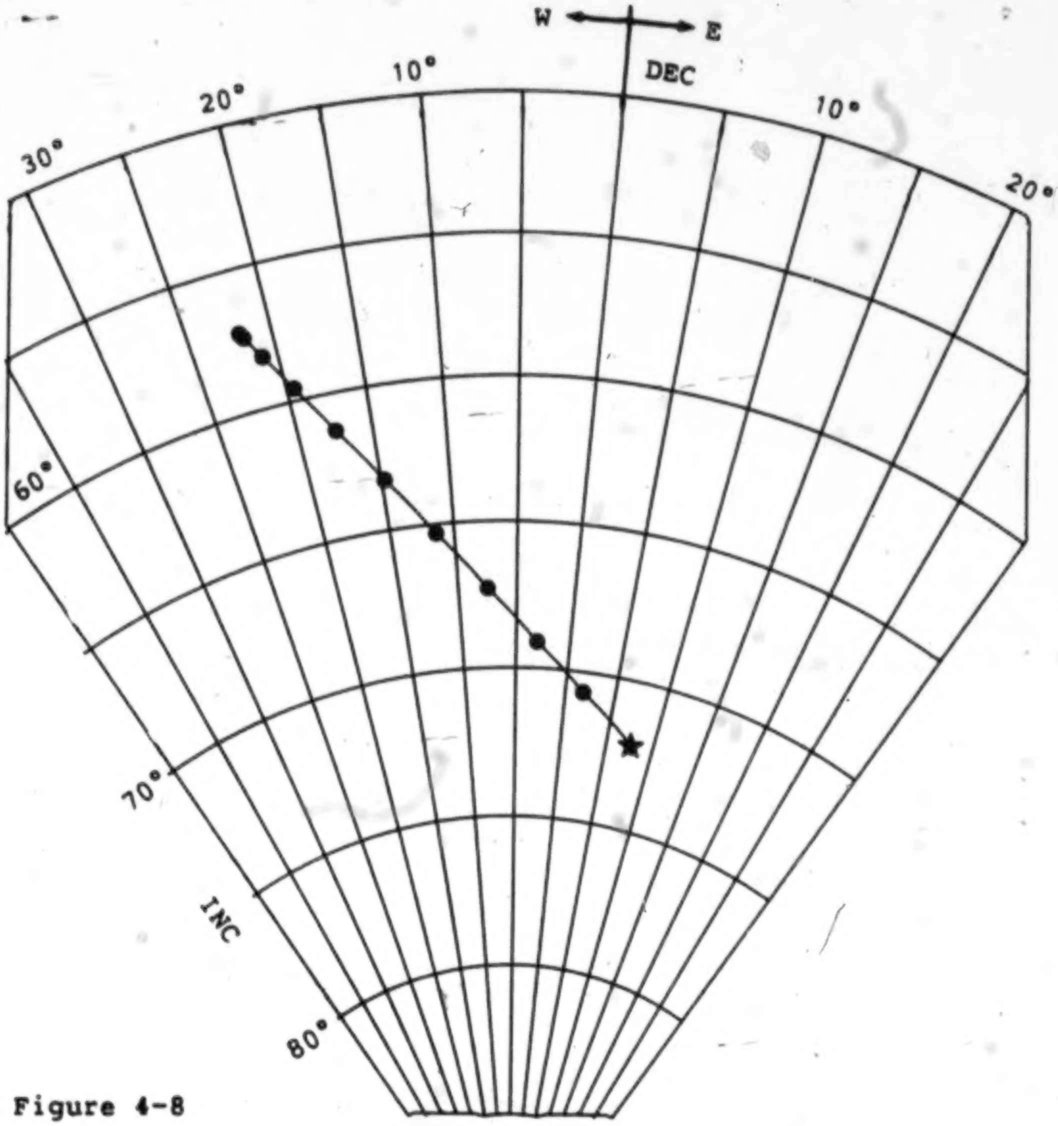

Figure 4-8

Bauer plot illustrating the path covered by the total geomagnetic field vector at site HH68-10 when a radial dipole, pointing toward the Earth's surface, and located at 250° E 63° N is superimposed on to the Earth's main dipole and sinusoidally varies in amplitude between zero and a maximum of 0.0762 times the Earth's main dipole moment.

The east longitude and colatitude of the Earth's main dipole are 197.7° and 168.8° respectively. The star represents the field vector that results from such a dipole with no non-dipole field superimposed. See figure 3-24 for the corresponding observed perturbations (from -550 to -419 cm and -241 to -11 cm).
(equal area projection)

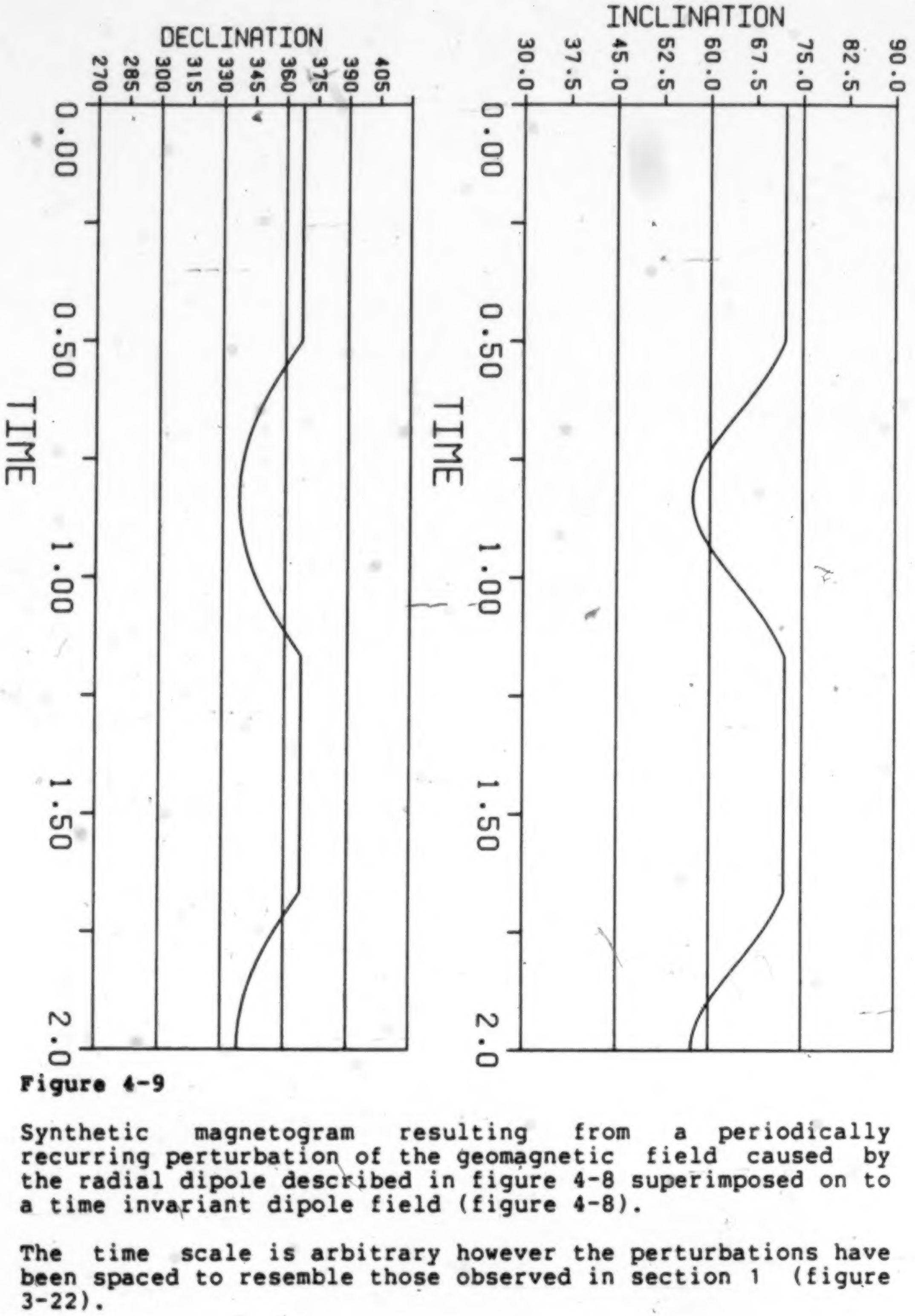

**Figure 4-9**

Synthetic magnetogram resulting from a periodically recurring perturbation of the geomagnetic field caused by the radial dipole described in figure 4-8 superimposed on to a time invariant dipole field (figure 4-8).

The time scale is arbitrary however the perturbations have been spaced to resemble those observed in section 1 (figure 3-22).

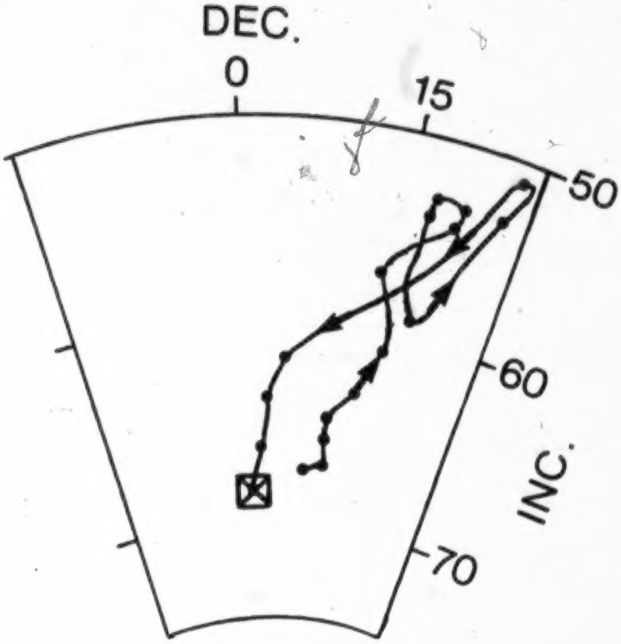

Figure 4-10

Bauer plot of a perturbation of the paleomagnetic field observed by Turner et al (1982) in sediments ≃ 20000 to 30000 years old located at Besette Creek in S.E. British Columbia.

The square with an inscribed diagonal cross represents the field due to an axial geocentric dipole at this site.

From Evans (1984)

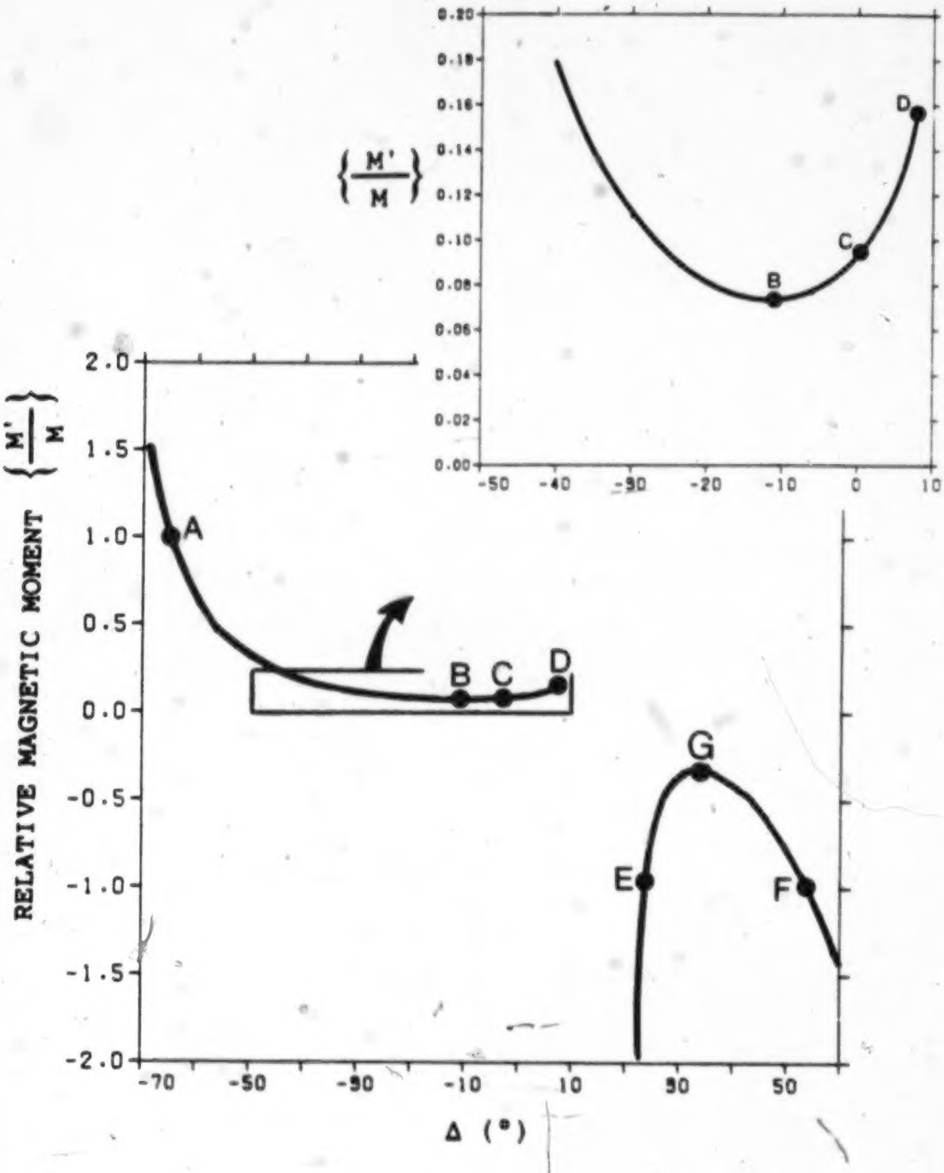

**Figure 4-11**

The magnetic moments of radial dipoles situated at the core-mantle boundary along curve 2 (figure 4-6) required to cause the maximum paleomagnetic field perturbation observed by Turner etal (1982) (figure 4-10).

For further details see figure 4-7.

favour of the possibility of a single source. There is a degree of uncertainty regarding the true paths covered by the perturbations in figure 3-24. The $\alpha95$ statistics that apply to each point range up to 5° (figure 3-22), and thus the perturbation itself should be contained within an *envelope* within which it is 95% certain the true perturbation lies. This envelope would directly map onto an envelope surrounding curve 1 in figure 4-6 (the same would of course be true for curve 2). Although the curves themselves do not coincide, the 95% confidence envelopes may. Furthermore, it is very possible that the actual source(s) may not have been perfectly radial. By manipulating the orientation of the dipole used in the model it would be a simple matter to make the curves coincide. In addition, although the RD has been described as being stationary, on long timescales (greater than 10 times that of the perturbations themselves say) the dipole may not be completely fixed in location but may migrate as the postulated bump, or inhomogeneity, at the core-mantle interface that is causing it is influenced by the convection cells in the outer core. The minima in curves 1 and 2 (points X and B respectively) are only separated by an angular distance of some 15° and thus the required migratory motion would not have to be great.

If it is indeed true that the perturbations located in this study and by Turner et al were caused by the same source it would have to have existed for at least 80,000 years and perhaps throughout its existance it may have periodically flared up to cause localized perturbations of the geomagnetic field. Admittedly this conclusion is highly speculative, no sediments covering the time gap between these two sections have been studied to verify the link, and to date there is no evidence to support the longevity of RDs, but it does seem plausible. A third section covering the time from 100,000 to 20,000 years B.P. would not only test this theory but if it contained perturbations due to the same RD it would be possible to locate it on the core-mantle boundary with much greater precision.

This explanation for the perturbations observed in section 1 seems to be the most tenable solution. Since the fluid in the outer core is in constant motion, and since it is generally accepted that the core-mantle interface is not perfectly smooth, one would expect small scale disturbances of the overall convective motion that produces the dipole field as that fluid encounters these irregularities. These disturbances in fluid flow would result in small scale disturbances in the magnetic field.

Striking support for this theory comes from the study of the directly observed magnetic field over recent times. As discussed by Merrill and McElhinny (1983) maps of the vertical component of the non-dipole field made in 1829 and 1980 (fig. 1-1) reveal a prominent stationary anomaly has existed in Mongolia and has in fact increased in magnitude some 50% to 36,000 nT. This anomaly, which is believed to result from fluid motion at the core-mantle boundary, may be a modern day analog of the process which caused the perturbation observed in this study. In addition to this study and that by Turner et al (1982) a perturbation with similar characteristics (i.e. involving path coincidence on a Bauer plot) has been located by Doell and Cox (1965) in Hawaii. It seems that evidence, both direct and indirect, is mounting to support the theory that stationary anomalies in the non-dipole field exist.

## Space Series Analysis

For completeness a space series analysis of data in section 1 was carried out to elucidate its power spectrum. The program POLFILT2, supplied by Dr. J. C. Samson of the Physics Department, University of Alberta, was used because of its ability to handle multichannel data (in this study each of the orthogonal components of magnetization, X,Y and Z, require one channel) as well as its ability to determine the pure state power spectrum (that power at each frequency directed along the direction of polarization) as well as the total power. To avoid the effect of smoothing, the data illustrated in figure 3-20 was used. Prior to the analysis the two points at each horizon were averaged and then the entire suite was linearly interpolated to give a new suite of the data points spaced at 5 cm intervals. The entire set was *padded* with zeros to give 200 points.

The total, and pure state power spectra were essentially identical and for convenience and simplicity only the former is illustrated (figure 4-12). The power spectrum is completely dominated by the third harmonic, which is due to $3\frac{1}{3}$ metre wavelength energy. Inspection of figures 3-20, 3-22 and 3-24 reveals that this is clearly due to the perturbations between -550 and -419 cm and between -241 and -11 cm. The degree of polarization at this frequency is high (0.76) and thus the validity of this peak is supported. (The degree of polarization ranges from 0 to 1 and is an assessment of the anisotropy of the power distribution; a completely isotropic power distribution has a degree of polarization of 0 and is likely due to random noise. Values above 0.6 generally indicate that the source of the power is real.). There is a hint of some power at the fifteenth harmonic ( 67 cm wavelength energy) which could be due to features between +25 and -50 cm, and between -250 and -425 cm, but since the degree of polarization is only 0.26, and their amplitudes are not much greater than the 95% confidence envelope, illustrated in figure 3-22, they are not believed to be significant.

Although the degree of polarization result confirms the reality of the power at the $3\frac{1}{3}$ metre wavelength, and thus the perturbations modelled earlier, it is clear that the elucidation of the power spectrum has not greatly enhanced this study. Because of the lack of dating information the power spectrum necessarily remains a function of spatial,

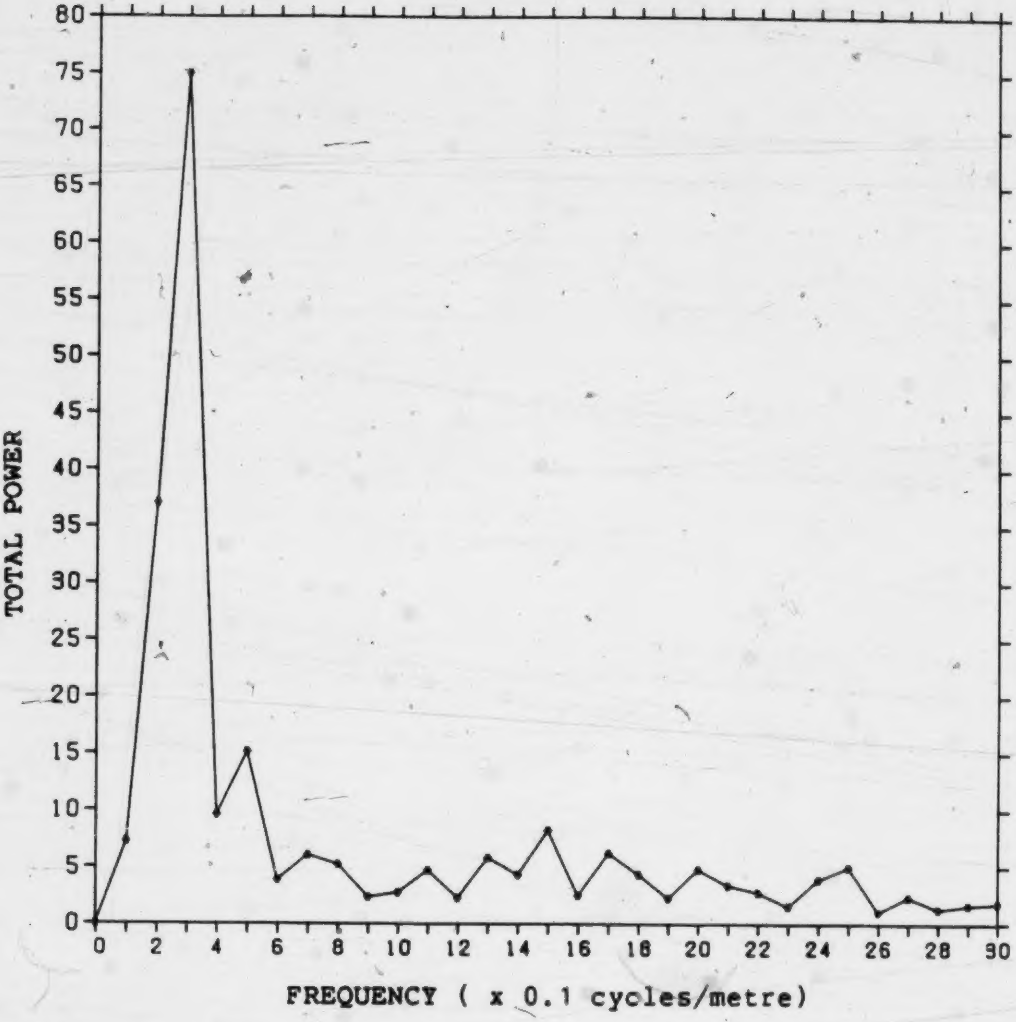

Figure 4-12

A plot illustrating the total power spectrum of section 1

The data set (illustrated in figure 3-20) has been padded with 75 zeros to give a total of 200 points, each separated by 5 cm. The harmonics are multiples of the 0.1 cycles per metre frequency.

not temporal, frequency. If dating information had been available, a more detailed analysis taking into account the varying sedimentation rates would have been warranted.

## D. Dispersion Analysis

An analysis of the angular dispersion (the degree of scatter about the mean) of paleomagnetic *field directions* is commonly applied to suites of measurements taken from lava flows because of the difficulty in obtaining adequate time series, in fact in some cases even the time sequence is unknown. Angular dispersion in paleomagnetic field directions is caused by variations in the intensity and direction of the dipole and non-dipole fields (this includes dipole wobble and secular variation) as well as inaccuracies in the measuring process. It has become common practice to consider the dispersion of the *Virtual Geomagnetic Poles (VGPs)*. A VGP is determined from one field measurement and is the location at which the axis of the main dipole would intersect the Earth's surface provided the geomagnetic field were purely dipolar.

Dispersion can be estimated in two ways:

1) from Fisher's precision parameter k. The angular variance ($s^2$) is given by

$$s^2=\left(\frac{6561}{k}\right) \text{ degrees} \qquad 4-1$$

2) by determining the mean square angular difference

between each field direction and the mean ($\delta$). The angular variance is then given by

$$s^2=\left(\frac{1}{(N-1)}\right)\Sigma\delta^2 \text{ degrees} \qquad 4\text{-}2$$

When N (the number of data points) is greater than 25 these methods give essentially the same results.

By comparing the dispersion present in suites of measurements collected from widely scattered locations around the globe, several workers (McElhinny and Merrill,1975; McFadden and McElhinny,1984) have noted a strong latitude dependence of VGP angular dispersion; it increases with increasing latitude (fig. 4-13). Since the 1950's several models have been proposed to explain this latitude dependence. The latest (called Model F by McFadden and McElhinny, 1984), takes into account the desirable features of earlier models but supercedes them by virtue of its completeness. The observed total dispersion at any latitude has two components, one from the dipole field and one from the non-dipole field. To a good approximation the total dispersion (St) is given by

$$St^2 = Sd^2 + Sn^2 \qquad 4\text{-}3$$

where Sd and Sn are the dispersions due to the dipole and non-dipole fields respectively.

The best fit curve through VGP dispersions observed in lava

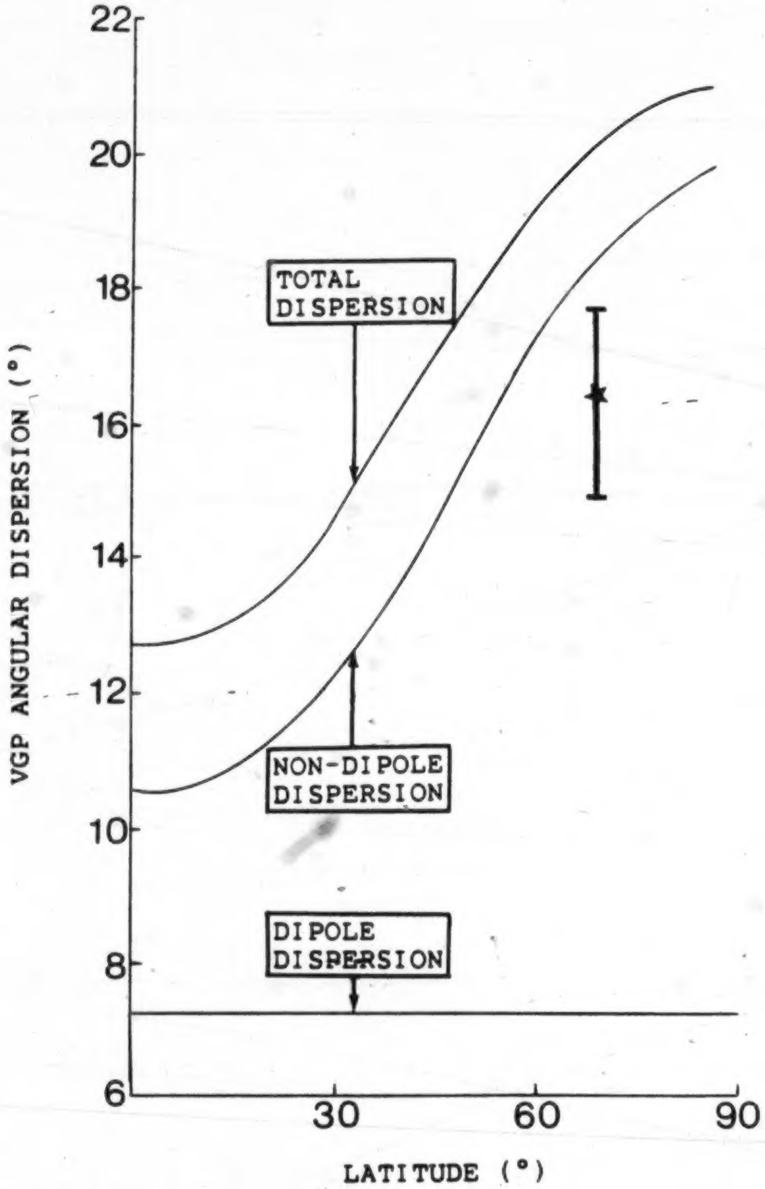

**Figure 4-13**

The dipole, non-dipole and total VGP dispersions predicted by model F.

The total dispersion curve was obtained by a least squares fit to the dispersion observed in lava flows less than 5 million years old. The data point is the dispersion (± standard error) in this study.

flows less than 5 million years old yields Sd = 7.2°. This is the dipole wobble. The non-dipole field provides 10.6° of dispersion at the equator increasing by a factor of 2 at the poles (fig. 4-13).

Considering the data of section 1 (illustrated in figure 3-22) the VGP dispersion is 16.3°±1.4° (N=127) (the starred data point in figure 4-~~13~~). This value is 3° lower than that predicted by model F.

Since dipole wobble is generally believed to occur on a timescale much longer than non-dipole fluctuations the reduced angular dispersion most likely reflects a lack of dipole wobble due to the fact that the time span covered by section 1 is short relative to the timescale of dipole wobble. Using equation 4-3 to isolate the non-dipole VGP dispersion from the total illustrated in figure 4-13 gives a predicted non-dipole dispersion of 18.0°. This figure is almost within the 95% confidence limits of the value obtained in this study and it seems fair to conclude that the observed perturbations are indeed non-dipole effects. This very important result supports the same conclusion reached in section 4-C. The time span covered by the section must therefore be short relative to the time covered by one period of dipole wobble. If dipole wobble indeed has a period on the order of $10^5$ years then the time span estimate of up to 60,000 years reached in section 4-B may be slightly high. In the next section further support is given to the conclusion that dipole wobble was not averaged out in section 1.

## E. The time averaged paleomagnetic field vector

If the time span of the set of measurements is great enough, the corresponding suite of VGPs should average out all phenomena such as dipole wobble and secular variation and one obtains a *paleomagnetic pole* which should coincide with the rotation axis.

The average of the VGPs obtained from all data points in section 1 does not coincide with the rotation axis, but lies at 75.9° N, 49.4° E ($\alpha95 = 2.7°$), and using Wilson's terminology (Wilson, 1971) is thus slightly far-sided and left-handed (fig. 4-14), that is, when viewed from the site, the average VGP lies beyond the geographic pole (by 14°) and to the left of the meridian through the site. Since the perturbations (discussed at length above) are to a relatively low inclination, some of this far-sidedness is due to them. Considering only those points that do not fall in the perturbations (ie. do not lie below -419 cm, or between -11 cm and -241 cm) the average VGP is still far-sided (by 11°) and lies at 79.1° N, 19.4° E ($\alpha95 = 3.3°$). In general such a far-sidedness could have a number of causes, and these are now discussed separately.

### Landslip

This is one factor that must be considered when studying poorly-consolidated sediments exposed by a

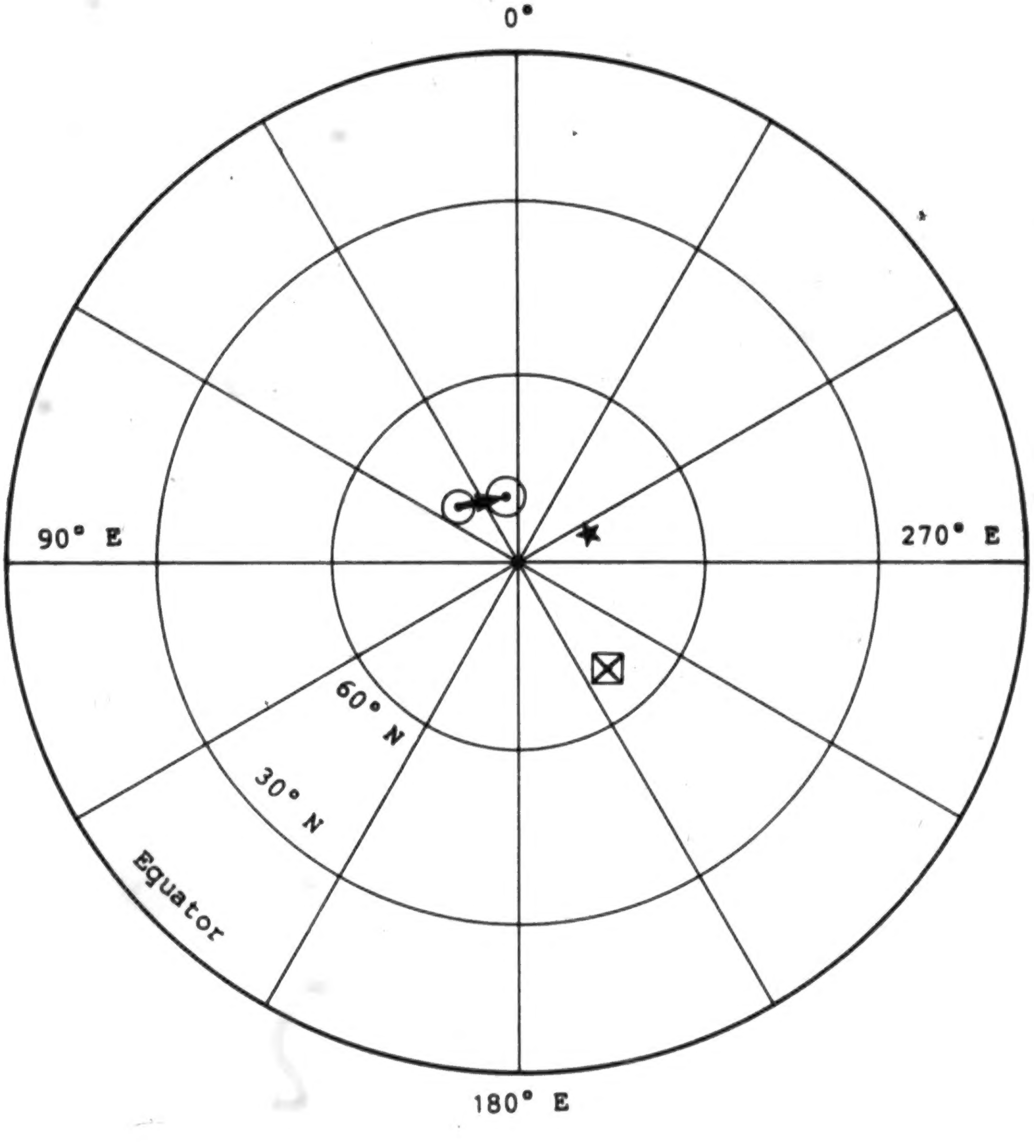

Figure 4-14

The average VGP's from section 1 before and after removing the perturbations between -550 and -419 cm and between -241 and -11 cm (see figure 3-24).

95% confidence limits are included.

The star represents the location of the present boreal geomagnetic pole.
The square with an inscribed diagonal cross represents the location of site HH68-10.

meandering river. Landslip of such sediments not only amounts to a translation but often to a rigid body rotation in which the axis of rotation parallels the riverbank exposure itself. Therefore, provided the landslip is severe enough, one would expect a re-orientation of the paleomagnetic record held by the sediments. At the location of section 1, the exposure trends N 005° E. As a result, slumping would primarily effect the declination of preserved magnetization, not the inclination, and thus could not lead to far-sidedness. Furthermore, the beds are observed to be horizontal and there is no visible evidence of landslip (figure 2-3).

## Depositional Inclination Error

As discussed by King and Rees(1966), studies conducted on artifically deposited sediments, in which the magnetization preserved was a pure DRM, revealed that they invariably preserved an inclination (PI) that was less than the ambient field inclination (I). Although it has not been confirmed by microscopic examination of the sediments a possible explanation for this is that at the moment of deposition some elongate particles present may be acted on by gravitational forces and be rotated to a more horizontal position. The magnitude of the resulting inclination error would depend on the proportion and degree of elongation of these particles and the inclination of the ambient field. King (1955) found that for one sediment studied the inclination corresponded very closely to the formula:

$$\tan(PI)=f*\tan(I) \qquad 4\text{-}4$$

where f is determined by grain elongation and ≃ 0.4.

Assuming that the sediments in the current study posess a pure DRM, using this formula it is possible to account for the far-sidedness observed in section 1. (Using an f of 0.4, equation 4-4 gives a far-sidedness of 23°). However, it now seems likely (Creer et al, 1983) that most sediments, and probably those in this study, posess a PDRM which tends to allow a re-alignment of the magnetic particles and thus largely corrects for inclination error. The artificial sediments studied by King and Rees are unlike most real sediments since they posess no post-depositional remanence. Furthermore, the true value of f that applies to these sediments is not known. Although this sedimentological source of far-sidedness cannot be entirely ruled out, a far superior alternative is available (dipole wobble) and is discussed below.

## Quadrupole far-sidedness

A survey by Wilson (1971) of over 90 VGPs spanning upper Tertiary, Quaternary and Recent times revealed that they tended to be far-sided. This result is true regardless of the location of the site on the Earth's surface, or whether the field had normal or reversed polarity. Wilson proposed that a quadrupole component is superimposed onto the dipole field. Physically this quadrupole component could be due to the center of the Earth's main dipole being displaced from the geocenter. The magnitude of the quadrupole term $g_2^0$ can be determined explicitly knowing the site colatitude ($\theta$) and the local inclination (I):

$$g_2^0 = \frac{g_1^0 * (-\tan(I)\sin(\theta) + 2*\cos(\theta))}{(3*\cos(\theta)\sin(\theta)\tan(I) - 4.5*\cos^2(\theta) + 1.5)} \qquad 4\text{-}5$$

where $g_1^0$ = the magnitude of the dipole term.

In the present study, the average I (excluding the two perturbations delineated earlier) is 72.9°, the site colatitude is 22.1° and thus if the far-sidedness of 11° is caused by the presence of a quadrupole component the ratio $g_2^0/g_1^0$ is equal to 0.61 . This value is extremely high (compared to the present ratio of 0.06) and corresponds to a displacement of the dipole from the geocenter of 920 km (Wilson, 1971). Because this displacement is so large, it is not believed the observed far-sidedness could be due entirely to the quadrupole component.

**Dipole Wobble**

As discussed in the previous section it is likely that the 6m of sediments sampled in this study comprise only a fraction of the time required to average out the effect of dipole wobble. As a result these sediments may have been deposited at a time when the dipole was offset from the rotation axis. If the dipole was offset 11° in the appropriate direction the observed far-sidedness would result. This seems to be by far the most reasonable and simple suggestion. The three other possible explanations are all highly contrived since they involve unreasonable assumptions. Taking into account the conclusions of sections 4-C and 4-D, reached by independent means, that dipole wobble has not been averaged out in the sediments covered by section 1, it seems that this must be the cause of the far-sidedness. It seems that the time span covered by section 1 is so brief relative to that covered by one period of dipole wobble, that it has by chance caught the dipole at one point it its normal cycle of movement when it happened to be on the far side of the geographic pole.

### F. The Absence of the Blake Event

As discussed in chapters 1 and 2, the Blake event, which is believed to have been a time of global reversed polarity, was expected to have been preserved in sediments just beneath the Old Crow Tephra at site HH68-10. It had been located in that position in three locations close to this site (by Westgate et al,1985 and Marino, 1977); the closest being at site HH228 just 35 km to the southwest, and involving an unmistakably full reversal of the geomagnetic field just 2.5 metres beneath the Old Crow Tephra (fig. 4-15).

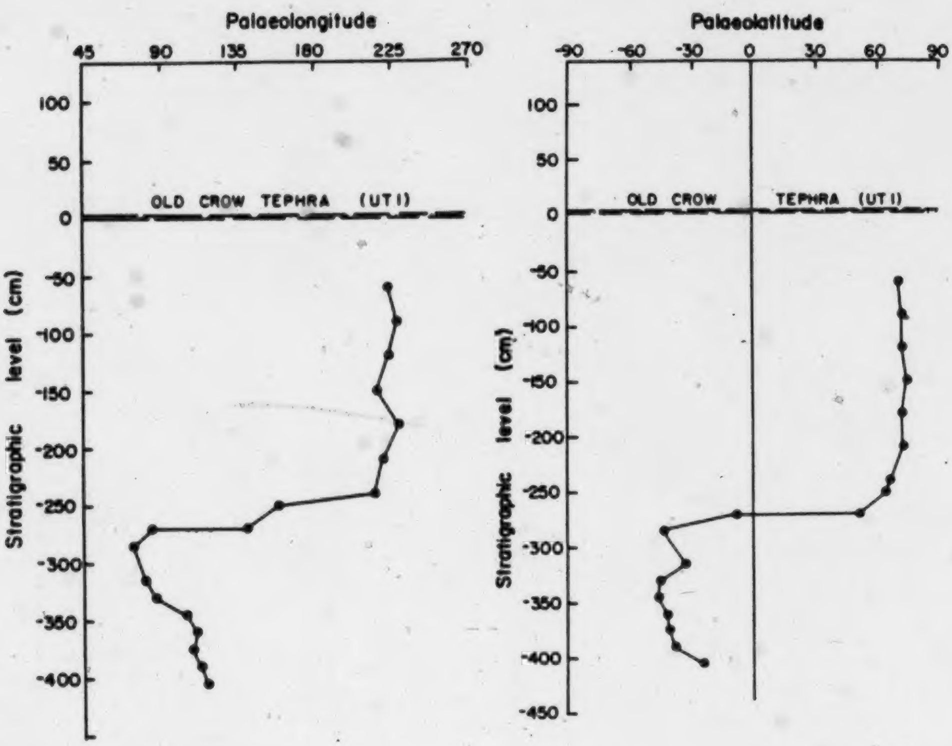

**Figure 4-15**

The paleolongitude and paleolatitude of the virtual geomagnetic pole as a function of stratigraphic level relative to the Old Crow tephra in sediments near the town of Old Crow (at 67° 28' N, 139° 54' W).

From Westgate etal (1985)

No reversed interval was located in section 1, or in section 2, at either the 0, 10 or 20 mT demagnetization levels. As mentioned in chapter 3, section B, 3 pilot samples, all located about 2 metres beneath the Old Crow Tephra, tended toward negatively inclined magnetizations under high levels of demagnetization, giving an indication of an originally reversed magnetization. This evidence is far from compelling not only because a negatively inclined magnetization was never reached, but because other samples adjacent to these 3 which were demagnetized to roughly equivalent levels showed no sign of such movement. The question regarding why the Blake was absent from these sections arises. There are two possible explanations which seem likely.

There is a slight possibility that the Blake may have been present in these sections but was overlooked by the discrete sampling. As discussed in chapter 1 it is believed that the Blake lasted anywhere from 5,000 to 40,000 years. Earlier in this chapter it was concluded that the average time between sampled horizons does not exceed 400 years, but it may be true that the occasional consecutive horizons, spaced further apart, could be separated by enough time to miss the Blake Event. This explanation is contrived and thus not very satisfactory.

It is more likely that erosion, or non-deposition, has eliminated the Blake Event from these sections. As discussed in chapter 4, section B, at least one unconformity of unknown duration is preserved in section 1 roughly 2 metres beneath the Old Crow Tephra (this is roughly the level the Blake Event was located at in similar sediments by Westgate et al,1985 , at HH228). There exists the possibility that the unconformity at the level of the cryoturbation occurred during the Blake Event and the perturbation between -241 and -11 cm, which spans the cryoturbated interval, represents the beginning and end of the event (the central part, involving a complete reversal having been eroded away). It is felt that this is unlikely. An unconformity placed at such a location would invariably lead to a jump in the field vector movement. No such jump was observed, the field vector possessed a very continuous movement. It is more likely that a different unconformity has completely removed the Blake Event.

Although the Blake Event has not been recorded in section 1 a completely unexpected, and scientifically significant, form of secular variation has. This form, which is uniquely distinguished by its path coincidence on a Bauer plot, has rarely been observed in the past and is therefore poorly documented, but is strongly indicative of a stationary dipole located just beneath the core-mantle boundary. Such stationary sources, which have time varying amplitudes, provide an additional source of secular variation and it is hoped that with further study they will become better understood. The ramifications of such stationary sources will be dealt with further in the concluding chapter.

# 5. SUMMARY AND CONCLUSIONS

Four six-metre vertical sections of samples were retrieved from Pleistocene sediments, exposed by the Old Crow River in the northern Yukon, for the purpose of studying the recent high-latitude behavior of the geomagnetic field. Although difficulties involved with dating the strata have prevented the precise delineation of the time span involved it is believed to cover some or all of the time between 80,000 and 140,000 years B.P.. The initial goal of this research was to study any secular variation that occurred in this time span. However the single geomagnetic feature of greatest interest was the Blake Event which is believed to be a time of global reversed polarity that occurred about 100,000 years ago. It was hoped that the observation of this event might provide another date to aid the geological and archaeological interpretations of this area as well as provide much needed information on the Blake Event itself.

Although a full reversal is recorded in sediments of similar age just 35 km to the southwest, and has been interpreted as being due to the Blake Event, no reversed interval is located in any of the four sections sampled. It was concluded that this is most likely due to a hiatus. What is preserved, however, are two linear perturbations of the geomagnetic field that involve outward trajectories of 22° to a westerly declination and a shallow inclination with superimposed return trajectories. The existence of these perturbations is supported not only by the fact that they are recorded with strikingly similar character in each section but by a time series analysis which reveals a strong power peak, with a high degree of polarization, at the wavelength corresponding to the perturbations.

Crucial to determining the cause of the perturbations is an analysis of the angular dispersion of the VGPs in section 1 which reveals that an abnormally low average angular dispersion is preserved, relative to that predicted by theory. Regardless of the time span covered by a suite of paleomagnetic field measurements, logic dictates that any lack of dispersion must be due to the absence of the longer period geomagnetic field variations. The two most likely sources of secular variation in these sediments are non-dipole fluctuations (of period $10^3$ to $10^4$ years) and dipole wobble (of period $\geq 10^5$ years). Considering the dispersion due to non-dipole fluctuations alone gives an expected value just outside the standard error of the observed dispersion and it was therefore concluded that the lack of dispersion was due to dipole wobble not being averaged out. This conclusion is supported by consideration of likely sedimentation rates which reveals that the 6m of sediments sampled likely cover a length of time significantly less than than expected to be required for one period of dipole wobble. Furthermore, the displacement of the time-averaged virtual geomagnetic pole supports this conclusion. After reviewing all the likely causes of the far-sidedness of the time averaged VGP it was concluded it was most likely due to dipole wobble, the span of results being insufficient to provide anything more than a *snapshot*.

All points of analysis indicate that the pertubations must be due to fluctuations in the non-dipole field and thus the source was likely located just below the core-mantle boundary. More specifically, the linear nature of the perturbations, and the fact that they appear repeatedly, demanded that the source must have been stationary and have a time varying amplitude. A likely source is a liquid Ni-Fe eddy located under a bump, or inhomogeneity, at the core-mantle boundary. Such an eddy would most likely lead to a radially oriented magnetic dipole. The likelihood that such a radial dipole was the cause of these perturbations is further supported by elementary magnetostatic theory which reveales such a perturbation could be caused by a radial dipole with a magnetic moment as low as 8% of that of the Earth's main dipole. The possibility that a very similar perturbation located in southeast British Columbia in sediments ≃ 20,000 to 30,000 years old could be caused by the same source suggests that it could have existed for 80,000 years or more, although this conclusion is admittedly highly speculative.

The most recent work on the nature of the magnetic field at the core-mantle boundary has been undertaken by Bloxham and Gubbins (1985). They analysed six sets of direct observations of the total magnetic field covering the time from 1715 to 1980 AD. These workers were able to downward continue these data sets to the core-mantle boundary and produce maps of the radial component of the magnetic field at this level. This is a remarkable achievement considering the inherent instability of the downward continuation process. When viewed successively these maps constitute a sort of movie in which each frame is separated by some 50 years. Although a number of very interesting features are apparent from this movie, most relevant to this work is the presence of high concentrations of radially oriented flux (flux bundles) some of which have drifted and others, in the polar regions, that have remained stationary over the last 250 years. Although the stationary flux bundles are believed to give rise to the dipole field, not the non-dipole field, and thus cannot be the sources of perturbations similar to the ones studied in this work, it is this concentration of radially oriented flux into small areas that lends support to the theory that RDs exist at the core-mantle boundary. It is hoped that in the future studies of a similar nature will be undertaken to try to resolve further flux bundles to determine if any are stationary. It is work of this nature that is critical to testing the conclusions reached earlier in this thesis.

As discussed in section 4-E, it has been noted for several years that average observed inclinations at sites tend to be slightly more negative than those predicted assuming a purely dipolar field. Several models have been developed to explain this observation. One, by Wilson (1971), suggests that the main dipole may be shifted northward from the geocenter. This would superimpose a quadrupole component onto the dipole field and cause inclinations at sites all around the globe to be more negative. Cox (1975) felt this model was inadequate because he claimed to observe positively, not negatively, biassed field inclinations in the polar regions (above 50° N and S latitude). He suggested that this could be caused by permanent, or temporarily active, radial dipoles at the core-mantle boundary. Cox postulated that the flux from these radial dipoles is linked and emerges from the core in the equatorial region and re-enters the core in the polar regions. This would bias the observed inclinations negatively over the entire globe, except for the polar regions where the inclinations would become slightly more positive. The discovery of periodically recurring pertubations that cause a relatively shallow average field in this study (at 67° 51' N latitude) and by Turner et al (1982) (at 50° N latitude) casts serious doubt on Cox's hypothesis and may provide a third explanation for the biassing of the field inclinations. Temporarily active, outwardly directed, radial dipoles at the core-mantle boundary will not only cause the observed biassing of the average field all over the globe, but if randomly located on the core-mantle boundary they will, on average, lead to the greatest degree of biassing in the equatorial regions, where the unperturbed field is not only weak but roughly horizontal. (In addition because progressively more surface area is occupied by the more equatorial latitudes, random scattering of RDs will naturally concentrate more of them near the equator (50% would be between ±30° latitude), thus still more biassing would be expected at the lower latitudes.) The biassing would decrease to a minimum at the poles. A recent study by Merrill and McElhinny (1977) of the paleomagnetic field has shown that the biassing is greatest at the equator (involving some 5°) and decreases to zero near the poles. For this model to be tenable, as discussed above, such stationary RDs must generally be composed of outwardly directed flux. This has yet to be demonstrated by theoretical, or observational, work and it is hoped that further studies will be conducted into this problem. Given that this is true the presence of such RDs may explain the far-sidedness of the average VGPs that have been consistently observed in paleomagnetic studies over the last 20 years.

The sedimentary record is clearly not perfect. Some intervals are probably missing and others have been cryoturbated (which in some cases may have led to a resetting of the magnetization at a time significantly later than the time of deposition). Nevertheless the non-erratic paleomagnetic field vector movement clearly indicates that at least some segments contain an unbroken history of the geomagnetic field. Two of these segments of sediments reveal perturbations of the field that appear to be significant. The repeated observation of the perturbations with similar character (separated both in time in the same section and in space from section to section) argues strongly for their reality. It is hoped that further study of sequentially ordered samples will reveal further linear perturbations and permit a deeper understanding.

# BIBLIOGRAPHY

Adam,N.V., Benkova,N.P, Orlov,V.P., Tyurmina,L.O., 1964, Western drift of the geomagnetic field, *Geomag. Aeron.*, *4*, 434-441.

Allredge,L.D. and Hurwitz,L., 1964, Radial dipoles as sources of the Earth's main magnetic field, *J. Geophys. Res.*, *69*, 2631-2640.

Bloxham,J. and Gubbins,D., 1985, The secular variation of the Earth's magnetic field, *Nature*, *317*, 777-781.

Bullard,E.C., Freedman,C., Gellman,H., Nixon,J. 1950, The westward drift of the Earth's magnetic field, *Phil. Trans. Roy. Soc. London*, *A243*, 67-92.

Bullard,C.E., 1968, Reversals of the Earth's magnetic field, *Phil. Trans. Roy. Soc. London*, *A263*, 481.

Burlatskaya,S.P., Nechayva,T.B., Petrova,G.N., 1965, The westward drift of the secular variation of magnetic inclination and variations of the earth's magnetic moment according to archeomagnetic data, *Amer. Geophys. Union English Ed.*, *6*, 380.

Cox,A.V., 1968, Lengths of geomagnetic polarity intervals, *J. Geophys. Res.*, *73*, 3247.

Cox,A.V., 1969, A paleomagnetic study of secular variation in New Zealand, *Earth Planet. Sci. Lett.*, *6*, 257-267.

Cox,A.V., 1975, The frequency of geomagnetic reversals and the symmetry of the non-dipole field, *Reviews of Phys. and Space Phys.*, *13*, 35-51.

Creer,K.M., Georgi,D.T., Lowrie,W., 1973, On the representation of the Quaternary and Late Tertiary geomagnetic field in terms of dipoles and quadrupoles, *Geophys. J. Roy. Astron. Soc.*, *33*, 323-345.

Creer,K.M., 1977, Geomagnetic secular variations during the last 25000 years: an interpretation of data obtained from rapidly deposited sediments, *Geophys. J. Roy. Astron. Soc.*, *48*, 91-109.

Creer,K.M., Readman,P.W., Jacobs,A.M., 1980, Paleomagnetic and palentological dating of a section at Gioia Tauro, Italy:identification of the Blake Event, *Earth Planet. Sci. Lett.*, *50*, 289.

Creer, K.M., Tucholka, P., Barton, C.E., 1983, *Geomagnetism of baked clays and recent sediments*, Elsevier Science Publishing.

Denham,C.R., Anderson,R.F., Bacon,M.P., 1977, Paleomagnetism and radiochemical age estimates for late Brunhes polarity episodes, *Earth Planet. Sci. Lett.*, *35*, 384-397.

Doell,R.R. and Cox,A.V., 1965, Paleomagnetism in Hawaiian lava flows, *J. Geophys. Res.*, *70*, 3377.

Doell,R.R., 1970, Paleomagnetic secular variation study of lavas from the Massif Central, France, *Earth Planet. Sci. Lett.*, *8*, 352-362.

Doell,R.R., 1972, Paleosecular variation of the Honolulu volcanic series, Oahu, Hawaii, *J. Geoph. Res.*, *77*, 2129-2138.

Evans,M.E., 1984, Paleomagnetic evidence for stationary sources of geomagnetic secular variation, *Phys. Earth Planet. Interiors*, *35*, 223-226.

Fisher,R.A., 1953, Dispersion on a sphere, *Proc. Roy. Soc.*, *A217*, 295-305.

Harrison,C.G.A. and Ramirez,E., 1975, Areal coverage of spurious reversals of the Earth's magnetic field, *J. Geomagn. Geoelec.*, *27*, 139.

Harwood,J.M. and Malin,S.R.C., 1976, Present trends in the Earth's magnetic field, *Nature, 259*, 469-471.

Hoye,G.S., 1981, Archeomagnetic secular variation record of Mount Vesuvius, *Nature, 291*, 216-218.

Hughes,O.L., 1969, Pleistocene stratigraphy, Porcupine and Old Crow rivers, Yukon Territory, *Geological Survey of Canada, Paper 69-1*, 209-212.

Hughes,O.L., 1972, Surficial geology of northern Yukon Territory and northwestern district of Mackenzie, Northwest Territories, *Geological Survey of Canada, Paper 69-36*.

Hurwitz, L., 1960, Eccentric dipoles and spherical harmonic analysis,*J. Geophys. Res., 65*, 2555-2556.

Irving,E., *Paleomagnetism and its application to geological and geophysical problems*, 399 pp., John Wiley, New York.

Jacobs,J.A., 1984, *Reversals of the Earth's magnetic field*, 230pp., Adam Hilger Ltd., Bristol.

King,R.F., 1955, The remanent magnetism of artificially deposited sediments, *Monthly Notices, Roy. Astron. Soc., Geophys Suppl.,7*,115-134.

King,R.F., Rees,A.I., 1966, Detrital magnetism in sediments: An examination of some theoretical models, *J. Geophys. Res., 71*,561-571.

Kukal,Z., 1971, *Geology of Recent Sediments*, Academia Publ. House of the Czechoslovak Academy of Sciences, Prague, Published in English by Academic Press, London and New York.

Malin,S.R.C. and Bullard,E.C., 1981, The direction of the Earth's magnetic field at London, 1570-1975, *Philos. Trans. R. Soc. London, Ser A, 299* 357-423.

Marino,R.J., 1977, *Paleomagnetism of two lake sediment cores from Seward Peninsula, Alaska*, Unpub. M.Sc. thesis, Ohio State Univ., 183pp.

McElhinny,M.W., 1966, An improved method for demagnetizing rocks in alternating magnetic fields, *Geophys. J. Roy. Astron. Soc.*, *10*, 369-374.

McElhinny,M.W., 1973, *Paleomagnetism and Plate Tectonics*, 386 pp., Cambridge University Press, New York.

McElhinny,M.W. and Merrill, R.T., 1975, Geomagnetic secular variation over the past 5 m.y., *Rev. Geoph. Space Phys*, *13*, 687.

McFadden,P.L. and McElhinny,M.W., 1984, A physical model for paleosecular variation, *Geophys. J. Roy. Astron. Soc.*, *78*, 809-830.

Merrill,R.T. and McElhinny,M.W., 1977, Anomalies in the time averaged paleomagnetic field and their implication for the lower mantle, *Reviews of Geophys. and Space Phys.*, *15*,309-323.

Merrill,R.T. and McElhinny,M.W., 1983, *The Earth's Magnetic Field*, 401 pp., Academic Press,International Geophysics Series , 32.

Molyneux,L., 1971, A complete result magnetometer for measuring the remanent magnetization of rocks, *Geophys. J. Roy. Astr. Soc.*, *24*, 429-433.

Morlan,R.E., 1980, *Taphonomy and Archaeology in the Upper Pleistocene of northern Yukon Territory: A glimpse of the peopling of the New World*, National Museum of Man (Mercury Series), Archaeological Survey of Canada, Paper 94.

Morlan,R.E., 1986, *New Dates on the Old Crow Pleistocene*, Unpub. paper presented to the Archaeological Association, Toronto, 1986.

Murthy,G.S., 1969, *Paleomagnetic Studies in the Canadian Shield*, Unpub. Ph.D. thesis, Univ. of Alberta.

Oberg,C.J., 1978, *Quaternary paleomagnetic/geomagnetic studies in western Canada*, Unpub. M.Sc. thesis, Univ. of Alberta.

Opdyke,N.D., 1962, *Paleoclimatology and continental drift*, *In Runcorn,S.K.*, ed. Continental drift, Academic Press, N.Y., 41-65.

Parker,E.N., 1955, Hydromagnetic dynamo models, *Astrophys. J.*, *122*, 293-314.

Pearce,G.W., Westgate,J.A., Robertson,S., 1982, Magnetic reversal history of Pleistocene sediments at Old Crow , northwestern Yukon Territory, *Can. J. Earth Sciences*, *19*, 919-929.

Putnam, W.C. and Bassett, A.B., 1971, *Geology*, Oxford University Press 586 pp.

Reid,A.B., 1972, *A paleomagnetic study at 1,800 million years in Canada*, Unpub. Ph.D. thesis, Univ. of Alberta.

Sasajima,S., Nishimura,S., Hirooka,K, 1980, Studies on the Blake episode with special emphasis to East Asian results obtained , *Rock Magnetism and Paleomagnetism*, *7*, 90.

Shumskii,P.A., 1959, Podzemnye l'dy:274-327 (Glava Ix) m Inst Merzlotovedeniya im. V.A. Obrucheva, Osnovy, geokriologii (merzlotovedeniya), Chast pervaya, obshchaya geokriologiya, Moskva, Akad. Nauk S.S.S.R. (459 pp).

Smith,D.J. and Foster,J.H., 1969, Geomagnetic reversal in Brunhes normal polarity epoch, *Science*, *163*, 565.

Tucker,P., 1983, Magnetic remanence acquisition in IPOD leg 73 sediments. Init. Rep. *Deep Sea Drilling Project 73*.

Turner,G.M., Evans,M.E., Hussin,I.B., 1982, A Geomagnetic secular variation study (32,000-19,500 bp) in western Canada, *Geophys J. Roy. Astron. Soc., 71*, 159-171.

Verosub,K.L. and Banerjee,S.K., 1977, Geomagnetic excursions and their paleomagnetic record, *Reviews of Geoph. and Space Phys., 15*, 145-155.

Walde,K., 1986, *Pollen Analysis and Taphonomy of locality 15 Alluvial sediments, Old Crow Basin, Yukon*, Unpub. M.A. thesis, Univ of Alberta, Department of Anthropology.

Watkins,N.D. and Nougier,J., 1973, Excursions and secular variation of the Brunhes Epoch geomagnetic field in the Indian ocean region, *J. Geoph. Res., 78*, 6060-6068.

Watson, G.S., 1956a, Analysis of dispersion on a sphere, *Mon. Not. Roy. Ast. Soc., Geophys Supp., 7*, 153-159.

Westgate,J.A., Walter,R.C., Pearce,G.W., Gorton,M.P., 1985, Distribution, stratigraphy, petrochemistry, and paleomagnetism of the late Pleistocene Old Crow tephra in Alaska and the Yukon, *Can. J. Earth Sci., 22*, 893-906.

Westgate, J.A. and Wintle,A.G., 1986, Thermoluminescence age of Old Crow tephra in Alaska, *Unpub. paper*.

Wilson,R.L., 1971, Dipole offset-time averaged paleomagnetic field over the past 25 million years, *Geophys J. Roy. Astron. Soc., 22*, 491.

Yaskawa,K., Nakajima,T., Kawai,N., Torii,M., Notsuhara,N., Horie,S., 1973, Paleomagnetism of a core from Lake Biwa, *J. Geomag. Geoelec., 25*, 447.

Yukutake,T., 1962, The westward drift of the magnetic field of the Earth, *Bull. Earthq. Res. Inst., 40*, 1-65.

Yukutake,T., 1967, The westward drift of the Earth's magnetic field in historic times, *J. Jeomag. Geoelec., 19*, 103-116.

Yukutake,T. and Tachinaka,H., 1968, The non-dipole part of the Earth's magnetic field, *Bull. Earthq. Res. Inst., Tokyo*, *46*, 1027-1074.

# APPENDIX A (UNIT DESCRIPTIONS)

Due to the similarity of the units in sections A and B these strata are described once only. Correlations between sections C and D were not as apparent in the field so they have individual descriptions. Likely correlations are noted in the section D unit descriptions. Elevations in sections 1 and C are in centimeters from the Old Crow Tephra (positive above). Elevations in section D are relative to the disconformity A due to the absence of the Old Crow Tephra.

## A. Section 1

| Unit | Interval | | Description |
|---|---|---|---|
| | A | B | |
| AB-1 | +50→+2 | +50→+3 | Thinly interbedded fine sands and clayey silts. Sand layers 0.1 to 0.5 cm thick are light brown to cream. Occasional stringer of coarse sand (grains up to 0.5 mm across). Clayey layers 0.5 to 1.5 cm thick and dark grey to dark brown. |
| AB-2 | +2→0 | +3→0 | (Old Crow Tephra) Individual particles indistinquishable and cluster into furry clumps, steely grey. |
| AB-3 | 0→-23 | 0→-18 | Clayey silt, more massive, very dark grey, occasional thin bed |

| | | | |
|---|---|---|---|
| | | | (up to 0.5 cm) of light grey silt. |
| AB-4 | -23→-35 | -18→-32 | Light brown fine grained pebbly sands, 1 cm thick, interbedded with dark brown discontinuous organics up to 0.5 cm thick. Quite friable. |
| AB-5 | -35→-61 | -32→-75 | Fine grain sand, massive, rusty red, extremely friable. Contains small pods of dark red silt and dark grey pebbles up to 0.1 cm in diameter. |
| AB-6 | -61→-164 | -75→-202 | Interbedded dark grey silty clays and light brown to rusty red fine sands. All beds 0.5 to 2.0 cm thick. Some beds contain extremely fine undulating lamination (less than 0.1 cm thick) consisting of alternating silts and clays. Appears to lie unconformably on the underlying unit. |
| AB-7 | -164→-175 | -202→-216 | Light grey thinly bedded friable sand containing thin beds (less than 0.5 cm thick) of pebbly sand (pebbles up to 0.1 cm across and black to grey to |

| | | | |
|---|---|---|---|
| | | | white). Unit thickness extremely variable (from 5 to 50 cm in one place). Seems to have been caused by cryoturbation. |
| AB-8 | -175→-320 | -216→-335 | Dark grey clayey silts predominate but contain thin (less than 1 cm) beds of light grey silts. Clayey silts contain ripple marks. The upper 1 metre of the unit has been strongly affected by cryoturbation. Bedding has been distorted into convoluted patterns. Ice wedges are present. In places has been oxidized to a rusty red colour. |
| AB-9 | -320→-460 | -335→-460 | Predominantly light grey silts to fine sands which contain ripple marks involving dark brown organics. Beds range from 10 to 20 cm thick. Contain thinner (roughly 3 cm) beds of dark grey clayey silts. Vivianite present. In lower 40 cm reddish, fine sand predominates. |
| AB-10 | -460→-462 | -460→-462 | Twigs, peaty material and black, brown and red smooth but poorly |

| | | | |
|---|---|---|---|
| | | | rounded pebbles, 1 to 4 mm across. |
| AB-11 | -462→-550 | -462→-550 | Predominantly dark grey, very clayey silt, containing thin beds (less than 1 cm) of dark brown organics. Also contains discontinuous stringers (less than 0.5 cm) of light to dark grey silt which are in places ripple marked. Appears to have been slightly cryoturbated. |

**B. Section C**

| Unit | Interval | Description |
|---|---|---|
| C-1 | +86 and above | Laminated fine grain sands and silts, light brown to grey. Bottom of this interval is disconformity A. |
| C-2 | +86→+15 | Interbedded dark grey to brown to rusty red clayey silts. Beds are from 0.5 to 1 cm thick. Bottom 30 centimeters are in places cryoturbated. |
| C-3 | +15→0 | (Old Crow Tephra). Already described in section 1. Here it is more friable. |
| C-4 | 0→-60 | Dark grey very clayey silt that |

| | | |
|---|---|---|
| | | contains thin laminae of light brown silt to fine sand. |
| C-5 | -60→-81 | Interbedded light brown to cream silts and dark grey silty clays. Each of the beds contain very fine laminations. Lies unconformably on unit C-6. |
| C-6 | -81→-159 | Organic creamy brown to red brown silts. Beds range from 0.1 to 1 cm thick. Has been cryoturbated in places. Ice wedges present. |
| C-7 | -159→-167 | Creamy fine grained sand. Beds 3 to 5 cm thick. |
| C-8 | -167→-265 | Predominantly dark grey very clayey silt with 0.3 to 1 cm thick beds of light brown, probably organic, silt. Contains a couple of 1 cm thick beds of laminated and sometimes ripple marked silts. |
| C-9 | -265→-307 | Creamy medium grain sand with less than 1 cm thick dark grey very clayey silts and dark brown organic material. |
| C-10 | -307→-311 | Twigs and pebbles. |
| C-11 | -311→-406 | Predominantly massive dark grey |

| | | |
|---|---|---|
| | | very clayey silt. Less than 1 cm thick beds of light brown silt. Becomes more silty in lower 30 cm. |
| C-12 | -406→-550 | Interbedded tan to medium brown friable sands and dark brown silts. Occasional organic layer up to 2 cm thick. |

### C. Section D

| Unit | Interval | Description |
|---|---|---|
| D-1 | above 0 | Same as unit C-1 |
| D-2 | 0→-100 | Interbedded dark grey to brown to rusty red clayey silts 0.5 to 1 cm thick. Has been cryoturbated (containing small scale frost cracks) so than bedding is slightly convoluted. Correlates to unit C-2. |
| D-3 | -100→-129 | Massive dark grey silty clay. |
| D-4 | -129→-145 | Predominantly light grey fine sands containing less than 1 cm thick beds of dark grey and rusty red silt. Correlates to unit C-5. |
| D-5 | -145→-195 | Rusty red (oxidized) massive silt. Becomes coarser (sandy) |

| | | |
|---|---|---|
| | | and lighter red in bottom 10 cm. Massive nature makes it difficult to discern cryoturbation. |
| D-6 | -195→-306 | Interbedded light grey to tan fine sands containing ripple marks and dark brown laminated organic silts. Beds 1 to 5 cm thick. |
| D-7 | -306→-366 | Predominantly dark grey clayey silt containing less than 1 cm thick beds of medium brown organic laminated silt. Strongly resembles unit C-8. |
| D-8 | -366→-488 | Interbedded dark grey clayey silts and tan ripple marked sands. Sands are discontinuous in places. |

# APPENDIX B (THE INCLINOMETER)

In the past it has been common practice to fully orientate plastic sampling cubes inserted into vertical exposures using a Brunton compass. Although the Brunton can easily be used to determine strike with an accuracy of 0.5°, it is an awkward and time-consuming task to determine dip and roll using it. The primary difficulty is caused by the face and sides of the trench which make it very difficult to place the Brunton in the proper position against the cube and simultaneously view the inclination reading. Because the Brunton was not specifically designed for such a task it was decided that a specially designed inclinometer would prove useful.

The main objectives in the design were:

1) to produce an instrument with an accuracy comparable to the Brunton (0.5°),and

2) to allow viewing the level bubble from above the instrument while it is placed on the cube.

The design settled upon is sketched in figure B-1. In practice this inclinometer greatly facilitated the field work. In a good 10 hour day it is quite possible to collect 100 samples.

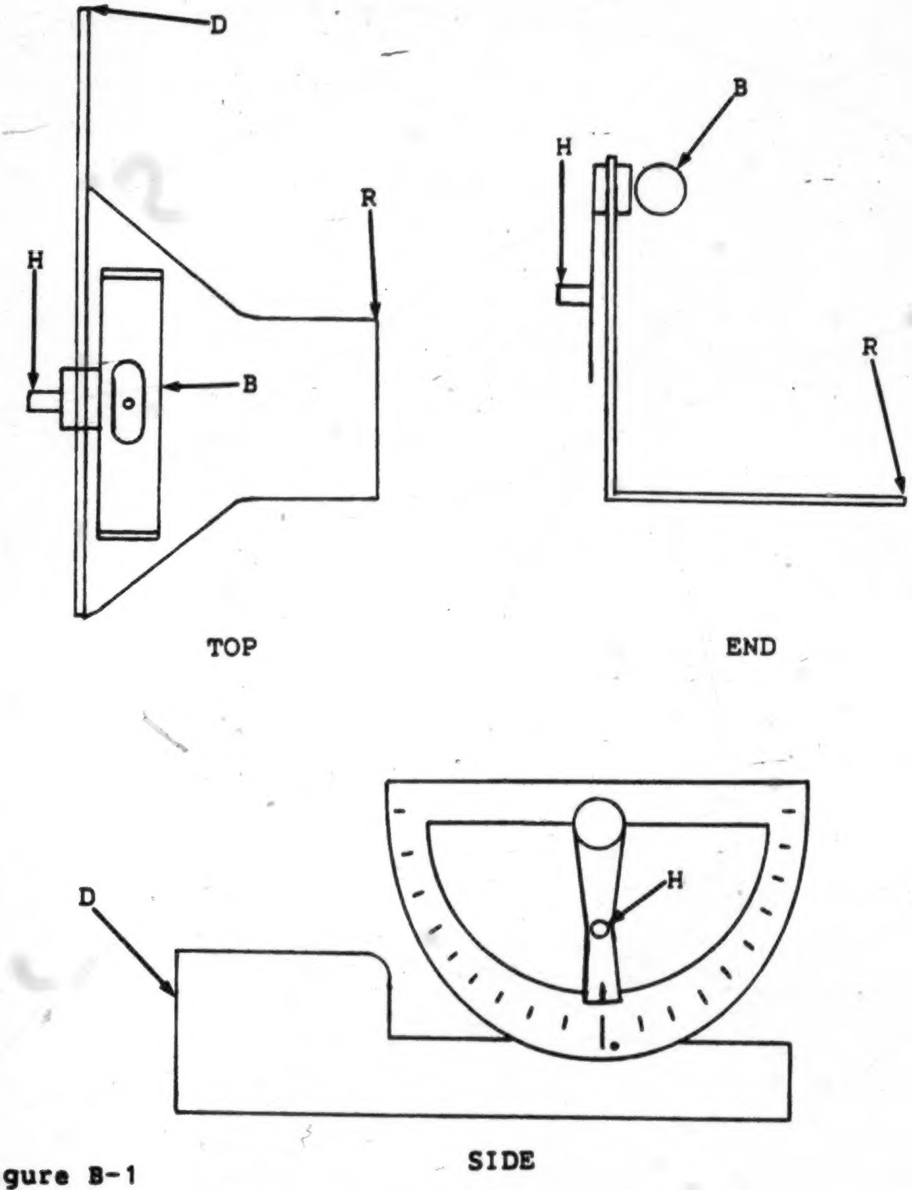

**Figure B-1**

A full scale drawing of the inclinometer designed by the author and Dr. M. E. Evans that was used in the orientation of samples for this study.

D denotes the surface used to determine Dip.
R denotes the surface used to determine Roll.
B denotes the bubble chamber.
H denotes the handle used to level the bubble chamber.

# APPENDIX C (MODELLING OF GEOMAGNETIC PERTURBATIONS)

The following magnetostatic theory is used in the program MODEL to delineate the great circles along which radial dipoles (RDs) at the core mantle boundary could cause observed perturbations of the geomagnetic field, and to determine the necessary magnetic moments required to cause a given perturbation.

A RD with magnetic moment $M_d$ is located any distance $R_d$ from the geocenter and at a colatitude $\theta_d$ and an east longitude $\phi_d$. The observation point is a distance $R_s$ from the geocenter and at a colatitude $\theta_s$ and east longitude $\phi_s$. The distance from the RD to the observation point equals

$$D=\sqrt{}(R_d^2 + R_s^2 \; 2R_dR_s\cos(\lambda))$$

where:

$$\lambda=\cos^{-1}\{ \cos(\theta_d)\cos(\theta_s) + \sin(\theta_d)\sin(\theta_s)\cos(\phi_s-\phi_d)\}$$

Letting: $A = \frac{M_d}{R_s^3}$, $B = \frac{D}{R_s}$, $C = \frac{R_d}{R_s}$

the potential (V) due to this dipole at the observation point equals

$$V = \{(A)(R_s)(\cos(\lambda) - \frac{R_d}{R_s})\}/B^3$$

The rectilinear components of the field are

$$X=-\frac{A}{B^3}\left(1+\frac{3C(\cos(\lambda)-R_d)}{B^2}\right)\cos\theta_d\sin\theta_s-\sin\theta_d\cos\theta_s\cos(\phi_s-\phi_d)$$

$$Y = \left(\frac{A}{B^3}\right)\left(1 + \frac{3C(\cos\lambda)-R_d}{B^2}\right)\left( \sin(\theta_d)\sin(\phi_s-\phi_d)\right)$$

$$Z = \left(\frac{A}{B^3}\right)\left(\cos(\lambda) - \frac{3(\cos(\lambda)-R_d)(1-R_d\cos(\lambda))}{B^2}\right)$$

where +X points toward geographic north, +Y points east and +Z points toward the geocenter (Alldredge and Hurwitz,1964). See figure 1-4 for a diagram illustrating the eccentric dipole involved.

```
      PROGRAM MODEL
C
C     THIS PROGRAM DETERMINES THE GEOGRAPHIC LOCATIONS
C     AND MAGNETIC MOMENTS, RELATIVE TO THE EARTH'S MAIN
C     DIPOLE, OF STATIONARY, RADIAL DIPOLES (RD'S)
C     SITUATED AT THE CORE-MANTLE INTERFACE THAT ARE
C     REQUIRED TO CAUSE AN OBSERVED PERTURBATION OF THE
C     GEOMAGNETIC FIELD.
C
C     THE COLATITUDES AND EAST LONGITUDES OF CANDIDATE
C     DIPOLES ARE ENTERED (FORMAT 2F6.1). THE PROGRAM
C     ADJUSTS THE LONGITUDE SO THE RD CAN CAUSE THE
C     OBSERVED GEOMAGNETIC PERTURBATION. IT THEN CALCULATES
C     AND CHECKS THE RD'S MAGNETIC MOMENT TO ELIMINATE ANY
C     POSSIBLE ARC TRIG FUNCTION ERRORS CAUSED BY THE
C     COMPUTER.
C
C     INPUT AND OUTPUT PARAMETERS ARE AS FOLLOWS:
C
C     PERINC=THE GEOMAGNETIC FIELD'S PERTURBED INCLINATION
C         (DEG).
C     PERDEC=THE GEOMAGNETIC FIELD'S PERTURBED DECLINATION
C         (DEG).
C     ELONMI AND CLAMI=THE EAST LONGITUDE AND COLATITUDE OF
C         THE RD CLOSEST TO THE SITE (DEG).
C     ELONGM AND CLATM=THE EAST LONGITUDE AND COLATITUDE
C         OF THE EARTH'S MAIN DIPOLE (DEG).
C     ELONGS AND CLATS=THE EAST LONGITUDE AND COLATITUDE
C         OF OBSERVATION POINT (DEG).
C     ELONGD AND CLATD=THE EAST LONGITUDE AND COLATITUDE
C         OF THE RD'S (DEG).
C     RADM=THE DISTANCE FROM THE GEOCENTER OF THE EARTH'S
C         MAIN DIPOLE (M).
C     RADD=THE DISTANCE FROM THE GEOCENTER OF THE RADIAL
C         DIPOLES (M).
C     RADS=THE DISTANCE FROM THE GEOCENTER OF THE
C         OBSERVATION POINT (M).
C     AMPM=THE MAGNETIC MOMENT OF THE EARTH'S MAIN DIPOLE
C         (AM**2).
C     AMPD=THE MAGNETIC MOMENT OF THE RD'S (AM**2).
C     COLATT=THE EPICENTRAL DISTANCE FROM THE RD TO THE RD
C         CLOSEST TO THE OBSERVATION POINT (DEG).
C     RATIO=THE RATIO OF THE RD'S AND THE EARTH'S MAIN
C         DIPOLE MOMENT.
C
      REAL INC
      INTEGER DIRN
C
   15 FORMAT(2F6.1)
   25 FORMAT(3F9.4,2X,F7.4)
C
C     HARD TERM INITIALIZATION
C
C     IF THE PERTURBING DIPOLE POINTS TOWARD THE EARTH'S
```

```
C     CENTER LET DIRN=1, ELSE LET DIRN=0
C
      DIRN=1
      PERINC=57.0
      PERDEC=-23.0
      ELONMI=241.0
      CLAMI=18.0
      ELONGM=197.7
      CLATM=168.8
      ELONGS=220.2
      CLATS=22.1
      RADM=0.
      RADD=2900000.
      RADS=6371000.
      AMPM=8.06E+22
      AMPD=AMPM
      PI=3.141592654
      CONV=PI/180.
      COUNT=0.
      PERINC=PERINC*CONV
      PERDEC=PERDEC*CONV
      ELONGM=ELONGM*CONV
      ELONGD=ELONGD*CONV
      ELONGS=ELONGS*CONV
      ELONMI=ELONMI*CONV
      CLATM=CLATM*CONV
      CLATD=CLATD*CONV
      CLATS=CLATS*CONV
      CLAMI=CLAMI*CONV
      XXS=SIN(CLATS)*COS(ELONGS)
      YYS=SIN(CLATS)*SIN(ELONGS)
      ZZS=COS(CLATS)
      XXM=SIN(CLATM)*COS(ELONGM)
      YYM=SIN(CLATM)*SIN(ELONGM)
      ZZM=COS(CLATM)
      XXMI=SIN(CLAMI)*COS(ELONMI)
      YYMI=SIN(CLAMI)*SIN(ELONMI)
      ZZMI=COS(CLAMI)
C
C     CALCULATE FIELD OF MAIN DIPOLE
C
      DLONGM=ELONGS-ELONGM
      C4M=SIN(CLATM)*SIN(CLATS)
      COSGAM=COS(CLATM)*COS(CLATS)+C4M*COS(DLONGM)
      DESQM=RADS**2
      AKPM=AMPM/(RADS**3)
      DPM=(SQRT(DESQM))/RADS
      C1M=AKPM/(DPM**3)
      C2M=COSGAM
      C3M=COS(CLATM)*SIN(CLATS)-SIN(CLATM)*COS(CLATS)
     + *COS(DLONGM)
      XM=-C1M*C3M*100.
      YM=C1M*SIN(CLATM)*SIN(DLONGM)*100.
      ZM=C1M*(COSGAM-3.*C2M/(DPM**2))*100.
```

```
C
C     CALCULATE THE RECTILINEAR COMPONENTS OF THE PERTURBED
C     VECTOR.
C
      XP=COS(PERINC)*COS(PERDEC)
      YP=COS(PERINC)*SIN(PERDEC)
      ZP=SIN(PERINC)
C
C     DETERMINE THE CROSS PRODUCT OF THE MAIN AND
C     PERTURBED VECTORS.
C
      CROSSX=YM*ZP-YP*ZM
      CROSSY=XP*ZM-XM*ZP
      CROSSZ=XM*YP-XP*YM
C
C
C     DETERMINE THE ANGLE BETWEEN THE UNPERTURBED AND
C     PERTURBED VECTORS.
C
      CALL ANGLE(XP,YP,ZP,RP,XM,YM,ZM,RM,THETA1)
C
C     DETERMINE THE RECTILINEAR COMPONENTS OF THE
C     PERTURBING VECTOR
C
   10 READ(5,15,END=20) ELONGD,CLATD
      IFLAG=0
      ELONGD=ELONGD*CONV
      CLATD=CLATD*CONV
   11 COUNT=COUNT+1.
      IF(COUNT.GT.4000)THEN
        COUNT=0.
        PRINT*, 'NO RD AT THIS LATITUDE CAN CAUSE
        PERTURBATION'
        GOTO10
      ENDIF
      IF(ELONGD.GT.2*PI)ELONGD=ELONGD-2*PI
      XXD=SIN(CLATD)*COS(ELONGD)
      YYD=SIN(CLATD)*SIN(ELONGD)
      ZZD=COS(CLATD)
      DLONGD=ELONGS-ELONGD
      C4D=SIN(CLATD)*SIN(CLATS)
      COSGAD=COS(CLATD)*COS(CLATS)+C4D*COS(DLONGD)
      DESQD=RADD**2+RADS**2-2.*RADD*RADS*COSGAD
      DPD=(SQRT(DESQD))/RADS
      RPD=RADD/RADS
      C2D=COSGAD-RPD
      C3D=COS(CLATD)*SIN(CLATS)-SIN(CLATD)*COS(CLATS)
     +*COS(DLONGD)
      AKPD=AMPD/(RADS**3)
      C1D=AKPD/(DPD**3)
      XD=-C1D*(1.+3.*RPD*C2D/(DPD**2))*C3D*100.
      YD=C1D*(1.+3.*RPD*C2D/(DPD**2))*SIN(CLATD)
     +*SIN(DLONGD)*100.
      ZD=C1D*(COSGAD-3.*C2D*(1.-RPD*COSGAD)/(DPD**2))*100.
      RDOLD=SQRT(XD**2+YD**2+ZD**2)
C
C     DETERMINE THE ANGLE BETWEEN THE CROSS PRODUCT OF
C     THE DIPOLE AND PERTURBED VECTORS AND THE THE
C     PERTURBING VECTOR (SHOULD BE CLOSE TO 90 DEGREES).
C
      CALL ANGLE(CROSSX,CROSSY,CROSSZ,CROSSR,XD,YD,ZD,RD,A)
      IF(A.GT.PI)A=A-PI
      IF(A.LT.-PI)A=A+PI
      IF(A.GT.1.58)THEN
        ELONGD=ELONGD+.005
        GOTO11
      ENDIF
      IF(A.LT.1.56.AND.A.GT.0.)THEN
        ELONGD=ELONGD-.005
        GOTO11
      ENDIF
      IF(A.LT.-1.58)THEN
        ELONGD=ELONGD-.005
        GOTO11
      ENDIF
      IF(A.GT.-1.56.AND.A.LT.0.)THEN
        ELONGD=ELONGD+.005
        GOTO11
      ENDIF
C
C     DETERMINE THE ANGLES BETWEEN THE PERTURBING VECTOR AND
C     THE DIPOLE AND PERTURBED VECTORS
C
      IF(DIRN.EQ.1)THEN
        XD=XD*(-1.0)
        YD=YD*(-1.0)
        ZD=ZD*(-1.0)
      ENDIF
      CALL ANGLE(XD,YD,ZD,RD,XM,YM,ZM,RM,THETA2)
      CALL ANGLE(XD,YD,ZD,RD,XP,YP,ZP,RP,THETA3)
C
C     DETERMINE THE NECESSARY PERTURBING VECTOR LENGTH
C
      RD=RM*SIN(THETA1)/SIN(THETA3)
      XD=XD*RD/RDOLD
      YD=YD*RD/RDOLD
      ZD=ZD*RD/RDOLD
      DINC=ATAN2(ZD,SQRT(XD**2+YD**2))
      DDEC=ATAN2(YD,XD)
C
C     DETERMINE THE COLATITUDES OF THE POINT
C     OF MINIMUM DIPOLE MAGNITUDE AND THE RATIO
C     OF THE MAIN TO PERTURBING DIPOLE MOMENTS.
C
      CALL ANGLE(XXS,YYS,ZZS,RRS,XXM,YYM,ZZM,RRM,COLATM)
      CALL ANGLE(XXS,YYS,ZZS,RRS,XXD,YYD,ZZD,RRD,COLATD)
      CALL ANGLE(XXMI,YYMI,ZZMI,RRMI,XXD,YYD,ZZD,RRD,COLATT)
      TOP=RD*(DESQD**1.5)*SQRT(1.+3.*(COS(COLATM)**2))
      BOTTOM=SQRT(1.+3.*(COS(COLATD)**2))*RM*(RADS**3)
      RATIO=TOP/BOTTOM
      XT=XD+XM
      YT=YD+YM
      ZT=ZD+ZM
      TINC=ATAN2(ZT,SQRT(XT**2+YT**2))/CONV
      TDEC=ATAN2(YT,XT)/CONV
C
C     CHECK RATIO TO MAKE SURE ITS CORRECT
C
   86 AMPD=AMPM*RATIO
      C4D=SIN(CLATD)*SIN(CLATS)
      COSGAD=COS(CLATD)*COS(CLATS)+C4D*COS(DLONGD)
      DESQD=RADD**2+RADS**2-2.*RADD*RADS*COSGAD
      DPD=(SQRT(DESQD))/RADS
      RPD=RADD/RADS
      C2D=COSGAD-RPD
      C3D=COS(CLATD)*SIN(CLATS)-SIN(CLATD)*COS(CLATS)
     + *COS(DLONGD)
      AKPD=AMPD/(RADS**3)
      C1D=AKPD/(DPD**3)
      XD=-C1D*(1.+3.*RPD*C2D/(DPD**2))*C3D*100.
      YD=C1D*(1.+3.*RPD*C2D/(DPD**2))*SIN(CLATD)
     + *SIN(DLONGD)*100.
      ZD=C1D*(COSGAD-3.*C2D*(1.-RPD*COSGAD)/(DPD**2))*100.
      XT=XD+XM
      YT=YD+YM
      ZT=ZD+ZM
      RRINC=ATAN2(ZT,SQRT(XT**2+YT**2))
      IF(RRINC.GT.PERINC)THEN
        RATIO=RATIO*1.01
        IFLAG=1
        GOTO86
      ENDIF
      IF(IFLAG.EQ.1)THEN
        RATIO=RATIO/1.01
      ENDIF
      WRITE(6,25) ELONGD/CONV,CLATD/CONV,COLATT/CONV,RATIO
      GOTO10
   20 END
C
      SUBROUTINE ANGLE(X1,Y1,Z1,R1,X2,Y2,Z2,R2,THETA)
        PI=3.141592654
        DOTPRO=X1*X2+Y1*Y2+Z1*Z2
        R1=SQRT(X1*X1+Y1*Y1+Z1*Z1)
        R2=SQRT(X2*X2+Y2*Y2+Z2*Z2)
        THETA=ACOS(DOTPRO/(R1*R2))
        RETURN
        END
```

## APPENDIX D (DATA ARCHIVE)

The data used in this thesis is arranged into 10 columns as follows:

| | |
|---|---|
| COLUMN 1: | Section name. |
| COLUMN 2: | Sample number (starred samples were collected from cryoturbated strata). |
| COLUMN 3: | A.F. demagnetization field in mT. |
| COLUMNS 4 to 6: | Strike, Dip and Roll respectively (in degrees,see fig. 2-7). |
| COLUMNS 7 to 9: | The X, Y and Z components of magnetization as measured by the Digico magnetometer (specimen frame). These components form a right handed orthogonal system with +Y parallel to the front of the cube (the side with the hole) and pointing to the right. Multiply by 8 x $10^{-2}$ to obtain intensity in $Am^{-1}$. |
| COLUMN 10: | Elevation of sample. In sections A,B and C this figure is relative to the Old Crow Tephra. In section D it is relative to Disconformity A. |

NOTE 1: At the time of sample collection (June,1985) the local magnetic declination was 33°30' E.

NOTE 2: No data at demagnetization levels of 10 and 20 mT for section C more than 3.5 metres below the Old Crow Tephra is present because the intensities of these samples approach the noise level of the Digico magnetometer resulting in internal variances of unacceptably high levels.

| | | | | | | | | | |
|---|---|---|---|---|---|---|---|---|---|
| A | 1 | 0 | 328.0 | 1.0 | 0.0 | -0.475 | 5.422 | 18.461 | 50 |
| A | 1 | 10 | 328.0 | 1.5 | 0.0 | -0.532 | 3.142 | 12.885 | 50 |
| A | 1 | 20 | 328.0 | 1.5 | 0.0 | -0.340 | 1.972 | 7.994 | 50 |
| A | 2 | 0 | 329.5 | 6.5 | -0.5 | 1.199 | 4.693 | 17.179 | 50 |
| A | 2 | 10 | 329.5 | 6.5 | -0.5 | 1.126 | 3.040 | 11.587 | 50 |
| A | 2 | 20 | 329.5 | 6.5 | -0.5 | 0.689 | 1.937 | 7.541 | 50 |
| A | 3 | 0 | 329.0 | -2.0 | -1.5 | -0.474 | 0.359 | 6.742 | 45 |
| A | 3 | 10 | 329.0 | -2.0 | -1.5 | -0.163 | 0.309 | 4.155 | 45 |
| A | 3 | 20 | 329.0 | -2.0 | -1.5 | -0.056 | 0.278 | 2.518 | 45 |
| A | 4 | 0 | 328.5 | -1.0 | -1.0 | -1.303 | 2.253 | 6.849 | 45 |
| A | 4 | 10 | 328.5 | -1.0 | -1.0 | -0.699 | 1.379 | 4.438 | 45 |
| A | 4 | 20 | 328.5 | -1.0 | -1.0 | -0.351 | 0.870 | 2.757 | 45 |
| A | 5 | 0 | 332.0 | 0.0 | -1.0 | -0.438 | 0.372 | 7.467 | 40 |
| A | 5 | 10 | 332.0 | 0.0 | -1.0 | 0.211 | -0.124 | 5.136 | 40 |
| A | 5 | 20 | 332.0 | 0.0 | -1.0 | 0.002 | -0.025 | 3.366 | 40 |
| A | 6 | 0 | 334.0 | 0.5 | -1.0 | -0.670 | 1.459 | 6.111 | 40 |
| A | 6 | 10 | 334.0 | 0.5 | -1.0 | -0.130 | 1.127 | 4.165 | 40 |
| A | 6 | 20 | 334.0 | 0.5 | -1.0 | -0.033 | 0.620 | 2.439 | 40 |
| A | 7 | 0 | 331.5 | -1.0 | 0.5 | -0.409 | 0.549 | 6.071 | 35 |
| A | 7 | 10 | 331.5 | -1.0 | 0.5 | -0.042 | 0.151 | 4.062 | 35 |
| A | 7 | 20 | 331.5 | -1.0 | 0.5 | 0.015 | 0.063 | 2.635 | 35 |
| A | 8 | 0 | 330.0 | -4.0 | 1.0 | -0.574 | 0.137 | 5.799 | 35 |
| A | 8 | 10 | 330.0 | -4.0 | 1.0 | -0.169 | 0.033 | 3.691 | 35 |
| A | 8 | 20 | 330.0 | -4.0 | 1.0 | -0.139 | 0.003 | 2.219 | 35 |
| A | 9 | 0 | 326.0 | -2.0 | -0.5 | -1.162 | 0.712 | 6.500 | 32 |
| A | 9 | 10 | 326.0 | -2.0 | -0.5 | -0.495 | 0.307 | 4.082 | 32 |
| A | 9 | 20 | 326.0 | -2.0 | -0.5 | -0.296 | 0.182 | 2.979 | 32 |
| A | 10 | 0 | 331.0 | 2.0 | 1.5 | -0.348 | 0.957 | 6.057 | 32 |
| A | 10 | 10 | 331.0 | 2.0 | 1.5 | 0.052 | 0.848 | 4.156 | 32 |
| A | 10 | 20 | 331.0 | 2.0 | 1.5 | -0.038 | 0.454 | 2.581 | 32 |
| A | 11 | 0 | 331.0 | 2.0 | -1.0 | -0.852 | 1.452 | 8.548 | 24 |
| A | 11 | 10 | 331.0 | 2.0 | -1.0 | -0.253 | 0.726 | 5.565 | 24 |
| A | 11 | 20 | 331.0 | 2.0 | -1.0 | -0.154 | 0.397 | 3.631 | 24 |
| A | 12 | 0 | 331.0 | 1.0 | -2.0 | 0.273 | 0.958 | 8.347 | 24 |
| A | 12 | 10 | 331.0 | 1.0 | -2.0 | 0.258 | 0.599 | 5.514 | 24 |
| A | 12 | 20 | 331.0 | 1.0 | -2.0 | 0.204 | 0.431 | 3.358 | 24 |
| A | 13 | 0 | 330.5 | 6.5 | 1.0 | 0.993 | 2.342 | 9.689 | 18 |
| A | 13 | 10 | 330.5 | 6.5 | 1.0 | 1.042 | 1.430 | 5.403 | 18 |
| A | 13 | 20 | 330.5 | 6.5 | 1.0 | 0.688 | 0.995 | 3.468 | 18 |
| A | 14 | 0 | 331.5 | 2.0 | 0.0 | 0.596 | 1.312 | 8.379 | 18 |
| A | 14 | 10 | 331.5 | 2.0 | 0.0 | 0.590 | 0.560 | 4.965 | 18 |
| A | 14 | 20 | 331.5 | 2.0 | 0.0 | 0.491 | 0.236 | 2.933 | 18 |
| A | 15 | 0 | 328.0 | 1.0 | 0.0 | -0.542 | 2.464 | 10.675 | 14 |
| A | 15 | 10 | 328.0 | 1.0 | 0.0 | -0.107 | 1.462 | 6.624 | 14 |
| A | 15 | 20 | 328.0 | 1.0 | 0.0 | -0.242 | 0.889 | 4.243 | 14 |
| A | 16 | 0 | 328.0 | 0.5 | -2.0 | -0.799 | 2.666 | 11.930 | 14 |
| A | 16 | 10 | 328.0 | 0.5 | -2.0 | -0.338 | 1.739 | 8.010 | 14 |
| A | 16 | 20 | 328.0 | 0.5 | -2.0 | -0.180 | 1.338 | 4.952 | 14 |
| A | 17 | 0 | 326.5 | 1.0 | 0.5 | -0.265 | 3.386 | 11.166 | 9 |
| A | 17 | 10 | 326.5 | 1.0 | 0.5 | 0.399 | 2.706 | 7.682 | 9 |
| A | 17 | 20 | 326.5 | 1.0 | 0.5 | 0.226 | 1.489 | 4.869 | 9 |
| A | 17 | 50 | 326.5 | 1.0 | 0.5 | -0.217 | 0.155 | 1.453 | 9 |
| A | 17 | 60 | 326.5 | 1.0 | 0.5 | 0.020 | 0.239 | 1.017 | 9 |
| A | 17 | 80 | 326.5 | 1.0 | 0.5 | -0.230 | 0.101 | 0.100 | 9 |
| A | 18 | 0 | 331.5 | 1.5 | -2.0 | -0.620 | 3.602 | 13.283 | 9 |
| A | 18 | 10 | 331.5 | 1.5 | -2.0 | -0.061 | 2.640 | 9.506 | 9 |
| A | 18 | 20 | 331.5 | 1.5 | -2.0 | 0.191 | 1.522 | 5.689 | 9 |
| A | 18 | 30 | 331.5 | 1.5 | -2.0 | 0.106 | 1.079 | 3.566 | 9 |
| A | 18 | 40 | 331.5 | 1.5 | -2.0 | 0.227 | 0.667 | 2.618 | 9 |
| A | 18 | 50 | 331.5 | 1.5 | -2.0 | 0.156 | 0.415 | 2.037 | 9 |
| A | 18 | 60 | 331.5 | 1.5 | -2.0 | -0.097 | 0.234 | 0.920 | 9 |
| A | 18 | 80 | 331.5 | 1.5 | -2.0 | -0.007 | 0.366 | 0.649 | 9 |
| A | 19 | 0 | 325.0 | 0.0 | 0.0 | -1.283 | 5.481 | 12.278 | 4 |
| A | 19 | 10 | 325.0 | 0.0 | 0.0 | -0.494 | 3.511 | 7.832 | 4 |
| A | 19 | 20 | 325.0 | 0.0 | 0.0 | -0.122 | 2.351 | 4.927 | 4 |
| A | 20 | 0 | 330.0 | 2.0 | 0.5 | -1.129 | 4.573 | 10.573 | 4 |
| A | 20 | 10 | 330.0 | 2.0 | 0.5 | -0.671 | 3.143 | 6.856 | 4 |
| A | 20 | 20 | 330.0 | 2.0 | 0.5 | -0.387 | 1.942 | 4.199 | 4 |
| A | 21 | 0 | 324.5 | -0.5 | -1.0 | -3.815 | 9.578 | 35.043 | 0 |
| A | 21 | 10 | 324.5 | -0.5 | -1.0 | -2.264 | 6.318 | 21.793 | 0 |
| A | 21 | 20 | 324.5 | -0.5 | -1.0 | -1.986 | 4.303 | 12.429 | 0 |
| A | 22 | 0 | 333.5 | -2.0 | 0.0 | -2.226 | 9.682 | 27.442 | 0 |
| A | 22 | 10 | 333.5 | -2.0 | 0.0 | -1.138 | 6.771 | 17.252 | 0 |
| A | 22 | 20 | 333.5 | -2.0 | 0.0 | -0.238 | 4.003 | 10.193 | 0 |
| A | 23 | 0 | 324.5 | -1.5 | -3.5 | -1.745 | 2.975 | 7.881 | -5 |
| A | 23 | 10 | 324.5 | -1.5 | -3.5 | -1.011 | 2.229 | 4.838 | -5 |
| A | 23 | 20 | 324.5 | -1.5 | -3.5 | -0.583 | 1.374 | 2.989 | -5 |
| A | 24 | 0 | 328.5 | -1.5 | 0.0 | -1.106 | 2.927 | 8.263 | -5 |
| A | 24 | 10 | 328.5 | -1.5 | 0.0 | -0.553 | 1.962 | 5.265 | -5 |
| A | 24 | 20 | 328.5 | -1.5 | 0.0 | -0.514 | 1.330 | 3.171 | -5 |
| A | 25 | 0 | 323.5 | -1.0 | 2.0 | -1.151 | 1.836 | 6.838 | -10 |
| A | 25 | 10 | 323.5 | -1.0 | 2.0 | -0.508 | 1.162 | 3.998 | -10 |
| A | 25 | 20 | 323.5 | -1.0 | 2.0 | -0.234 | 0.635 | 2.417 | -10 |
| A | 26 | 0 | 328.5 | 0.5 | -1.0 | -0.922 | 1.253 | 5.314 | -10 |
| A | 26 | 10 | 328.5 | 0.5 | -1.0 | -0.586 | 0.689 | 3.057 | -10 |
| A | 26 | 20 | 328.5 | 0.5 | -1.0 | -0.218 | 0.454 | 1.710 | -10 |
| A | 27 | 0 | 324.0 | 3.0 | -1.0 | -0.232 | 1.306 | 5.185 | -15 |
| A | 27 | 10 | 324.0 | 3.0 | -1.0 | -0.056 | 0.879 | 2.957 | -15 |
| A | 27 | 20 | 324.0 | 3.0 | -1.0 | -0.181 | 0.564 | 1.779 | -15 |
| A | 28 | 0 | 328.0 | -2.0 | -2.0 | -0.924 | 1.512 | 5.295 | -15 |
| A | 28 | 10 | 328.0 | -2.0 | -2.0 | -0.632 | 0.854 | 3.080 | -15 |
| A | 28 | 20 | 328.0 | -2.0 | -2.0 | -0.172 | 0.324 | 1.766 | -15 |
| A | 29 | 0 | 315.5 | 4.0 | 3.0 | -0.013 | 0.995 | 3.891 | -20 |
| A | 29 | 10 | 315.5 | 4.0 | 3.0 | 0.033 | 0.451 | 2.201 | -20 |
| A | 29 | 20 | 315.5 | 4.0 | 3.0 | -0.207 | 0.505 | 1.180 | -20 |
| A | 30 | 0 | 325.0 | 0.0 | -2.0 | -0.819 | 0.898 | 4.241 | -20 |
| A | 30 | 10 | 325.0 | 0.0 | -2.0 | -0.588 | 0.671 | 2.431 | -20 |
| A | 30 | 20 | 325.0 | 0.0 | -2.0 | -0.342 | 0.364 | 1.430 | -20 |
| A | 31 | 0 | 331.0 | 4.0 | -4.0 | -0.183 | 0.559 | 2.341 | -25 |
| A | 31 | 10 | 331.0 | 4.0 | -4.0 | 0.047 | 0.387 | 1.168 | -25 |
| A | 31 | 20 | 331.0 | 4.0 | -4.0 | 0.173 | 0.306 | 0.695 | -25 |
| A | 32 | 0 | 321.0 | 6.0 | -5.5 | -1.843 | 0.228 | 3.264 | -25 |
| A | 32 | 10 | 321.0 | 6.0 | -5.5 | 1.326 | 0.174 | 2.052 | -25 |
| A | 32 | 20 | 321.0 | 6.0 | -5.5 | 0.575 | -0.452 | 0.529 | -25 |
| A | 33 | 0 | 329.0 | 3.5 | 0.5 | -0.372 | 1.150 | 3.485 | -30 |
| A | 34 | 0 | 341.5 | 7.0 | -3.0 | 1.169 | 0.795 | 3.892 | -30 |
| A | 35 | 0 | 330.5 | 1.0 | -1.0 | -0.058 | 0.598 | 3.114 | -62 |
| A | 35 | 10 | 330.5 | 1.0 | -1.0 | 0.299 | 0.459 | 1.955 | -62 |
| A | 35 | 20 | 330.5 | 1.0 | -1.0 | 0.163 | 0.389 | 1.402 | -62 |
| A | 36 | 0 | 330.5 | 3.0 | -1.5 | -0.216 | 0.938 | 3.899 | -62 |
| A | 36 | 10 | 330.5 | 3.0 | -1.5 | 0.105 | 0.485 | 2.563 | -62 |
| A | 36 | 20 | 330.5 | 3.0 | -1.5 | 0.154 | 0.426 | 1.745 | -62 |
| A | 37 | 0 | 332.5 | 0.0 | -4.0 | 0.262 | 1.377 | 4.996 | -72 |
| A | 37 | 10 | 332.5 | 0.0 | -4.0 | 0.597 | 0.597 | 2.582 | -72 |
| A | 37 | 20 | 332.5 | 0.0 | -4.0 | 0.460 | 0.235 | 1.261 | -72 |
| A | 38 | 0 | 343.0 | 4.5 | -1.5 | 0.086 | 0.866 | 4.530 | -72 |
| A | 38 | 10 | 343.0 | 4.5 | -1.5 | 0.379 | 0.529 | 2.467 | -72 |
| A | 38 | 20 | 343.0 | 4.5 | -1.5 | 0.312 | 0.339 | 1.669 | -72 |
| A | 39 | 0 | 331.0 | 4.0 | -0.5 | 1.205 | 2.447 | 5.175 | -79 |
| A | 39 | 10 | 331.0 | 4.0 | -0.5 | 0.873 | 1.736 | 3.239 | -79 |

```
A   39    20 331.0    4.0  -0.5      0.617      1.194      2.009   -79
A   40     0 339.0    4.5   3.5      1.072      2.202      4.392   -79
A   40    10 339.0    4.5   3.5      1.037      1.516      2.752   -79
A   40    20 339.0    4.5   3.5      0.996      1.211      1.844   -79
A   41     0 334.0    0.5   1.5      0.333      1.230      4.632   -88
A   41    10 334.0    0.5   1.5      0.559      0.778      2.775   -88
A   41    20 334.0    0.5   1.5      0.541      0.389      1.609   -88
A   42     0 338.0    2.5   1.0     -0.021      1.751      5.391   -88
A   42    10 338.0    2.5   1.0      0.541      0.832      2.842   -88
A   42    20 338.0    2.5   1.0      0.624      0.531      2.034   -88
A   43     0 330.0    5.0   1.5      1.326      1.984      4.266   -96
A   43    10 330.0    5.0   1.5      1.234      1.373      2.501   -96
A   43    20 330.0    5.0   1.5      0.583      0.787      1.358   -96
A   44     0 344.5    5.5  -1.0      1.430      2.724      6.705   -96
A   44    10 344.5    5.5  -1.0      1.390      1.580      4.049   -96
A   44    20 344.5    5.5  -1.0      1.036      0.890      2.589   -96
A   45     0 333.5    3.0  -1.0      0.027      2.515      7.166  -105
A   45    10 333.5    3.0  -1.0      0.612      1.632      3.996  -105
A   45    20 333.5    3.0  -1.0      0.327      0.998      2.482  -105
A   46     0 340.0    9.0  -1.5      0.601      1.721      6.324  -105
A   46    10 340.0    9.0  -1.5      1.030      1.058      3.387  -105
A   46    20 340.0    9.0  -1.5      0.830      0.760      1.948  -105
A   47     0 328.0   11.0  -2.0      5.607      5.442     14.030  -111
A   47    10 328.0   11.0  -2.0      3.956      3.242      8.307  -111
A   47    20 328.0   11.0  -2.0      2.550      1.966      5.342  -111
A   48     0 348.0    8.5  -1.0      3.679      3.945     13.070  -111
A   48    10 348.0    8.5  -1.0      2.941      2.415      7.701  -111
A   48    20 348.0    8.5  -1.0      1.859      1.485      5.012  -111
A   49     0 331.0    8.5  -6.0      2.834      4.488     18.711  -116
A   49    10 331.0    8.5  -6.0      2.952      3.342     12.133  -116
A   49    20 331.0    8.5  -6.0      1.976      1.932      8.105  -116
A   50     0 346.0    6.5  -6.5      5.287      3.770     18.528  -116
A   50    10 346.0    6.5  -6.5      4.517      2.744     11.442  -116
A   50    20 346.0    6.5  -6.5      3.135      1.917      7.552  -116
A   51     0 323.0    1.0  -2.5      0.985      6.098     22.149  -121
A   51    10 323.0    1.0  -2.5      2.076      4.643     14.632  -121
A   51    20 323.0    1.0  -2.5      1.341      2.964      9.399  -121
A   52     0 320.0    0.0  -4.0     -1.118      5.615     20.833  -121
A   52    10 320.0    0.0  -4.0      0.886      4.708     14.184  -121
A   52    20 320.0    0.0  -4.0      0.659      2.808      8.342  -121
A   53     0 325.0    3.0  -2.0      1.393      2.639      9.388  -127
A   53    10 325.0    3.0  -2.0      1.458      2.070      6.677  -127
A   53    20 325.0    3.0  -2.0      1.184      1.696      4.861  -127
A   54     0 319.0   -1.5  -3.0      0.594      2.637      7.862  -127
A   54    10 319.0   -1.5  -3.0      0.819      2.105      6.036  -127
A   54    20 319.0   -1.5  -3.0      0.600      1.399      4.572  -127
A   55     0 320.5   -1.0   0.0     -0.148      2.866      9.190  -134
A   55    10 320.5   -1.0   0.0      0.538      1.715      5.864  -134
A   55    20 320.5   -1.0   0.0      0.458      0.961      3.889  -134
A   56     0 324.0   -1.0  -1.0     -0.100      4.867     14.445  -134
A   56    10 320.5   -1.0   0.0      0.854      3.933     10.016  -134
A   56    20 324.0   -1.0  -1.0      0.849      2.004      7.662  -134
A   57     0 320.5    2.0  -1.5      0.523      5.154     11.357  -140
A   57    10 320.5    2.0  -1.5      1.129      4.330      7.567  -140
A   57    20 320.5    2.0  -1.5      0.763      2.936      5.110  -140
A   58     0 322.0    7.5  -3.0      2.196      5.369     11.977  -140
A   58    10 322.0    7.5  -3.0      2.531      3.818      7.889  -140
A   58    20 322.0    7.5  -3.0      1.425      2.291      5.671  -140
A   59     0 326.0    3.0  -1.5      2.224      5.656     11.999  -145
A   59    10 326.0    3.0  -1.5      2.444      4.764      8.966  -145
```

```
A   59    20 326.0    3.0  -1.5      1.972      3.088      5.159  -145
A   60     0 327.0    4.0  -1.5      1.655      5.157     11.861  -145
A   60    10 327.0    4.0  -1.5      2.085      3.843      7.630  -145
A   60    20 327.0    4.0  -1.5      1.589      2.876      4.842  -145
A   61     0 320.0    1.0  -3.0      0.797      5.046      9.396  -150
A   61    10 320.0    1.0  -3.0      1.063      3.801      6.173  -150
A   61    20 320.0    1.0  -3.0      0.522      2.651      4.206  -150
A   62     0 328.0    0.0  -4.0     -0.156      2.424      7.653  -150
A   62    10 328.0    0.0  -4.0      0.513      1.598      4.637  -150
A   62    20 328.0    0.0  -4.0      0.310      0.854      3.118  -150
A   63     0 323.0    3.5  -2.0      1.399      6.098     13.804  -157
A   63    10 323.0    3.5  -2.0      1.608      4.710      8.692  -157
A   63    20 323.0    3.5  -2.0      1.406      2.983      6.183  -157
A   64     0 327.0    1.5  -5.5      0.689      6.547     16.513  -157
A   64    10 327.0    1.5  -5.5      1.411      5.006     10.720  -157
A   64    20 327.0    1.5  -5.0      0.999      3.565      7.698  -157
A   65     0 323.0    2.5  -4.0     -1.622      3.826     18.420  -164
A   65    10 323.0    2.5  -4.0      0.483      3.301      8.912  -164
A   65    20 323.0    2.5  -4.0      0.700      2.112      5.819  -164
A   66     0 324.5    5.5  -2.5      1.629      4.090     10.600  -164
A   66    10 324.5    5.5  -2.5      1.644      2.756      6.602  -164
A   66    20 324.5    5.5  -2.5      1.048      1.818      4.706  -164
A   67     0 328.0    0.0  -2.0     -0.530      2.469      8.701  -177
A   67    10 328.0    0.0  -2.0      0.233      2.167      5.554  -177
A   67    20 328.0    0.0  -2.0     -0.101      1.495      4.225  -177
A   68     0 335.0    1.5  -3.5     -0.913      0.956      8.269  -177
A   68    10 335.0    1.5  -3.5     -0.110      0.877      5.000  -177
A   68    20 335.0    1.5  -3.5     -0.142      0.398      3.483  -177
A   69     0 326.0   -1.0  -1.5     -1.414      2.635      9.659  -182
A   69    10 326.0   -1.0  -1.5     -0.385      1.875      6.466  -182
A   69    20 326.0   -1.0  -1.5     -0.066      1.189      4.119  -182
A   69    30 326.0   -1.0  -1.5     -0.086      0.931      2.881  -182
A   69    40 326.0   -1.0  -1.5     -0.139      0.774      1.725  -182
A   69    60 326.0   -1.0  -1.5     -0.060      0.397      1.273  -182
A   69    80 326.0   -1.0  -1.5      0.204      0.563      0.524  -182
A   70     0 335.0    2.5  -3.0     -0.561      1.731     12.689  -182
A   70    10 335.0    2.5  -3.0      0.169      1.181      9.720  -182
A   70    20 335.0    2.5  -3.0      0.239      1.023      6.517  -182
A   70    30 335.0    2.5  -3.0      0.109      0.705      4.015  -182
A   70    40 335.0    2.5  -3.0      0.294      0.352      2.771  -182
A   70    60 335.0    2.5  -3.0     -0.060      0.397      1.273  -182
A   70    80 335.0    2.5  -3.0     -0.165      0.527      0.708  -182
A   71     0 324.5    0.0  -1.5      2.925     -2.062     13.490  -188
A   71    10 324.5    0.0  -1.5      3.477     -1.960      9.520  -188
A   71    20 324.5    0.0  -1.5      2.605     -1.398      5.929  -188
A   71    30 324.5    0.0  -1.5      2.399     -1.235      3.902  -188
A   71    40 324.5    0.0  -1.5      2.109     -1.047      2.595  -188
A   71    50 324.5    0.0  -1.5      1.797     -0.960      1.425  -188
A   71    60 324.5    0.0  -1.5      1.394     -0.732      0.576  -188
A   71    70 324.5    0.0  -1.5      1.459     -0.569      0.841  -188
A   71    80 324.5    0.0  -1.5      1.100     -0.482      0.288  -188
A   71   100 324.5    0.0  -1.5      0.798     -0.464      0.523  -188
A   71   120 324.5    0.0  -1.5      1.087     -0.371      0.122  -188
A   71   140 324.5    0.0  -1.5      0.808     -0.517      0.589  -188
A   72     0 336.0    0.0  -1.5     -3.876     -6.271     22.457  -188
A   72    10 336.0    0.0  -1.5     -2.380     -5.315     17.460  -188
A   72    20 336.0    0.0  -1.5     -1.756     -4.058     12.890  -188
A   72    30 336.0    0.0  -1.5     -1.253     -3.262      9.099  -188
A   72    40 336.0    0.0  -1.5     -0.872     -3.020      6.176  -188
A   72    50 336.0    0.0  -1.5     -0.659     -2.842      5.232  -188
```

| | | | | | | | | | |
|---|---|---|---|---|---|---|---|---|---|
| A | 72 | 60 | 336.0 | 0.0 | -1.5 | -0.563 | -1.949 | 4.114 | -188 |
| A | 72 | 70 | 336.0 | 0.0 | -1.5 | -1.259 | -2.084 | 3.768 | -188 |
| A | 72 | 80 | 336.0 | 0.0 | -1.5 | -0.378 | -1.430 | 2.980 | -188 |
| A | 72 | 100 | 336.0 | 0.0 | -1.5 | -0.839 | -2.541 | 2.640 | -186 |
| A | 72 | 120 | 336.0 | 0.0 | -1.5 | -0.103 | -1.465 | 2.162 | -188 |
| A | 72 | 140 | 336.0 | 0.0 | -1.5 | -0.283 | -1.150 | 1.754 | -188 |
| A | 73 | 0 | 325.0 | -3.0 | -1.0 | -0.943 | 2.066 | 6.369 | -193 |
| A | 73 | 10 | 325.0 | -3.0 | -1.0 | -0.341 | 1.746 | 4.999 | -193 |
| A | 73 | 20 | 325.0 | -3.0 | -1.0 | -0.123 | 1.156 | 3.563 | -193 |
| A | 73 | 30 | 325.0 | -3.0 | -1.0 | -0.124 | 0.837 | 2.451 | -193 |
| A | 73 | 40 | 325.0 | -3.0 | -1.0 | -0.227 | 0.689 | 1.588 | -193 |
| A | 73 | 60 | 325.0 | -3.0 | -1.0 | -0.129 | 0.184 | 1.008 | -193 |
| A | 73 | 80 | 325.0 | -3.0 | -1.0 | -0.161 | 0.438 | 1.139 | -193 |
| A | 74 | 0 | 328.5 | 2.0 | -1.5 | -0.348 | 2.168 | 7.861 | -193 |
| A | 74 | 10 | 328.5 | 2.0 | -1.5 | 0.197 | 1.647 | 5.667 | -193 |
| A | 74 | 20 | 328.5 | 2.0 | -1.5 | 0.189 | 1.005 | 3.496 | -193 |
| A | 74 | 30 | 328.5 | 2.0 | -1.5 | -0.003 | 0.700 | 2.507 | -193 |
| A | 74 | 40 | 328.5 | 2.0 | -1.5 | 0.037 | 0.449 | 1.720 | -193 |
| A | 74 | 60 | 328.5 | 2.0 | -1.5 | 0.017 | 0.424 | 0.746 | -193 |
| A | 75 | 0 | 321.5 | -1.0 | 2.0 | -1.372 | 2.391 | 7.469 | -199 |
| A | 75 | 10 | 321.5 | -1.0 | 2.0 | -0.482 | 1.626 | 4.950 | -199 |
| A | 75 | 20 | 321.5 | -1.0 | 2.0 | -0.312 | 1.268 | 3.493 | -199 |
| A | 76 | 0 | 325.5 | -1.5 | -1.5 | -1.715 | 2.340 | 9.099 | -199 |
| A | 76 | 10 | 325.5 | -1.5 | -1.5 | -0.727 | 1.641 | 5.968 | -199 |
| A | 76 | 20 | 325.5 | -1.5 | -1.5 | -0.430 | 1.148 | 4.444 | -199 |
| A | 77 | 0 | 330.5 | 1.5 | -4.5 | 0.406 | 3.472 | 8.548 | -203 |
| A | 77 | 10 | 330.5 | 1.5 | -4.5 | 0.619 | 2.571 | 5.893 | -203 |
| A | 77 | 20 | 330.5 | 1.5 | -4.5 | 0.390 | 3.215 | 7.453 | -203 |
| A | 78 | 0 | 330.5 | -1.5 | -3.0 | -0.390 | 4.047 | 10.849 | -203 |
| A | 78 | 10 | 330.5 | -1.5 | -3.0 | 0.390 | 3.215 | 7.453 | -203 |
| A | 78 | 20 | 330.5 | -1.5 | -3.0 | 0.204 | 2.294 | 5.436 | -203 |
| A | 79 | 0 | 326.5 | -0.5 | -4.0 | 0.172 | 1.948 | 8.168 | -209 |
| A | 79 | 10 | 326.5 | -0.5 | -4.0 | 0.472 | -0.003 | 0.859 | -209 |
| A | 80 | 0 | 328.0 | -0.5 | -5.0 | -0.493 | 1.610 | 7.653 | -209 |
| A | 80 | 10 | 328.0 | -0.5 | -5.0 | 0.333 | 1.217 | 4.916 | -209 |
| A | 81 | 0 | 336.0 | -1.0 | -6.0 | -0.708 | 1.795 | 6.854 | -214 |
| A | 81 | 10 | 336.0 | -1.0 | -6.0 | -0.088 | 1.411 | 4.777 | -214 |
| A | 81 | 20 | 336.0 | -1.0 | -6.0 | -0.015 | 1.136 | 3.640 | -214 |
| A | 82 | 0 | 341.5 | -2.0 | 1.0 | -1.276 | 2.784 | 10.815 | -214 |
| A | 82 | 10 | 341.5 | -2.0 | 1.0 | -0.244 | 1.791 | 7.131 | -214 |
| A | 82 | 20 | 341.5 | -2.0 | 1.0 | -0.105 | 1.190 | 4.673 | -214 |
| A | 83 | 0 | 328.0 | -3.0 | -4.5 | -1.052 | 0.933 | 6.340 | -218 |
| A | 83 | 10 | 328.0 | -3.0 | -4.5 | -0.448 | 0.723 | 4.568 | -218 |
| A | 83 | 20 | 328.0 | -3.0 | -4.5 | -0.309 | 0.510 | 3.003 | -218 |
| A | 84 | 0 | 328.5 | 2.5 | -4.0 | -0.210 | 1.427 | 6.021 | -218 |
| A | 84 | 10 | 328.5 | 2.5 | -4.0 | 0.071 | 1.260 | 4.379 | -218 |
| A | 84 | 20 | 328.5 | 2.5 | -4.0 | 0.228 | 0.879 | 3.075 | -218 |
| A | 85 | 0 | 331.0 | 4.0 | -4.0 | -0.638 | 1.496 | 6.269 | -224 |
| A | 85 | 10 | 331.0 | 4.0 | -4.0 | -0.050 | 1.221 | 4.038 | -224 |
| A | 85 | 20 | 331.0 | 4.0 | -4.0 | -0.005 | 0.784 | 2.859 | -224 |
| A | 86 | 0 | 336.0 | -6.0 | -5.0 | -2.418 | 1.575 | 8.191 | -224 |
| A | 86 | 10 | 336.0 | -6.0 | -5.0 | -0.478 | 0.839 | 3.458 | -224 |
| A | 86 | 20 | 336.0 | -6.0 | -5.0 | -0.303 | 0.580 | 2.120 | -224 |
| A | 87 | 0 | 328.5 | -3.0 | -2.5 | -2.437 | 2.608 | 6.723 | -230 |
| A | 87 | 10 | 328.5 | -3.0 | -2.5 | -1.093 | 1.779 | 3.782 | -230 |
| A | 87 | 20 | 328.5 | -3.0 | -2.5 | -1.151 | 1.819 | 3.678 | -230 |
| A | 88 | 0 | 335.0 | -3.5 | -2.0 | -1.084 | 2.186 | 4.949 | -230 |
| A | 88 | 10 | 335.0 | -3.5 | -2.0 | -0.367 | 1.482 | 3.179 | -230 |
| A | 88 | 20 | 335.0 | -3.5 | -2.0 | -0.130 | 0.955 | 2.183 | -230 |
| A | 89 | 0 | 334.0 | 3.5 | -4.0 | -0.403 | 0.988 | 4.272 | -235 |
| A | 89 | 10 | 334.0 | 3.5 | -4.0 | -0.041 | 0.630 | 2.508 | -235 |
| A | 89 | 20 | 334.0 | 3.5 | -4.0 | 0.009 | 0.517 | 1.803 | -235 |
| A | 90 | 0 | 337.0 | 1.0 | -4.0 | -0.461 | 0.844 | 3.995 | -235 |
| A | 90 | 10 | 337.0 | 1.0 | -4.0 | -0.136 | 0.590 | 2.588 | -235 |
| A | 90 | 20 | 337.0 | 1.0 | -4.0 | -0.029 | 0.457 | 1.768 | -235 |
| A | 91 | 0 | 332.0 | 5.0 | -8.0 | 0.296 | 0.841 | 4.453 | -240 |
| A | 91 | 10 | 332.0 | 5.0 | -8.0 | 0.285 | 0.547 | 2.628 | -240 |
| A | 91 | 20 | 332.0 | 5.0 | -8.0 | 0.494 | 0.284 | 1.904 | -240 |
| A | 92 | 0 | 331.0 | 0.5 | -1.5 | -0.512 | 0.993 | 3.694 | -240 |
| A | 92 | 10 | 331.0 | 0.5 | -1.5 | -0.123 | 0.800 | 2.614 | -240 |
| A | 92 | 20 | 331.0 | 0.5 | -1.5 | -0.132 | 0.733 | 1.912 | -240 |
| A | 93 | 0 | 322.5 | 4.5 | -4.0 | -0.175 | 2.749 | 5.667 | -245 |
| A | 93 | 10 | 322.5 | 4.5 | -4.0 | 0.097 | 2.356 | 3.785 | -245 |
| A | 93 | 20 | 322.5 | 4.5 | -4.0 | 0.035 | 1.825 | 2.954 | -245 |
| A | 94 | 0 | 332.5 | 5.0 | -5.5 | -0.601 | 1.614 | 3.834 | -245 |
| A | 94 | 10 | 332.5 | 5.0 | -5.5 | -0.310 | 1.379 | 2.838 | -245 |
| A | 94 | 20 | 332.5 | 5.0 | -5.5 | -0.332 | 0.913 | 2.120 | -245 |
| A | 95 | 0 | 335.0 | 6.0 | -6.5 | -0.365 | 2.429 | 6.130 | -250 |
| A | 95 | 10 | 335.0 | 6.0 | -6.5 | 0.087 | 2.078 | 4.269 | -250 |
| A | 95 | 20 | 335.0 | 6.0 | -6.5 | 0.045 | 1.510 | 2.848 | -250 |
| A | 96 | 0 | 334.5 | 4.0 | -6.5 | -0.268 | 2.782 | 7.997 | -250 |
| A | 96 | 10 | 334.5 | 4.0 | -6.5 | 0.093 | 2.005 | 4.193 | -250 |
| A | 96 | 20 | 334.5 | 4.0 | -6.5 | 0.258 | 1.477 | 2.412 | -250 |
| A | 97 | 0 | 340.5 | -1.5 | -10.0 | -0.872 | 0.956 | 6.852 | -255 |
| A | 97 | 10 | 340.5 | -1.5 | -10.0 | -0.431 | 0.682 | 4.214 | -255 |
| A | 97 | 20 | 340.5 | -1.5 | -10.0 | -0.338 | 0.477 | 3.110 | -255 |
| A | 98 | 0 | 334.5 | 1.5 | -6.0 | -0.457 | 1.068 | 3.736 | -255 |
| A | 98 | 10 | 334.5 | 1.5 | -6.0 | -0.110 | 0.640 | 2.726 | -255 |
| A | 98 | 20 | 334.5 | 1.5 | -6.0 | -0.279 | 0.413 | 1.895 | -255 |
| A | 99 | 0 | 318.5 | 0.0 | -2.0 | -0.376 | 0.696 | 4.183 | -263 |
| A | 99 | 10 | 318.5 | 0.0 | -2.0 | -0.536 | 0.513 | 2.952 | -263 |
| A | 99 | 20 | 318.5 | 0.0 | -2.0 | -0.361 | 0.193 | 2.425 | -263 |
| A | 100 | 0 | 321.5 | 0.0 | -2.0 | 0.474 | 3.762 | 8.730 | -263 |
| A | 100 | 10 | 321.5 | 0.0 | -2.0 | 0.210 | 2.766 | 5.596 | -263 |
| A | 100 | 20 | 321.5 | 0.0 | -2.0 | 0.163 | 1.754 | 4.389 | -263 |
| A | 101 | 0 | 323.0 | 0.5 | -1.5 | -1.272 | 1.802 | 7.354 | -269 |
| A | 101 | 10 | 323.0 | 0.5 | -1.5 | -0.950 | 1.215 | 5.035 | -269 |
| A | 101 | 20 | 323.0 | 0.5 | -1.5 | -0.649 | 0.772 | 3.741 | -269 |
| A | 102 | 0 | 321.0 | 1.0 | -0.5 | -0.809 | 1.441 | 6.491 | -269 |
| A | 102 | 10 | 321.0 | 1.0 | -0.5 | -0.563 | 0.849 | 4.359 | -269 |
| A | 102 | 20 | 321.0 | 1.0 | -0.5 | -0.308 | 0.742 | 3.299 | -269 |
| A | 103 | 0 | 323.0 | 1.5 | -3.5 | 0.050 | 2.659 | 5.740 | -276 |
| A | 103 | 10 | 323.0 | 1.5 | -3.5 | 0.353 | 2.079 | 3.644 | -276 |
| A | 103 | 20 | 323.0 | 1.5 | -3.5 | 0.228 | 1.426 | 2.404 | -276 |
| A | 104 | 0 | 321.5 | 4.0 | -2.5 | -0.640 | 2.863 | 6.854 | -276 |
| A | 104 | 10 | 321.5 | 4.0 | -2.5 | -0.183 | 2.157 | 4.164 | -276 |
| A | 104 | 20 | 321.5 | 4.0 | -2.5 | -0.135 | 1.403 | 2.786 | -276 |
| A | 105 | 0 | 324.0 | 3.0 | -5.5 | 0.352 | 2.613 | 6.418 | -282 |
| A | 105 | 10 | 324.0 | 3.0 | -5.5 | 0.234 | 1.972 | 3.742 | -282 |
| A | 106 | 0 | 325.5 | 1.5 | -3.5 | -0.338 | 1.520 | 5.326 | -282 |
| A | 106 | 10 | 325.5 | 1.5 | -3.5 | 0.786 | -0.030 | 0.979 | -282 |
| A | 107 | 0 | 326.5 | 0.5 | -5.5 | -0.967 | 1.312 | 5.843 | -288 |
| A | 107 | 10 | 326.5 | 0.5 | -5.5 | -0.478 | 1.076 | 3.481 | -288 |
| A | 107 | 20 | 326.5 | 0.5 | -5.5 | -0.240 | 0.729 | 2.543 | -288 |
| A | 108 | 0 | 326.5 | -1.5 | -4.5 | -1.229 | 0.990 | 5.099 | -288 |
| A | 108 | 10 | 326.5 | -1.5 | -4.5 | -0.596 | 0.641 | 3.417 | -288 |
| A | 108 | 20 | 326.5 | -1.5 | -4.5 | -0.420 | 0.518 | 2.490 | -288 |
| A | 109 | 0 | 322.5 | 1.5 | -1.0 | -0.032 | 1.214 | 4.341 | -294 |
| A | 109 | 10 | 322.5 | 1.5 | -1.0 | 0.375 | 0.427 | 1.191 | -294 |
| A | 109 | 20 | 322.5 | 1.5 | -1.0 | 0.156 | 0.198 | 0.646 | -294 |

| | | | | | | | | | |
|---|---|---|---|---|---|---|---|---|---|
| A | 110 | 0 | 328.0 | 3.0 | -4.5 | -0.136 | 0.752 | 3.547 | -294 |
| A | 110 | 10 | 328.0 | 3.0 | -4.5 | 0.344 | 0.034 | 0.993 | -294 |
| A | 110 | 20 | 328.0 | 3.0 | -4.5 | 0.390 | -0.092 | 0.547 | -294 |
| A | 111 | 0 | 326.0 | 5.0 | -3.0 | -0.537 | 0.789 | 5.952 | -300 |
| A | 111 | 10 | 326.0 | 5.0 | -3.0 | 0.194 | 0.487 | 2.887 | -300 |
| A | 112 | 0 | 328.0 | 3.0 | -4.0 | -0.319 | 0.720 | 3.886 | -300 |
| A | 112 | 10 | 328.0 | 3.0 | -4.0 | 0.184 | -0.076 | 0.738 | -300 |
| A | 113 | 0 | 317.0 | 4.0 | -1.0 | -0.206 | 0.952 | 4.581 | -306 |
| A | 113 | 10 | 317.0 | 4.0 | -1.0 | -0.090 | 0.846 | 3.363 | -306 |
| A | 113 | 20 | 317.0 | 4.0 | -1.0 | 0.006 | 0.542 | 2.403 | -306 |
| A | 114 | 0 | 320.0 | 6.5 | -4.5 | 0.256 | 0.425 | 4.639 | -306 |
| A | 114 | 10 | 320.0 | 6.5 | -4.5 | 0.325 | 0.231 | 3.270 | -306 |
| A | 114 | 20 | 320.0 | 6.5 | -4.5 | 0.410 | 0.237 | 2.280 | -306 |
| A | 115 | 0 | 325.0 | 9.0 | -5.5 | -0.049 | 0.575 | 3.987 | -314 |
| A | 116 | 0 | 328.0 | 5.5 | -6.0 | -0.012 | 0.473 | 4.531 | -314 |
| A | 117 | 0 | 326.0 | 1.0 | -4.0 | -0.265 | 1.341 | 4.920 | -320 |
| A | 117 | 10 | 326.0 | 1.0 | -4.0 | -0.076 | 0.983 | 3.484 | -320 |
| A | 117 | 20 | 326.0 | 1.0 | -4.0 | -0.127 | 0.582 | 2.603 | -320 |
| A | 118 | 0 | 322.0 | 3.5 | -4.5 | -0.161 | 0.856 | 3.462 | -320 |
| A | 118 | 10 | 322.0 | 3.5 | -4.5 | -0.007 | 0.605 | 2.549 | -320 |
| A | 118 | 20 | 322.0 | 3.5 | -4.5 | 0.082 | 0.499 | 1.693 | -320 |
| A | 119 | 0 | 344.0 | 9.0 | -6.5 | 0.754 | 0.387 | 5.895 | -326 |
| A | 119 | 10 | 344.0 | 9.0 | -6.5 | 0.559 | 0.382 | 4.169 | -326 |
| A | 119 | 20 | 344.0 | 9.0 | -6.5 | 0.366 | 0.151 | 3.201 | -326 |
| A | 120 | 0 | 343.0 | 8.0 | -7.0 | 0.593 | 0.153 | 8.581 | -326 |
| A | 120 | 10 | 343.0 | 8.0 | -7.0 | 0.604 | 0.022 | 6.026 | -326 |
| A | 120 | 20 | 343.0 | 8.0 | -7.0 | 0.428 | 0.097 | 4.708 | -326 |
| A | 121 | 0 | 321.0 | 7.0 | -5.0 | 0.264 | 0.496 | 3.228 | -336 |
| A | 121 | 10 | 321.0 | 7.0 | -5.0 | 0.196 | 0.311 | 1.689 | -336 |
| A | 121 | 20 | 321.0 | 7.0 | -5.0 | 0.210 | 0.239 | 1.155 | -336 |
| A | 122 | 0 | 320.0 | 9.0 | -6.0 | 0.289 | 0.439 | 3.361 | -336 |
| A | 122 | 10 | 320.0 | 9.0 | -6.0 | 0.315 | 0.374 | 2.012 | -336 |
| A | 122 | 20 | 320.0 | 9.0 | -6.0 | 0.167 | 0.139 | 1.261 | -336 |
| A | 123 | 0 | 317.5 | 5.5 | -5.5 | -0.037 | 0.665 | 4.850 | -342 |
| A | 123 | 10 | 317.5 | 5.5 | -5.5 | -0.069 | 0.314 | 3.441 | -342 |
| A | 123 | 20 | 317.5 | 5.5 | -5.5 | -0.010 | 0.376 | 2.406 | -342 |
| A | 124 | 0 | 318.0 | 5.5 | -5.0 | 0.212 | 1.175 | 4.827 | -342 |
| A | 124 | 10 | 318.0 | 5.5 | -5.5 | 0.352 | 1.030 | 3.254 | -342 |
| A | 124 | 20 | 318.0 | 5.5 | -5.5 | 0.267 | 0.629 | 2.301 | -342 |
| A | 125 | 0 | 308.0 | 0.0 | -3.5 | -0.468 | 0.699 | 3.813 | -348 |
| A | 125 | 10 | 308.0 | 0.0 | -3.5 | -0.315 | 0.541 | 2.385 | -348 |
| A | 125 | 20 | 308.0 | 0.0 | -3.5 | -0.117 | 0.413 | 1.646 | -348 |
| A | 126 | 0 | 317.0 | 2.0 | -4.0 | -0.464 | 0.645 | 3.414 | -348 |
| A | 126 | 10 | 317.0 | 2.0 | -4.0 | -0.275 | 0.542 | 1.880 | -348 |
| A | 126 | 20 | 317.0 | 2.0 | -4.0 | -0.277 | 0.394 | 1.381 | -348 |
| A | 127 | 0 | 309.0 | -5.0 | -3.0 | -0.835 | 0.556 | 4.707 | -355 |
| A | 127 | 10 | 309.0 | -5.0 | -3.0 | -0.417 | 0.562 | 2.967 | -355 |
| A | 127 | 20 | 309.0 | -5.0 | -3.0 | -0.302 | 0.221 | 2.228 | -355 |
| A | 128 | 0 | 315.5 | -6.5 | -3.5 | -1.716 | 1.390 | 4.664 | -355 |
| A | 128 | 10 | 315.5 | -6.5 | -3.5 | -0.887 | 0.857 | 2.779 | -355 |
| A | 128 | 20 | 315.5 | -6.5 | -3.5 | -0.631 | 0.656 | 2.128 | -355 |
| A | 129 | 0 | 306.0 | 5.0 | -4.5 | -0.293 | 1.084 | 4.076 | -362 |
| A | 129 | 10 | 306.0 | 5.0 | -4.5 | -0.101 | 0.428 | 2.635 | -362 |
| A | 129 | 20 | 306.0 | 5.0 | -4.5 | 0.051 | 0.403 | 1.961 | -362 |
| A | 130 | 0 | 319.0 | -4.0 | -4.5 | -0.129 | 0.980 | 3.706 | -362 |
| A | 130 | 10 | 319.0 | -4.0 | -4.5 | 0.096 | 0.630 | 2.351 | -362 |
| A | 130 | 20 | 319.0 | -4.0 | -4.5 | -0.007 | 0.537 | 1.746 | -362 |
| A | 131 | 0 | 309.0 | 3.0 | -3.0 | 0.044 | 0.396 | 1.742 | -369 |
| A | 131 | 10 | 309.0 | 3.0 | -3.0 | 0.118 | 0.327 | 1.106 | -369 |
| A | 131 | 20 | 309.0 | 3.0 | -3.0 | 0.165 | 0.285 | 0.654 | -369 |
| A | 132 | 0 | 318.5 | -4.0 | -6.0 | -0.159 | 0.440 | 2.360 | -369 |
| A | 132 | 10 | 318.5 | -4.0 | -6.0 | 0.010 | 0.355 | 1.308 | -369 |
| A | 132 | 20 | 318.5 | -4.0 | -6.0 | -0.054 | 0.275 | 1.099 | -369 |
| A | 133 | 0 | 309.5 | 5.0 | -3.5 | 0.337 | 1.370 | 3.719 | -375 |
| A | 133 | 10 | 309.5 | 5.0 | -3.5 | 0.494 | 0.988 | 2.688 | -375 |
| A | 134 | 0 | 312.5 | 5.0 | -4.0 | 0.022 | 0.633 | 2.782 | -375 |
| A | 134 | 10 | 312.5 | 5.0 | -4.0 | 0.194 | 0.508 | 2.213 | -375 |
| A | 135 | 0 | 309.0 | 3.0 | -3.5 | -2.046 | 1.213 | 12.322 | -384 |
| A | 135 | 10 | 309.0 | 3.0 | -3.5 | -0.801 | 1.347 | 4.735 | -384 |
| A | 135 | 20 | 309.0 | 3.0 | -3.5 | -0.573 | 0.876 | 3.158 | -384 |
| A | 136 | 0 | 315.0 | 2.5 | -2.5 | -0.791 | 1.871 | 4.674 | -384 |
| A | 136 | 10 | 315.0 | 2.5 | -2.5 | -0.367 | 1.388 | 2.889 | -384 |
| A | 136 | 20 | 315.0 | 2.5 | -2.5 | -0.110 | 1.067 | 2.024 | -384 |
| A | 137 | 0 | 310.5 | -3.7 | -7.5 | -1.177 | 0.546 | 4.142 | -390 |
| A | 137 | 10 | 310.5 | -3.5 | -7.5 | -0.660 | 0.385 | 3.091 | -390 |
| A | 137 | 20 | 310.5 | -3.5 | -7.5 | -0.637 | 0.233 | 2.330 | -390 |
| A | 138 | 0 | 313.0 | -2.0 | -3.0 | -0.364 | 0.945 | 4.125 | -390 |
| A | 138 | 10 | 313.0 | -2.0 | -3.0 | -0.196 | 0.765 | 3.034 | -390 |
| A | 138 | 20 | 313.0 | -2.0 | -3.0 | -0.157 | 0.383 | 2.236 | -390 |
| A | 139 | 0 | 311.5 | -0.5 | -8.5 | -1.098 | -0.717 | 7.817 | -397 |
| A | 139 | 10 | 311.5 | -0.5 | -8.5 | 0.018 | -0.345 | 3.576 | -397 |
| A | 140 | 0 | 310.5 | 2.5 | -4.0 | 0.175 | 0.267 | 3.231 | -397 |
| A | 140 | 10 | 310.5 | 2.5 | -4.0 | 0.375 | 0.051 | 1.586 | -397 |
| A | 141 | 0 | 311.0 | -1.0 | -5.0 | -0.820 | 1.232 | 3.941 | -403 |
| A | 141 | 10 | 311.0 | -1.0 | -5.0 | -0.479 | 0.840 | 2.707 | -403 |
| A | 141 | 20 | 311.0 | -1.0 | -5.0 | -0.283 | 0.695 | 1.846 | -403 |
| A | 142 | 0 | 310.5 | -2.5 | -9.0 | -0.713 | 0.412 | 3.307 | -403 |
| A | 142 | 10 | 310.5 | -2.5 | -9.0 | -0.381 | 0.310 | 2.124 | -403 |
| A | 142 | 20 | 310.5 | -2.5 | -9.0 | -0.262 | 0.179 | 1.657 | -403 |
| A | 143 | 0 | 311.5 | 0.0 | -4.0 | -0.761 | 0.877 | 3.518 | -410 |
| A | 143 | 10 | 311.5 | 0.0 | -4.0 | -0.425 | 0.532 | 2.095 | -410 |
| A | 143 | 20 | 311.5 | 0.0 | -4.0 | -0.442 | 0.421 | 1.461 | -410 |
| A | 144 | 0 | 311.5 | 3.0 | -4.0 | -0.655 | 1.122 | 3.260 | -410 |
| A | 144 | 10 | 311.5 | 3.0 | -4.0 | -0.399 | 0.746 | 2.004 | -410 |
| A | 144 | 20 | 311.5 | 3.0 | -4.0 | -0.292 | 0.539 | 1.586 | -410 |
| A | 145 | 0 | 308.5 | 3.5 | -3.0 | -0.750 | 0.855 | 3.707 | -418 |
| A | 145 | 10 | 308.5 | 3.5 | -3.0 | -0.417 | 0.645 | 2.690 | -418 |
| A | 145 | 20 | 308.5 | 3.5 | -3.0 | -0.098 | 0.393 | 1.790 | -418 |
| A | 145 | 30 | 308.5 | 3.5 | -3.0 | -0.065 | 0.286 | 1.020 | -418 |
| A | 145 | 40 | 308.5 | 3.5 | -3.0 | -0.012 | 0.243 | 0.962 | -418 |
| A | 145 | 60 | 308.5 | 3.5 | -3.0 | -0.088 | 0.118 | 0.250 | -418 |
| A | 146 | 0 | 310.5 | 0.5 | -3.5 | -0.716 | 0.742 | 3.088 | -418 |
| A | 146 | 10 | 310.5 | 0.5 | -3.5 | -0.586 | 0.534 | 2.245 | -418 |
| A | 146 | 20 | 310.5 | 0.5 | -3.5 | -0.299 | 0.322 | 1.300 | -418 |
| A | 146 | 30 | 310.5 | 0.5 | -3.5 | -0.229 | 0.385 | 1.002 | -418 |
| A | 146 | 40 | 310.5 | 0.5 | -3.5 | -0.055 | 0.071 | 0.648 | -418 |
| A | 146 | 60 | 310.5 | 0.5 | -3.5 | -0.069 | 0.173 | 0.359 | -418 |
| A | 147 | 0 | 306.0 | 1.0 | -3.5 | -0.628 | 0.880 | 3.132 | -424 |
| A | 147 | 10 | 306.0 | 1.0 | -3.5 | -0.199 | 0.674 | 1.887 | -424 |
| A | 147 | 20 | 306.0 | 1.0 | -3.5 | -0.158 | 0.412 | 1.152 | -424 |
| A | 148 | 0 | 314.5 | 3.0 | -4.5 | 0.073 | 1.257 | 4.212 | -424 |
| A | 148 | 10 | 314.5 | 3.0 | -4.5 | 0.095 | 0.937 | 2.647 | -424 |
| A | 148 | 20 | 314.5 | 3.0 | -4.5 | 0.179 | 0.751 | 1.779 | -424 |
| A | 149 | 0 | 302.5 | 4.0 | -2.5 | -0.118 | 0.359 | 2.336 | -430 |
| A | 149 | 10 | 302.5 | 4.0 | -2.5 | -0.233 | 0.263 | 1.870 | -430 |
| A | 149 | 20 | 302.5 | 4.0 | -2.5 | -0.108 | 0.174 | 1.278 | -430 |
| A | 150 | 0 | 307.0 | 4.0 | -3.0 | 0.063 | 0.291 | 2.548 | -430 |
| A | 150 | 10 | 307.0 | 4.0 | -3.0 | 0.170 | 0.293 | 1.812 | -430 |
| A | 150 | 20 | 307.0 | 4.0 | -3.0 | -0.040 | 0.080 | 1.449 | -430 |
| A | 151 | 0 | 325.0 | 0.0 | -1.0 | 0.040 | 1.423 | 4.717 | -448 |

| | | | | | | | | | |
|---|---|---|---|---|---|---|---|---|---|
| A | 151 | 10 | 325.0 | 0.0 | -1.0 | 0.112 | 1.015 | 3.152 | -448 |
| A | 151 | 20 | 325.0 | 0.0 | -1.0 | 0.167 | 0.838 | 2.183 | -448 |
| A | 152 | 0 | 331.0 | 2.5 | -2.0 | -0.101 | 1.532 | 5.503 | -448 |
| A | 152 | 10 | 331.0 | 2.5 | -2.0 | 0.155 | 1.085 | 3.592 | -448 |
| A | 152 | 20 | 331.0 | 2.5 | -2.0 | 0.094 | 0.646 | 2.666 | -448 |
| A | 153 | 0 | 322.5 | 0.0 | -1.0 | -0.303 | 2.491 | 7.681 | -457 |
| A | 153 | 10 | 322.5 | 0.0 | -1.0 | 0.221 | 1.720 | 5.150 | -457 |
| A | 153 | 20 | 322.5 | 0.0 | -1.0 | 0.237 | 1.314 | 3.620 | -457 |
| A | 154 | 0 | 325.0 | 0.5 | -2.0 | -0.720 | 1.778 | 6.268 | -457 |
| A | 154 | 10 | 325.0 | 0.5 | -2.0 | -0.156 | 1.510 | 4.211 | -457 |
| A | 154 | 20 | 325.0 | 0.5 | -2.0 | -0.088 | 1.029 | 3.155 | -457 |
| A | 155 | 0 | 325.0 | 4.0 | -2.0 | 0.149 | 1.550 | 3.863 | -465 |
| A | 155 | 10 | 325.0 | 4.0 | -2.0 | 0.276 | 1.083 | 2.401 | -465 |
| A | 155 | 20 | 325.0 | 4.0 | -2.0 | 0.192 | 0.726 | 1.914 | -465 |
| A | 156 | 0 | 331.5 | 1.0 | 0.0 | -0.028 | 1.596 | 3.687 | -465 |
| A | 156 | 10 | 331.5 | 1.0 | 0.0 | 0.500 | 1.066 | 2.241 | -465 |
| A | 156 | 20 | 331.5 | 1.0 | 0.0 | 0.294 | 0.814 | 1.658 | -465 |
| A | 157 | 0 | 329.5 | -4.0 | -4.0 | -0.264 | 1.775 | 4.720 | -472 |
| A | 157 | 10 | 329.5 | -4.0 | -4.0 | -0.044 | 1.258 | 2.967 | -472 |
| A | 157 | 20 | 329.5 | -4.0 | -4.0 | 0.032 | 0.917 | 2.078 | -472 |
| A | 158 | 0 | 334.5 | -6.0 | 0.5 | -0.513 | 1.426 | 4.467 | -472 |
| A | 158 | 10 | 334.5 | -6.0 | 0.5 | -0.171 | 0.900 | 2.938 | -472 |
| A | 158 | 20 | 334.5 | -6.0 | 0.5 | -0.185 | 0.719 | 2.128 | -472 |
| A | 159 | 0 | 342.5 | -3.0 | -3.5 | 0.849 | 2.029 | 6.255 | -478 |
| A | 159 | 10 | 342.5 | -3.0 | -3.5 | 1.270 | 1.568 | 4.406 | -478 |
| A | 159 | 20 | 342.5 | -3.0 | -3.5 | 0.802 | 1.200 | 3.252 | -478 |
| A | 160 | 0 | 342.5 | -4.0 | -3.0 | -0.363 | 0.868 | 5.064 | -478 |
| A | 160 | 10 | 342.5 | -4.0 | -3.0 | 0.699 | 0.607 | 3.558 | -478 |
| A | 160 | 20 | 342.5 | -4.0 | -3.0 | 0.533 | 0.462 | 2.509 | -478 |
| A | 161 | 0 | 342.5 | -4.5 | -1.0 | -0.131 | 1.673 | 5.450 | -484 |
| A | 161 | 10 | 342.5 | -4.5 | -1.0 | 0.223 | 1.509 | 3.978 | -484 |
| A | 161 | 20 | 342.5 | -4.5 | -1.0 | 0.414 | 1.183 | 3.123 | -484 |
| A | 162 | 0 | 344.0 | -6.0 | 0.0 | 0.318 | 1.912 | 4.436 | -484 |
| A | 162 | 10 | 344.0 | -6.0 | 0.0 | 0.672 | 1.456 | 3.062 | -484 |
| A | 162 | 20 | 344.0 | -6.0 | 0.0 | 0.448 | 1.061 | 2.236 | -484 |
| A | 163 | 0 | 342.0 | -4.5 | 1.0 | 1.264 | 1.783 | 5.522 | -490 |
| A | 163 | 10 | 342.0 | -4.5 | 1.0 | 1.619 | 1.529 | 4.044 | -490 |
| A | 163 | 20 | 342.0 | -4.5 | 1.0 | 1.205 | 1.033 | 2.917 | -490 |
| A | 164 | 0 | 345.0 | -6.0 | -1.0 | -0.085 | 1.045 | 5.359 | -490 |
| A | 164 | 10 | 345.0 | -6.0 | -1.0 | 0.702 | 0.954 | 3.717 | -490 |
| A | 164 | 20 | 345.0 | -6.0 | -1.0 | 0.736 | 0.565 | 2.880 | -490 |
| A | 165 | 0 | 344.0 | -4.0 | 1.0 | -0.164 | 1.507 | 5.128 | -496 |
| A | 165 | 10 | 344.0 | -4.0 | 1.0 | 0.870 | 1.274 | 3.654 | -496 |
| A | 165 | 20 | 344.0 | -4.0 | 1.0 | 0.760 | 0.806 | 2.835 | -496 |
| A | 166 | 0 | 342.5 | -6.0 | 0.0 | 2.669 | 2.522 | 6.395 | -496 |
| A | 166 | 10 | 342.5 | -6.0 | 0.0 | 2.807 | 2.214 | 4.856 | -496 |
| A | 166 | 20 | 342.5 | -6.0 | 0.0 | 2.069 | 1.564 | 3.716 | -496 |
| A | 167 | 0 | 346.0 | -5.0 | 1.0 | 0.209 | 1.482 | 3.316 | -502 |
| A | 167 | 10 | 346.0 | -5.0 | 1.0 | 0.267 | 0.983 | 2.092 | -502 |
| A | 167 | 20 | 346.0 | -5.0 | 1.0 | 0.154 | 0.756 | 1.526 | -502 |
| A | 168 | 0 | 346.5 | -7.0 | 0.0 | 0.424 | 1.824 | 3.611 | -502 |
| A | 168 | 10 | 346.5 | -7.0 | 0.0 | 0.516 | 1.272 | 2.105 | -502 |
| A | 168 | 20 | 346.5 | -7.0 | 0.0 | 0.271 | 1.021 | 1.560 | -502 |
| A | 169 | 0 | 335.0 | -5.0 | -1.5 | 0.141 | 1.001 | 2.508 | -513 |
| A | 169 | 10 | 335.0 | -5.0 | -1.5 | 0.471 | 0.614 | 1.470 | -513 |
| A | 169 | 20 | 335.0 | -5.0 | -1.5 | 0.333 | 0.446 | 1.011 | -513 |
| A | 170 | 0 | 332.5 | -5.5 | 4.0 | 0.263 | 0.944 | 2.739 | -513 |
| A | 170 | 10 | 332.5 | -5.5 | 4.0 | 0.292 | 0.690 | 1.534 | -513 |
| A | 170 | 20 | 332.5 | -5.5 | 4.0 | 0.253 | 0.459 | 1.211 | -513 |
| A | 171 | 0 | 335.0 | -7.0 | 0.5 | 1.604 | 1.552 | 4.523 | -519 |
| A | 171 | 10 | 335.0 | -7.0 | 0.5 | 1.633 | 1.251 | 3.039 | -519 |
| A | 171 | 20 | 335.0 | -7.0 | 0.5 | 1.232 | 0.892 | 2.173 | -519 |
| A | 172 | 0 | 335.0 | -5.5 | 0.5 | 0.304 | 1.193 | 3.246 | -519 |
| A | 172 | 10 | 335.0 | -5.5 | 0.5 | 0.434 | 0.788 | 1.939 | -519 |
| A | 172 | 20 | 335.0 | -5.5 | 0.5 | 0.285 | 0.473 | 1.352 | -519 |
| A | 173 | 0 | 335.0 | -4.0 | 1.5 | -0.135 | 0.367 | 2.635 | -527 |
| A | 173 | 10 | 335.0 | -4.0 | 1.5 | -0.0 | 0.330 | 1.740 | -527 |
| A | 173 | 20 | 335.0 | -4.0 | 1.5 | 0.102 | 0.164 | 1.237 | -527 |
| A | 174 | 0 | 337.0 | 1.0 | -1.5 | 0.140 | 0.270 | 2.781 | -527 |
| A | 174 | 10 | 337.0 | 1.0 | -1.5 | 0.259 | 0.324 | 1.792 | -527 |
| A | 174 | 20 | 337.0 | 1.0 | -1.5 | 0.212 | 0.123 | 1.026 | -527 |
| A | 175 | 0 | 337.0 | -4.0 | 0.0 | 1.418 | 1.869 | 5.154 | -533 |
| A | 175 | 10 | 337.0 | -4.0 | 0.0 | 1.543 | 1.339 | 3.441 | -533 |
| A | 175 | 20 | 337.0 | -4.0 | 0.0 | 1.108 | 1.022 | 2.503 | -533 |
| A | 176 | 0 | 335.5 | -2.0 | 1.0 | 1.755 | 3.083 | 5.669 | -533 |
| A | 176 | 10 | 335.5 | -2.0 | 1.0 | 1.717 | 2.425 | 4.015 | -533 |
| A | 176 | 20 | 335.5 | -2.0 | 1.0 | 1.358 | 1.879 | 3.088 | -533 |
| A | 177 | 0 | 332.5 | -2.0 | 3.5 | 3.305 | 4.392 | 6.671 | -539 |
| A | 177 | 10 | 332.5 | -2.0 | 3.5 | 2.855 | 3.639 | 4.919 | -539 |
| A | 177 | 20 | 332.5 | -2.0 | 3.5 | 2.372 | 2.799 | 3.786 | -539 |
| A | 178 | 0 | 334.0 | -1.5 | 0.0 | 3.810 | 3.122 | 8.154 | -539 |
| A | 178 | 10 | 334.0 | -1.5 | 0.0 | 3.557 | 2.471 | 6.162 | -539 |
| A | 178 | 20 | 334.0 | -1.5 | 0.0 | 2.939 | 2.100 | 4.701 | -539 |
| A | 179 | 0 | 332.0 | -5.0 | 3.0 | 2.320 | 3.514 | 5.939 | -550 |
| A | 179 | 10 | 332.0 | -5.0 | 3.0 | 2.309 | 2.965 | 4.418 | -550 |
| A | 179 | 20 | 332.0 | -5.0 | 3.0 | 1.961 | 2.353 | 3.344 | -550 |
| A | 180 | 0 | 334.0 | -5.0 | 3.0 | 1.645 | 3.900 | 5.622 | -550 |
| A | 180 | 10 | 334.0 | -5.0 | 3.0 | 1.607 | 3.294 | 4.120 | -550 |
| A | 180 | 20 | 334.0 | -5.0 | 3.0 | 1.349 | 2.655 | 3.146 | -550 |
| A | 181• | 0 | 291.5 | -4.0 | -0.5 | -3.477 | 2.824 | 14.850 | -173 |
| A | 181• | 10 | 291.5 | -4.0 | -0.5 | -2.166 | 2.375 | 10.690 | -173 |
| A | 181• | 20 | 291.5 | -4.0 | -0.5 | -1.543 | 1.886 | 7.934 | -173 |
| A | 182• | 0 | 290.0 | -8.0 | -1.0 | -3.765 | 3.360 | 12.137 | -173 |
| A | 182• | 10 | 290.0 | -8.0 | -1.0 | -2.651 | 2.631 | 8.634 | -173 |
| A | 182• | 20 | 290.0 | -8.0 | -1.0 | -1.766 | 1.960 | 6.205 | -173 |
| A | 183• | 0 | 291.0 | -4.5 | 4.5 | -3.123 | 3.321 | 15.009 | -179 |
| A | 183• | 10 | 291.0 | -4.5 | 4.5 | -1.922 | 2.364 | 9.050 | -179 |
| A | 183• | 20 | 291.0 | -4.5 | 4.5 | -0.979 | 1.792 | 5.794 | -179 |
| A | 184• | 0 | 292.0 | -5.5 | -1.0 | -1.779 | 3.178 | 10.700 | -179 |
| A | 184• | 10 | 292.0 | -5.5 | -1.0 | -1.258 | 2.532 | 7.497 | -179 |
| A | 184• | 20 | 292.0 | -5.5 | -1.0 | -0.590 | 1.909 | 5.607 | -179 |
| A | 185• | 0 | 290.5 | -3.0 | 0.0 | -3.463 | 5.381 | 11.867 | -186 |
| A | 185• | 10 | 290.5 | -3.0 | 0.0 | -2.295 | 3.692 | 7.558 | -186 |
| A | 185• | 20 | 290.5 | -3.0 | 0.0 | -1.194 | 2.791 | 4.657 | -186 |
| A | 186• | 0 | 291.5 | -2.5 | -1.5 | -2.494 | 2.312 | 9.035 | -186 |
| A | 186• | 10 | 291.5 | -2.5 | -1.5 | -1.583 | 1.490 | 6.033 | -186 |
| A | 186• | 20 | 291.5 | -2.5 | -1.5 | -1.193 | 1.210 | 4.223 | -186 |
| A | 187• | 0 | 288.5 | -4.0 | 1.0 | -2.733 | 2.388 | 12.421 | -192 |
| A | 187• | 10 | 288.5 | -4.0 | 1.0 | -1.397 | 1.783 | 7.267 | -192 |
| A | 187• | 20 | 288.5 | -4.0 | 1.0 | -1.124 | 1.224 | 4.265 | -192 |
| A | 188• | 0 | 287.0 | -3.5 | 0.5 | -2.503 | 2.223 | 12.938 | -192 |
| A | 188• | 10 | 287.0 | -3.5 | 0.5 | -1.547 | 1.414 | 8.152 | -192 |
| A | 188• | 20 | 287.0 | -3.5 | 0.5 | -1.020 | 0.787 | 4.966 | -192 |
| A | 189• | 0 | 289.0 | -4.0 | 0.0 | -2.013 | 3.315 | 8.507 | -199 |
| A | 189• | 10 | 289.0 | -4.0 | 0.0 | -1.516 | 2.425 | 5.171 | -199 |
| A | 189• | 20 | 289.0 | -4.0 | 0.0 | -1.010 | 1.795 | 3.561 | -199 |
| A | 190• | 0 | 290.5 | -3.0 | -2.0 | -1.150 | 2.079 | 7.807 | -199 |
| A | 190• | 10 | 290.5 | -3.0 | -2.0 | -0.746 | 1.605 | 4.848 | -199 |
| A | 190• | 20 | 290.5 | -3.0 | -2.0 | -0.478 | 1.167 | 2.802 | -199 |
| A | 191• | 0 | 292.0 | 1.0 | -2.0 | -1.188 | 2.461 | 5.852 | -206 |

| | | | | | | | | | |
|---|---|---|---|---|---|---|---|---|---|
| A | 191• | 10 | 292.0 | 1.0 | -2.0 | -0.159 | 1.358 | 5.453 | -206 |
| A | 191• | 20 | 289.0 | -2.5 | 0.0 | -0.113 | 0.820 | 3.548 | -206 |
| A | 192• | 0 | 290.0 | 1.0 | -1.0 | -1.851 | 3.052 | 7.113 | -206 |
| A | 192• | 10 | 290.0 | 1.0 | -1.0 | -1.368 | 2.650 | 3.643 | -206 |
| A | 192• | 20 | 290.0 | 1.0 | -1.0 | -1.059 | 1.633 | 2.346 | -206 |
| A | 193• | 0 | 290.5 | -1.0 | -0.5 | -1.793 | 2.255 | 14.624 | -213 |
| A | 193• | 10 | 290.5 | -1.0 | -0.5 | -1.126 | 1.238 | 8.725 | -213 |
| A | 193• | 20 | 290.5 | -1.0 | -0.5 | -0.430 | 0.783 | 5.305 | -213 |
| A | 194• | 0 | 292.0 | 1.0 | -2.0 | -1.188 | 2.461 | 5.852 | -213 |
| A | 194• | 10 | 292.0 | 1.0 | -2.0 | -1.140 | 2.042 | 3.899 | -213 |
| A | 194• | 20 | 292.0 | 1.0 | -2.0 | -0.564 | 1.403 | 2.594 | -213 |
| A | 195• | 0 | 290.5 | 4.0 | 1.0 | -0.846 | 2.341 | 7.103 | -219 |
| A | 195• | 10 | 290.5 | 4.0 | 1.0 | -0.598 | 1.924 | 4.775 | -219 |
| A | 195• | 20 | 290.5 | 4.0 | 1.0 | -0.448 | 1.226 | 3.229 | -219 |
| A | 196• | 0 | 289.0 | 4.0 | -4.0 | 0.005 | 1.556 | 6.413 | -219 |
| A | 196• | 10 | 289.0 | 4.0 | -4.0 | -0.114 | 1.214 | 4.006 | -219 |
| A | 196• | 20 | 289.0 | 4.0 | -4.0 | -0.185 | 0.868 | 2.861 | -219 |
| B | 1 | 0 | 317.5 | 5.5 | 3.5 | 0.184 | 0.963 | 5.152 | 30 |
| B | 1 | 10 | 317.5 | 5.5 | 3.5 | 0.350 | 0.493 | 2.993 | 30 |
| B | 1 | 20 | 317.5 | 5.5 | 3.5 | 0.171 | 0.208 | 1.669 | 30 |
| B | 2 | 0 | 322.0 | 0.0 | 1.0 | -0.089 | 0.921 | 5.265 | 30 |
| B | 2 | 10 | 322.0 | 0.0 | 1.0 | 0.216 | 0.547 | 3.175 | 30 |
| B | 2 | 20 | 322.0 | 0.0 | 1.0 | 0.004 | 0.264 | 1.492 | 30 |
| B | 3 | 0 | 322.0 | 4.0 | 0.0 | -1.900 | 0.738 | 8.385 | 24 |
| B | 3 | 10 | 320.0 | -0.5 | -2.0 | -1.114 | 0.176 | 4.633 | 24 |
| B | 3 | 20 | 320.0 | -0.5 | -2.0 | -0.487 | 0.182 | 2.742 | 24 |
| B | 4 | 0 | 322.0 | 4.0 | 0.0 | -0.229 | 1.936 | 8.721 | 24 |
| B | 4 | 10 | 322.0 | 4.0 | 0.0 | 0.311 | 1.292 | 4.940 | 24 |
| B | 4 | 20 | 322.0 | 4.0 | 0.0 | 0.076 | 0.720 | 3.092 | 24 |
| B | 5 | 0 | 321.5 | 1.0 | -3.5 | -0.720 | 1.229 | 7.949 | 18 |
| B | 6 | 0 | 319.0 | -1.5 | 2.0 | -1.711 | 2.317 | 10.068 | 18 |
| B | 7 | 0 | 318.0 | 3.0 | -1.0 | -0.299 | 0.912 | 5.049 | 12 |
| B | 7 | 10 | 318.0 | 3.0 | -1.0 | -0.301 | 0.772 | 3.631 | 12 |
| B | 7 | 20 | 318.0 | 3.0 | -1.0 | -0.129 | 0.332 | 2.231 | 12 |
| B | 8 | 0 | 318.0 | -1.0 | -1.5 | -0.657 | 1.191 | 4.599 | 12 |
| B | 8 | 10 | 318.0 | -1.0 | -1.5 | -0.258 | 0.861 | 2.878 | 12 |
| B | 8 | 20 | 318.0 | -1.0 | -1.5 | -0.226 | 0.482 | 1.780 | 12 |
| B | 9 | 0 | 319.0 | 3.5 | -2.0 | -0.722 | 2.804 | 11.193 | 6 |
| B | 9 | 10 | 319.0 | 3.5 | -2.0 | -0.239 | 2.282 | 8.136 | 6 |
| B | 9 | 20 | 319.0 | 3.5 | -2.0 | -0.478 | 1.552 | 4.772 | 6 |
| B | 10 | 0 | 316.0 | 0.0 | 0.0 | -0.874 | 1.715 | 7.217 | 6 |
| B | 10 | 10 | 316.0 | 0.0 | 0.0 | -0.598 | 1.311 | 4.866 | 6 |
| B | 10 | 20 | 316.0 | 0.0 | 0.0 | -0.416 | 0.845 | 2.859 | 6 |
| B | 11 | 0 | 317.0 | 3.0 | -1.5 | -2.210 | 3.938 | 17.480 | 0 |
| B | 11 | 10 | 317.0 | 3.0 | -1.5 | -1.432 | 2.953 | 11.354 | 0 |
| B | 11 | 20 | 317.0 | 3.0 | -1.5 | -0.914 | 1.666 | 6.176 | 0 |
| B | 12 | 0 | 318.0 | 1.0 | -2.5 | -4.041 | 6.055 | 19.332 | 0 |
| B | 12 | 10 | 318.0 | 1.0 | -2.5 | -2.517 | 3.814 | 10.972 | 0 |
| B | 12 | 20 | 318.0 | 1.0 | -2.5 | -1.366 | 2.422 | 6.235 | 0 |
| B | 13 | 0 | 319.5 | 5.5 | -4.5 | -1.363 | 3.938 | 13.038 | -6 |
| B | 13 | 10 | 319.5 | 5.5 | -4.5 | -0.886 | 2.686 | 8.919 | -6 |
| B | 13 | 20 | 319.5 | 5.5 | -4.5 | -0.481 | 1.734 | 5.513 | -6 |
| B | 14 | 0 | 321.5 | 2.0 | -2.0 | -2.045 | 2.804 | 9.920 | -6 |
| B | 14 | 10 | 321.5 | 2.0 | -2.0 | -1.499 | 2.153 | 6.554 | -6 |
| B | 14 | 20 | 321.5 | 2.0 | -2.0 | -0.790 | 1.367 | 4.130 | -6 |
| B | 15 | 0 | 323.5 | 1.0 | -2.0 | -1.889 | 2.851 | 8.749 | -12 |
| B | 15 | 10 | 323.5 | 1.0 | -2.0 | -1.130 | 2.002 | 5.435 | -12 |
| B | 15 | 20 | 323.5 | 1.0 | -2.0 | -0.632 | 1.370 | 3.290 | -12 |
| B | 16 | 0 | 323.5 | 2.0 | -3.0 | -2.685 | 1.860 | 9.029 | -12 |
| B | 16 | 10 | 323.5 | 2.0 | -3.0 | -1.473 | 1.279 | 5.702 | -12 |
| B | 16 | 20 | 323.5 | 2.0 | -3.0 | -0.965 | 0.784 | 3.378 | -12 |
| B | 17 | 0 | 318.5 | 1.0 | -1.0 | -0.874 | 1.002 | 5.938 | -18 |
| B | 17 | 10 | 318.5 | 1.0 | -2.0 | -0.244 | 0.634 | 3.197 | -18 |
| B | 17 | 20 | 318.5 | 1.0 | -2.0 | -0.275 | 0.384 | 2.011 | -18 |
| B | 18 | 0 | 323.5 | 3.5 | -1.0 | -0.417 | 0.968 | 5.625 | -18 |
| B | 18 | 10 | 323.5 | 2.0 | -3.0 | -0.120 | 0.580 | 2.524 | -18 |
| B | 18 | 20 | 323.5 | 2.0 | -3.0 | -0.176 | 0.249 | 1.628 | -18 |
| B | 19 | 0 | 320.5 | 4.5 | -3.0 | 0.023 | 0.570 | 5.594 | -24 |
| B | 19 | 10 | 320.5 | 4.5 | -3.0 | 0.179 | 0.221 | 3.370 | -24 |
| B | 19 | 20 | 320.5 | 4.5 | -3.0 | 0.124 | 0.144 | 2.365 | -24 |
| B | 20 | 0 | 318.0 | 1.0 | -1.0 | -0.142 | 1.168 | 6.377 | -24 |
| B | 20 | 10 | 318.0 | 1.0 | -1.0 | 0.387 | 0.993 | 4.234 | -24 |
| B | 20 | 20 | 318.0 | 1.0 | -1.0 | 0.029 | 0.416 | 2.786 | -24 |
| B | 21 | 0 | 318.5 | 4.5 | -1.0 | 0.145 | 0.793 | 4.410 | -30 |
| B | 21 | 10 | 318.5 | 4.5 | -1.0 | 0.141 | 0.434 | 3.251 | -30 |
| B | 21 | 20 | 318.5 | 4.5 | -1.0 | 0.111 | 0.394 | 2.466 | -30 |
| B | 22 | 0 | 321.5 | 8.0 | -4.0 | -0.035 | 0.233 | 2.137 | -30 |
| B | 22 | 10 | 321.5 | 8.0 | -4.0 | 0.043 | 0.202 | 1.397 | -30 |
| B | 22 | 20 | 321.5 | 8.0 | -4.0 | -0.017 | 0.175 | 1.166 | -30 |
| B | 23 | 0 | 320.0 | 4.5 | 2.0 | -0.204 | 0.387 | 2.001 | -40 |
| B | 23 | 10 | 320.0 | 4.5 | -1.0 | 0.023 | 0.236 | 1.407 | -40 |
| B | 23 | 20 | 320.0 | 4.5 | -1.0 | -0.009 | 0.104 | 0.919 | -40 |
| B | 24 | 0 | 323.5 | 4.5 | 2.0 | -0.184 | 0.574 | 2.009 | -40 |
| B | 24 | 10 | 323.5 | 4.5 | 2.0 | -0.087 | 0.470 | 1.560 | -40 |
| B | 24 | 20 | 323.5 | 4.5 | 2.0 | -0.139 | 0.367 | 1.189 | -40 |
| B | 25 | 0 | 329.0 | 5.0 | -2.0 | 0.714 | 1.544 | 4.704 | -77 |
| B | 25 | 10 | 329.0 | 5.0 | -2.0 | 0.333 | -0.162 | 0.150 | -77 |
| B | 26 | 0 | 331.5 | 4.0 | 0.0 | 0.720 | 1.303 | 4.516 | -77 |
| B | 26 | 10 | 331.5 | 4.0 | 0.0 | 0.793 | 0.433 | 1.041 | -77 |
| B | 27 | 0 | 326.5 | 8.0 | 1.0 | 0.620 | 1.076 | 3.953 | -85 |
| B | 27 | 10 | 326.5 | 8.0 | 1.0 | 0.866 | 1.022 | 2.811 | -85 |
| B | 27 | 20 | 326.5 | 8.0 | 1.0 | 0.557 | 0.903 | 1.955 | -85 |
| B | 28 | 0 | 327.5 | 8.0 | -2.0 | 1.167 | 1.071 | 3.911 | -85 |
| B | 28 | 10 | 327.5 | 8.0 | -2.0 | 1.248 | 1.061 | 2.994 | -85 |
| B | 28 | 20 | 327.5 | 8.0 | -2.0 | 0.897 | 0.818 | 2.145 | -85 |
| B | 29 | 0 | 327.0 | 3.0 | 0.5 | 0.174 | 0.943 | 3.876 | -90 |
| B | 29 | 10 | 327.0 | 3.0 | 0.5 | 0.366 | 0.738 | 2.603 | -90 |
| B | 29 | 20 | 327.0 | 3.0 | 0.5 | 0.179 | 0.453 | 1.860 | -90 |
| B | 30 | 0 | 330.0 | 5.0 | 0.0 | 0.145 | 0.912 | 4.250 | -90 |
| B | 30 | 10 | 330.0 | 5.0 | 0.0 | 0.293 | 0.699 | 2.992 | -90 |
| B | 30 | 20 | 330.0 | 5.0 | 0.0 | 0.267 | 0.457 | 2.282 | -90 |
| B | 31 | 0 | 324.0 | 4.5 | -1.0 | -0.037 | 0.604 | 1.784 | -98 |
| B | 31 | 10 | 324.0 | 4.5 | -1.0 | 0.062 | 0.416 | 1.074 | -98 |
| B | 31 | 20 | 324.0 | 4.5 | -1.0 | 0.019 | 0.221 | 0.733 | -98 |
| B | 32 | 0 | 324.0 | 0.5 | -0.5 | -0.018 | 0.175 | 1.406 | -98 |
| B | 32 | 10 | 324.0 | 0.5 | -0.5 | -0.104 | 0.128 | 0.888 | -98 |
| B | 32 | 20 | 324.0 | 0.5 | -0.5 | -0.119 | 0.053 | 0.772 | -98 |
| B | 33 | 0 | 331.5 | 0.0 | -1.5 | -0.047 | 1.564 | 4.621 | -102 |
| B | 33 | 10 | 331.5 | 0.0 | -1.5 | 0.394 | 1.047 | 3.156 | -102 |
| B | 33 | 20 | 331.5 | 0.0 | -1.5 | 0.235 | 0.837 | 2.110 | -102 |
| B | 34 | 0 | 332.5 | -3.0 | -2.5 | -0.197 | 1.061 | 4.201 | -102 |
| B | 34 | 10 | 332.5 | -3.0 | -2.5 | 0.252 | 0.787 | 2.875 | -102 |
| B | 34 | 20 | 332.5 | -3.0 | -2.5 | 0.091 | 0.673 | 1.784 | -102 |
| B | 35 | 0 | 327.0 | 2.0 | -1.5 | 0.179 | 2.846 | 16.150 | -109 |
| B | 35 | 10 | 327.0 | 2.0 | -1.5 | 0.743 | 2.522 | 10.861 | -109 |
| B | 35 | 20 | 327.0 | 2.0 | -1.5 | 0.442 | 1.938 | 7.616 | -109 |
| B | 36 | 0 | 326.0 | 3.0 | -1.5 | 1.936 | 2.819 | 12.084 | -109 |
| B | 36 | 10 | 326.0 | 3.0 | -1.5 | 2.066 | 2.200 | 8.210 | -109 |
| B | 36 | 20 | 326.0 | 3.0 | -1.5 | 1.389 | 1.271 | 6.119 | -109 |
| B | 37 | 0 | 330.0 | 4.0 | 0.5 | 2.427 | 5.828 | 18.495 | -114 |

| | | | | | | | | | |
|---|---|---|---|---|---|---|---|---|---|
| B | 37 | 10 | 330.0 | 4.0 | 0.5 | 2.676 | 4.724 | 13.116 | -114 |
| B | 37 | 20 | 330.0 | 4.0 | 0.5 | 1.512 | 2.943 | 8.140 | -114 |
| B | 38 | 0 | 331.5 | 5.0 | 2.0 | 2.612 | 6.235 | 8.719 | -114 |
| B | 38 | 10 | 331.5 | 5.0 | 2.0 | 2.540 | 4.380 | 12.598 | -114 |
| B | 38 | 20 | 331.5 | 5.0 | 2.0 | 1.597 | 3.145 | 7.963 | -114 |
| B | 39 | 0 | 332.0 | 2.0 | -1.0 | 0.268 | 3.895 | 17.112 | -119 |
| B | 39 | 10 | 332.0 | 2.0 | -1.0 | 1.067 | 3.068 | 11.111 | -119 |
| B | 39 | 20 | 332.0 | 2.0 | -1.0 | 1.103 | 2.584 | 7.165 | -119 |
| B | 40 | 0 | 336.0 | 2.5 | -2.0 | 1.346 | 3.636 | 15.884 | -119 |
| B | 40 | 10 | 336.0 | 2.5 | -2.0 | 2.341 | 3.117 | 10.731 | -119 |
| B | 40 | 20 | 336.0 | 2.5 | -2.0 | 1.440 | 2.099 | 7.080 | -119 |
| B | 41 | 0 | 331.5 | -2.0 | -4.0 | 2.391 | 5.341 | 18.132 | -125 |
| B | 41 | 10 | 331.5 | -2.0 | -4.0 | 2.835 | 4.502 | 12.480 | -125 |
| B | 41 | 20 | 331.5 | -2.0 | -4.0 | 1.645 | 2.933 | 8.278 | -125 |
| B | 42 | 0 | 335.0 | 0.0 | -2.5 | 1.594 | 7.150 | 20.475 | -125 |
| B | 42 | 10 | 335.0 | 0.0 | -2.5 | 2.419 | 4.963 | 13.897 | -125 |
| B | 42 | 20 | 335.0 | 0.0 | -2.5 | 2.165 | 3.437 | 9.149 | -125 |
| B | 43 | 0 | 328.0 | -1.0 | -3.0 | 3.371 | 8.791 | 18.643 | -132 |
| B | 43 | 10 | 328.0 | -1.0 | -3.0 | 3.573 | 6.900 | 11.815 | -132 |
| B | 43 | 20 | 328.0 | -1.0 | -3.0 | 2.471 | 4.959 | 8.335 | -132 |
| B | 44 | 0 | 333.0 | -1.0 | -0.5 | 4.326 | 8.971 | 15.934 | -132 |
| B | 44 | 10 | 333.0 | -1.0 | -0.5 | 4.006 | 7.103 | 9.769 | -132 |
| B | 44 | 20 | 333.0 | -1.0 | -0.5 | 3.131 | 4.788 | 6.899 | -132 |
| B | 45 | 0 | 325.0 | 1.0 | -4.0 | 4.910 | 9.312 | 15.802 | -139 |
| B | 45 | 10 | 325.0 | 1.0 | -4.0 | 3.975 | 7.431 | 11.516 | -139 |
| B | 45 | 20 | 325.0 | 1.0 | -4.0 | 2.780 | 5.188 | 7.738 | -139 |
| B | 46 | 0 | 332.5 | 2.0 | -4.0 | 7.427 | 5.884 | 14.893 | -139 |
| B | 46 | 10 | 332.5 | 2.0 | -4.0 | 6.444 | 4.978 | 9.998 | -139 |
| B | 46 | 20 | 332.5 | 2.0 | -4.0 | 4.639 | 3.531 | 6.789 | -139 |
| B | 47 | 0 | 329.0 | 2.5 | -4.0 | 2.154 | 4.293 | 9.535 | -146 |
| B | 47 | 10 | 329.0 | 2.5 | -4.0 | 2.212 | 3.578 | 6.168 | -146 |
| B | 47 | 20 | 329.0 | 2.5 | -4.0 | 1.732 | 2.395 | 4.169 | -146 |
| B | 48 | 0 | 333.0 | 0.0 | -4.0 | 2.385 | 3.336 | 8.997 | -146 |
| B | 48 | 10 | 333.0 | 0.0 | -4.0 | 2.144 | 2.781 | 5.658 | -146 |
| B | 48 | 20 | 333.0 | 0.0 | -4.0 | 1.537 | 1.826 | 3.599 | -146 |
| B | 49 | 0 | 327.0 | 2.0 | -3.0 | 3.554 | 6.560 | 14.747 | -153 |
| B | 49 | 10 | 327.0 | 2.0 | -3.0 | 3.253 | 4.639 | 9.478 | -153 |
| B | 49 | 20 | 327.0 | 2.0 | -3.0 | 2.473 | 2.678 | 7.029 | -153 |
| B | 50 | 0 | 328.0 | 2.0 | -3.0 | 3.605 | 5.845 | 12.864 | -153 |
| B | 50 | 10 | 328.0 | 2.0 | -3.0 | 3.142 | 4.059 | 7.477 | -153 |
| B | 50 | 20 | 328.0 | 2.0 | -3.0 | 2.485 | 2.865 | 4.808 | -153 |
| B | 51 | 0 | 325.0 | 0.0 | -3.0 | 1.171 | 3.982 | 13.048 | -159 |
| B | 51 | 10 | 325.0 | 0.0 | -3.0 | 1.139 | 2.932 | 8.399 | -159 |
| B | 51 | 20 | 325.0 | 0.0 | -3.0 | 0.939 | 2.370 | 5.712 | -159 |
| B | 52 | 0 | 332.0 | 1.0 | -3.0 | 2.056 | 3.394 | 10.121 | -159 |
| B | 52 | 10 | 332.0 | 1.0 | -3.0 | 1.782 | 2.575 | 6.361 | -159 |
| B | 52 | 20 | 332.0 | 1.0 | -3.0 | 1.462 | 1.639 | 4.594 | -159 |
| B | 53 | 0 | 326.5 | 2.0 | -4.0 | 2.802 | 5.461 | 12.166 | -165 |
| B | 53 | 10 | 326.5 | 2.0 | -4.0 | 2.467 | 4.412 | 7.996 | -165 |
| B | 53 | 20 | 326.5 | 2.0 | -4.0 | 1.834 | 3.171 | 5.571 | -165 |
| B | 54 | 0 | 332.5 | 2.0 | -4.5 | 4.715 | 7.187 | 12.836 | -165 |
| B | 54 | 10 | 332.5 | 2.0 | -4.5 | 4.511 | 4.968 | 8.232 | -165 |
| B | 54 | 20 | 332.5 | 2.0 | -4.5 | 2.904 | 3.513 | 5.571 | -165 |
| B | 55 | 0 | 325.0 | 5.0 | -2.0 | -0.083 | 3.996 | 7.862 | -170 |
| B | 55 | 10 | 325.0 | 5.0 | -2.0 | 0.155 | 2.917 | 4.778 | -170 |
| B | 55 | 20 | 325.0 | 5.0 | -2.0 | -0.213 | 1.769 | 3.231 | -170 |
| B | 56 | 0 | 328.0 | 3.0 | -4.5 | 0.219 | 4.920 | 9.125 | -170 |
| B | 56 | 10 | 328.0 | 3.0 | -4.5 | 0.318 | 2.794 | 5.693 | -170 |
| B | 56 | 20 | 328.0 | 3.0 | -4.5 | 0.480 | 1.903 | 3.644 | -170 |
| B | 57 | 0 | 325.5 | 3.0 | -3.5 | 1.700 | 4.076 | 9.662 | -176 |
| B | 57 | 10 | 325.5 | 3.0 | -3.5 | 1.213 | 3.219 | 5.801 | -176 |
| B | 57 | 20 | 325.5 | 3.0 | -3.5 | 0.544 | 2.068 | 3.559 | -176 |
| B | 58 | 0 | 325.5 | 3.0 | -3.5 | 1.054 | 4.456 | 10.638 | -176 |
| B | 58 | 10 | 325.5 | 3.0 | -3.5 | 0.968 | 2.988 | 6.569 | -176 |
| B | 58 | 20 | 325.5 | 3.0 | -3.5 | 0.631 | 2.475 | 4.393 | -176 |
| B | 59 | 0 | 323.5 | 2.0 | -6.0 | 3.539 | 5.734 | 15.459 | -182 |
| B | 59 | 10 | 323.5 | 2.0 | -6.0 | 2.546 | 4.048 | 9.242 | -182 |
| B | 59 | 20 | 323.5 | 2.0 | -6.0 | 2.044 | 2.433 | 6.783 | -182 |
| B | 60 | 0 | 327.0 | 2.5 | -3.5 | 2.738 | 5.665 | 14.692 | -182 |
| B | 60 | 10 | 327.0 | 2.5 | -3.5 | 2.197 | 4.378 | 9.761 | -182 |
| B | 60 | 20 | 327.0 | 2.5 | -3.5 | 1.476 | 3.437 | 6.480 | -182 |
| B | 61 | 0 | 322.5 | 1.0 | -2.0 | 1.045 | 4.402 | 10.051 | -189 |
| B | 61 | 10 | 322.5 | 1.0 | -2.0 | 1.059 | 3.181 | 6.426 | -189 |
| B | 61 | 20 | 322.5 | 1.0 | -2.0 | 1.156 | 2.363 | 4.557 | -189 |
| B | 62 | 0 | 325.0 | -2.0 | -4.0 | 1.415 | 4.542 | 12.353 | -189 |
| B | 62 | 10 | 325.0 | -2.0 | -4.0 | 1.248 | 3.609 | 7.621 | -189 |
| B | 62 | 20 | 325.0 | -2.0 | -4.0 | 1.196 | 2.673 | 5.177 | -189 |
| B | 63 | 0 | 330.0 | -2.5 | -1.5 | 1.561 | 3.675 | 7.913 | -194 |
| B | 63 | 10 | 330.0 | -2.5 | -1.5 | 1.728 | 2.953 | 5.419 | -194 |
| B | 63 | 20 | 330.0 | -2.5 | -1.5 | 1.150 | 2.141 | 3.647 | -194 |
| B | 64 | 0 | 328.0 | 1.5 | -4.5 | 1.164 | 4.676 | 9.798 | -194 |
| B | 64 | 10 | 328.0 | 1.5 | -4.5 | 1.498 | 3.515 | 6.737 | -194 |
| B | 64 | 20 | 328.0 | 1.5 | -4.5 | 1.208 | 2.088 | 4.701 | -194 |
| B | 65 | 0 | 325.0 | 6.0 | -4.5 | 2.414 | 7.079 | 22.423 | -202 |
| B | 65 | 10 | 325.0 | 6.0 | -4.5 | 3.064 | 4.588 | 10.217 | -202 |
| B | 65 | 20 | 325.0 | 6.0 | -4.5 | 1.847 | 3.610 | 7.278 | -202 |
| B | 66 | 0 | 330.5 | 3.5 | -4.5 | 2.485 | 5.259 | 12.676 | -202 |
| B | 66 | 10 | 330.5 | 3.5 | -4.5 | 2.273 | 3.722 | 7.266 | -202 |
| B | 66 | 20 | 330.5 | 3.5 | -4.5 | 1.639 | 2.645 | 5.597 | -202 |
| B | 67 | 0 | 310.5 | 2.5 | -1.0 | 0.861 | 3.769 | 9.407 | -222 |
| B | 67 | 10 | 310.5 | 2.5 | -1.0 | 1.115 | 2.618 | 5.076 | -222 |
| B | 67 | 20 | 310.5 | 2.5 | -1.0 | 0.888 | 1.764 | 3.017 | -222 |
| B | 68 | 0 | 317.5 | 0.5 | 0.0 | -0.029 | 4.455 | 11.887 | -222 |
| B | 68 | 10 | 317.5 | 0.5 | 0.0 | 0.686 | 3.040 | 6.960 | -222 |
| B | 68 | 20 | 317.5 | 0.5 | 0.0 | 0.478 | 2.115 | 4.272 | -222 |
| B | 69 | 0 | 323.5 | -1.0 | -2.5 | -0.578 | 2.287 | 5.998 | -230 |
| B | 69 | 10 | 323.5 | -1.0 | -2.5 | -0.190 | 1.640 | 3.639 | -230 |
| B | 69 | 20 | 323.5 | -1.0 | -2.5 | -0.124 | 1.154 | 2.577 | -230 |
| B | 70 | 0 | 325.0 | 4.0 | -4.5 | -0.010 | 1.607 | 6.653 | -230 |
| B | 70 | 10 | 325.0 | 4.0 | -4.5 | 0.146 | 1.181 | 3.827 | -230 |
| B | 70 | 20 | 325.0 | 4.0 | -4.5 | 0.162 | 0.880 | 2.661 | -230 |
| B | 71 | 0 | 316.5 | 0.0 | -3.0 | -2.404 | 2.954 | 14.207 | -234 |
| B | 71 | 10 | 316.5 | 0.0 | -3.0 | -1.730 | 2.190 | 10.176 | -234 |
| B | 71 | 20 | 316.5 | 0.0 | -3.0 | -1.216 | 1.366 | 7.483 | -234 |
| B | 72 | 0 | 318.5 | 3.0 | -4.0 | -1.854 | 4.354 | 15.357 | -234 |
| B | 72 | 10 | 318.5 | 3.0 | -4.0 | -0.937 | 3.283 | 10.334 | -234 |
| B | 72 | 20 | 318.5 | 3.0 | -4.0 | -0.640 | 2.301 | 7.505 | -234 |
| B | 73 | 0 | 321.0 | 4.0 | -2.0 | -0.173 | 1.142 | 6.470 | -240 |
| B | 73 | 10 | 321.0 | 4.0 | -2.0 | -0.019 | 0.977 | 4.757 | -240 |
| B | 73 | 20 | 321.0 | 4.0 | -2.0 | 0.106 | 0.721 | 3.514 | -240 |
| B | 74 | 0 | 321.0 | -1.5 | -3.0 | -0.298 | 1.157 | 6.980 | -240 |
| B | 74 | 10 | 321.0 | -1.5 | -3.0 | -0.194 | 0.909 | 4.907 | -240 |
| B | 74 | 20 | 321.0 | -1.5 | -3.0 | -0.172 | 0.825 | 3.796 | -240 |
| B | 75 | 0 | 323.0 | -2.0 | -3.5 | -0.220 | 1.624 | 5.459 | -246 |
| B | 75 | 10 | 323.0 | -2.0 | -3.5 | -0.080 | 1.312 | 3.837 | -246 |
| B | 75 | 20 | 323.0 | -2.0 | -3.5 | -0.111 | 0.840 | 2.939 | -246 |
| B | 76 | 0 | 323.0 | -2.0 | -3.0 | -0.158 | 1.433 | 5.983 | -246 |
| B | 76 | 10 | 323.0 | -2.0 | -3.0 | 0.092 | 1.317 | 4.182 | -246 |
| B | 76 | 20 | 323.0 | -2.0 | -3.0 | -0.042 | 0.701 | 3.079 | -246 |
| B | 77 | 0 | 324.0 | 1.5 | -3.5 | -0.337 | 3.151 | 13.537 | -252 |

| | | | | | | | | | |
|---|---|---|---|---|---|---|---|---|---|
| B | 77 | 10 | 324.0 | 1.5 | -3.5 | 0.463 | 2.273 | 8.192 | -252 |
| B | 77 | 20 | 324.0 | 1.5 | -3.5 | 0.389 | 1.751 | 5.654 | -252 |
| B | 78 | 0 | 324.0 | 2.0 | -2.5 | 0.121 | 3.629 | 10.272 | -252 |
| B | 78 | 10 | 324.0 | 2.0 | -2.5 | 0.312 | 3.025 | 7.390 | -252 |
| B | 78 | 20 | 324.0 | 2.0 | -2.5 | 0.366 | 2.165 | 5.344 | -252 |
| B | 79 | 0 | 326.0 | 3.5 | -1.0 | -2.210 | 2.685 | 18.415 | -258 |
| B | 79 | 10 | 326.0 | 3.5 | -1.0 | -0.052 | 1.837 | 7.173 | -258 |
| B | 79 | 20 | 326.0 | 3.5 | -1.0 | -0.119 | 1.352 | 5.237 | -258 |
| B | 80 | 0 | 323.5 | 1.5 | -1.0 | -3.266 | 3.679 | 19.713 | -258 |
| B | 80 | 10 | 323.5 | 1.5 | -1.0 | -0.118 | 2.285 | 8.357 | -258 |
| B | 80 | 20 | 323.5 | 1.5 | -1.0 | 0.049 | 1.813 | 4.747 | -258 |
| B | 81 | 0 | 326.0 | 5.0 | -5.0 | 0.093 | 1.426 | 5.930 | -270 |
| B | 81 | 10 | 326.0 | 5.0 | -5.0 | -0.063 | 0.851 | 3.824 | -270 |
| B | 81 | 20 | 326.0 | 5.0 | -5.0 | 0.067 | 1.511 | [illegible] | -270 |
| B | 82 | 0 | 326.5 | 4.5 | -4.0 | 0.259 | 1.072 | 6.310 | -270 |
| B | 82 | 10 | 326.5 | 4.5 | -4.0 | 0.346 | 0.831 | 4.947 | -270 |
| B | 82 | 20 | 326.5 | 4.5 | -4.0 | 0.347 | 0.465 | 4.008 | -270 |
| B | 83 | 0 | 326.0 | 3.5 | -5.0 | -1.788 | 1.030 | 8.905 | -276 |
| B | 83 | 10 | 326.0 | 3.5 | -5.0 | -1.167 | 0.759 | 5.524 | -276 |
| B | 83 | 20 | 326.0 | 3.5 | -5.0 | -0.744 | 0.448 | 3.640 | -276 |
| B | 84 | 0 | 325.5 | 6.0 | -6.0 | -1.625 | 0.453 | 10.929 | -276 |
| B | 84 | 10 | 325.5 | 6.0 | -6.0 | -0.852 | 0.288 | 6.309 | -276 |
| B | 84 | 20 | 325.5 | 6.0 | -6.0 | -0.420 | 0.210 | 3.931 | -276 |
| B | 85 | 0 | 328.0 | 4.5 | -4.0 | -2.047 | 2.751 | 11.688 | -282 |
| B | 85 | 10 | 328.0 | 4.5 | -4.0 | -0.547 | 2.274 | 6.668 | -282 |
| B | 85 | 20 | 328.0 | 4.5 | -4.0 | -0.329 | 1.632 | 4.395 | -282 |
| B | 86 | 0 | 329.0 | 5.5 | -4.0 | -0.950 | 1.466 | 13.017 | -282 |
| B | 86 | 10 | 329.0 | 5.5 | -4.0 | -0.168 | 1.031 | 8.031 | -282 |
| B | 86 | 20 | 329.0 | 5.5 | -4.0 | -0.070 | 0.817 | 5.582 | -282 |
| B | 87 | 0 | 326.0 | -2.0 | -5.0 | -0.636 | 3.267 | 10.559 | -288 |
| B | 88 | 0 | 323.5 | -4.0 | -4.0 | 6.353 | 2.927 | 14.248 | -288 |
| B | 89 | 0 | 322.0 | 3.0 | -1.5 | -1.019 | 1.334 | 7.225 | -294 |
| B | 89 | 10 | 322.0 | 3.0 | -1.5 | -0.382 | 0.742 | 4.581 | -294 |
| B | 89 | 20 | 322.0 | 3.0 | -1.5 | -0.316 | 0.464 | 3.251 | -294 |
| B | 90 | 0 | 323.0 | 2.5 | -4.0 | -1.394 | 1.563 | 8.294 | -294 |
| B | 90 | 10 | 323.0 | 2.5 | -4.0 | -0.834 | 1.332 | 4.634 | -294 |
| B | 90 | 20 | 323.0 | 2.5 | -4.0 | -0.526 | 0.880 | 3.243 | -294 |
| B | 91 | 0 | 324.5 | -5.0 | 1.5 | -0.688 | 2.467 | 4.848 | -297 |
| B | 91 | 10 | 324.5 | -5.0 | 1.5 | -0.394 | 2.137 | 3.702 | -297 |
| B | 91 | 20 | 324.5 | -5.0 | 1.5 | -0.342 | 1.301 | 2.643 | -297 |
| B | 92 | 0 | 328.0 | -4.5 | -1.5 | -1.394 | 2.983 | 6.265 | -297 |
| B | 92 | 10 | 328.0 | -4.5 | -1.5 | -0.993 | 2.471 | 4.565 | -297 |
| B | 92 | 20 | 328.0 | -4.5 | -1.5 | -0.881 | 1.907 | 3.383 | -297 |
| B | 93 | 0 | 326.5 | -0.5 | -2.0 | -0.521 | 1.478 | 4.147 | -303 |
| B | 93 | 10 | 326.5 | -0.5 | -2.0 | -0.364 | 1.004 | 2.827 | -303 |
| B | 93 | 20 | 326.5 | -0.5 | -2.0 | -0.266 | 0.723 | 2.028 | -303 |
| B | 94 | 0 | 328.5 | -2.0 | -2.5 | -0.700 | 1.083 | 4.619 | -303 |
| B | 94 | 10 | 328.5 | -2.0 | -2.5 | -0.805 | 0.936 | 3.385 | -303 |
| B | 94 | 20 | 328.5 | -2.0 | -2.5 | -0.550 | 0.784 | 2.543 | [illegible] |
| B | 95 | 0 | 330.5 | 2.5 | -2.0 | 0.151 | 1.568 | 3.799 | -309 |
| B | 95 | 10 | 330.5 | 2.5 | -2.0 | 0.130 | 1.373 | 2.548 | -309 |
| B | 95 | 20 | 330.5 | 2.5 | -2.0 | 0.311 | 1.045 | 1.864 | -309 |
| B | 96 | 0 | 333.5 | 1.0 | -1.0 | -0.687 | 3.423 | 5.708 | -309 |
| B | 96 | 10 | 333.5 | 1.0 | -1.0 | -0.450 | 3.061 | 4.131 | -309 |
| B | 96 | 20 | 333.5 | 1.0 | -1.0 | -0.391 | 2.297 | 3.168 | -309 |
| B | 97 | 0 | 315.5 | -1.5 | -1.5 | -0.673 | 0.477 | 3.541 | -315 |
| B | 97 | 10 | 315.5 | -1.5 | -1.5 | -0.226 | 0.494 | 2.705 | -315 |
| B | 97 | 20 | 315.5 | -1.5 | -1.5 | -0.328 | 0.213 | 1.940 | -315 |
| B | 98 | 0 | 325.5 | 0.5 | -1.0 | -1.064 | 0.836 | 4.338 | -315 |
| B | 98 | 10 | 325.5 | 0.5 | -1.0 | -0.736 | 0.784 | 3.450 | -315 |
| B | 98 | 20 | 325.5 | 0.5 | -1.0 | -0.438 | 0.583 | 2.428 | -315 |
| B | 99 | 0 | 321.5 | 4.0 | 1.0 | -0.018 | 1.057 | 4.000 | -321 |
| B | 99 | 10 | 321.5 | 4.0 | 1.0 | 0.233 | 0.809 | 2.591 | -321 |
| B | 99 | 20 | 321.5 | 4.0 | 1.0 | -0.059 | 0.623 | 1.788 | -321 |
| B | 100 | 0 | 328.0 | 6.0 | 0.5 | 0.266 | 1.232 | 3.972 | -321 |
| B | 100 | 10 | 328.0 | 6.0 | 0.5 | 0.463 | 0.926 | 2.955 | -321 |
| B | 100 | 20 | 328.0 | 6.0 | 0.5 | 0.096 | 0.741 | 2.174 | -321 |
| B | 101 | 0 | 331.0 | 0.0 | 0.0 | 0.006 | 4.609 | 7.712 | -329 |
| B | 101 | 10 | 331.0 | 0.0 | 0.0 | 0.400 | 3.515 | 4.903 | -329 |
| B | 101 | 20 | 331.0 | 0.0 | 0.0 | 0.193 | 2.596 | 3.585 | -329 |
| B | 102 | 0 | 330.5 | -2.0 | -1.5 | -0.065 | 4.236 | 7.318 | -329 |
| B | 102 | 10 | 330.5 | -2.0 | -1.5 | 0.130 | 3.092 | 4.907 | -329 |
| B | 102 | 20 | 330.5 | -2.0 | -1.5 | 0.253 | 2.299 | 3.425 | -329 |
| B | 103 | 0 | 336.0 | 1.0 | -1.5 | 1.784 | 4.148 | 5.845 | -334 |
| B | 103 | 10 | 336.0 | 1.0 | -1.5 | 1.677 | 3.222 | 3.868 | -334 |
| B | 103 | 20 | 336.0 | 1.0 | -1.5 | 1.198 | 2.539 | 2.661 | -334 |
| B | 104 | 0 | 337.5 | 0.0 | 0.0 | 0.273 | 4.499 | 5.915 | -334 |
| B | 104 | 10 | 336.0 | 1.0 | -1.5 | 0.508 | 3.565 | 3.812 | -334 |
| B | 104 | 20 | 336.0 | 1.0 | -1.5 | 0.327 | 2.467 | 2.665 | -334 |
| B | 105 | 0 | 339.0 | 0.0 | -1.5 | 1.792 | 1.316 | 24.750 | -340 |
| B | 105 | 10 | 339.0 | 0.0 | -1.5 | 1.473 | 0.802 | 16.676 | -340 |
| B | 105 | 20 | 339.0 | 0.0 | -1.5 | 1.275 | 0.778 | 13.136 | -340 |
| B | 106 | 0 | 338.0 | 1.0 | -1.5 | -0.284 | 0.593 | 5.187 | -340 |
| B | 106 | 10 | 338.0 | 1.0 | -0.5 | -0.098 | 0.430 | 3.571 | -340 |
| B | 106 | 20 | 338.0 | 1.0 | -0.5 | -0.158 | 0.267 | 2.916 | -340 |
| B | 107 | 0 | 318.5 | 7.0 | -3.0 | -0.092 | 0.737 | 4.284 | -346 |
| B | 107 | 10 | 318.5 | 7.0 | -3.0 | 0.021 | 0.570 | 3.141 | -346 |
| B | 107 | 20 | 318.5 | 7.0 | -3.0 | 0.037 | 0.465 | 2.432 | -346 |
| B | 108 | 0 | 326.5 | 3.0 | -1.0 | -0.619 | 1.265 | 6.056 | -346 |
| B | 108 | 10 | 326.5 | 3.0 | -1.0 | -0.262 | 1.021 | 4.089 | -346 |
| B | 108 | 20 | 326.5 | 3.0 | -1.0 | -0.276 | 0.660 | 3.043 | -346 |
| B | 109 | 0 | 322.5 | 4.5 | -1.5 | -0.011 | 0.768 | 13.877 | -354 |
| B | 109 | 10 | 322.5 | 4.5 | -1.5 | -0.196 | 1.184 | 6.296 | -354 |
| B | 109 | 20 | 322.5 | 4.5 | -1.5 | -0.088 | 0.881 | 4.832 | -354 |
| B | 110 | 0 | 322.0 | 4.0 | -2.0 | -0.414 | 1.469 | 7.054 | -354 |
| B | 110 | 10 | 322.0 | 4.0 | -2.0 | -0.328 | 1.415 | 4.944 | -354 |
| B | 110 | 20 | 322.0 | 4.0 | -2.0 | -0.348 | 1.000 | 3.782 | -354 |
| B | 111 | 0 | 323.5 | 2.0 | -3.0 | -0.731 | 0.590 | 5.010 | -359 |
| B | 111 | 10 | 323.5 | 2.0 | -3.0 | -0.451 | 0.476 | 3.738 | -359 |
| B | 111 | 20 | 323.5 | 2.0 | -3.0 | -0.487 | 0.189 | 2.770 | -359 |
| B | 112 | 0 | 326.5 | 0.0 | -2.0 | -1.005 | 0.951 | 5.344 | -359 |
| B | 112 | 10 | 326.5 | 0.0 | -2.0 | -0.696 | 0.796 | 4.014 | -359 |
| B | 112 | 20 | 326.5 | 0.0 | -2.0 | -0.598 | 0.605 | 3.153 | -359 |
| B | 113 | 0 | 323.5 | 2.5 | -1.0 | -0.418 | 0.449 | 4.887 | -365 |
| B | 113 | 10 | 323.5 | 2.5 | -1.0 | -0.073 | 0.196 | 3.149 | -365 |
| B | 113 | 20 | 323.5 | 2.5 | -1.0 | -0.163 | 0.215 | 2.541 | -365 |
| B | 114 | 0 | 329.0 | 5.0 | -4.5 | -0.133 | 0.665 | 6.332 | -365 |
| B | 114 | 10 | 329.0 | 5.0 | -4.5 | 0.086 | 0.411 | 3.564 | -365 |
| B | 114 | 20 | 329.0 | 5.0 | -4.5 | -0.116 | 0.339 | 2.562 | -365 |
| B | 115 | 0 | 319.5 | 3.5 | -3.5 | -0.380 | 0.358 | 4.810 | -374 |
| B | 115 | 10 | 319.5 | 3.5 | -3.5 | -0.061 | 0.346 | 1.317 | -374 |
| B | 115 | 20 | 319.5 | 3.5 | -3.5 | 0.005 | 0.266 | 1.333 | -374 |
| B | 116 | 0 | 325.0 | 2.0 | -3.5 | -0.992 | 0.300 | 6.040 | -374 |
| B | 116 | 10 | 325.0 | 2.0 | -3.5 | -0.218 | 0.316 | 2.194 | -374 |
| B | 116 | 20 | 325.0 | 2.0 | -3.5 | -0.055 | 0.203 | 1.201 | -374 |
| B | 117 | 0 | 313.0 | 0.5 | -2.0 | -0.258 | 2.021 | 4.550 | -383 |
| B | 117 | 10 | 313.0 | 0.5 | -2.0 | 0.022 | 1.617 | 2.943 | -383 |
| B | 117 | 20 | 313.0 | 0.5 | -2.0 | -0.070 | 1.241 | 2.274 | -383 |
| B | 118 | 0 | 324.0 | -0.5 | -2.0 | -0.022 | 1.284 | 3.925 | -383 |
| B | 118 | 10 | 324.0 | -0.5 | -2.0 | 0.103 | 0.983 | 1.949 | -383 |

| | | | | | | | | | |
|---|---|---|---|---|---|---|---|---|---|
| B | 118 | 20 | 324.0 | -0.5 | -2.0 | 0.089 | 0.768 | 1.327 | -383 |
| B | 119 | 0 | 316.0 | -4.0 | 0.5 | -0.608 | 1.351 | 4.690 | -390 |
| B | 119 | 10 | 316.0 | -4.0 | 0.5 | -0.178 | 1.125 | 3.414 | -390 |
| B | 119 | 20 | 316.0 | -4.0 | 0.5 | -0.114 | 0.725 | 2.568 | -390 |
| B | 120 | 0 | 323.5 | -8.5 | 0.5 | -0.532 | 0.813 | 3.311 | -390 |
| B | 120 | 10 | 323.5 | -8.5 | 0.5 | -0.350 | 0.710 | 2.584 | -390 |
| B | 120 | 20 | 323.5 | -8.5 | 0.5 | -0.452 | 0.402 | 1.952 | -390 |
| B | 121 | 0 | 312.0 | -6.5 | -2.5 | -1.043 | 0.716 | 3.659 | -396 |
| B | 121 | 10 | 312.0 | -6.5 | -2.5 | -0.486 | 0.317 | 2.667 | -396 |
| B | 121 | 20 | 312.0 | -6.5 | -2.5 | -0.698 | 0.297 | 2.188 | -396 |
| B | 122 | 0 | 313.0 | -3.0 | -3.5 | -0.934 | 0.369 | 4.403 | -396 |
| B | 122 | 10 | 313.0 | -3.0 | -3.5 | -0.527 | 0.330 | 3.047 | -396 |
| B | 122 | 20 | 313.0 | -3.0 | -3.5 | -0.554 | 0.235 | 2.357 | -396 |
| B | 123 | 0 | 315.0 | -8.0 | -2.0 | -0.487 | 0.231 | 3.695 | -401 |
| B | 123 | 10 | 315.0 | -8.0 | -2.0 | -0.399 | 0.218 | 2.570 | -401 |
| B | 123 | 20 | 315.0 | -8.0 | -2.0 | -0.381 | 0.194 | 2.017 | -401 |
| B | 124 | 0 | 322.0 | -6.0 | -2.5 | -0.525 | 0.196 | 4.250 | -401 |
| B | 124 | 10 | 322.0 | -6.0 | -2.5 | -0.320 | 0.238 | 2.875 | -401 |
| B | 124 | 20 | 322.0 | -6.0 | -2.5 | -0.232 | 0.060 | 2.298 | -401 |
| B | 125 | 0 | 311.0 | -3.0 | -0.5 | -3.493 | 2.579 | 11.135 | -407 |
| B | 125 | 10 | 311.0 | -3.0 | -0.5 | -2.109 | 1.910 | 6.818 | -407 |
| B | 125 | 20 | 311.0 | -3.0 | -0.5 | -1.609 | 1.483 | 5.253 | -407 |
| B | 126 | 0 | 317.5 | -5.5 | 1.5 | -4.411 | 2.917 | 12.792 | -407 |
| B | 126 | 10 | 317.5 | -5.5 | 1.5 | -2.521 | 2.115 | 7.824 | -407 |
| B | 126 | 20 | 317.5 | -5.5 | 1.5 | -1.603 | 1.519 | 5.914 | -407 |
| B | 127 | 0 | 310.5 | -5.0 | -1.5 | -0.689 | 2.580 | 4.614 | -412 |
| B | 127 | 10 | 310.5 | -5.0 | -1.5 | -0.479 | 1.884 | 2.973 | -412 |
| B | 127 | 20 | 310.5 | -5.0 | -1.5 | -0.285 | 1.438 | 2.298 | -412 |
| B | 128 | 0 | 316.0 | -12.0 | -0.5 | -1.289 | 2.298 | 4.322 | -412 |
| B | 128 | 10 | 316.0 | -12.0 | -0.5 | -0.563 | 1.667 | 2.839 | -412 |
| B | 128 | 20 | 316.0 | -12.0 | -0.5 | -0.391 | 1.315 | 2.057 | -412 |
| B | 129 | 0 | 316.0 | -8.0 | 0.5 | -0.939 | 1.396 | 3.619 | -420 |
| B | 129 | 10 | 316.0 | -8.0 | 0.5 | -0.379 | 1.027 | 1.956 | -420 |
| B | 129 | 20 | 316.0 | -8.0 | 0.5 | -0.227 | 0.818 | 1.391 | -420 |
| B | 130 | 0 | 321.0 | -3.0 | 0.0 | -0.811 | 1.645 | 3.343 | -420 |
| B | 130 | 10 | 321.0 | -3.0 | 0.0 | -0.255 | 1.188 | 1.973 | -420 |
| B | 130 | 20 | 321.0 | -3.0 | 0.0 | -0.167 | 0.671 | 1.416 | -420 |
| B | 131 | 0 | 325.0 | -5.0 | -4.5 | -0.842 | 0.114 | 4.399 | -426 |
| B | 131 | 10 | 325.0 | -5.0 | -4.5 | -0.488 | 0.144 | 2.764 | -426 |
| B | 131 | 20 | 325.0 | -5.0 | -4.5 | -0.393 | 0.119 | 2.246 | -426 |
| B | 132 | 0 | 321.5 | 0.0 | 0.0 | -0.589 | 0.479 | 4.966 | -426 |
| B | 132 | 10 | 321.5 | 0.0 | 0.0 | -0.371 | 0.360 | 2.911 | -426 |
| B | 132 | 20 | 321.5 | 0.0 | 0.0 | -0.376 | 0.313 | 2.347 | -426 |
| B | 133 | 0 | 328.5 | -5.5 | -3.0 | -0.331 | 0.227 | 2.031 | -432 |
| B | 133 | 10 | 328.5 | -5.5 | -3.0 | -0.150 | 0.173 | 1.304 | -432 |
| B | 133 | 20 | 328.5 | -5.5 | -3.0 | -0.149 | 0.156 | 0.944 | -432 |
| B | 134 | 0 | 330.0 | -5.0 | -2.0 | -0.280 | -0.103 | 1.966 | -432 |
| B | 134 | 10 | 330.0 | -5.0 | -2.0 | -0.182 | -0.103 | 1.045 | -432 |
| B | 134 | 20 | 330.0 | -5.0 | -2.0 | -0.217 | -0.187 | 0.783 | -432 |
| B | 135 | 0 | 322.0 | 2.0 | -5.0 | -0.061 | 0.179 | 0.764 | -438 |
| B | 135 | 10 | 322.0 | 2.0 | -5.0 | 0.103 | 0.111 | 0.573 | -438 |
| B | 135 | 20 | 322.0 | 2.0 | -5.0 | 0.011 | 0.016 | 0.397 | -438 |
| B | 136 | 0 | 326.5 | -5.0 | -4.5 | -0.094 | 0.012 | 0.718 | -438 |
| B | 136 | 10 | 326.5 | -5.0 | -4.5 | -0.056 | 0.098 | 0.525 | -438 |
| B | 136 | 20 | 326.5 | -5.0 | -4.5 | 0.022 | -0.043 | 0.337 | -438 |
| B | 137 | 0 | 325.0 | -2.5 | -2.0 | -0.181 | 0.292 | 1.517 | -448 |
| B | 137 | 10 | 325.0 | -2.5 | -2.0 | -0.037 | 0.202 | 1.013 | -448 |
| B | 137 | 20 | 325.0 | -2.5 | -2.0 | 0.042 | -0.056 | 0.756 | -448 |
| B | 138 | 0 | 323.5 | 0.0 | -2.0 | -0.051 | 0.151 | 1.130 | -448 |
| B | 138 | 10 | 323.5 | 0.0 | -2.0 | 0.130 | 0.088 | 1.073 | -448 |
| B | 138 | 20 | 323.5 | 0.0 | -2.0 | -0.052 | 0.055 | 0.751 | -448 |
| B | 139 | 0 | 325.5 | -5.0 | -3.5 | -0.384 | 0.153 | 1.671 | -453 |
| B | 139 | 10 | 325.5 | -5.0 | -3.5 | -0.144 | 0.107 | 1.303 | -453 |
| B | 139 | 20 | 325.5 | -5.0 | -3.5 | -0.121 | 0.006 | 0.964 | -453 |
| B | 140 | 0 | 330.0 | -1.0 | -3.0 | -0.224 | 0.107 | 1.522 | -453 |
| B | 140 | 10 | 330.0 | -1.0 | -3.0 | -0.105 | -0.023 | 0.952 | -453 |
| B | 140 | 20 | 330.0 | -1.0 | -3.0 | -0.067 | 0.043 | 0.774 | -453 |
| B | 141 | 0 | 332.0 | -5.0 | -3.5 | -0.388 | 0.677 | 2.621 | -459 |
| B | 141 | 10 | 332.0 | -5.0 | -3.5 | -0.088 | 0.466 | 1.577 | -459 |
| B | 141 | 20 | 332.0 | -5.0 | -3.5 | -0.039 | 0.430 | 1.051 | -459 |
| B | 142 | 0 | 337.5 | -7.0 | -3.0 | -0.333 | 0.604 | 2.989 | -459 |
| B | 142 | 10 | 337.5 | -7.0 | -3.0 | -0.190 | 0.355 | 1.828 | -459 |
| B | 142 | 20 | 337.5 | -7.0 | -3.0 | -0.137 | [illegible] | 1.315 | -459 |
| B | 143 | 0 | 332.5 | -5.5 | 1.0 | -0.209 | [illegible] | 2.395 | -492 |
| B | 143 | 10 | 332.5 | -5.5 | 1.0 | -0.150 | 0.324 | 1.199 | -492 |
| B | 143 | 20 | 332.5 | -5.5 | 1.0 | -0.130 | 0.348 | 0.841 | -492 |
| B | 144 | 0 | 338.0 | -2.5 | 0.5 | -0.164 | 0.451 | 2.133 | -492 |
| B | 144 | 10 | 338.0 | -2.5 | 0.5 | -0.038 | 0.300 | 1.297 | -492 |
| B | 144 | 20 | 338.0 | -2.5 | 0.5 | 0.009 | 0.193 | 0.942 | -492 |
| B | 145 | 0 | 323.0 | -4.5 | 3.5 | -0.227 | 1.075 | 2.614 | -500 |
| B | 145 | 10 | 323.0 | -4.5 | 3.5 | -0.053 | 0.553 | 1.520 | -500 |
| B | 145 | 20 | 323.0 | -4.5 | 3.5 | -0.064 | 0.447 | 1.105 | -500 |
| B | 146 | 0 | 332.0 | -4.5 | 2.0 | -0.083 | 0.877 | 2.717 | -500 |
| B | 146 | 10 | 332.0 | -4.5 | 2.0 | 0.026 | 0.576 | 1.517 | -500 |
| B | 146 | 20 | 332.0 | -4.5 | 2.0 | 0.052 | 0.370 | 1.118 | -500 |
| B | 147 | 0 | 331.0 | 1.5 | 1.5 | 0.851 | 1.443 | 3.536 | -507 |
| B | 147 | 10 | 331.0 | 1.5 | 1.5 | 0.826 | 1.286 | 2.371 | -507 |
| B | 147 | 20 | 331.0 | 1.5 | 1.5 | 0.602 | 0.848 | 1.726 | -507 |
| B | 148 | 0 | 330.0 | 2.0 | 3.0 | -0.110 | 1.419 | 3.328 | -507 |
| B | 148 | 10 | 330.0 | 2.0 | 3.0 | 0.022 | 1.312 | 2.343 | -507 |
| B | 148 | [illegible] | 330.0 | 2.0 | 3.0 | 0.007 | 0.927 | 1.617 | -507 |
| B | 149 | 0 | 326.5 | -3.0 | 1.5 | 0.322 | 1.434 | 4.709 | -513 |
| B | 149 | 10 | 326.5 | -3.0 | 1.5 | 0.247 | 1.157 | 3.498 | -513 |
| B | 149 | 20 | 326.5 | -3.0 | 1.5 | 0.147 | 0.789 | 2.329 | -513 |
| B | 150 | 0 | 326.0 | -3.5 | 0.0 | 0.232 | 1.463 | 4.537 | -513 |
| B | 150 | 10 | 326.0 | -3.5 | 0.0 | 0.182 | 1.023 | 3.017 | -513 |
| B | 150 | 20 | 326.0 | -3.5 | 0.0 | 0.058 | 0.672 | 1.998 | -513 |
| B | 151 | 0 | 323.5 | 2.0 | -4.5 | 0.242 | 1.278 | 3.205 | -521 |
| B | 151 | 10 | 323.5 | 2.0 | -4.5 | 0.265 | 0.799 | 1.796 | -521 |
| B | 151 | 20 | 323.5 | 2.0 | -4.5 | 0.117 | 0.538 | 1.334 | -521 |
| B | 152 | 0 | 327.5 | 0.5 | 1.5 | 1.107 | 1.759 | 3.326 | -521 |
| B | 152 | 10 | 327.5 | 0.5 | 1.5 | 0.743 | 1.163 | 1.854 | -521 |
| B | 152 | 20 | 327.5 | 0.5 | 1.5 | 0.598 | 0.979 | 1.422 | -521 |
| B | 153 | 0 | 329.0 | -1.5 | -0.5 | -0.766 | 2.010 | 5.455 | -529 |
| B | 153 | 10 | 329.0 | -1.5 | -0.5 | -0.528 | 1.876 | 4.560 | -529 |
| B | 153 | 20 | 329.0 | -1.5 | -0.5 | -0.106 | 0.376 | 0.828 | -529 |
| B | 154 | 0 | 330.0 | 2.0 | -2.0 | -1.114 | 3.691 | 5.932 | -529 |
| B | 154 | 10 | 330.0 | 2.0 | -2.0 | -0.854 | 3.436 | 4.890 | -529 |
| B | 154 | 20 | 330.0 | 2.0 | -2.0 | -0.582 | 2.639 | 3.816 | -529 |
| B | 155 | 0 | 325.5 | 1.0 | -0.5 | -0.139 | 0.498 | 1.379 | -538 |
| B | 155 | 10 | 325.5 | 1.0 | -0.5 | -0.083 | 0.582 | 0.985 | -538 |
| B | 155 | 20 | 325.5 | 1.0 | -0.5 | -0.106 | 0.376 | 0.828 | -538 |
| B | 156 | 0 | 329.5 | 0.5 | -4.5 | -0.063 | 0.429 | 1.350 | -538 |
| B | 156 | 10 | 329.5 | 0.5 | -4.5 | -0.114 | 0.469 | 1.079 | -538 |
| B | 156 | 20 | 329.5 | 0.5 | -4.5 | -0.075 | 0.257 | 0.666 | -538 |
| B | 157 | 0 | 325.0 | 1.5 | -1.5 | -0.061 | 0.522 | 1.424 | -548 |
| B | 157 | 10 | 325.0 | 1.5 | -1.5 | -0.047 | 0.460 | 1.021 | -548 |
| B | 157 | 20 | 325.0 | 1.5 | -1.5 | -0.130 | 0.463 | 0.863 | -548 |
| B | 158 | 0 | 326.0 | 0.0 | -7.0 | 0.002 | 0.474 | 1.397 | -548 |
| B | 158 | 10 | 326.0 | 0.0 | -7.0 | -0.082 | 0.499 | 1.114 | -548 |

```
B 158   20 326.0   0.0  -7.0   -0.024   0.288   0.761 -548
C   1    0 346.5  -2.0  -2.0    0.422   1.064   6.424   84
C   1   10 346.5  -2.0  -2.0    0.536   0.626   3.964   84
C   1   20 346.5  -2.0  -2.0   -0.086   0.603   1.977   84
C   2    0 347.0   1.0  -3.0    0.0     1.279   5.854   84
C   2   10 347.0   1.0  -3.0    0.316   1.048   5.933   84
C   2   20 347.0   1.0  -3.0   -0.086   0.603   1.977   84
C   3    0 347.5  -4.0  -1.0    0.139   0.783   4.647   78
C   3   10 347.5  -4.0  -1.0    0.040   0.201   2.997   78
C   3   20 347.5  -4.0  -1.0    0.076   0.224   1.603   78
C   4    0 345.0  -5.0  -3.5    0.539   0.874   6.144   78
C   4   10 345.0  -5.0  -3.5    0.608   0.468   3.614   78
C   4   20 345.0  -5.0  -3.5    0.457   0.265   2.358   78
C   5    0 345.5  -3.5  -4.0    0.003   0.971   7.493   72
C   5   10 345.5  -3.5  -4.0    0.253   0.825   4.913   72
C   5   20 345.5  -3.5  -4.0    0.280   0.589   3.051   72
C   6    0 347.0  -2.5  -2.0    0.283   1.254   7.912   72
C   6   10 347.0  -2.5  -2.0    0.552   0.915   5.257   72
C   6   20 347.0  -2.5  -2.0    0.402   0.631   3.505   72
C   7    0 344.0   1.0   0.0    1.249   1.564   8.024   66
C   7   10 344.0   1.0   0.0    1.226   1.123   5.381   66
C   7   20 344.0   1.0   0.0    0.672   0.794   3.473   66
C   8    0 346.0  -1.0  -3.5    1.335   0.920   8.401   66
C   8   10 346.0  -1.0  -3.5    1.251   0.551   5.838   66
C   8   20 346.0  -1.0  -3.5    1.377   1.158   3.068   66
C   9    0 344.0   1.0  -3.0    0.732   1.195   6.421   59
C   9   10 344.0   1.0  -3.0    0.705   0.839   3.927   59
C   9   20 344.0   1.0  -3.0    0.402   0.557   2.666   59
C  10    0 344.0   1.5  -3.0    0.853   0.956   5.596   59
C  10   10 344.0   1.5  -3.0    0.636   0.585   3.556   59
C  10   20 344.0   1.5  -3.0    0.581   0.481   2.143   59
C  11    0 345.0  -2.5  -2.5   -0.248   0.884   4.740   54
C  11   10 345.0  -2.5  -2.5   -0.249   0.860   2.545   54
C  11   20 345.0  -2.5  -2.5   -0.062   0.433   1.573   54
C  12    0 349.0  -0.5  -2.5    0.426   0.729   4.941   54
C  12   10 349.0  -0.5  -2.5    0.440   0.110   2.734   54
C  12   20 349.0  -0.5  -2.5    0.308   0.218   1.787   54
C  13    0 344.5  -6.0  -0.5    0.098   0.644   5.885   48
C  13   10 344.5  -6.0  -0.5    0.233   0.212   3.472   48
C  13   20 344.5  -6.0  -0.5    0.162   0.249   2.143   48
C  14    0 345.5   1.0  -3.0    0.479   1.258   5.092   48
C  14   10 345.5   1.0  -3.0    0.464   0.776   2.733   48
C  14   20 345.5   1.0  -3.0    0.235   0.453   1.725   48
C  15    0 342.0  -3.0  -3.0    0.781   0.690   4.684   41
C  15   10 342.0  -3.0  -3.0    0.753   0.581   2.506   41
C  15   20 342.0  -3.0  -3.0    0.296   0.192   1.638   41
C  16    0 344.5  -6.5   0.0    0.303   0.640   5.577   41
C  16   10 344.5  -6.5   0.0    0.406   0.371   3.022   41
C  16   20 344.5  -6.5   0.0    0.283   0.216   1.798   41
C  17    0 340.5  -4.0  -2.0    1.052   0.819   6.145   32
C  17   10 340.5  -4.0  -2.0    0.936   0.334   3.816   32
C  17   20 340.5  -4.0  -2.0    0.773   0.245   2.514   32
C  18    0 345.0  -2.5  -3.0    0.347   0.366   5.592   32
C  18   10 345.0  -2.5  -3.0    0.206  -0.025   3.178   32
C  18   20 345.0  -2.5  -3.0    0.333   0.007   2.162   32
C  19    0 335.0   0.5  -0.5   -0.146   0.794   4.883   25
C  19   10 335.0   0.5  -0.5   -0.029   0.356   2.946   25
C  19   20 335.0   0.5  -0.5   -0.130   0.337   1.873   25
C  20    0 340.0   1.0  -3.0   -0.119   0.713   5.084   25
C  20   10 340.0   1.0  -3.0   -0.096   0.364   2.872   25

C  20   20 340.0   1.0  -3.0   -0.126   0.262   1.773   25
C  21    0 340.5 -10.0   3.0   -0.424   1.207   4.116   -3
C  21   10 340.5 -10.0   3.0   -0.075   0.666   1.958   -3
C  21   20 340.5 -10.0   3.0   -0.163   0.451   1.117   -3
C  22    0 349.5 -11.0  -0.5   -0.742   1.049   3.693   -3
C  22   10 349.5 -11.0  -0.5   -0.118   0.652   1.674   -3
C  22   20 349.5 -11.0  -0.5   -0.034   0.520   1.032   -3
C  23    0 334.0 -10.0   1.5   -0.381   0.886   3.300  -11
C  23   10 334.0 -10.0   1.5    0.303   0.365   1.700  -11
C  23   20 334.0 -10.0   1.5   -0.043   0.243   0.966  -11
C  24    0 348.0  -8.0   4.0   -0.085   1.280   3.590  -11
C  24   10 348.0  -8.0   4.0    0.202   0.684   2.172  -11
C  24   20 348.0  -8.0   4.0    0.028   0.361   1.240  -11
C  25    0 341.0  -4.0  -1.0    0.187   0.818   4.052  -16
C  25   10 341.0  -4.0  -1.0    0.496   0.394   1.778  -16
C  25   20 341.0  -4.0  -1.0    0.553   0.218   1.009  -16
C  26    0 348.0  -3.5  -1.0   -0.014   0.719   3.707  -16
C  26   10 348.0  -3.5  -1.0    0.274   0.240   2.192  -16
C  26   20 348.0  -3.5  -1.0    0.051   0.231   1.849  -16
C  27    0 333.5  -7.5   4.0   -0.116   0.689   3.406  -21
C  27   10 333.5  -7.5   4.0   -0.132   0.412   2.427  -21
C  27   20 333.5  -7.5   4.0    0.191   0.105   1.628  -21
C  28    0 336.0 -11.0   4.0   -0.541   1.048   3.805  -21
C  28   10 336.0 -11.0   4.0   -0.219   0.683   2.393  -21
C  28   20 336.0 -11.0   4.0    0.011   0.323   1.780  -21
C  29    0 338.0  -1.0   5.0    0.115   0.877   3.775  -28
C  29   10 338.0  -1.0   5.0    0.074   0.506   2.646  -28
C  29   20 338.0  -1.0   5.0    0.160   0.155   1.475  -28
C  30    0 342.0  -6.0   2.5    0.098   0.873   3.922  -28
C  30   10 342.0  -6.0   2.5    0.194   0.330   2.080  -28
C  30   20 342.0  -6.0   2.5    0.246   0.310   1.130  -28
C  31    0 335.5  -2.0   2.0    0.006   0.654   2.836  -34
C  31   10 335.5  -2.0   2.0    0.240   0.284   1.769  -34
C  31   20 335.5  -2.0   2.0    0.010   0.132   1.152  -34
C  32    0 342.0  -2.5   2.5   -0.116   0.517   2.817  -34
C  32   10 342.0  -2.5   2.5    0.100   0.317   1.841  -34
C  32   20 342.0  -2.5   2.5    0.013   0.143   1.199  -34
C  33    0 344.0  -3.0   0.5   -0.049   0.737   3.148  -41
C  33   10 344.0  -3.0   0.5    0.032   0.390   2.003  -41
C  33   20 344.0  -3.0   0.5   -0.035   0.207   1.289  -41
C  34    0 343.5  -3.0   0.0   -0.014   0.639   3.205  -41
C  34   10 343.5  -3.0   0.0   -0.058   0.168   1.772  -41
C  34   20 343.5  -3.0   0.0    0.272  -0.044   1.335  -41
C  35    0 335.0  -7.0   2.5   -0.368   1.842   8.980  -46
C  35   10 335.0  -7.0   2.5   -0.085   1.401   6.038  -46
C  35   20 335.0  -7.0   2.5   -0.173   1.161   5.092  -46
C  36    0 349.5  -4.5  -1.0   -0.060   0.686   5.112  -46
C  36   10 349.5  -4.5  -1.0    0.064   0.237   3.009  -46
C  36   20 349.5  -4.5  -1.0   -0.138   0.358   1.984  -46
C  37    0 335.0  -7.5   1.0   -0.547   0.845   5.242  -51
C  37   10 335.0  -7.5   1.0   -0.257   0.491   3.146  -51
C  37   20 335.0  -7.5   1.0   -0.128   0.446   2.250  -51
C  38    0 336.0  -2.5   0.0   -0.103   1.245   5.968  -51
C  38   10 336.0  -2.5   0.0    0.007   0.750   3.701  -51
C  38   20 336.0  -2.5   0.0    0.143   0.477   2.634  -51
C  39    0 343.5  -4.0   1.5   -0.193   1.039   6.074  -56
C  39   10 343.5  -4.0   1.5    0.007   0.809   4.195  -56
C  39   20 343.5  -4.0   1.5   -0.120   0.483   2.934  -56
C  40    0 354.0  -7.5   1.5   -0.073   0.712   4.360  -56
C  40   10 354.0  -7.5   1.5    0.034   0.602   2.734  -56
```

```
C 40   20 354.0  -7.5   1.5    0.102    0.370    1.790   -56
C 41    0 358.0  -2.5  -2.0    0.413    1.017    8.753   -62
C 41   10 358.0  -2.5  -2.0    0.392    0.667    6.565   -62
C 41   20 358.0  -2.5  -2.0    0.221    0.522    4.849   -62
C 42    0   6.5  -3.0  -2.0    0.611    0.988    8.738   -62
C 42   10   6.5  -3.0  -2.0    0.567    0.792    6.724   -62
C 42   20   6.5  -3.0  -2.0    0.433    0.517    5.022   -62
C 43    0 356.5  -3.5  -2.0    0.233    0.676    7.410   -65
C 43   10 356.5  -3.5  -2.0    0.229    0.612    5.309   -65
C 43   20 356.5  -3.5  -2.0    0.294    0.321    3.687   -65
C 44    0 357.5  -4.0  -0.5    0.675    0.872    7.445   -65
C 44   10 357.5  -4.0  -0.5    0.604    0.488    5.329   -65
C 44   20 357.5  -4.0  -0.5    0.381    0.452    4.124   -65
C 45    0 357.5  -6.0   0.0    0.495    1.243    8.892   -70
C 45   10 357.5  -6.0   0.0    0.607    0.925    5.967   -70
C 45   20 357.5  -6.0   0.0    0.539    0.634    4.523   -70
C 46    0 357.0  -4.5  -3.5    0.532    0.953    8.692   -70
C 46   10 357.0  -4.5  -3.5    0.581    0.468    6.187   -70
C 46   20 357.0  -4.5  -3.5    0.599    0.507    4.432   -70
C 47    0 358.0  -1.5  -2.0    2.337    3.162   14.796   -76
C 47   10 358.0  -1.5  -2.0    2.084    2.361   10.569   -76
C 47   20 358.0  -1.5  -2.0    1.518    1.732    8.277   -76
C 48    0 356.5  -2.5  -5.0    2.771    2.887   20.819   -76
C 48   10 356.5  -2.5  -5.0    2.682    2.034   15.674   -76
C 48   20 356.5  -2.5  -5.0    1.935    1.516   12.684   -76
C 49    0 343.0   0.0   4.0    0.242    1.044    3.170   -83
C 49   10 343.0   0.0   4.0    0.136    0.833    2.575   -83
C 49   20 343.0   0.0   4.0    0.224    0.681    1.854   -83
C 50    0 341.0  -0.5   3.0   -0.031    1.036    2.816   -83
C 50   10 341.0  -0.5   3.0   -0.084    0.913    2.274   -83
C 50   20 341.0  -0.5   3.0    0.010    0.680    1.729   -83
C 51    0 344.0   0.0   0.0    0.025    0.590    2.591   -90
C 51   10 344.0   0.0   0.0    0.067    0.642    2.272   -90
C 51   20 344.0   0.0   0.0    0.086    0.437    1.729   -90
C 52    0 347.0   5.0   0.0    0.232    0.701    3.679   -90
C 52   10 347.0   5.0   0.0    0.348    0.678    2.836   -90
C 52   20 347.0   5.0   0.0    0.169    0.433    2.269   -90
C 53    0 345.0  -1.5   1.0   -0.001    0.349    2.107   -96
C 53   10 345.0  -1.5   1.0    0.095    0.339    1.589   -96
C 53   20 345.0  -1.5   1.0    0.131    0.244    1.347   -96
C 54    0 342.0  -1.0   0.5    0.118    0.694    4.601   -96
C 54   10 342.0  -1.0   0.5    0.334    0.651    4.230   -96
C 54   20 342.0  -1.0   0.5    0.248    0.595    3.387   -96
C 55    0 344.0  -3.0   1.0    0.139    0.655    3.439  -101
C 55   10 344.0  -3.0   1.0    0.215    0.633    2.982  -101
C 55   20 344.0  -3.0   1.0    0.271    0.475    2.469  -101
C 56    0 345.0  -4.5   2.0    0.040    0.747    4.238  -101
C 56   10 345.0  -4.5   2.0    0.109    0.848    3.853  -101
C 56   20 345.0  -4.5   2.0    0.068    0.587    2.906  -101
C 57    0 340.5  -4.0  -2.5    0.104    0.633    2.989  -107
C 57   10 340.5  -4.0  -2.5    0.363    0.673    2.506  -107
C 57   20 340.5  -4.0  -2.5    0.210    0.428    1.893  -107
C 58    0 340.5  -5.5  -2.0    0.207    0.499    2.556  -107
C 58   10 340.5  -5.5  -2.0    0.323    0.617    2.181  -107
C 58   20 340.5  -5.5  -2.0    0.188    0.379    1.702  -107
C 59    0 331.0  -5.5  -1.0    0.067    0.751    2.380  -112
C 59   10 331.0  -5.5  -1.0    0.260    0.626    1.866  -112
C 59   20 331.0  -5.5  -1.0    0.172    0.483    1.282  -112
C 60    0 331.5  -4.0   2.5    0.083    0.646    2.669  -112
C 60   10 331.5  -4.0   2.5    0.236    0.461    2.003  -112
```

```
C 60   20 331.5  -4.0   2.5    0.127    0.328    1.395  -112
C 61    0 332.0  -4.0   1.5   -0.024    0.531    2.419  -118
C 61   10 332.0  -4.0   1.5    0.046    0.519    1.664  -118
C 61   20 332.0  -4.0   1.5    0.044    0.392    1.455  -118
C 62    0 331.0  -3.5   1.5    0.055    0.492    2.368  -118
C 62   10 331.0  -3.5   1.5    0.140    0.455    2.029  -118
C 62   20 331.0  -3.5   1.5    0.188    0.286    1.666  -118
C 63    0 332.5  -5.0   0.0    0.140    1.350    3.285  -123
C 63   10 332.5  -5.0   0.0    0.236    1.299    2.806  -123
C 63   20 332.5  -5.0   0.0    0.072    0.929    1.856  -123
C 64    0 331.0  -4.0   0.0    0.225    1.068    3.192  -123
C 64   10 331.0  -4.0   0.0    0.369    1.080    2.760  -123
C 64   20 331.0  -4.0   0.0    0.299    0.825    1.845  -123
C 65    0 335.0  -1.0   1.5    0.423    1.183    2.571  -128
C 65   10 335.0  -1.0   1.5    0.338    0.967    1.849  -128
C 65   20 335.0  -1.0   1.5    0.280    0.748    1.394  -128
C 66    0 335.5   1.0   2.0    0.445    1.158    2.756  -128
C 66   10 335.5   1.0   2.0    0.424    0.903    1.868  -128
C 66   20 335.5   1.0   2.0    0.336    0.521    1.392  -128
C 67    0 334.0  -3.0   1.0    0.188    0.621    1.815  -133
C 67   10 334.0  -3.0   1.0    0.223    0.499    1.308  -133
C 67   20 334.0  -3.0   1.0    0.254    0.379    0.896  -133
C 68    0 338.0  -1.5   1.0    0.269    0.677    1.734  -133
C 68   10 338.0  -1.5   1.0    0.180    0.429    1.030  -133
C 68   20 338.0  -1.5   1.0    0.169    0.352    0.851  -133
C 69    0 338.0  -4.5   2.0    0.687    2.057    4.024  -139
C 69   10 338.0  -4.5   2.0    0.686    1.658    2.837  -139
C 69   20 338.0  -4.5   2.0    0.550    1.224    2.039  -139
C 70    0 340.0  -1.0  -5.0    0.493    1.800    3.949  -139
C 70   10 340.0  -1.0  -5.0    0.538    1.388    2.705  -139
C 70   20 340.0  -1.0  -5.0    0.228    0.960    2.080  -139
C 71    0 341.0  -1.0  -1.0    0.706    1.545    3.094  -144
C 71   10 341.0  -1.0  -1.0    0.553    1.106    2.144  -144
C 71   20 341.0  -1.0  -1.0    0.288    0.920    1.716  -144
C 72    0 340.0  -1.0   0.0    0.783    1.982    4.038  -144
C 72   10 340.0  -1.0   0.0    0.769    1.731    2.711  -144
C 72   20 340.0  -1.0   0.0    0.581    1.144    2.090  -144
C 73    0 338.5  -1.0  -1.0    1.368    1.497    3.446  -149
C 73   10 338.5  -1.0  -1.0    1.213    1.251    2.479  -149
C 73   20 338.5  -1.0  -1.0    0.973    0.984    1.739  -149
C 74    0 340.5  -3.0  -3.0    1.376    1.621    3.558  -149
C 74   10 340.5  -3.0  -3.0    1.119    1.267    2.542  -149
C 74   20 340.5  -3.0  -3.0    0.869    1.094    1.906  -149
C 75    0 331.5  -1.5   2.0    1.812    2.896    5.310  -154
C 75   10 331.5  -1.5   2.0    1.769    2.582    4.503  -154
C 75   20 331.5  -1.5   2.0    1.275    1.766    3.066  -154
C 76    0 337.5  -2.5   2.0    1.868    3.081    5.370  -154
C 76   10 337.5  -2.5   2.0    1.821    2.687    4.159  -154
C 76   20 337.5  -2.5   2.0    1.274    1.877    3.118  -154
C 77    0 340.0   0.0   2.0    1.043    1.327    4.438  -159
C 77   10 340.0   0.0   2.0    0.941    1.057    3.132  -159
C 77   20 340.0   0.0   2.0    0.724    0.773    2.414  -159
C 78    0 341.5   1.0   0.5    1.323    1.262    4.107  -159
C 78   10 341.5   1.0   0.5    1.180    1.098    2.974  -159
C 78   20 341.5   1.0   0.5    0.827    0.742    2.139  -159
C 79    0 333.0  -8.0   3.5    0.397    1.394    3.062  -169
C 79   10 333.0  -8.0   3.5    0.329    1.192    2.223  -169
C 79   20 333.0  -8.0   3.5    0.286    0.995    1.536  -169
C 80    0 343.0  -4.5   0.0    0.649    1.095    3.115  -169
C 80   10 343.0  -4.5   0.0    0.605    1.065    2.272  -169
```

```
C  80   20 343.0  -4.5   0.0     0.581     0.722     1.605  -169
C  81    0 328.5  -6.0   4.0     0.222     1.438     2.594  -175
C  81   20 328.5  -6.0   4.0     0.222     0.828     1.348  -175
C  82    0 329.5  -6.5   3.0     0.581     1.357     2.775  -175
C  82   20 329.5  -6.5   3.0     0.279     0.748     1.480  -175
C  83    0 330.0  -4.0   0.5    -0.102     1.153     2.234  -182
C  83   10 330.0  -4.0   0.5     0.011     1.005     1.483  -182
C  83   20 330.0  -4.0   0.5     0.002     0.672     1.095  -182
C  84    0 330.5  -5.0   0.0     0.156     0.995     2.457  -182
C  84   10 330.5  -5.0   0.0     0.131     0.813     1.739  -182
C  84   20 330.5  -5.0   0.0     0.209     0.474     1.389  -182
C  85    0 327.0  -6.5   1.5    -0.002     1.062     2.766  -188
C  85   10 327.0  -6.5   1.5     0.202     0.814     1.950  -188
C  85   20 327.0  -6.5   1.5     0.059     0.621     1.323  -188
C  86    0 330.0  -4.0  -1.5    -0.153     1.143     2.650  -188
C  86   10 330.0  -4.0  -1.5    -0.013     0.901     1.808  -188
C  86   20 330.0  -4.0  -1.5    -0.103     0.510     1.350  -188
C  86   40 330.0  -4.0  -1.5    -0.037     0.210     0.466  -188
C  87    0 331.0  -2.5   2.5     0.924     0.890     2.385  -194
C  87   10 331.0  -2.5   2.5     0.841     0.763     1.457  -194
C  87   20 331.0  -2.5   2.5     0.560     0.451     0.984  -194
C  87   30 331.0  -2.5   2.5     0.539     0.374     0.860  -194
C  87   40 331.0  -2.5   2.5     0.406     0.312     0.744  -194
C  87   60 331.0  -2.5   2.5     0.333     0.187     0.387  -194
C  87   70 331.0  -2.5   2.5     0.381     0.238     0.401  -194
C  87   80 331.0  -2.5   2.5     0.264    -0.105     0.414  -194
C  87  100 331.0  -2.5   2.5     0.247    -0.025     0.270  -194
C  88    0 332.5  -3.0   3.0     0.661     0.633     2.304  -194
C  88   10 332.5  -3.0   3.0     0.535     0.385     1.343  -194
C  88   20 332.5  -3.0   3.0     0.555     0.337     1.000  -194
C  88   30 332.5  -3.0   3.0     0.368     0.338     0.753  -194
C  88   40 332.5  -3.0   3.0     0.245     0.223     0.518  -194
C  88   60 332.5  -3.0   3.0     0.090     0.163     0.388  -194
C  88   70 332.5  -3.0   3.0     0.156     0.090     0.332  -194
C  88   80 332.5  -3.0   3.0     0.333     0.0       0.152  -194
C  88  100 332.5  -3.0   3.0     0.132     0.100     0.154  -194
C  89    0 333.0  -2.5  -0.5    -0.131    -0.257     2.166  -201
C  89   10 333.0  -2.5  -0.5    -0.069    -0.219     1.247  -201
C  89   20 333.0  -2.5  -0.5    -0.034    -0.183     0.742  -201
C  89   30 333.0  -2.5  -0.5    -0.025    -0.265     0.712  -201
C  89   40 333.0  -2.5  -0.5     0.037    -0.239     0.482  -201
C  89   45 333.0  -2.5  -0.5    -0.177    -0.046     0.516  -201
C  89   50 333.0  -2.5  -0.5    -0.037    -0.206     0.375  -201
C  89   55 333.0  -2.5  -0.5    -0.009    -0.379     0.414  -201
C  89   60 333.0  -2.5  -0.5     0.071    -0.310     0.440  -201
C  89   70 333.0  -2.5  -0.5    -0.075    -0.328     0.406  -201
C  89   70 333.0  -2.5  -0.5    -0.055    -0.223     0.298  -201
C  89  100 333.0  -2.5  -0.5     0.037    -0.240     0.167  -201
C  90    0 333.5  -5.0  -1.0     0.232    -0.055     2.451  -201
C  90   10 333.5  -5.0  -1.0     0.353    -0.115     1.525  -201
C  90   20 333.5  -5.0  -1.0     0.349    -0.187     1.161  -201
C  90   30 333.5  -5.0  -1.0     0.407     0.043     1.001  -201
C  90   35 333.5  -5.0  -1.0     0.310    -0.102     0.966  -201
C  90   40 333.5  -5.0  -1.0     0.146    -0.081     0.987  -201
C  90   45 333.5  -5.0  -1.0     0.198    -0.048     0.659  -201
C  90   50 333.5  -5.0  -1.0     0.158    -0.018     0.486  -201
C  90   55 333.5  -5.0  -1.0     0.025    -0.148     0.583  -201
C  90   60 333.5  -5.0  -1.0     0.150    -0.048     0.344  -201
C  90   70 333.5  -5.0  -1.0     0.149    -0.177     0.452  -201
C  90   80 333.5  -5.0  -1.0     0.171    -0.114     0.235  -201
```

```
C  90  100 333.5  -5.0  -1.0     0.208    -0.206     0.392  -201
C  91    0 335.5  -1.5   1.0     0.181     0.666     2.411  -207
C  91   10 335.5  -1.5   1.0     0.197     0.396     1.569  -207
C  91   20 335.5  -1.5   1.0     0.130     0.268     1.084  -207
C  91   30 335.5  -1.5   1.0     0.141     0.291     1.030  -207
C  91   40 335.5  -1.5   1.0     0.128     0.111     0.631  -207
C  91   50 335.5  -1.5   1.0     0.303     0.161     0.609  -207
C  91   60 335.5  -1.5   1.0    -0.037     0.063     0.362  -207
C  92    0 337.0  -6.5   0.5     0.081     0.132     2.506  -207
C  92   10 337.0  -6.5   0.5     0.168     0.172     1.577  -207
C  92   20 337.0  -6.5   0.5     0.053     0.030     1.163  -207
C  92   30 337.0  -6.5   0.5     0.049     0.098     0.836  -207
C  92   40 337.0  -6.5   0.5     0.007    -0.067     0.623  -207
C  92   50 337.0  -6.5   0.5    -0.007    -0.025     0.671  -207
C  92   60 337.0  -6.5   0.5     0.030    -0.007     0.532  -207
C  93    0 333.5  -3.0  -0.5     0.345     0.124     2.794  -213
C  93   10 333.5  -3.0  -0.5     0.287     0.102     1.958  -213
C  93   20 333.5  -3.0  -0.5     0.359    -0.035     1.135  -213
C  93   30 333.5  -3.0  -0.5     0.220    -0.085     0.750  -213
C  93   40 333.5  -3.0  -0.5    -0.099     0.231    -1.970  -213
C  93   45 333.5  -3.0  -0.5    -0.166     0.964    -1.348  -213
C  93   50 333.5  -3.0  -0.5     0.067     1.441    -1.533  -213
C  93   55 333.5  -3.0  -0.5     0.337     1.223    -1.061  -213
C  93   60 333.5  -3.0  -0.5     0.463     1.102    -0.721  -213
C  93   70 333.5  -3.0  -0.5     0.339     0.580    -0.103  -213
C  93   80 333.5  -3.0  -0.5     0.199     0.443     0.149  -213
C  93  100 333.5  -3.0  -0.5     0.048     0.385     0.241  -213
C  94    0 339.5  -7.0   0.0     0.452    -0.045     2.585  -213
C  94   10 339.5  -7.0   0.0     0.430    -0.049     1.804  -213
C  94   20 339.5  -7.0   0.0     0.409     0.002     1.011  -213
C  94   30 339.5  -7.0   0.0     0.396     0.175     0.595  -213
C  94   35 339.5  -7.0   0.0     0.355    -0.101     0.485  -213
C  94   40 339.5  -7.0   0.0     0.099    -0.405     0.341  -213
C  94   45 339.5  -7.0   0.0     0.095    -0.398     0.352  -213
C  94   50 339.5  -7.0   0.0     0.107    -0.329     0.223  -213
C  94   55 339.5  -7.0   0.0     0.117    -0.127     0.334  -213
C  94   60 339.5  -7.0   0.0     0.171     0.083     0.283  -213
C  94   70 339.5  -7.0   0.0     0.090    -0.126     0.354  -213
C  94   80 339.5  -7.0   0.0     0.211    -0.030     0.431  -213
C  95    0 335.5  -1.5  -1.0     0.543     0.719     2.127  -220
C  95   10 335.5  -1.5  -1.0     0.439     0.530     1.335  -220
C  95   20 335.5  -1.5  -1.0     0.319     0.352     0.951  -220
C  96    0 339.0  -3.5  -4.0     0.596     0.480     2.234  -220
C  96   10 339.0  -3.5  -4.0     0.599     0.340     1.336  -220
C  96   20 339.0  -3.5  -4.0     0.456     0.295     0.993  -220
C  97    0 358.0   1.0   0.0     0.181     0.369     2.095  -228
C  97   10 358.0   1.0   0.0     0.028     0.258     1.059  -228
C  97   20 358.0   1.0   0.0    -0.008     0.159     0.689  -228
C  98    0   0.0  -3.0  -0.5     0.384     0.578     2.196  -228
C  98   10   0.0  -3.0  -0.5     0.290     0.317     1.224  -228
C  98   20   0.0  -3.0  -0.5     0.264     0.203     0.783  -228
C  99    0 358.0   2.0  -1.0     0.159     0.674     1.910  -233
C  99   10 358.0   2.0  -1.0     0.048     0.595     1.134  -233
C  99   20 358.0   2.0  -1.0     0.022     0.381     0.871  -233
C 100    0 359.5  -1.5  -1.5     0.098     0.483     1.609  -233
C 100   10 359.5  -1.5  -1.5     0.089     0.374     0.991  -233
C 100   20 359.5  -1.5  -1.5     0.050     0.325     0.647  -233
C 101    0 356.0   1.5  -1.5    -0.100     0.628     1.625  -244
C 101   10 356.0   1.5  -1.5    -0.059     0.420     0.992  -244
C 101   20 356.0   1.5  -1.5    -0.058     0.365     0.688  -244
```

|  |  |  |  |  |  |  |  |  |  |
|---|---|---|---|---|---|---|---|---|---|
| C | 102 | 0 | 359.5 | -2.0 | -1.0 | -0.027 | 0.401 | 1.502 | -244 |
| C | 102 | 10 | 359.5 | -2.0 | -1.0 | -0.054 | 0.292 | 0.964 | -244 |
| C | 102 | 20 | 359.5 | -2.0 | -1.0 | -0.022 | 0.231 | 0.657 | -244 |
| C | 103 | 0 | 359.0 | -0.5 | -1.0 | -0.118 | 0.596 | 1.859 | -249 |
| C | 103 | 10 | 359.0 | -0.5 | -1.0 | -0.084 | 0.419 | 1.108 | -249 |
| C | 103 | 20 | 359.0 | -0.5 | -1.0 | 0.0 | 0.395 | 0.720 | -249 |
| C | 104 | 0 | 1.5 | 2.0 | -0.5 | 0.080 | 0.549 | 2.043 | -249 |
| C | 104 | 10 | 1.5 | 2.0 | -0.5 | 0.090 | 0.366 | 1.128 | -249 |
| C | 104 | 20 | 1.5 | 2.0 | -0.5 | 0.041 | 0.280 | 0.778 | -249 |
| C | 105 | 0 | 350.0 | -2.0 | 3.5 | 0.253 | 0.304 | 1.413 | -256 |
| C | 105 | 10 | 350.0 | -2.0 | 3.5 | 0.246 | 0.157 | 0.961 | -256 |
| C | 105 | 20 | 350.0 | -2.0 | 3.5 | 0.212 | 0.202 | 0.658 | -256 |
| C | 106 | 0 | 354.5 | -4.0 | 2.0 | 0.059 | 0.376 | 1.607 | -256 |
| C | 106 | 10 | 354.5 | -4.0 | 2.0 | 0.055 | 0.227 | 1.016 | -256 |
| C | 106 | 20 | 354.5 | -4.0 | 2.0 | 0.123 | 0.192 | 0.739 | -256 |
| C | 107 | 0 | 353.5 | -2.0 | -2.0 | 0.270 | 0.700 | 1.247 | -262 |
| C | 107 | 10 | 353.5 | -2.0 | -2.0 | 0.310 | 0.552 | 0.753 | -262 |
| C | 107 | 20 | 353.5 | -2.0 | -2.0 | 0.178 | 0.347 | 0.489 | -262 |
| C | 108 | 0 | 348.5 | -1.0 | 0.5 | 0.106 | 0.667 | 1.220 | -262 |
| C | 108 | 10 | 348.5 | -1.0 | 0.5 | 0.148 | 0.577 | 0.794 | -262 |
| C | 108 | 20 | 348.5 | -1.0 | 0.5 | 0.064 | 0.397 | 0.518 | -262 |
| C | 109 | 0 | 353.0 | 0.0 | -2.0 | 0.334 | 0.788 | 1.884 | -267 |
| C | 109 | 10 | 353.0 | 0.0 | -2.0 | 0.430 | 0.671 | 1.576 | -267 |
| C | 109 | 20 | 353.0 | 0.0 | -2.0 | 0.338 | 0.533 | 1.061 | -267 |
| C | 110 | 0 | 346.5 | -0.5 | 5.0 | -0.145 | 0.553 | 1.293 | -267 |
| C | 110 | 10 | 346.5 | -0.5 | 5.0 | -0.017 | 0.414 | 0.913 | -267 |
| C | 110 | 20 | 346.5 | -0.5 | 5.0 | -0.036 | 0.290 | 0.688 | -267 |
| C | 111 | 0 | 350.0 | -2.0 | 5.0 | 0.103 | 0.185 | 0.702 | -275 |
| C | 111 | 10 | 350.0 | -2.0 | 5.0 | 0.054 | 0.162 | 0.487 | -275 |
| C | 111 | 20 | 350.0 | -2.0 | 5.0 | 0.129 | 0.126 | 0.346 | -275 |
| C | 112 | 0 | 351.5 | -4.0 | 6.0 | 0.049 | 0.150 | 0.526 | -275 |
| C | 112 | 10 | 351.5 | -4.0 | 6.0 | 0.057 | 0.082 | 0.352 | -275 |
| C | 112 | 20 | 351.5 | -4.0 | 6.0 | 0.111 | 0.061 | 0.256 | -275 |
| C | 113 | 0 | 358.5 | 2.0 | 3.0 | 0.039 | 0.323 | 0.695 | -293 |
| C | 113 | 10 | 358.5 | 2.0 | 3.0 | 0.050 | 0.237 | 0.512 | -293 |
| C | 113 | 20 | 358.5 | 2.0 | 3.0 | 0.015 | 0.196 | 0.352 | -293 |
| C | 114 | 0 | 6.5 | 4.5 | 3.0 | 0.070 | 0.176 | 0.803 | -293 |
| C | 114 | 10 | 6.5 | 4.5 | 3.0 | 0.034 | 0.044 | 0.516 | -293 |
| C | 114 | 20 | 6.5 | 4.5 | 3.0 | 0.033 | -0.016 | 0.376 | -293 |
| C | 115 | 0 | 352.0 | 1.5 | -1.0 | 0.356 | 0.179 | 1.289 | -303 |
| C | 115 | 10 | 352.0 | 1.5 | -1.0 | 0.288 | 0.087 | 0.827 | -303 |
| C | 115 | 20 | 352.0 | 1.5 | -1.0 | 0.228 | 0.112 | 0.606 | -303 |
| C | 116 | 0 | 353.0 | 4.5 | 1.5 | 0.262 | 0.257 | 1.232 | -303 |
| C | 116 | 10 | 353.0 | 4.5 | 1.5 | 0.175 | 0.157 | 0.817 | -303 |
| C | 116 | 20 | 353.0 | 4.5 | 1.5 | 0.150 | 0.119 | 0.496 | -303 |
| C | 117 | 0 | 0.0 | 3.5 | -3.5 | 0.083 | 0.149 | 0.666 | -316 |
| C | 117 | 10 | 0.0 | 3.5 | -3.5 | 0.108 | -0.031 | 0.480 | -316 |
| C | 117 | 20 | 0.0 | 3.5 | -3.5 | 0.038 | -0.046 | 0.352 | -316 |
| C | 118 | 0 | 1.0 | 1.0 | -5.5 | 0.064 | 0.175 | 0.743 | -316 |
| C | 118 | 10 | 1.0 | 1.0 | -5.5 | 0.030 | 0.103 | 0.476 | -316 |
| C | 118 | 20 | 1.0 | 1.0 | -5.5 | 0.056 | 0.073 | 0.299 | -316 |
| C | 119 | 0 | 1.5 | 0.0 | -4.0 | 0.047 | 0.151 | 0.614 | -322 |
| C | 119 | 10 | 1.5 | 0.0 | -4.0 | 0.048 | 0.109 | 0.373 | -322 |
| C | 119 | 20 | 1.5 | 0.0 | -4.0 | 0.061 | 0.086 | 0.226 | -322 |
| C | 120 | 0 | 0.0 | 2.0 | -2.5 | 0.083 | 0.130 | 0.631 | -322 |
| C | 120 | 10 | 0.0 | 2.0 | -2.5 | 0.119 | 0.069 | 0.357 | -322 |
| C | 120 | 20 | 0.0 | 2.0 | -2.5 | 0.083 | 0.025 | 0.214 | -322 |
| C | 121 | 0 | 358.5 | 8.0 | -2.0 | 0.156 | 0.283 | 0.717 | -329 |
| C | 121 | 10 | 358.5 | 8.0 | -2.0 | 0.080 | 0.197 | 0.367 | -329 |
| C | 121 | 20 | 358.5 | 8.0 | -2.0 | 0.117 | 0.162 | 0.270 | -329 |
| C | 122 | 0 | 0.5 | 6.5 | -2.0 | 0.099 | 0.213 | 0.634 | -329 |
| C | 122 | 10 | 0.5 | 6.5 | -2.0 | 0.076 | 0.121 | 0.339 | -329 |
| C | 122 | 20 | 0.5 | 6.5 | -2.0 | 0.090 | 0.078 | 0.213 | -329 |
| C | 123 | 0 | 359.0 | 15.5 | 1.5 | 0.347 | 0.214 | 0.744 | -335 |
| C | 123 | 10 | 359.0 | 15.5 | 1.5 | 0.265 | 0.159 | 0.342 | -335 |
| C | 123 | 20 | 359.0 | 15.5 | 1.5 | 0.185 | 0.169 | 0.224 | -335 |
| C | 124 | 0 | 359.5 | 15.5 | -0.5 | 0.288 | 0.171 | 0.707 | -335 |
| C | 124 | 10 | 359.0 | 15.5 | -0.5 | 0.221 | 0.135 | 0.331 | -335 |
| C | 124 | 20 | 359.0 | 15.5 | -0.5 | 0.130 | 0.094 | 0.220 | -335 |
| C | 125 | 0 | 340.0 | 3.0 | 0.5 | 0.213 | 0.305 | 0.702 | -343 |
| C | 125 | 10 | 340.0 | 3.0 | 0.5 | 0.187 | 0.183 | 0.434 | -343 |
| C | 125 | 20 | 340.0 | 3.0 | 0.5 | 0.119 | 0.108 | 0.259 | -343 |
| C | 126 | 0 | 344.0 | 2.0 | -1.5 | 0.221 | 0.160 | 0.565 | -343 |
| C | 126 | 10 | 344.0 | 2.0 | -1.5 | 0.145 | 0.063 | 0.358 | -343 |
| C | 126 | 20 | 344.0 | 2.0 | -1.5 | 0.148 | 0.061 | 0.319 | -343 |
| C | 127 | 0 | 340.0 | 1.0 | 0.0 | 0.331 | 0.256 | 0.593 | -350 |
| C | 128 | 0 | 341.0 | 1.0 | 2.0 | 0.088 | 0.361 | 0.628 | -350 |
| C | 129 | 0 | 337.5 | 4.0 | -1.5 | 0.154 | 0.378 | 0.661 | -358 |
| C | 130 | 0 | 341.5 | 1.5 | -1.5 | 0.190 | 0.475 | 0.760 | -358 |
| C | 131 | 0 | 339.0 | 5.5 | -1.5 | 0.228 | 0.269 | 0.779 | -366 |
| C | 132 | 0 | 341.5 | 3.0 | -1.0 | -0.149 | 0.013 | 0.336 | -366 |
| C | 133 | 0 | 340.0 | 7.0 | -2.0 | 0.332 | 0.353 | 0.726 | -375 |
| C | 134 | 0 | 342.0 | 7.0 | -2.0 | 0.127 | 0.172 | 0.753 | -375 |
| C | 135 | 0 | 340.0 | 4.5 | 2.0 | -0.041 | 0.396 | 0.902 | -383 |
| C | 136 | 0 | 340.5 | 1.5 | -2.0 | -0.047 | 0.326 | 0.778 | -383 |
| C | 137 | 0 | 355.0 | -6.5 | 1.0 | 0.074 | 0.082 | 0.617 | -389 |
| C | 138 | 0 | 354.0 | -2.0 | -1.0 | 0.196 | 0.124 | 0.797 | -389 |
| C | 139 | 0 | 357.0 | 0.0 | -2.0 | 0.161 | 0.184 | 1.053 | -395 |
| C | 140 | 0 | 356.5 | 2.0 | 1.0 | 0.194 | 0.162 | 0.836 | -395 |
| C | 141 | 0 | 358.0 | -6.0 | -1.5 | 0.018 | 0.233 | 0.753 | -401 |
| C | 142 | 0 | 0.5 | -1.5 | -0.5 | 0.096 | 0.155 | 0.824 | -401 |
| C | 143 | 0 | 357.5 | 3.5 | 1.0 | 0.124 | 0.056 | 0.346 | -411 |
| C | 144 | 0 | 358.5 | 4.0 | 3.0 | -0.068 | -0.007 | 0.422 | -411 |
| C | 145 | 0 | 353.0 | -2.0 | 3.0 | -0.011 | 0.085 | 0.337 | -422 |
| C | 146 | 0 | 2.5 | -5.0 | 0.0 | 0.059 | 0.071 | 0.399 | -422 |
| C | 147 | 0 | 345.0 | 3.5 | 4.0 | 0.059 | 0.075 | 0.35[illegible] | -432 |
| C | 148 | 0 | 349.0 | 0.5 | 6.0 | -0.026 | 0.126 | 0.3[illegible] | -432 |
| C | 149 | 0 | 348.0 | 0.5 | 3.0 | -0.027 | 0.075 | 0.460 | -438 |
| C | 150 | 0 | 352.5 | 6.5 | 1.0 | 0.069 | 0.081 | 0.578 | -438 |
| C | 151 | 0 | 349.0 | 1.5 | 4.5 | 0.094 | 0.132 | 0.472 | -443 |
| C | 152 | 0 | 351.0 | 2.0 | -0.5 | 0.021 | 0.035 | 0.363 | -443 |
| C | 153 | 0 | 354.5 | 2.5 | 0.5 | 0.069 | 0.072 | 0.438 | -448 |
| C | 154 | 0 | 356.0 | 0.0 | -4.0 | 0.107 | -0.030 | 0.396 | -448 |
| C | 155 | 0 | 357.5 | 0.0 | -1.5 | 1.221 | 0.156 | 2.739 | -457 |
| C | 156 | 0 | 357.0 | 3.0 | 0.0 | 1.166 | 0.139 | 2.115 | -457 |
| C | 157 | 0 | 346.5 | 4.5 | 1.0 | 0.473 | 0.313 | 1.448 | -463 |
| C | 158 | 0 | 350.0 | 8.0 | -2.5 | 0.718 | 0.300 | 1.399 | -463 |
| C | 159 | 0 | 346.0 | 1.0 | 1.0 | 0.751 | 0.359 | 1.716 | -468 |
| C | 160 | 0 | 348.0 | 2.0 | 0.5 | 0.242 | 0.214 | 0.873 | -468 |
| C | 161 | 0 | 341.5 | 0.0 | 2.0 | 0.724 | 0.491 | 1.490 | -474 |
| C | 162 | 0 | 346.0 | -2.0 | 0.0 | 0.812 | 0.617 | 1.914 | -474 |
| C | 163 | 0 | 337.0 | -3.0 | 0.5 | 0.183 | 0.553 | 1.160 | -487 |
| C | 164 | 0 | 339.0 | -0.5 | 4.0 | 0.098 | 0.280 | 1.372 | -487 |
| C | 165 | 0 | 332.0 | 3.0 | -1.0 | 0.444 | 0.670 | 2.013 | -492 |
| C | 166 | 0 | 337.0 | 3.0 | -3.0 | 0.339 | 0.743 | 2.317 | -492 |
| C | 167 | 0 | 337.0 | -1.0 | 1.0 | 0.588 | 0.387 | 1.288 | -498 |
| C | 168 | 0 | 349.0 | -2.0 | -3.0 | 0.483 | 0.286 | 1.227 | -498 |
| C | 169 | 0 | 341.5 | 2.0 | -1.0 | 0.485 | 0.585 | 1.904 | -510 |
| C | 170 | 0 | 348.0 | 1.5 | -4.5 | 0.662 | 0.353 | 2.580 | -510 |
| C | 171 | 0 | 335.0 | 1.0 | -1.0 | 0.497 | 0.475 | 1.164 | -514 |

```
C 172     0 335.5   2.5   0.0      0.591      0.773      1.510  -514
C 173     0 335.5  -2.0  -2.0      0.371      0.722      2.464  -520
C 174     0 336.0   4.0  -2.5      0.634      0.311      2.305  -520
C 175     0 335.5   3.0   0.0      0.210      0.262      0.935  -526
C 176     0 336.0   1.5  -1.5      0.172      0.250      0.945  -526
C 177     0 332.5   0.0   0.5      0.746      0.696      2.306  -533
C 178     0 334.5   1.0   0.0      0.856      0.554      2.711  -533
C 179     0 335.5   4.0  -1.0      0.355      0.452      1.191  -539
C 180     0 337.5   4.0  -1.5      0.478      0.633      1.698  -539
C 181     0 335.0   2.5   1.0      0.754      0.634      1.909  -546
C 182     0 334.5   4.0   0.0      0.746      0.702      2.028  -546
C 183•    0  11.0   0.0  -4.0      1.141      0.668      4.825  -109
C 184•    0   7.0   0.0   1.5      1.153      1.211      5.236  -109
C 185•    0   9.5   2.0  -4.0      1.903      1.103      6.219  -116
C 186•    0   6.0   3.5  -5.5      1.679      0.998      5.884  -116
C 187•    0   6.5   3.0  -5.0      0.750      0.730      3.591  -123
C 188•    0   3.0   1.0  -3.0      1.103      1.065      4.175  -123
C 189•    0   1.5   1.5  -0.5      0.814      1.023      4.581  -128
C 190•    0   5.5   2.0  -6.0      1.058      0.602      3.819  -128
C 191•    0   4.0  -1.0  -5.0      0.501      0.725      2.997  -134
C 192•    0   3.5   0.5  -6.0      0.828      0.693      3.327  -134
C 193•    0 359.5  -1.0   0.0      0.638      0.726      2.476  -142
C 194•    0   4.0   3.0  -3.0      0.803      0.722      3.075  -142
D   1     0 292.0  -2.0  -5.0     -0.767      0.685      3.611   -71
D   1    10 292.0  -2.0  -5.0     -0.250      0.780      2.129   -71
D   1    20 292.0  -2.0  -5.0     -0.350      0.328      1.270   -71
D   2     0 289.0  -2.5  -1.0     -0.974      0.747      3.129   -71
D   2    10 289.0  -2.5  -1.0     -0.536      0.591      1.780   -71
D   2    20 289.0  -2.5  -1.0     -0.724      0.301      1.058   -71
D   3     0 292.5   1.5  -5.0     -0.653      0.582      4.076   -78
D   3    10 292.5   1.5  -5.0     -0.507      0.473      2.394   -78
D   3    20 292.5   1.5  -5.0     -0.313      0.280      1.551   -78
D   4     0 295.0   0.0  -0.5     -0.558      1.269      4.324   -78
D   4    10 295.0   0.0  -0.5     -0.464      1.037      2.409   -78
D   4    20 295.0   0.0  -0.5     -0.133      0.511      1.665   -78
D   5     0 295.5  -4.0  -6.0     -0.544      0.470      4.751   -84
D   5    10 295.5  -4.0  -6.0     -0.343      0.356      2.762   -84
D   5    20 295.5  -4.0  -6.0     -0.250      0.279      2.053   -84
D   6     0 295.0  -1.5  -5.0     -0.410      0.746      4.896   -84
D   6    10 295.0  -1.5  -5.0     -0.160      0.588      3.098   -84
D   6    20 295.0  -1.5  -5.0     -0.130      0.462      2.123   -84
D   7     0 291.0  -4.0  -1.0     -0.739      0.711      3.886   -89
D   7    10 291.0  -4.0  -1.0     -0.461      0.584      2.392   -89
D   7    20 291.0  -4.0  -1.0     -0.400      0.343      1.507   -89
D   8     0 299.5  -1.0  -3.0     -0.597      0.465      4.772   -89
D   8    10 299.5  -1.0  -3.0     -0.323      0.381      2.956   -89
D   8    20 299.5  -1.0  -3.0     -0.289      0.441      2.067   -89
D   9     0 294.0   2.5  -3.0      0.006      0.893      5.244   -95
D   9    10 294.0   2.5  -3.0      0.041      0.414      3.215   -95
D   9    20 294.0   2.5  -3.0      0.103      0.248      2.354   -95
D  10     0 294.0   2.0  -3.0     -0.746      0.672      5.233   -95
D  10    10 294.0   2.0  -3.0     -0.546      0.405      2.905   -95
D  10    20 294.0   2.0  -3.0     -0.332      0.250      2.188   -95
D  11     0 295.0  -1.0  -5.0     -0.377      0.512      2.805  -101
D  11    20 295.0  -1.0  -5.0     -0.169      0.242      1.118  -107
D  12     0 296.0  -3.0  -4.5     -0.373      0.414      3.107  -101
D  12    20 296.0  -3.0  -4.5     -0.315      0.191      1.107  -107
D  13     0 292.5  -2.5  -3.0     -0.479      0.156      2.154  -107
D  13    10 292.5  -2.5  -3.0     -0.400      0.113      1.369  -107
D  13    20 292.5  -2.5  -3.0     -0.317      0.065      0.834  -107
```

```
D  14     0 299.5  -2.0  -6.0     -0.382      0.540      2.270  -107
D  14    10 299.5  -2.0  -6.0     -0.175      0.382      1.379  -107
D  14    20 299.5  -2.0  -6.0     -0.099      0.340      0.963  -107
D  15     0 296.0  -2.0  -3.0     -0.768      0.826      2.738  -114
D  15    10 296.0  -2.0  -3.0     -0.359      0.599      1.717  -114
D  15    20 296.0  -2.0  -3.0     -0.287      0.438      1.255  -114
D  16     0 299.5   0.5  -5.0     -0.628      0.841      2.619  -114
D  16    10 299.5   0.5  -5.0     -0.422      0.557      1.616  -114
D  16    20 299.5   0.5  -5.0     -0.342      0.527      1.166  -114
D  17     0 297.5   0.0  -4.0     -0.311      0.389      3.000  -119
D  17    10 297.5   0.0  -4.0     -0.091      0.290      1.759  -119
D  17    20 297.5   0.0  -4.0     -0.061      0.272      1.153  -119
D  18     0 297.5   3.0  -7.0     -0.354      0.607      3.796  -119
D  18    10 297.5   3.0  -7.0     -0.215      0.267      1.719  -119
D  18    20 297.5   3.0  -7.0     -0.199      0.323      1.137  -119
D  19     0 296.0   0.0  -5.5     -0.394      1.048      4.566  -124
D  19    10 296.0   0.0  -5.5     -0.089      0.711      2.688  -124
D  19    20 296.0   0.0  -5.5     -0.061      0.524      1.559  -124
D  20     0 297.5   2.0  -5.0     -0.338      1.202      7.236  -124
D  20    10 297.5   2.0  -5.0     -0.212      0.736      4.140  -124
D  20    20 297.5   2.0  -5.0     -0.083      0.710      3.002  -124
D  21     0 314.0  -5.0  -2.0     -0.869      2.389     11.137  -131
D  21    10 314.0  -5.0  -2.0     -0.457      1.728      7.936  -131
D  21    20 314.0  -5.0  -2.0     -0.173      1.527      6.168  -131
D  22     0 320.0  -9.0  -4.0     -2.373      1.457     11.692  -131
D  22    10 320.0  -9.0  -4.0     -1.800      1.158      8.580  -131
D  22    20 320.0  -9.0  -4.0     -1.245      1.140      7.095  -131
D  23     0 310.0  -1.5  -4.0     -1.528      1.503     10.022  -139
D  23    10 310.0  -1.5  -4.0     -0.916      0.872      7.293  -139
D  23    20 310.0  -1.5  -4.0     -0.599      0.696      5.996  -139
D  24     0 316.0  -2.0   0.0     -1.087      5.890     27.358  -139
D  24    10 316.0  -2.0   0.0     -1.037      4.851     22.055  -139
D  24    20 316.0  -2.0   0.0     -0.269      4.907     20.033  -139
D  25     0 304.0  -3.0  -1.0     -0.945      1.335      4.415  -147
D  25    10 304.0  -3.0  -1.0     -0.480      0.849      2.528  -147
D  25    20 304.0  -3.0  -1.0     -0.194      0.542      1.576  -147
D  26     0 313.5  -0.5   1.0     -0.220      1.496      3.697  -147
D  26    10 313.5  -0.5   1.0     -0.142      0.658      1.775  -147
D  26    20 313.5  -0.5   1.0      0.054      0.297      0.949  -147
D  27     0 312.5  -2.5   0.5     -0.111      1.738      4.439  -154
D  27    10 312.5  -2.5   0.5     -0.136      1.281      2.710  -154
D  27    20 312.5  -2.5   0.5     -0.101      1.022      1.720  -154
D  28     0 315.5   1.5  -1.5      0.101      1.090      4.581  -154
D  28    10 315.5   1.5  -1.5      0.186      0.818      2.831  -154
D  28    20 315.5   1.5  -1.5      0.203      0.725      1.976  -154
D  29     0 312.0  -2.5   3.0     -0.178      1.535      4.900  -160
D  29    10 312.0  -2.5   3.0      0.353      1.145      3.376  -160
D  29    20 312.0  -2.5   3.0      0.135      0.634      2.248  -160
D  30     0 314.5  -2.5  -1.5     -0.051      0.740      5.171  -160
D  30    10 314.5  -2.5  -1.5     -0.060      0.670      3.348  -160
D  30    20 314.5  -2.5  -1.5      0.0        0.424      2.317  -160
D  31     0 316.5   4.0  -2.5     -0.199      1.338      4.660  -167
D  31    10 316.5   4.0  -2.5      0.026      1.005      3.190  -167
D  31    20 316.5   4.0  -2.5      0.042      0.757      2.285  -167
D  32     0 321.0 [illegible]  -8.5     -0.078      0.617      4.554  -167
D  32    10 321.0 [illegible]  -8.5      0.160      0.689      3.014  -167
D  32    20 321.0   5.0  -8.5      0.260      0.441      2.125  -167
D  33     0 314.0   1.0  -1.0     -0.058      2.070      4.412  -172
D  33    10 314.0   1.0  -1.0     -0.055      1.504      2.872  -172
D  33    20 314.0   1.0  -1.0     -0.111      1.218      2.158  -172
```

```
D  34    0 319.0   3.5  -1.0     0.063     1.291     4.372  -172        D  54    0 327.0   2.0  -2.5     1.663     2.060     3.888  -231
D  34   10 319.0   3.5  -1.0     0.080     0.982     3.002  -172        D  54   10 327.0   2.0  -2.5     1.369     1.507     2.431  -231
D  34   20 319.0   3.5  -1.0     0.095     0.855     2.374  -172        D  54   20 327.0   2.0  -2.5     0.836     1.092     1.751  -231
D  35    0 317.5   6.0  -4.0     0.357     0.890     4.328  -178        D  55    0 315.0   3.0   1.0    -0.053     1.529     2.067  -236
D  35   10 317.5   3.0  -0.5     0.351     0.472     2.861  -178        D  55   10 315.0   3.0   1.0     0.024     1.108     1.298  -236
D  35   20 317.5   3.0  -0.5     0.229     0.379     2.249  -178        D  55   20 315.0   3.0   1.0     0.096     0.806     1.034  -236
D  36    0 319.0   5.0  -5.0     0.160     0.929     4.669  -178        D  56    0 323.0   6.0   2.0     0.207     1.642     2.074  -236
D  36   10 319.0   5.0  -5.0     0.217     0.756     3.010  -178        D  56   10 323.0   6.0   2.0     0.154     1.198     1.237  -236
D  36   20 319.0   5.0  -5.0     0.313     0.543     2.413  -178        D  56   20 323.0   6.0   2.0     0.111     0.938     0.890  -236
D  37    0 317.5   3.0  -0.5     0.639     1.357     4.397  -184        D  57    0 317.0   5.5   0.0     0.032     1.571     2.173  -242
D  37   10 317.5   6.0  -4.0     0.455     1.153     2.873  -184        D  57   10 317.0   5.5   0.0     0.143     1.086     1.280  -242
D  37   20 317.5   6.0  -4.0     0.275     0.754     1.929  -184        D  57   20 317.0   5.5   0.0     0.070     0.699     0.897  -242
D  38    0 320.0   2.0  -1.0     0.132     1.135     4.956  -184        D  58    0 324.0   7.5   1.5     0.306     2.060     2.236  -242
D  38   10 320.0   2.0  -1.0     0.317     0.786     3.178  -184        D  58   10 324.0   7.5   1.5     0.209     1.490     1.339  -242
D  38   20 320.0   2.0  -1.0     0.313     0.427     2.140  -184        D  58   20 324.0   7.5   1.5     0.145     1.142     1.000  -242
D  39    0 318 0   4.0   0.5     0.822     1.150     4.586  -189        D  59    0 321.0   6.0   1.0     0.501     2.417     2.579  -248
D  39   10 318.0   4.0   0.5     0.624     0.677     3.266  -189        D  59   10 321.0   6.0   1.0     0.524     1.861     1.962  -248
D  39   20 318.0   4.0   0.5     0.454     0.562     2.134  -189        D  59   20 321.0   6.0   1.0     0.418     1.435     1.445  -248
D  40    0 313.5  -3.0   0.0    -0.646     0.813     3.767  -189        D  60    0 321.0   5.0  -1.5     0.473     1.930     2.361  -248
D  40   10 313.5  -3.0   0.0    -0.283     0.629     2.563  -189        D  60   10 321.0   5.0  -1.5     0.502     1.582     1.668  -248
D  40   20 313.5  -3.0   0.0    -0.142     0.505     1.902  -189        D  60   20 321.0   5.0  -1.5     0.405     0.997     1.198  -248
D  41    0 312.5  10.0  -4.0     2.346     3.987     4.895  -195        D  61    0 321.0   6.0  -1.5     0.257     0.485     1.043  -254
D  41   10 312.5  10.0  -4.0     1.451     2.495     2.852  -195        D  61   10 321.0   6.0  -1.5     0.156     0.417     0.814  -254
D  41   20 312.5  10.0  -4.0     0.801     1.311     2.029  -195        D  61   20 321.0   6.0  -1.5     0.146     0.258     0.533  -254
D  42    0 314.0   0.5  -3.5     0.101     1.539     4.087  -195        D  62    0 325.0   8.0  -2.0     0.113     0.408     1.023  -254
D  42   10 314.0   0.5  -3.5     0.076     1.252     2.717  -195        D  62   10 325.0   8.0  -2.0     0.027     0.270     0.593  -254
D  42   20 314.0   0.5  -3.5     0.134     0.840     1.954  -195        D  62   20 325.0   8.0  -2.0     0.049     0.154     0.473  -254
D  43    0 313.5   4.0  -3.5     0.044     1.502     3.724  -201        D  63    0 322.5   4.0  -1.5     0.704     1.423     2.929  -260
D  43   10 313.5   4.0  -3.5     0.131     1.242     2.813  -201        D  63   10 322.5   4.0  -1.5     0.635     1.202     2.214  -260
D  43   20 313.5   4.0  -3.5    -0.025     0.952     2.203  -201        D  63   20 322.5   4.0  -1.5     0.415     0.893     1.619  -260
D  44    0 317.5   2.5  -2.0     0.168     1.317     4.207  -201        D  64    0 320.5   6.0   0.0     0.818     1.332     2.689  -260
D  44   10 317.5   2.5  -2.0    -0.014     1.113     3.216  -201        D  64   10 320.5   6.0   0.0     0.698     1.024     2.041  -260
D  44   20 317.5   2.5  -2.0     0.063     0.775     2.562  -201        D  64   20 320.5   6.0   0.0     0.340     0.709     1.597  -260
D  45    0 315.0   1.0  -1.5     0.056     1.110     3.823  -207        D  65    0 323.0   5.0  -4.0     1.071     1.986     3.968  -266
D  45   10 315.0   1.0  -1.5     0.091     0.775     2.730  -207        D  65   10 323.0   5.0  -4.0     0.869     1.582     3.024  -266
D  45   20 315.0   1.0  -1.5     0.043     0.730     2.242  -207        D  65   20 323.0   5.0  -4.0     0.757     1.317     2.384  -266
D  46    0 320.0   4.0  -5.0     0.037     1.160     4.282  -207        D  66    0 322.0   4.0   1.0     0.980     2.074     3.484  -266
D  46   10 320.0   4.0  -5.0     0.168     0.867     3.287  -207        D  66   10 322.0   4.0   1.0     0.853     1.849     2.614  -266
D  46   20 320.0   4.0  -5.0     0.227     0.576     2.565  -207        D  66   20 322.0   4.0   1.0     0.740     1.340     1.954  -266
D  47    0 316.0   0.0  -4.0    -0.192     1.956     3.504  -212        D  67    0 325.5   1.0   0.5    -0.011     1.451     2.350  -276
D  47   10 316.0   0.0  -4.0    -0.134     1.458     2.290  -212        D  67   10 325.5   1.0   0.5    -0.025     1.253     1.936  -276
D  47   20 316.0   0.0  -4.0    -0.086     1.112     1.602  -212        D  67   20 325.5   1.0   0.5    -0.044     0.947     1.346  -276
D  48    0 318.0   4.0   0.0     0.039     2.085     3.585  -212        D  68    0 335.5   1.0  -1.5     0.291     1.351     2.445  -276
D  48   10 318.0   4.0   0.0     0.197     1.582     2.164  -212        D  68   10 335.5   1.0  -1.5     0.215     1.131     1.794  -276
D  48   20 318.0   4.0   0.0     0.090     1.162     1.583  -212        D  68   20 335.5   1.0  -1.5     0.223     0.986     1.398  -276
D  49    0 318.0   3.5  -1.0    -0.134     1.635     3.108  -217        D  69    0 325.5   0.0   0.0     0.193     2.323     4.407  -281
D  49   10 318.0   3.5  -1.0     0.005     1.438     1.968  -217        D  69   10 325.5   0.0   0.0     0.111     2.132     3.734  -281
D  49   20 318.0   3.5  -1.0     0.046     0.992     1.472  -217        D  69   20 325.5   0.0   0.0     0.165     1.722     2.770  -281
D  50    0 319.0   4.0  -2.5     0.264     1.830     3.214  -217        D  70    0 329.0   3.0   0.5     0.585     2.233     4.667  -281
D  50   10 319.0   4.0  -2.5     0.268     1.685     2.333  -217        D  70   10 329.0   3.0   0.5     0.437     1.859     4.089  -281
D  50   20 319.0   4.0  -2.5     0.142     1.141     1.523  -217        D  70   20 329.0   3.0   0.5     0.414     1.554     2.995  -281
D  51    0 324.0   2.0  -4.0    -0.242     0.442     1.682  -220        D  71    0 326.0   1.5   1.0     0.816     1.496     2.671  -286
D  51   10 324.0   2.0  -4.0    -0.288     0.376     1.172  -220        D  71   10 326.0   1.5   1.0     0.677     1.272     2.205  -286
D  51   20 324.0   2.0  -4.0    -0.277     0.251     0.938  -220        D  71   20 326.0   1.5   1.0     0.683     1.116     1.491  -286
D  52    0 324.0   1.0  -5.0     0.234     0.187     1.512  -220        D  72    0 325.0   0.0   1.0     0.014     1.296     2.561  -286
D  52   10 324.0   1.0  -5.0     0.177     0.119     0.994  -220        D  72   10 325.0   0.0   1.0     0.039     0.999     2.066  -286
D  52   20 324.0   1.0  -5.0     0.080     0.069     0.752  -220        D  72   20 325.0   0.0   1.0     0.281     0.933     1.514  -286
D  53    0 316.5   2.5  -0.5     1.335     2.145     3.573  -231        D  73    0 325.0  -1.0   3.0     0.274     1.397     2.697  -291
D  53   10 316.5   2.5  -0.5     0.947     1.634     2.277  -231        D  73   10 325.0  -1.0   3.0     0.031     1.099     1.771  -291
D  53   20 316.5   2.5  -0.5     0.754     1.338     1.684  -231        D  73   20 325.0  -1.0   3.0     0.034     0.824     1.218  -291
```

| | | | | | | | | | |
|---|---|---|---|---|---|---|---|---|---|
| D | 74 | 0 | 326.5 | 3.0 | 0.0 | 0.399 | 1.304 | 2.721 | -291 |
| D | 74 | 10 | 326.5 | 3.0 | 0.0 | 0.183 | 0.844 | 1.549 | -291 |
| D | 74 | 20 | 326.5 | 3.0 | 0.0 | 0.234 | 0.732 | 1.143 | -291 |
| D | 75 | 0 | 323.0 | 0.0 | -3.0 | -0.302 | 1.753 | 3.038 | -301 |
| D | 75 | 10 | 323.0 | 0.0 | -3.0 | -0.181 | 1.381 | 2.061 | -301 |
| D | 75 | 20 | 323.0 | 0.0 | -3.0 | -0.091 | 0.953 | 1.375 | -301 |
| D | 76 | 0 | 323.0 | 1.0 | 1.0 | 0.410 | 0.810 | 2.642 | -301 |
| D | 76 | 10 | 323.0 | 1.0 | 1.0 | 0.232 | 0.801 | 1.842 | -301 |
| D | 76 | 20 | 323.0 | 1.0 | 1.0 | 0.188 | 0.659 | 1.281 | -301 |
| D | 77 | 0 | 323.5 | -0.5 | -0.5 | -0.219 | 0.481 | 2.308 | -308 |
| D | 77 | 10 | 323.5 | -0.5 | -0.5 | -0.093 | 0.319 | 1.150 | -308 |
| D | 77 | 20 | 323.5 | -0.5 | -0.5 | -0.010 | 0.238 | 0.756 | -308 |
| D | 78 | 0 | 321.0 | 0.0 | 4.0 | -0.215 | 0.382 | 2.395 | -308 |
| D | 78 | 10 | 321.0 | 0.0 | 4.0 | -0.012 | 0.303 | 1.311 | -308 |
| D | 78 | 20 | 321.0 | 0.0 | 4.0 | -0.053 | 0.153 | 0.860 | -308 |
| D | 79 | 0 | 319.0 | -3.0 | 2.0 | -0.433 | 0.627 | 2.606 | -312 |
| D | 79 | 10 | 319.0 | -3.0 | 2.0 | -0.372 | 0.410 | 1.659 | -312 |
| D | 79 | 20 | 319.0 | -3.0 | 2.0 | -0.180 | 0.207 | 1.205 | -312 |
| D | 80 | 0 | 324.0 | 3.0 | 0.0 | -0.405 | 0.986 | 2.726 | -312 |
| D | 80 | 10 | 324.0 | 3.0 | 0.0 | -0.299 | 0.742 | 1.592 | -312 |
| D | 80 | 20 | 324.0 | 3.0 | 0.0 | -0.295 | 0.506 | 1.157 | -312 |
| D | 81 | 0 | 323.5 | -2.0 | 0.0 | 0.487 | 1.396 | 2.929 | -320 |
| D | 81 | 10 | 323.5 | -2.0 | 0.0 | 0.488 | 1.253 | 2.123 | -320 |
| D | 81 | 20 | 323.5 | -2.0 | 0.0 | 0.424 | 0.889 | 1.688 | -320 |
| D | 82 | 0 | 329.0 | 3.5 | 0.0 | 0.222 | 1.585 | 3.138 | -320 |
| D | 82 | 10 | 329.0 | 3.5 | 0.0 | 0.109 | 1.331 | 2.296 | -320 |
| D | 82 | 20 | 329.0 | 3.5 | 0.0 | 0.084 | 1.061 | 1.892 | -320 |
| D | 83 | 0 | 323.5 | -2.0 | 1.5 | -0.853 | 1.199 | 2.152 | -326 |
| D | 83 | 10 | 323.5 | -2.0 | 1.5 | -0.596 | 1.050 | 1.469 | -326 |
| D | 83 | 20 | 323.5 | -2.0 | 1.5 | -0.484 | 0.797 | 0.967 | -326 |
| D | 84 | 0 | 321.5 | 3.5 | 1.0 | -0.767 | 1.162 | 2.081 | -326 |
| D | 84 | 10 | 321.5 | 3.5 | 1.0 | -0.646 | 1.050 | 1.227 | -326 |
| D | 84 | 20 | 321.5 | 3.5 | 1.0 | -0.560 | 0.789 | 0.888 | -326 |
| D | 85 | 0 | 328.0 | -0.5 | 2.0 | -0.626 | 1.859 | 2.662 | -332 |
| D | 85 | 10 | 328.0 | -0.5 | 2.0 | -0.449 | 1.541 | 1.863 | -332 |
| D | 85 | 20 | 328.0 | -0.5 | 2.0 | -0.329 | 1.090 | 1.312 | -332 |
| D | 86 | 0 | 327.0 | 0.0 | 2.0 | -0.716 | 1.877 | 2.923 | -332 |
| D | 86 | 10 | 327.0 | 0.0 | 2.0 | -0.708 | 1.615 | 2.047 | -332 |
| D | 86 | 20 | 327.0 | 0.0 | 2.0 | -0.489 | 1.146 | 1.453 | -332 |
| D | 87 | 0 | 337.5 | 2.5 | -0.5 | -0.083 | 1.442 | 2.743 | -338 |
| D | 87 | 10 | 337.5 | 2.5 | -0.5 | -0.058 | 1.285 | 2.239 | -338 |
| D | 87 | 20 | 337.5 | 2.5 | -0.5 | -0.098 | 0.969 | 1.407 | -338 |
| D | 88 | 0 | 330.5 | -2.0 | -1.0 | -0.499 | 0.843 | 2.092 | -338 |
| D | 88 | 10 | 330.5 | -2.0 | -1.0 | -0.397 | 0.647 | 1.572 | -338 |
| D | 88 | 20 | 330.5 | -2.0 | -1.0 | -0.194 | 0.455 | 0.993 | -338 |
| D | 89 | 0 | 326.5 | 0.5 | 0.0 | -0.352 | 0.919 | 2.486 | -345 |
| D | 89 | 10 | 326.5 | 0.5 | 0.0 | -0.262 | 0.552 | 1.413 | -345 |
| D | 89 | 20 | 326.5 | 0.5 | 0.0 | -0.287 | 0.475 | 0.955 | -345 |
| D | 90 | 0 | 326.5 | 1.0 | 0.0 | -0.571 | 0.902 | 2.698 | -345 |
| D | 90 | 10 | 326.5 | 1.0 | 0.0 | -0.305 | 0.639 | 1.599 | -345 |
| D | 90 | 20 | 326.5 | 1.0 | 0.0 | -0.205 | 0.536 | 1.123 | -345 |
| D | 91 | 0 | 326.0 | -1.0 | 1.0 | -0.258 | 1.016 | 1.655 | -352 |
| D | 91 | 10 | 326.0 | -1.0 | 1.0 | -0.248 | 0.685 | 0.738 | -352 |
| D | 91 | 20 | 326.0 | -1.0 | 1.0 | -0.113 | 0.496 | 0.529 | -352 |
| D | 92 | 0 | 327.0 | 1.0 | 2.0 | -0.278 | 1.063 | 1.708 | -352 |
| D | 92 | 10 | 327.0 | 1.0 | 2.0 | -0.220 | 0.717 | 0.953 | -352 |
| D | 92 | 20 | 327.0 | 1.0 | 2.0 | -0.134 | 0.472 | 0.597 | -352 |
| D | 93 | 0 | 312.5 | -5.0 | -8.0 | -0.709 | 1.627 | 3.088 | -357 |
| D | 93 | 10 | 312.5 | -5.0 | -8.0 | -0.522 | 1.560 | 2.555 | -357 |
| D | 93 | 20 | 312.5 | -5.0 | -8.0 | -0.464 | 1.162 | 1.919 | -357 |
| D | 94 | 0 | 308.5 | -4.5 | -4.0 | -0.873 | 1.636 | 2.801 | -357 |
| D | 94 | 10 | 308.5 | 0.0 | -8.5 | -0.665 | 1.448 | 2.078 | -357 |
| D | 94 | 20 | 308.5 | 0.0 | -8.5 | -0.595 | 1.235 | 1.491 | -357 |
| D | 95 | 0 | 309.0 | -3.0 | -8.0 | 0.175 | 2.207 | 4.237 | -362 |
| D | 95 | 10 | 309.0 | -3.0 | -8.0 | 0.285 | 2.143 | 3.268 | -362 |
| D | 95 | 20 | 309.0 | -3.0 | -8.0 | 0.287 | 1.639 | 2.436 | -362 |
| D | 96 | 0 | 308.5 | 0.0 | -8.5 | 0.471 | 2.214 | 3.723 | -362 |
| D | 96 | 10 | 308.5 | 0.0 | -8.5 | 0.398 | 2.132 | 2.975 | -362 |
| D | 96 | 20 | 308.5 | 0.0 | -8.5 | 0.266 | 1.651 | 2.089 | -362 |
| D | 97 | 0 | 307.0 | -5.0 | -8.0 | -0.644 | 0.357 | 2.314 | -368 |
| D | 97 | 10 | 307.0 | -5.0 | -8.0 | -0.493 | 0.226 | 1.427 | -368 |
| D | 97 | 20 | 307.0 | -5.0 | -8.0 | -0.224 | 0.173 | 0.865 | -368 |
| D | 98 | 0 | 309.0 | -5.0 | -12.0 | -1.112 | 0.948 | 1.936 | -368 |
| D | 98 | 10 | 309.0 | -5.0 | -12.0 | -0.853 | 0.845 | 1.199 | -368 |
| D | 98 | 20 | 309.0 | -5.0 | -12.0 | -0.562 | 0.711 | 0.806 | -368 |
| D | 99 | 0 | 310.0 | -4.0 | -8.0 | -1.372 | 2.561 | 2.610 | -374 |
| D | 99 | 10 | 310.0 | -4.0 | -8.0 | -1.047 | 1.897 | 1.693 | -374 |
| D | 99 | 20 | 310.0 | -4.0 | -8.0 | -0.668 | 1.322 | 1.260 | -374 |
| D | 100 | 0 | 311.5 | -3.0 | -8.0 | -0.762 | 1.988 | 2.269 | -374 |
| D | 100 | 10 | 311.5 | -3.0 | -8.0 | -0.573 | 1.344 | 1.282 | -374 |
| D | 100 | 20 | 311.5 | -3.0 | -8.0 | -0.368 | 1.044 | 0.991 | -374 |
| D | 101 | 0 | 308.5 | -2.5 | -7.0 | -1.074 | 0.917 | 1.535 | -379 |
| D | 101 | 10 | 308.5 | -2.5 | -7.0 | -0.899 | 0.786 | 1.015 | -379 |
| D | 101 | 20 | 308.5 | -2.5 | -7.0 | -0.735 | 0.659 | 0.775 | -379 |
| D | 102 | 0 | 311.0 | -3.0 | -10.0 | -1.189 | 1.379 | 2.050 | -379 |
| D | 102 | 10 | 311.0 | -3.0 | -10.0 | -0.993 | 1.205 | 1.330 | -379 |
| D | 102 | 20 | 311.0 | -3.0 | -10.0 | -0.647 | 0.997 | 0.941 | -379 |
| D | 103 | 0 | 310.0 | -4.0 | -5.0 | -1.093 | 1.364 | 2.068 | -385 |
| D | 103 | 10 | 310.0 | -4.0 | -5.0 | -0.870 | 1.016 | 1.309 | -385 |
| D | 103 | 20 | 310.0 | -4.0 | -5.0 | -0.681 | 0.788 | 1.013 | -385 |
| D | 104 | 0 | 313.0 | -5.0 | -7.0 | -0.764 | 1.325 | 1.907 | -385 |
| D | 104 | 10 | 313.0 | -5.0 | -7.0 | -0.596 | 1.305 | 1.192 | -385 |
| D | 104 | 20 | 313.0 | -5.0 | -7.0 | -0.456 | 0.844 | 0.828 | -385 |
| D | 105 | 0 | 315.0 | -5.0 | -7.5 | -0.390 | 0.680 | 1.848 | -391 |
| D | 105 | 10 | 315.0 | -5.0 | -7.5 | -0.109 | 0.762 | 1.204 | -391 |
| D | 105 | 20 | 315.0 | -5.0 | -7.5 | -0.052 | 0.507 | 0.856 | -391 |
| D | 106 | 0 | 313.0 | -3.0 | -9.0 | 0.100 | 0.853 | 2.024 | -391 |
| D | 106 | 10 | 313.0 | -3.0 | -9.0 | 0.042 | 0.683 | 1.384 | -391 |
| D | 106 | 20 | 313.0 | -3.0 | -9.0 | -0.034 | 0.434 | 1.023 | -391 |
| D | 107 | 0 | 313.0 | -3.0 | -6.5 | -0.168 | 0.782 | 1.906 | -397 |
| D | 107 | 10 | 313.0 | -3.0 | -6.5 | -0.083 | 0.463 | 1.083 | -397 |
| D | 107 | 20 | 313.0 | -3.0 | -6.5 | -0.069 | 0.360 | 0.745 | -397 |
| D | 108 | 0 | 318.0 | -1.0 | -6.5 | 0.294 | 0.904 | 1.774 | -397 |
| D | 108 | 10 | 313.0 | -3.0 | -6.5 | 0.227 | 0.631 | 0.974 | -397 |
| D | 108 | 20 | 313.0 | -3.0 | -6.5 | 0.192 | 0.487 | 0.791 | -397 |
| D | 109 | 0 | 315.0 | 0.5 | -6.0 | 0.551 | 0.882 | 2.720 | -404 |
| D | 109 | 10 | 315.0 | 0.5 | -6.0 | 0.443 | 0.694 | 1.737 | -404 |
| D | 109 | 20 | 315.0 | 0.5 | -6.0 | 0.415 | 0.574 | 1.277 | -404 |
| D | 110 | 0 | 315.5 | -3.5 | -8.0 | 0.051 | 0.616 | 2.480 | -404 |
| D | 110 | 10 | 315.5 | -3.5 | -8.0 | 0.138 | 0.497 | 1.625 | -404 |
| D | 110 | 20 | 315.5 | -3.5 | -8.0 | -0.091 | 0.383 | 1.185 | -404 |
| D | 111 | 0 | 317.0 | -1.5 | -3.0 | 0.720 | 1.412 | 2.280 | -409 |
| D | 111 | 10 | 317.0 | -1.5 | -3.0 | 0.544 | 0.945 | 1.535 | -409 |
| D | 111 | 20 | 317.0 | -1.5 | -3.0 | 0.318 | 0.640 | 1.061 | -409 |
| D | 112 | 0 | 318.0 | -3.0 | -1.5 | 0.352 | 1.129 | 2.255 | -409 |
| D | 112 | 10 | 318.0 | -3.0 | -1.5 | 0.303 | 0.745 | 1.487 | -409 |
| D | 112 | 20 | 318.0 | -3.0 | -1.5 | 0.229 | 0.467 | 1.037 | -409 |
| D | 113 | 0 | 320.5 | -3.0 | -3.0 | 0.406 | 1.562 | 2.599 | -414 |
| D | 113 | 10 | 320.5 | -3.0 | -3.0 | 0.420 | 1.010 | 1.619 | -414 |
| D | 113 | 20 | 320.5 | -3.0 | -3.0 | 0.325 | 0.765 | 1.199 | -414 |

| | | | | | | | | | |
|---|---|---|---|---|---|---|---|---|---|
| D | 114 | 0 | 321.5 | -5.0 | -1.5 | -0.065 | 1.276 | 2.438 | -414 |
| D | 114 | 10 | 321.5 | -5.0 | -1.5 | 0.159 | 1.011 | 1.569 | -414 |
| D | 114 | 20 | 321.5 | -5.0 | -1.5 | -0.253 | 0.695 | 1.109 | -414 |
| D | 115 | 0 | 319.0 | -5.0 | -5.0 | 0.401 | 1.755 | 2.510 | -420 |
| D | 115 | 10 | 319.0 | -5.0 | -5.0 | 0.532 | 1.566 | 1.810 | -420 |
| D | 115 | 20 | 319.0 | -5.0 | -5.0 | 0.441 | 1.115 | 1.326 | -420 |
| D | 116 | 0 | 314.5 | -1.0 | -5.0 | 0.405 | 1.395 | 2.164 | -420 |
| D | 116 | 10 | 314.5 | -1.0 | -5.0 | 0.458 | 1.223 | 1.681 | -420 |
| D | 116 | 20 | 314.5 | -1.0 | -5.0 | 0.360 | 0.939 | 1.188 | -420 |
| D | 117 | 0 | 318.0 | -0.5 | -5.0 | 0.549 | 1.191 | 2.158 | -424 |
| D | 117 | 10 | 318.0 | -0.5 | -5.0 | 0.495 | 0.976 | 1.458 | -424 |
| D | 117 | 20 | 318.0 | -0.5 | -5.0 | 0.410 | 0.767 | 1.071 | -424 |
| D | 118 | 0 | 309.0 | -0.5 | -0.5 | 0.505 | 1.473 | 2.457 | -424 |
| D | 118 | 10 | 309.0 | -0.5 | -0.5 | 0.444 | 1.423 | 1.728 | -424 |
| D | 118 | 20 | 309.0 | -0.5 | -0.5 | 0.288 | 1.035 | 1.325 | -424 |
| D | 119 | 0 | 316.0 | -2.0 | -4.0 | 0.189 | 0.782 | 1.483 | -429 |
| D | 119 | 10 | 316.0 | -2.0 | -4.0 | 0.241 | 0.627 | 1.064 | -429 |
| D | 119 | 20 | 316.0 | -2.0 | -4.0 | 0.229 | 0.500 | 0.749 | -429 |
| D | 120 | 0 | 316.0 | -2.0 | 0.0 | 0.314 | 0.679 | 1.191 | -429 |
| D | 120 | 10 | 316.0 | -2.0 | 0.0 | 0.401 | 0.531 | 0.799 | -429 |
| D | 120 | 20 | 316.0 | -2.0 | 0.0 | 0.355 | 0.401 | 0.587 | -429 |
| D | 121 | 0 | 330.0 | -0.5 | -5.0 | 0.455 | 1.152 | 1.983 | -434 |
| D | 121 | 10 | 330.0 | -0.5 | -5.0 | 0.570 | 0.903 | 1.533 | -434 |
| D | 121 | 20 | 330.0 | -0.5 | -5.0 | 0.400 | 0.738 | 1.021 | -434 |
| D | 122 | 0 | 327.0 | -5.0 | -7.0 | 0.326 | 1.094 | 2.008 | -434 |
| D | 122 | 10 | 327.0 | -5.0 | -7.0 | 0.298 | 1.062 | 1.461 | -434 |
| D | 122 | 20 | 327.0 | -5.0 | -7.0 | 0.220 | 0.664 | 1.113 | -434 |
| D | 123 | 0 | 322.5 | -12.5 | -5.0 | 0.317 | 0.777 | 1.636 | -439 |
| D | 123 | 10 | 322.5 | -12.5 | -5.0 | 0.390 | 0.767 | 1.318 | -439 |
| D | 123 | 20 | 322.5 | -12.5 | -5.0 | 0.338 | 0.598 | 1.033 | -439 |
| D | 124 | 0 | 328.5 | -11.0 | -4.0 | 0.377 | 1.129 | 1.771 | -439 |
| D | 124 | 10 | 328.5 | -11.0 | -4.0 | 0.332 | 0.934 | 1.360 | -439 |
| D | 124 | 20 | 328.5 | -11.0 | -4.0 | 0.280 | 0.785 | 0.987 | -439 |
| D | 125 | 0 | 323.0 | -8.0 | -4.0 | 0.689 | 0.610 | 1.807 | -444 |
| D | 125 | 10 | 323.0 | -8.0 | -4.0 | 0.489 | 0.468 | 1.482 | -444 |
| D | 125 | 20 | 323.0 | -8.0 | -4.0 | 0.407 | 0.381 | 1.150 | -444 |
| D | 126 | 0 | 324.0 | -4.0 | -1.0 | 0.546 | 0.809 | 1.852 | -444 |
| D | 126 | 10 | 324.0 | -4.0 | -1.0 | 0.403 | 0.564 | 1.310 | -444 |
| D | 126 | 20 | 324.0 | -4.0 | -1.0 | 0.436 | 0.494 | 1.032 | -444 |
| D | 127 | 0 | 325.5 | -6.0 | -3.0 | 0.119 | 0.846 | 1.652 | -451 |
| D | 127 | 10 | 325.5 | -6.0 | -3.0 | 0.083 | 0.686 | 1.226 | -451 |
| D | 127 | 20 | 325.5 | -6.0 | -3.0 | 0.037 | 0.615 | 0.987 | -451 |
| D | 128 | 0 | 326.5 | -6.0 | -7.5 | 0.380 | 0.707 | 1.678 | -451 |
| D | 128 | 10 | 326.5 | -6.0 | -7.5 | 0.404 | 0.578 | 1.323 | -451 |
| D | 128 | 20 | 326.5 | -6.0 | -7.5 | 0.376 | 0.433 | 1.079 | -451 |
| D | 129 | 0 | 330.0 | -0.5 | -5.0 | 0.626 | 1.036 | 2.273 | -457 |
| D | 129 | 10 | 330.0 | -0.5 | -5.0 | 0.484 | 0.906 | 1.625 | -457 |
| D | 129 | 20 | 330.0 | -0.5 | -5.0 | 0.383 | 0.605 | 1.180 | -457 |
| D | 130 | 0 | 329.5 | -1.0 | -5.0 | 0.501 | 0.733 | 2.294 | -457 |
| D | 130 | 10 | 329.5 | -1.0 | -5.0 | 0.480 | 0.663 | 1.625 | -457 |
| D | 130 | 20 | 329.5 | -1.0 | -5.0 | 0.377 | 0.418 | 1.220 | -457 |
| D | 131 | 0 | 328.0 | 5.0 | -5.5 | -0.052 | 0.225 | 0.600 | -462 |
| D | 131 | 10 | 328.0 | 5.0 | -5.5 | 0.002 | 0.127 | 0.375 | -462 |
| D | 131 | 20 | 328.0 | 5.0 | -5.5 | -0.008 | 0.109 | 0.294 | -462 |
| D | 132 | 0 | 329.5 | 0.5 | -3.5 | 0.180 | 0.253 | 0.572 | -462 |
| D | 132 | 10 | 329.5 | 0.5 | -3.5 | 0.151 | 0.118 | 0.467 | -462 |
| D | 132 | 20 | 329.5 | 0.5 | -3.5 | 0.175 | -0.031 | 0.372 | -462 |
| D | 133 | 0 | 328.0 | 0.5 | -5.0 | 0.673 | 0.813 | 1.457 | -469 |
| D | 133 | 10 | 328.0 | 0.5 | -5.0 | 0.580 | 0.693 | 1.123 | -469 |
| D | 133 | 20 | 328.0 | 0.5 | -5.0 | 0.479 | 0.607 | 0.854 | -469 |
| D | 134 | 0 | 330.0 | 0.0 | -2.0 | 0.638 | 0.690 | 1.367 | -469 |
| D | 134 | 10 | 330.0 | 0.0 | -2.0 | 0.609 | 0.619 | 1.063 | -469 |
| D | 134 | 20 | 330.0 | 0.0 | -2.0 | 0.493 | 0.560 | 0.782 | -469 |
| D | 135 | 0 | 326.0 | 1.0 | -2.0 | 0.107 | 0.047 | 0.573 | -474 |
| D | 135 | 10 | 326.0 | 1.0 | -2.0 | 0.104 | 0.006 | 0.446 | -474 |
| D | 135 | 20 | 326.0 | 1.0 | -2.0 | 0.042 | -0.038 | 0.304 | -474 |
| D | 136 | 0 | 331.5 | 1.0 | -5.5 | 0.108 | 0.060 | 0.627 | -474 |
| D | 136 | 10 | 331.5 | 1.0 | -5.5 | 0.153 | 0.090 | 0.395 | -474 |
| D | 136 | 20 | 331.5 | 1.0 | -5.5 | 0.132 | 0.050 | 0.357 | -474 |
| D | 137 | 0 | 330.5 | 0.0 | -2.0 | 0.576 | 0.891 | 1.746 | -481 |
| D | 137 | 10 | 330.5 | 0.0 | -2.0 | 0.460 | 0.729 | 1.237 | -481 |
| D | 137 | 20 | 330.5 | 0.0 | -2.0 | 0.341 | 0.607 | 0.966 | -481 |
| D | 138 | 0 | 331.0 | 1.5 | -2.0 | 0.731 | 0.753 | 2.148 | -481 |
| D | 138 | 10 | 331.0 | 1.5 | -2.0 | 0.644 | 0.592 | 1.316 | -481 |
| D | 138 | 20 | 331.0 | 1.5 | -2.0 | 0.540 | 0.526 | 1.144 | -481 |
| D | 139 | 0 | 332.0 | 2.0 | -4.0 | 0.838 | 0.772 | 1.737 | -486 |
| D | 139 | 10 | 332.0 | 2.0 | -4.0 | 0.815 | 0.725 | 1.258 | -486 |
| D | 139 | 20 | 332.0 | 2.0 | -4.0 | 0.662 | 0.509 | 0.953 | -486 |
| D | 140 | 0 | 334.0 | 2.5 | -4.0 | 0.639 | 0.686 | 1.514 | -486 |
| D | 140 | 10 | 334.0 | 2.5 | -4.0 | 0.639 | 0.518 | 1.078 | -486 |
| D | 140 | 20 | 334.0 | 2.5 | -4.0 | 0.625 | 0.538 | 0.886 | -486 |
| D | 141 | 0 | 328.0 | 1.0 | -1.5 | -0.028 | 0.042 | 0.838 | -490 |
| D | 141 | 10 | 328.0 | 1.0 | -1.5 | 0.004 | 0.035 | 0.605 | -490 |
| D | 141 | 20 | 328.0 | 1.0 | -1.5 | -0.008 | 0.002 | 0.435 | -490 |
| D | 142 | 0 | 327.0 | -1.0 | -5.0 | 0.026 | 0.021 | 0.584 | -490 |
| D | 142 | 10 | 327.0 | -1.0 | -5.0 | 0.086 | 0.154 | 0.419 | -490 |
| D | 142 | 20 | 327.0 | -1.0 | -5.0 | 0.062 | 0.088 | 0.432 | -490 |
| D | 143 | 0 | 326.0 | 2.5 | 1.0 | 0.629 | 0.126 | 0.423 | -496 |
| D | 143 | 10 | 326.0 | 2.5 | 1.0 | 0.447 | 0.116 | 0.327 | -496 |
| D | 143 | 20 | 326.0 | 2.5 | 1.0 | 0.073 | 0.011 | 0.284 | -496 |
| D | 144 | 0 | 332.5 | 5.0 | -2.5 | 0.210 | 0.013 | 0.733 | -496 |
| D | 144 | 10 | 332.5 | 5.0 | -2.5 | 0.166 | 0.030 | 0.468 | -496 |
| D | 144 | 20 | 332.5 | 5.0 | -2.5 | 0.107 | -0.050 | 0.283 | -496 |
| D | 145 | 0 | 325.0 | 4.0 | 0.0 | 0.082 | 0.315 | 0.958 | -501 |
| D | 145 | 10 | 325.0 | 4.0 | 0.0 | 0.123 | 0.248 | 0.690 | -501 |
| D | 145 | 20 | 325.0 | 4.0 | 0.0 | 0.099 | 0.174 | 0.449 | -501 |
| D | 146 | 0 | 333.0 | 0.0 | 1.0 | 0.082 | 0.234 | 0.817 | -501 |
| D | 146 | 10 | 333.0 | 0.0 | 1.0 | 0.136 | 0.252 | 0.542 | -501 |
| D | 146 | 20 | 333.0 | 0.0 | 1.0 | 0.102 | 0.150 | 0.319 | -501 |
| D | 147 | 0 | 325.0 | -3.0 | 1.0 | 0.143 | 0.379 | 0.879 | -506 |
| D | 147 | 10 | 325.0 | -3.0 | 1.0 | 0.108 | 0.351 | 0.581 | -506 |
| D | 147 | 20 | 325.0 | -3.0 | 1.0 | 0.114 | 0.249 | 0.394 | -506 |
| D | 148 | 0 | 334.0 | -1.0 | -3.0 | 0.149 | 0.293 | 0.878 | -506 |
| D | 148 | 10 | 334.0 | -1.0 | -3.0 | 0.151 | 0.204 | 0.500 | -506 |
| D | 148 | 20 | 334.0 | -1.0 | -3.0 | 0.187 | 0.143 | 0.334 | -506 |
| D | 149 | 0 | 331.0 | -1.0 | -2.5 | 0.113 | 0.320 | 0.902 | -516 |
| D | 149 | 10 | 331.0 | -1.0 | -2.5 | 0.193 | 0.269 | 0.658 | -516 |
| D | 149 | 20 | 331.0 | -1.0 | -2.5 | 0.128 | 0.223 | 0.399 | -516 |
| D | 150 | 0 | 330.5 | 1.0 | -1.0 | 0.161 | 0.295 | 1.024 | -516 |
| D | 150 | 10 | 330.5 | 1.0 | -1.0 | 0.138 | 0.228 | 0.751 | -516 |
| D | 150 | 20 | 330.5 | 1.0 | -1.0 | 0.102 | -0.134 | 0.500 | -516 |
| D | 151 | 0 | 337.5 | 3.0 | 0.0 | 0.119 | 0.087 | 0.605 | -522 |
| D | 151 | 10 | 337.5 | 3.0 | 0.0 | 0.071 | 0.064 | 0.401 | -522 |
| D | 151 | 20 | 337.5 | 3.0 | 0.0 | 0.039 | -0.013 | 0.246 | -522 |
| D | 152 | 0 | 335.0 | 4.0 | -1.0 | 0.135 | 0.099 | 0.767 | -522 |
| D | 152 | 10 | 335.0 | 4.0 | -1.0 | 0.138 | 0.052 | 0.368 | -522 |
| D | 152 | 20 | 335.0 | 4.0 | -1.0 | 0.033 | -0.034 | 0.182 | -522 |
| D | 153 | 0 | 328.5 | 0.5 | 0.0 | 0.102 | 0.116 | 0.591 | -549 |
| D | 153 | 10 | 328.5 | 0.5 | 0.0 | 0.115 | 0.048 | 0.324 | -549 |
| D | 153 | 20 | 328.5 | 0.5 | 0.0 | 0.232 | 0.028 | 0.237 | -549 |

|  |  |  |  |  |  |  |  |  |  |
|---|---|---|---|---|---|---|---|---|---|
| D | 154 | 0 | 329.0 | 0.0 | -1.0 | 0.116 | 0.120 | 0.474 | -549 |
| D | 154 | 10 | 329.0 | 0.0 | -1.0 | 0.045 | 0.113 | 0.280 | -549 |
| D | 154 | 20 | 329.0 | 0.0 | -1.0 | 0.080 | 0.205 | 0.274 | -549 |
| D | 155 | 0 | 329.0 | -2.0 | 0.0 | 0.002 | 0.130 | 0.727 | -555 |
| D | 155 | 10 | 329.0 | -2.0 | 0.0 | 0.081 | 0.006 | 0.404 | -555 |
| D | 156 | 0 | 334.0 | -0.5 | -3.5 | 0.097 | 0.116 | 0.699 | -555 |
| D | 156 | 10 | 334.0 | -0.5 | -3.5 | -0.042 | 0.055 | 0.453 | -555 |
| D | 157 | 0 | 326.5 | -1.5 | 0.5 | 0.041 | 0.043 | 0.778 | -561 |
| D | 158 | 0 | 328.0 | -0.5 | -1.5 | 0.104 | 0.040 | 0.820 | -561 |
| D | 159 | 0 | 324.0 | 1.0 | 1.0 | -0.066 | 0.074 | 0.648 | -567 |
| D | 160 | 0 | 326.5 | 1.5 | 1.0 | -0.064 | 0.104 | 0.662 | -567 |
| D | 161 | 0 | 330.5 | -5.0 | 4.0 | -0.181 | 0.823 | 8.028 | -16 |
| D | 161 | 10 | 330.5 | -5.0 | 4.0 | -0.013 | 0.430 | 3.802 | -16 |
| D | 161 | 20 | 330.5 | -5.0 | 4.0 | -0.013 | 0.401 | 2.621 | -16 |
| D | 162 | 0 | 336.5 | -0.5 | 0.0 | 0.508 | 0.499 | 6.596 | -16 |
| D | 162 | 10 | 336.5 | -0.5 | 0.0 | 0.260 | 0.448 | 3.298 | -16 |
| D | 162 | 20 | 336.5 | -0.5 | 0.0 | 0.048 | 0.191 | 2.418 | -16 |
| D | 163 | 0 | 331.5 | -3.0 | 2.0 | 1.216 | 1.652 | 5.246 | -26 |
| D | 163 | 10 | 331.5 | -3.0 | 2.0 | 1.156 | 1.123 | 2.760 | -26 |
| D | 163 | 20 | 331.5 | -3.0 | 2.0 | 0.792 | 0.436 | 1.614 | -26 |
| D | 164 | 0 | 335.5 | -4.0 | 2.0 | 1.134 | 1.558 | 5.989 | -26 |
| D | 164 | 10 | 335.5 | -4.0 | 2.0 | 0.793 | 0.859 | 3.070 | -26 |
| D | 164 | 20 | 335.5 | -4.0 | 2.0 | 0.492 | 0.516 | 1.940 | -26 |
| D | 165 | 0 | 329.5 | -3.0 | -0.5 | 1.192 | 1.528 | 5.976 | -34 |
| D | 165 | 10 | 329.5 | -3.0 | -0.5 | 0.924 | 0.926 | 2.793 | -34 |
| D | 165 | 20 | 329.5 | -3.0 | -0.5 | 0.593 | 0.554 | 1.867 | -34 |
| D | 166 | 0 | 330.5 | -0.5 | 0.0 | 0.788 | 0.890 | 5.166 | -34 |
| D | 166 | 10 | 330.5 | -0.5 | 0.0 | 0.557 | 0.503 | 2.525 | -34 |
| D | 166 | 20 | 330.5 | -0.5 | 0.0 | 0.360 | 0.336 | 1.772 | -34 |
| D | 167 | 0 | 327.0 | -0.5 | 3.5 | 1.266 | 1.975 | 8.871 | -42 |
| D | 167 | 10 | 327.0 | -0.5 | 3.5 | 0.799 | 1.061 | 5.143 | -42 |
| D | 167 | 20 | 327.0 | -0.5 | 3.5 | 0.508 | 0.657 | 3.248 | -42 |
| D | 168 | 0 | 332.5 | -3.5 | 3.0 | 0.738 | 0.782 | 6.532 | -42 |
| D | 168 | 10 | 332.5 | -3.5 | 3.0 | 0.411 | 0.377 | 3.585 | -42 |
| D | 168 | 20 | 332.5 | -3.5 | 3.0 | 0.299 | 0.140 | 2.515 | -42 |
| D | 169 | 0 | 331.0 | 0.0 | -2.0 | 0.297 | 0.518 | 4.395 | -52 |
| D | 169 | 10 | 331.0 | 0.0 | -2.0 | 0.163 | 0.457 | 2.060 | -52 |
| D | 169 | 20 | 331.0 | 0.0 | -2.0 | 0.221 | 0.222 | 1.344 | -52 |
| D | 170 | 0 | 334.0 | -2.0 | -2.0 | 0.667 | 0.670 | 4.490 | -52 |
| D | 170 | 10 | 334.0 | -2.0 | -2.0 | 0.452 | 0.403 | 2.396 | -52 |
| D | 170 | 20 | 334.0 | -2.0 | -2.0 | 0.221 | 0.168 | 1.696 | -52 |
| D | 171 | 0 | 333.0 | 1.5 | 0.0 | 1.520 | 1.247 | 5.420 | -60 |
| D | 171 | 10 | 333.0 | 1.5 | 0.0 | 0.581 | 0.421 | 1.542 | -60 |
| D | 171 | 20 | 333.0 | 1.5 | 0.0 | 0.463 | 0.275 | 0.828 | -60 |
| D | 172 | 0 | 333.0 | -1.0 | 0.0 | 0.624 | 1.170 | 4.830 | -60 |
| D | 172 | 10 | 333.0 | -1.0 | 0.0 | 0.431 | 0.649 | 2.565 | -60 |
| D | 172 | 20 | 333.0 | -1.0 | 0.0 | 0.235 | 0.434 | 1.642 | -60 |
| D | 173 | 0 | 334.0 | 0.0 | 0.0 | 1.177 | 1.168 | 4.444 | -66 |
| D | 173 | 10 | 334.0 | 0.0 | 0.0 | 0.935 | 0.915 | 2.994 | -66 |
| D | 173 | 20 | 334.0 | 0.0 | 0.0 | 0.564 | 0.717 | 1.963 | -66 |
| D | 174 | 0 | 334.0 | 1.5 | -1.0 | 0.240 | 0.758 | 3.475 | -66 |
| D | 174 | 10 | 334.0 | 1.5 | -1.0 | 0.359 | 0.522 | 2.126 | -66 |
| D | 174 | 20 | 334.0 | 1.5 | -1.0 | 0.226 | 0.367 | 1.435 | -66 |